



The  
University  
Of  
Sheffield.

***The Performance of Vertical Ground Source Heat Pumps  
(GSHPs) in Hot/Dry Climates: Saudi Arabia as a Case Study***

*A thesis submitted to the University of Sheffield for the degree of Doctor of  
Philosophy in the Faculty of Engineering*

By

**Faisal Ali Alshehri**

The University of Sheffield

Faculty of Engineering

Department of Mechanical Engineering

Submission Date

June 2022

## **Declaration**

---

I hereby declare that the work presented in this thesis has not been submitted for any other degree or professional qualification, and that it is the result of my own independent work.

Faisal Ali Alshehri

---

29/05/2021

---

## Abstract

---

Nowadays the use of renewal energy has become a fundamental choice in most developed and developing countries, in order to reduce the energy demand and CO<sub>2</sub> equivalent emissions. In order to reduce this demand, conventional air-conditioning technology should be replaced by more efficient renewable energy systems, such as those employing ground source heat pumps (GSHPs). The GSHP is cooling/heating system that transfer heat to or from the ground benefiting from the fact that the underground temperature remains almost constant all year-round at ten metres in depth or more. This means that the effect of the ambient temperature is limited and the difference in temperature between what is considered desirable (inside the building) and the surrounding medium (underground soil) is small compared to the outside temperature.

In a hot and dry country such as Saudi Arabia, air-conditioning systems consume seventy per cent of the electrical energy. In order to reduce this demand, the performance of groundsource heat pumps (GSHPs) compared to the conventional air source heat pump (ASHP) systems which have a poor performance when the air temperature is high. In Saudi Arabia, this can be as much as 50 °C. Unfortunately, the majority of the previous research into GSHPs has been focused on cold regions. Therefore, for the first time in such a hot/dry climate, the performance of ground source heat pumps (GSHPs) has been evaluated compared to the conventional air source heat pump (ASHP) systems in this type of climate. Both systems were comprehensively modelled and simulated using the Transient System Simulation (TRNSYS) and Ground Loop Design (GLD).

In order to assess this configuration, an evaluation of a model of a single-storey office building, based on the climatic conditions and geological characteristics that occur in the city of Riyadh in Saudi Arabia, was investigated. The period of evaluation was twenty years to determine the Coefficient of Performance (COP), Energy Efficiency Ratio (EER) and power consumption. Generally energy efficiency ratio is calculated by taking ratio of cooling or heating output in BTU

to electrical energy input in W.

The simulation results show that the GSHP system has high performance when compared to the ASHP. The average annual COP and EER were 4.1 and 15.5 for the GSHP, compared to 3.8 and 11 for the ASHP respectively, and the GSHP is a feasible alternative to the ASHP, with an 11-year payback period, with an 18% total cost saving over the simulation period and 36% lower annual energy consumption. The TRNSYS model shows that despite the positive results of the modelling, the high rate of the underground thermal imbalance (88%) could lead to a system failure in the long term.

In addition, Ground Loop Design software has been employed to conduct a sensitivity analysis of 12 parameters that most affect the behaviour of the system in order to determine the near-optimum design of a GSHP system. Thus, the entering water temperature (EWT) was selected to be the performance measure of the system. The results showed that the most important four design parameters are: the thermal conductivity, soil temperature, building load, and fluid flow rate. And the length of the ground heat exchanger and power consumption in the proposed design could be reduced by 15% and 1.12% respectively, compared to the baseline system.

Despite the high underground thermal imbalance and increase in the initial capital costs of GSHP, because of the extra expensive drilling costs for the ground loop heat exchanger and piping, the feasibility of GSHP system is worthy of investigation. These results can be used to simplify the design of buildings in similar arid regions worldwide.

## Publications associated with this research.

---

### List of Publications

Part of the contents in Chapters 4, 5 and 6 of this thesis are based on three journal articles listed below.

F. Alshehri, S. Beck, D. Ingham, L. Ma and M. Pourkashanian, "Techno-economic analysis of ground and air source heat pumps in hot dry climates", *Journal of Building Engineering*, vol. 26, pp. 100825, 2019.  
[DOI: 10.1016/j.jobe.2019.100825](https://doi.org/10.1016/j.jobe.2019.100825)

F. Alshehri, S. Beck, D. Ingham, L. Ma and M. Pourkashanian, "**Technico-economic modelling of ground and air source heat pumps in a hot and dry climate**", *Proceedings of the Institution of Mechanical Engineers, Part A: Journal of Power and Energy*, vol.235, 2020,  
[DOI: 10.1177/0957650920976051](https://doi.org/10.1177/0957650920976051)

F. Alshehri, S. Beck, D. Ingham, L. Ma and M. Pourkashanian, "**Sensitivity analysis of a vertical geothermal heat pump system in a hot dry climate**", *Journal of Renewable Energy*, vol. 178, pp. 785-801, 2021. [DOI: 10.1016/j.renene.2021.06.058](https://doi.org/10.1016/j.renene.2021.06.058)

## Acknowledgements

---

I would like to express my deepest appreciation to my supervisors, Derek Ingham, Stephen Beck, Mohammed Pourkashanian and Lin Ma. I am especially indebted to Prof. Derek for his invaluable support, advice and guidance during my PhD journey. My deepest thanks also to Prof. Stephen Beck for his encouragement throughout the project.

I am extremely grateful to my mum, who has been very patient during my journey. Your prayers have made my PhD journey possible.

I would also like to extend my deepest gratitude to my wife, Fadah, for her endless love and support in the pursuit of my academic goals. And many thanks to my children, Wasn, Fahad and Abdullah.

My sincere thanks are also due to my brother Fayeze, who has given direct or indirect support for all of my life.

Finally, I would like to acknowledge the scholarship grant bestowed by the Ministry of Education in Saudi Arabia in order to undertake this research work.

# Table of Contents

---

Declaration .....	I
Abstract .....	II
Publications associated with this research.....	IV
Acknowledgements .....	V
Table of Contents .....	VI
List of Figures .....	XIII
List of tables.....	XVI
List of Nomenclatures and acronyms.....	XVIII
Chapter 1: Introduction .....	1
1.1 Research Background.....	1
1.2 Saudi Arabia Vision 2030.....	2
1.3 Thesis Aims and Objectives .....	4
1.4 Structure of the Thesis.....	5
Chapter 2: Literature Review .....	7
2.1 Introduction .....	7
2.2 History of Energy Use .....	7
2.3 Renewable Energy.....	9
2.4 Renewable Energy Trend .....	9
2.5 Geothermal Energy.....	11
2.6 History of the Heat Pump .....	12
2.6.1 Heat Pump and Refrigerators .....	13
2.6.2 Heat pump components .....	14

2.6.3 Basic heat pump cycle .....	16
2.6.4 Performance of the heat pump.....	17
2.7 Ground Source Heat Pump Technology.....	18
2.8 Principle of Operation of GSHPs .....	19
2.8.1 Ground loop of GSHP .....	20
2.8.2 Heat pump of the GSHP .....	20
2.8.3 Distribution system of the GSHP .....	21
2.9 Factors Affecting GSHP Operations .....	21
2.10 Types of Geothermal Heat Pump Systems.....	23
2.10.1 Closed loop system.....	23
2.10.1.1 Vertical closed loop .....	23
2.10.1.2 Horizontal closed loop.....	24
2.10.1.3 Slinky closed loop .....	25
2.10.1.4 Closed pond loop.....	25
2.10.2 Open loop systems.....	26
2.11 Ground Source Heat Pumps in Hot and Dry Climates .....	27
2.11.1 Saudi Arabia .....	27
2.11.2 Erbil, Iraq.....	27
2.11.3 Tunisia.....	28
2.11.4 Qatar .....	29
2.11.5 Egypt .....	30
2.11.6 Palestine and Jordan .....	30
2.11.7 Algerian.....	31
2.11.8 Florida and Arizona, USA.....	31



2.12 GSHPs in Cold Climates .....	32
2.13 Large-scale GSHPs.....	35
2.14 Conclusion.....	37
Chapter 3: Ground Source Heat Pump Modelling .....	38
3.1 Introduction .....	38
3.2 Vertical Ground Source Heat Pump System Modelling.....	38
3.2.1 The line source model .....	41
3.2.2 Cylinder source model.....	41
3.3 Numerical Methods .....	42
3.3.1 G-function model .....	42
3.4 Simulation Software .....	43
3.4.1 System simulation using TRNSYS .....	44
3.4.2 Ground loop design software, GLD: .....	44
3.5 Conclusion.....	45
Chapter 4: The GSHP Potential in Saudi Arabia .....	47
4.1 Introduction .....	47
4.2 Climate Conditions in Saudi Arabia.....	47
4.3 Precipitation .....	48
4.4 Climatic Zones in Saudi Arabia .....	49
4.5 Geothermal Conditions in Saudi Arabia.....	51
4.6 Sizing a Geothermal Heat Pump in Saudi Arabia .....	57
4.7 Methods of Calculating the Length of a Vertical GHX .....	58
4.7.1 Description of generic model.....	59
4.7.2 Calculation of the length of the GHX based on the ASHRAE standards .....	61

4.8 Cost Analysis.....	66
4.8.1 Savings on the power consumption.....	66
4.8.2 Initial cost analysis .....	69
4.8.3 Simple payback periods.....	70
4.9 Underground Thermal Imbalance.....	71
4.10 Discussion of the Results of this Saudi Arabi Application .....	73
4.11 Conclusion.....	74
Chapter 5: Modelling of Ground and Air Source Heat Pumps in a Hot and Dry Climate.....	75
5.1 Introduction .....	75
5.2 Literature Review .....	75
5.3 System Simulation Using TRNSYS.....	77
5.3.1 Building envelope model.....	77
5.3.2 Building load estimation .....	80
5.3.3 Heat pump simulation .....	82
5.3.3.1 Air source heat pump.....	82
5.3.3.2 Ground source heat pump modelling.....	85
5.4 Sizing of the GHX.....	87
5.4.1 ASHREA standards method.....	88
5.4.2 Ground loop design software, GLD .....	88
5.5 Ground Source Heat Pump Simulation .....	89
5.6 Results .....	91
5.6.1 Savings on the power consumption.....	91
5.6.2 Initial cost analysis .....	93
5.6.3 Simple payback periods.....	94

5.6.4 Underground thermal imbalance .....	94
5.7 Discussion of the Results .....	97
5.8 Conclusion.....	99
Chapter 6: Sensitivity Analysis of GSHP Systems in a Hot Dry Climate .....	100
6.1 Introduction .....	100
6.2 Literature Reviews for the Sensitivity Analysis .....	100
6.3 Parameters Affecting the Design of the GSHP .....	104
6.4 Modelling of the GSHP System Using GLD .....	106
6.4.1 Sizing the GHX using GLD .....	106
6.4.2 Methodology and baseline model.....	108
6.5 System Simulation and Validation .....	110
6.5.1 System validation .....	110
6.6 Sensitivity Analysis Results .....	112
6.6.1 Soil thermal conductivity .....	114
6.6.2 Soil temperature .....	115
6.6.3 Entering water temperature .....	117
6.6.4 Soil diffusivity.....	118
6.6.5 Borehole geometry .....	119
6.6.5.1 Borehole separation .....	119
6.6.5.2 Borehole diameters .....	120
6.6.5.3 Radial pipe placement.....	121
6.6.5.4 U-Tube configuration .....	121
6.6.5.6 The fluid flowrate .....	125
6.6.6 Circulated fluid type.....	126

6.7 Parameter Evaluation .....	127
6.8 Additive Value Technique.....	129
6.9 The Best/worst-case Scenarios .....	132
6.10 Re-designing the System Using the Sensitivity Analysis.....	133
6.11 Conclusions .....	135
Chapter 7: Discussion, Conclusion and Future WorkClimate .....	137
7.1 Discussion .....	137
7.1.1 Research background .....	137
7.1.2 Aim and main findings of the thesis.....	137
7.1.3 Buildings and loads .....	141
7.1.4 Heat pump units.....	145
7.1.5 Ground loop heat exchangers .....	146
7.1.6 Grout material.....	147
7.1.7 Thermal imbalance .....	148
7.1.8 Soil thermal conductivity .....	149
7.1.9 Site characteristics .....	149
7.1.10 Limitations in installing and sizing GSHPs in Saudi Arabia.....	150
7.2 Conclusion.....	151
7.3 Future Work .....	153
References .....	155
Appendix 1: Cooling and heating load calculation for the bank building in Riyadh.....	165
a) Air System Sizing Summary for PACKAGE A/C UNIT .....	165
b) Summary for design cooling heating load .....	166
Appendix 2: Three contractors bid for pipes and drilling for GSHP system installation. ....	167

a) Pipes Prices .....	167
b) Derailing Price .....	167
APPENDIX 3. TRNSYS parameters and input data for modelling ASHP and GSHP.....	168
a) GSHP system .....	168
Input data:.....	171
b) ASHP system .....	172
Input data:.....	173
APPENDIX 4. Manufacture’s catalogue data for ASHP and GSHP. ....	176
a) ASHP catalogue data.....	176
b) GSHP catalogue data .....	182

## List of Figures

---

Figure 2-1 Estimated share of renewable energy in the total final energy consumption. ....	10
Figure 2-2 Geothermal energy classification depending on the resource temperature. ....	11
Figure 2-3 Geothermal energy applications based on the resource temperature.....	12
Figure 2-4 (a) The objective of a heat pump is to supply the heat $Q_H$ into the warmer space. (b) The objective of a refrigerator is to remove the heat $Q_L$ from the cold place.....	14
Figure 2-5 Schematic of the basic vapour-compression cycle. ....	15
Figure 2-6 Schematic of the basic thermodynamic heat pump cycle .....	17
Figure 2-7 Temperature as a function of depth (0–100m) below the Earth’s surface.....	19
Figure 2-8 Schematic of the basic ground source heat pump system components. ....	20
Figure 2-9 Schematic of the different types of geothermal heat pump systems.....	26
Figure 4-1 Average annual precipitation for Saudi Arabia. ....	49
Figure 4-2 The climatic zones in Saudi Arabia, adopted from.....	50
Figure 4-3 Map of Saudi Arabia, showing the two main parts, the Arabian Shield and the Arabian Plate.....	51
Figure 4-4 Difference between the ambient air and the ground at different depths in May 2008 ..	53
Figure 4-5 Layout of the first thermal response test in Saudi Arabia. ....	54
Figure 4-6 Inlet, outlet and mean fluid temperatures during the thermal response test. ....	54
Figure 4-7 The location of the five sites that were selected for the drilling of the boreholes by the Ministry of Petroleum and Mineral Resources in Saudi Arabia and the US Geological Survey to investigate the heat-flow measurements adopted from. ....	55
Figure 4-8 Underground temperature for Riyadh city at different depths.....	57
Figure 4-9 Schematics of ground and air source heat pump systems for a typical house in Saudi Arabia.....	59
Figure 5-1 (a) Schematic of the single-storey office building investigated. (b) Walls Construction	

Details.....	78
Figure 5-2 Saudi Arabia Climate Zones based on the Saudi Building Code. ....	79
Figure 5-3 Cooling and heating loads for the building created by TRNSYS.....	81
Figure 5-4 Outside and inside building temperature during the simulation period.....	83
Figure 5-5 COP for the ASHP unit. ....	84
Figure 5-6 Underground temperature for Riyadh city at different depths.....	86
Figure 5-7 Average entering water temperature to the GSHP unit for a 22 year period by the GLD. .....	88
Figure 5-8 The TRNSYS model.....	90
Figure 5-9 COP for the GSHP unit. ....	90
Figure 5-10 Comparison of the power consumption for the GSHP and the ASHP. ....	91
Figure 5-11 Comparison of the COP for the GSHP and the ASHP.....	92
Figure 5-12 Total heat rejected and extracted from/to the soil. ....	97
Figure 6-1 The most important parameters that affect the GSHP design and operations. ....	105
Figure 6-2 Illustration of the most important parameters employed in the sensitivity analysis....	106
Figure 6-3 A typical model of a vertical GSHP system developed in GLD.....	107
Figure 6-4 Flowchart of the proposed methodology. ....	110
Figure 6-5 Comparison between the predicted TRNSYS and GLD as regards (a) Borehole wall temperatures and (b) entering water temperatures. ....	111
Figure 6-6 Composition of Soil and types for the Al-Jubaila area - city of Riyadh.....	115
Figure 6-7 The effect of the soil temperature change on the (a) COP, (b) GHX length, and (c) WET. .....	117
Figure 6-8 The maximum EWT for the periods of 1, 20, and 40 years. ....	118
Figure 6-9 The g-function 3D map for the borehole separation: (a) 3m separation, and (b) 10m separation. ....	120

Figure 6-10 The position of the U-pipe legs inside the borehole. ....	121
Figure 6-11 The three commonly used shapes for the GHX: (A) single U-tube, (B) double U-tube, and (C) coaxial. ....	122
Figure 6-12 The effect of the pipe size on the borehole thermal resistance. ....	124
Figure 6-13 The effect of the fluid flowrate on the COP of the GSHP. ....	126
Figure 6-14 The effect of the parameter changes by $\pm 5\%$ on the borehole length. ....	127
Figure 6-15 The effect of a parameter change by $\pm 5\%$ on the power consumption. ....	128
Figure 6-16 The effect of the combination of two different parameters on the borehole length. .	130
Figure 6-17 The effect of the combination of two different parameters on the EWT. ....	131
Figure 7-1 The percentage of monthly cooling load compared to the maximum cooling load for the office building in the city of Riyadh. ....	143
Figure 7-2 The amount of cooling heat ejected to the soil for office and school buildings in Riyadh. ....	143
Figure 7-3 The relationship between the coolant type and system COP. ....	146
Figure 7-4 The proposed new fan and how it should be installed. ....	148
Figure 7-5 The caves that appear in the limestone bedrock in Saudi Arabia. ....	149
Figure 7-6 The effect of increasing the energy-efficiency ratio (EER) on power consumption for air conditioning units. ....	151



## List of tables

---

Table 1.1 The new electricity consumption tariffs for different sectors in Saudi Arabia, applied from 1/1/2018.....	3
Table 1.2 The comparison of old and new tariffs for residential buildings.....	3
Table 2.1 Thermal conductivity of different grouting material.....	24
Table 2.2 Size classification of ground source heat pumps.....	35
Table 2.3 Minimum COP and EER requirements for a small GSHP system.....	36
Table 3.1 The main analytical models' approach for GHX.....	40
Table 4.1 The climatic parameters for the identified and represented locations. ....	50
Table 4.2 Heat flow and thermal conductivity estimates from the five sites selected.....	56
Table 4.3 Geological and soil properties conditions of the ground heat exchangers. ....	56
Table 4.4 The data collected for the design calculation for the length of the GHX. ....	60
Table 4.5 The design conditions for the estimation of the cooling and heating loads. ....	60
Table 4.6 The annual primary power consumption for the ASHP and the GSHP. ....	67
Table 4.7 The initial cost analysis for the ASHP and the GSHP.....	70
Table 5.1 The U-Values for low-rise / residential buildings. ....	79
Table 5.2 Design conditions for the building investigated: summer period.....	80
Table 5.3 Estimated cooling and heating loads for the building investigated.....	81
Table 5.4 The annual COP and power consumption of the ASHP and GSHP units. ....	85
Table 5.5 Design input data of the GHSP. ....	87
Table 5.6 The cost analysis for the ASHP and GSHP for 22 years.....	93
Table 5.7 Monthly accumulated heat to the soil.....	96
Table 6.1 The baseline parameters' values.....	108
Table 6.2 GLD output of 1-year modelling for the GSHP system. ....	108

Table 6.3 Parameters analysed against the length of the GHX and energy consumption of the GSHP unit.....	113
Table 6.4 Parameters analysed against the length and power consumption of the GSHP based on the parameter type.....	114
Table 6.5 The most popular pipe sizes of the HDPE used in GSHP installations.....	124
Table 6.6 The notation for the four most important parameters influencing the length of the borehole. ....	129
Table 6.7 The impact of combination of the two different parameters on the borehole length (baseline, 100m).....	130
Table 6.8 The impact of the combination of the two different parameters on the EWT (baseline, 39.4°C).....	131
Table 6.9 The best/worst-case scenarios for the parameters which change by $\pm 5\%$ . ....	132
Table 6.10 The comparison of the results for the best/worst-case scenarios in comparison to the baseline case.....	133
Table 6.11 shows a comparison between the baseline and the proposed design parameters values. ....	134
Table 6.12 The comparison between the baseline and the proposed design parameters values....	134
Table 7.1 The baseline parameter values for the simulation of GSHPs in Riyadh and Qatar.....	140
Table 7.2 The main results for the simulation of GSHPs in Riyadh and Qatar.....	140

## List of Nomenclatures and acronyms

Symbol	Nomenclature
GSHP	Ground Source Heat Pump
H	Halala (The Saudi Riyal Is Made Up Of 100 Halala)
ASHP	Air Source Heat Pump
TRNSYS	Transient System Simulation
GLD	Ground Loop Design
COP	Coefficient of Performance
EER	Energy Efficiency Ratio
EWT	Entering Water Temperature
KACARE	King Abdullah City for Atomic and Renewable Energy
GHX	Ground Heat Exchanger
Mt	Metric Tons
MENA	Middle East and North Africa Region
SPF	Seasonal Performance Factor
BHE	Borehole Heat Exchanger
IGSHPA	International Ground Source Heat Pump Association
ASHRAE	American Society of Heating, Refrigerating and Air-Conditioning Engineers
TQBE	Thermal Quality of The Building Envelope
EED	Earth Energy Designer
EAHE	Earth-Air Heat Exchanger
HCUT	Heat Compensation Unit with A Thermosyphon
GSAHP	Ground Source Absorption Heat Pump
GSEHP	Ground Source Electrical Heat Pump
DOER	Department of Energy Resources
SGSHP	Solar Energy Coupled Ground Source Heat Pump System
LSM	Line Source Model
CSM	Cylindrical Source Model
BESTEST	Building Energy Simulation Test
ZEH	Zero Energy Houses
EFLH	Equivalent Full-Load Hours
Fo	Fourier Number
H/kWh	Halala per Kilowatt hours
kWh	kilowatt hours
EF	Emissions Factor
PBP	Payback Period
DOE	Department of Energy
<i>AEFLH</i>	<i>Annual Equivalent Full Load Hours</i>
TMY2	Typical Meteorological Years
LCCA	Life-Cycle Cost Analysis
NPV	Net Present Value
ROI	Return on Investment
IR	Imbalance Ratio
BTES	Borehole Thermal Energy Storage System
IH	Total Quantity of Injected Heat
SE	Storage Efficiency

HLP	Percentage of Heat Loss
ED	Energy Density
TRT	Thermal Response Test
PVT	Photovoltaic and Thermal Collector
CCHRC	Cold Climate Housing Research Centre
VRF	Variable Refrigerant Flow
SEEC	Saudi Energy Efficiency Centre
GHCP	Ground-Coupled Heat Pump System

# Chapter 1: Introduction

---

## 1.1 Research Background

Saudi Arabia is situated in western Asia, and it has a land mass of approximately 2,000,000 km<sup>2</sup> and a population of 32.5 million [1]. It has a hot temperature and becomes especially hot during the summer, except for the mountains in the south-western region. Also, the rainfall rate is very rare in the country and occurs only in a few months [2]. However, the climate condition in Saudi Arabia is particularly mild in the winter and very hot in summer, with the aforementioned exception of the south-western region. Most of the climatic features are due to the desert conditions that are predominant in the Kingdom.

In terms of energy consumption, energy supplies in Saudi Arabia almost totally depend on oil and gas power plants, and the energy consumption is extensively subsidized, leading to the overuse and misallocation of the oil and natural gas resources. The subsidization of energy has given little incentive for its fast-growing population to save energy consumption in different economic activities [3]. For this reason, the domestic energy consumption of oil has rapidly grown in the past 40-year period and has recently comprised one-fourth of the total oil production in the country. Over the last five years, Saudi Arabia's domestic energy consumption has rapidly grown - by 10% annually [4]. Also, the population growth of 3.4% per year has had a large impact on the consumption of domestic oil [5]. At this rate of growth, it has been estimated that by the year 2025 the electricity generation of Saudi Arabia may be more than double that of the existing demand [6]. Moreover, Saudi Arabia is classified as having a high per capita consumption of energy, making it one of the predominant global polluters (in terms of the energy used per capita). This has resulted in 16 metric tons of carbon dioxide emissions per capita in the year 2009, in comparison to a global average of about 4.7 metric tons. Therefore, the government of Saudi Arabia is attempting to reduce its greenhouse gas emissions by 130 metric tons

(Mt CO<sub>2</sub>), preferably by 2030.

In addition, research has projected that the peak demand for electricity will reach 70% in 2030 [7], with 70% of the consumption of the electrical energy per building being consumed for ventilation, heating, and air conditioning purposes (HVAC). For example, in 2010, due to the high temperatures during the summer and an outdoor temperature of 45 °C, buildings consumed 65% of the total electricity, which was 47% higher than the world average [8]. The actual power consumption in Saudi Arabia is three times more than the world average [9], and therefore special focus should be given to air conditioning systems. This can be achieved by setting higher efficiency standards, implementing adequate insulation measures, as well as through the use of renewable energy.

## **1.2 Saudi Arabia Vision 2030**

One of the main goals of the Saudi Arabia Vision 2030 is to transform the Kingdom's oil-dependent economy to one which is diverse, sustainable, and situated at the crossroads of international trade. A significant target under Vision 2030 is to decrease the energy consumption and greenhouse gas emissions from both the building and industrial sectors. Thus, the Saudi Arabia Renewable Energy programme started with the establishment of the King Abdullah City for Atomic and Renewable Energy (KACARE), which is responsible for the development of technology that relates to renewable energy, associated research, and the setting of the policies and legislative frameworks pertaining to Saudi Arabia's energy consumption [11]. Thus, the Saudi Arabia government intends to encourage enthusiastic programmes, with the purpose of harnessing renewable energy, for which there are not only great opportunities but also much room for improvement. Furthermore, they also want to increase their energy mix, which will include solar thermal, solar PV, waste, wind, and geothermal energy systems. Thus, the general aims and objectives of this research fall in line with the National Transformation Program in Saudi Arabia, which plans to cut public-sector subsidies, as a part of Vision

2030, by 2020. The Kingdom’s government plans to adjust the subsidies for petroleum products, water, and electricity over the next five years in order to achieve the efficient use of energy, as well as the conservation of natural resources [12]. In fact, the Saudi government has started implementing the new energy tariff since January 2018; Table 1.1 shows the electricity consumption tariff for different sectors in Saudi Arabia [13].

Table 1.1 The new electricity consumption tariffs for different sectors in Saudi Arabia, applied from 1/1/2018.

Consumption categories (kWh)	Residential (H/kWh)	Commercial (H/kWh)	Agricultural & Charities (H/kWh)	Governmental (H/ kWh)	Industrial (H/ kWh)	Private, educational, medical facilities (H/ kWh)
1-6000	18	20	16			
More than 6000	30	30	20	32	18	18

\*(Halala (The Saudi Riyal Is Made Up Of 100 Halala)

The residential segments expected to be the most affected by the new electricity tariff; Table 1.2 shows a comparison of the old and new tariffs for residential buildings. However, the new tariff may increase by the year 2025, and therefore new strategies should be considered in order to reduce the electricity consumption.

Table 1.2 The comparison of old and new tariffs for residential buildings.

	Total units consumed (kWh)			
	1500	2500	4500	6500
Old tariff	75	150	400	850
New tariff	270	450	810	1230
% Increase	260%	200%	103%	45%

### 1.3 Thesis Aims and Objectives

The majority of research on GSHP systems has been - and still is - undertaken in cold climate regions. This research is aiming to investigate and simulate the performance of vertical ground source heat pumps (GSHPs) in hot/dry climates like Saudi Arabia, where the cooling dominant effect applies most of the time. This is to provide a better understanding of the most important factors affecting the GSHPs' design as well as to reduce the initial and operational costs and the CO<sub>2</sub> emissions, along with saving energy. In order to fulfil this aim, a number of objectives are addressed as follows:

- The existing GSHP technology is critically reviewed in terms of GSHP types and performance analysis in various aspects, such as using GSHPs in different climates and sizes.
- The concept of the GSHP thermal performance is presented, and the various governing equations that are necessary for assessing the performance are presented and critically discussed. In addition, the existing modelling software is critically reviewed.
- A techno-economic analysis is employed to evaluate the use of GSHPs compared to the conventional ASHP systems, based on identifying and understanding the climate conditions and local geological characteristics that occur in the city of Riyadh in Saudi Arabia.
- To simulate and evaluate the performance of GSHP compared with systems employing ASHP, they were comprehensively modelled and simulated using the Transient System Simulation (TRNSYS). In order to assess this configuration, an evaluation of a model of a single-story office building, the cost analysis and energy savings across the forecast period were investigated.



- An in-depth novel sensitivity analysis approach has been developed and implemented in order to determine the most important parameters that affect the GSHP operation in a hot/dry climate. Ground Loop Design (GLD) software was used to design the length of the ground loop heat exchanger and evaluate the most important parameters that play the most important roles in GSHPs' design in the geographical conditions of Saudi Arabia.

## **1.4 Structure of the Thesis**

This thesis is divided into seven chapters as follows:

Chapter 1: introduces the research background, including the general picture of energy consumption and supplies in Saudi Arabia and the government plans. It also highlights the main aims, objectives, and methodology of the study.

Chapter 2: presents a critical literature review that includes a brief energy history and trends. This is followed by detailed explanations of the types of geothermal heat pumps, their theory of operation, and the current status of heat pump applications in different climate zones and geological characteristics.

Chapter 3: details the numerical approaches and modelling solutions for the GSHP design. In addition, a review of the design tools is critically presented.

Chapter 4: investigates the ability of employing a GSHP in a hot/dry climate. Mathematical approaches are employed using the ASHRAE standards method to determine the GHX length. The chapter also reviews the current geological and weather characteristics of the location of the proposed newsystem, namely the city of Riyadh.

Chapter 5: describes in detail the modelling used in the new study and includes a comparison between the GSHP and ASHP systems; the chapter also presents the results obtained from the simulations, including the cost analysis.

Chapter 6: discusses the major components and parameters that affect the GSHP system, using a sensitivity analysis approach. In addition, the optimum design of the system depends on the characteristics of the surrounding soil and a detailed discussion of this is included.

Chapter 7: presents a detailed discussion of the results and conclusions. Finally, the chapter suggests possible future work in the GSHP industry, based on hot/dry climates.

## **Chapter 2: Literature Review**

---

### **2.1 Introduction**

In this chapter, a critical literature review of the GSHP system is presented. Firstly, fundamental knowledge of geothermal energy history and trends is introduced. This includes a brief review of GSHP technology. An extensive literature review in using shallow geothermal energy in hot and cold regions and on small and large scales, especially in terms of how shallow geothermal energy works, has been done in the Middle East and North Africa (MENA) region.

### **2.2 History of Energy Use**

Energy has not only been regarded as a great resource in the past, but its importance and increased continuous use has resulted from technological changes. However, the use of energy dates back to prehistoric periods of humankind. During this age, humans have relied on the muscular power of animals for their survival [14]. Before the advent and development of the industrial sector, humankind has had limited energy requirements. The sun and wood were the main energy source for heat, shelter, warmth, and food [15]. Hence, a switch to a new type of fuel was necessary. This led to the use of coal, oil, and other natural gases as the main source of fuel. According to the International Correspondence Schools [16] the 17<sup>th</sup> century witnessed the use of steam engines and coal by humans, along with the discovery of natural gas, oil, and electricity [17]. In 1880, the steam engine was attached to an electrical generator and powered by coal [16]. Also, the fast flow of water was used for creating light energy and thereafter, a hydro-plant was built by Edison with the assistance of Henry Ford [18]. By the end of the 18<sup>th</sup> century, petroleum, along with gasoline, was being used as fuel to fire the combustion engines which were slowly being developed [19].

Because of the rapid development and invention of several energy sources and technologies, the 17<sup>th</sup> and 18<sup>th</sup> centuries have often been considered as the starting point of the Industrial Revolution [20]. The

world's human population and their energy usage saw a significant growth during this period. To achieve the increasing energy requirements worldwide, the world's energy production increased rapidly. This energy demand was supported by the larger power plants as well as hydroplants. A large variety of energy sources were being sought to generate more power and electricity was made available even in rural regions [21].

New technologies have been developed in the modern age. Due to the extensive use of natural gas, petroleum, and other fossil fuels that have been used to support the high energy demand, there was a great decline in the availability of these non-renewable fossil fuels. This called for the invention of new technologies and alternative sources of energy in order to generate the requisite amount of power. In the 20<sup>th</sup> century, nuclear power started to be used [22],[23]. In the end of 20<sup>th</sup> century can be regarded as the modern era with regard to energy usage, consumption, and technological developments. The development and advancement in the field of computers, IT sectors, space exploration, etc. have provided ample support towards exploring new energy sources in the modern era. Along with fossil fuels and petroleum, renewable energy sources have also been used to produce the required amount of energy [24]. At present, the use of renewable energy sources has been large-scale. Nowadays, many countries are quite dependent on solar and wind energy while eschewing their dependence on conventional sources of energy [19]. Along with harnessing wind and solar energy, developed countries have increased the funding of research activities aimed at identifying and harnessing different sources of energy including biomass, hydraulic, solar, wind, geothermal, wave, tidal, biogas, ocean, fuel cells, and hydrogen, in order to improve the ways of harnessing energy from sources and support a clean environment with no gaseous emissions [25].

### **2.3 Renewable Energy**

In 1973, the oil crisis in many countries made them think about alternatives to oil and they started looking for sources of renewable energy. Actually, there are numerous different sources and forms of energy. Broadly, there are two sources: renewable and non-renewable energy [26]. However, there is a slight difference between the two sources of energy; renewable energy is obtained from sources at a less, or equal, rate in which the source replenishes itself. In other words, it is derived from sources which will never be completely depleted and will continue to provide energy for many years to come. Examples of renewable energy include, but are not limited to, solar, wind, geothermal, biomass, ocean waves, and hydropower energy. On the other hand, non-renewable energy sources are obtained at a rate which exceeds the rate at which the sources replenish themselves, e.g. uranium (which is used for nuclear fusion) and fossil fuels [27].

### **2.4 Renewable Energy Trend**

Over the last few decades, excessive use of fossil fuels has resulted in an increase in carbon dioxide emissions. Due to the massive use of oil and the high demand for energy, developed and developing countries are seeking to apply advanced technological innovations that meet the requirements of safe and efficient energy and do not adversely affect the climate [26],[28]. Although technological innovation is a key driver of energy transition, there are many other related factors which include, but are not limited to, politics, culture, economy, and geography. These considerations are important when selecting distinct technologies which are to be adopted in the course of harnessing energy sources as well as providing other energy-related services worldwide. Also, developed countries have increased the funds allotted towards research activities regarding different sources of renewable energy, in order to support a clean environment with no emissions [25].

According to the renewable global status report [30] the increase in the demand of renewable energy

has taken place in several directions and can be summarized as follows:

- Growth: In 2015, the use of renewable energy amounted to about 19.3% of the global energy consumption.
- Energy Policy: 176 countries had renewable energy targets, 126 countries had power policies, 68 countries had transport policies, and 21 countries had heating and cooling policies.
- Job Opportunity: In 2016, the renewable energy industry employed around 9.8 million to their workforce, which was 1.1% higher than their employment percentile in 2015.
- Investment: The market share of renewable energy was 241.6 billion USD in 2016. For the past five years, the investment in the sector of renewable power energy has been almost double of what has been invested in harnessing the energy based on fossil fuels.

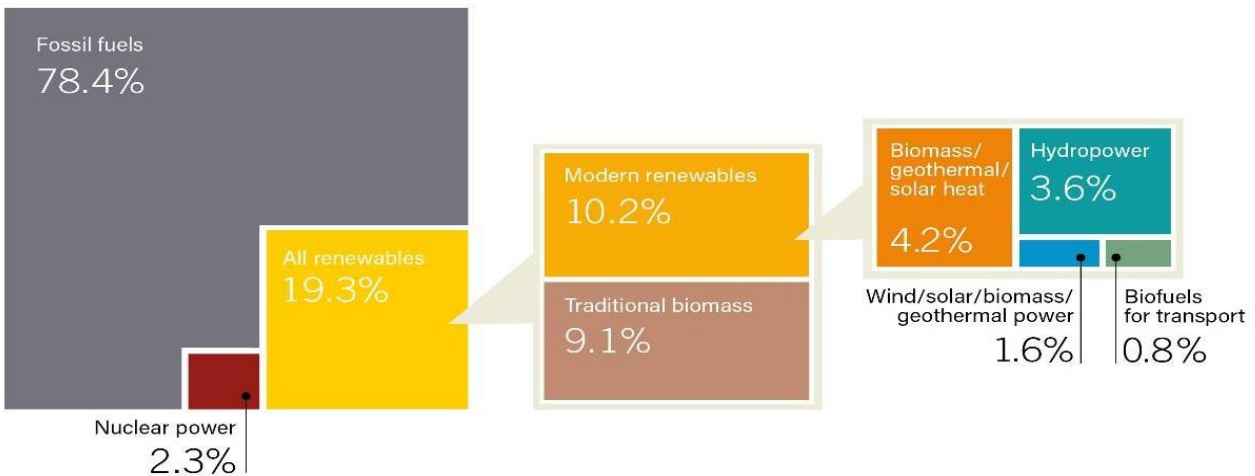
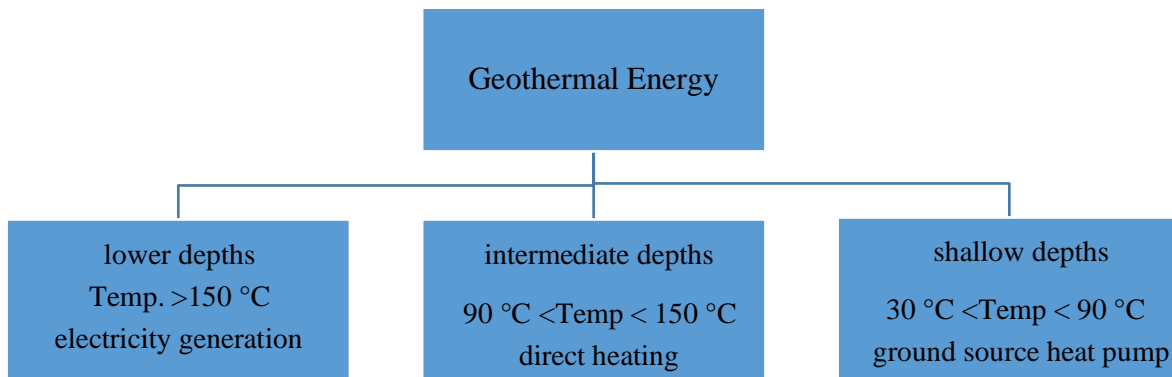


Figure 2-1 Estimated share of renewable energy in the total final energy consumption [30].

## 2.5 Geothermal Energy

Geothermal energy is a clean, efficient, sustainable, environment friendly, and cost-effective form of renewable energy. Its sources are as follows: hot molten lava in the Earth's core, heat produced by the decay of radioactive elements inside the Earth, and solar radiation which warms the Earth's surface [31].

Geothermal energy has various applications with regard to power generation including thermal baths, spas, heating and cooling, along with industrial and agricultural applications [32]. Geothermal power can be classified into three categories—lower depth, intermediate depth, and shallow depth—depending on the resource temperature and regardless of its distance from the Earth's surface as shown in Figure 2.2. In addition, Figure 2.3 shows some geothermal applications based on the resource temperature. However, analysis of the lower depth and intermediate depths are beyond the scope of this literature review, which focuses on the geothermal heat pump (which pertains to shallow depth).



*Figure 2-2 Geothermal energy classification depending on the resource temperature [32].*

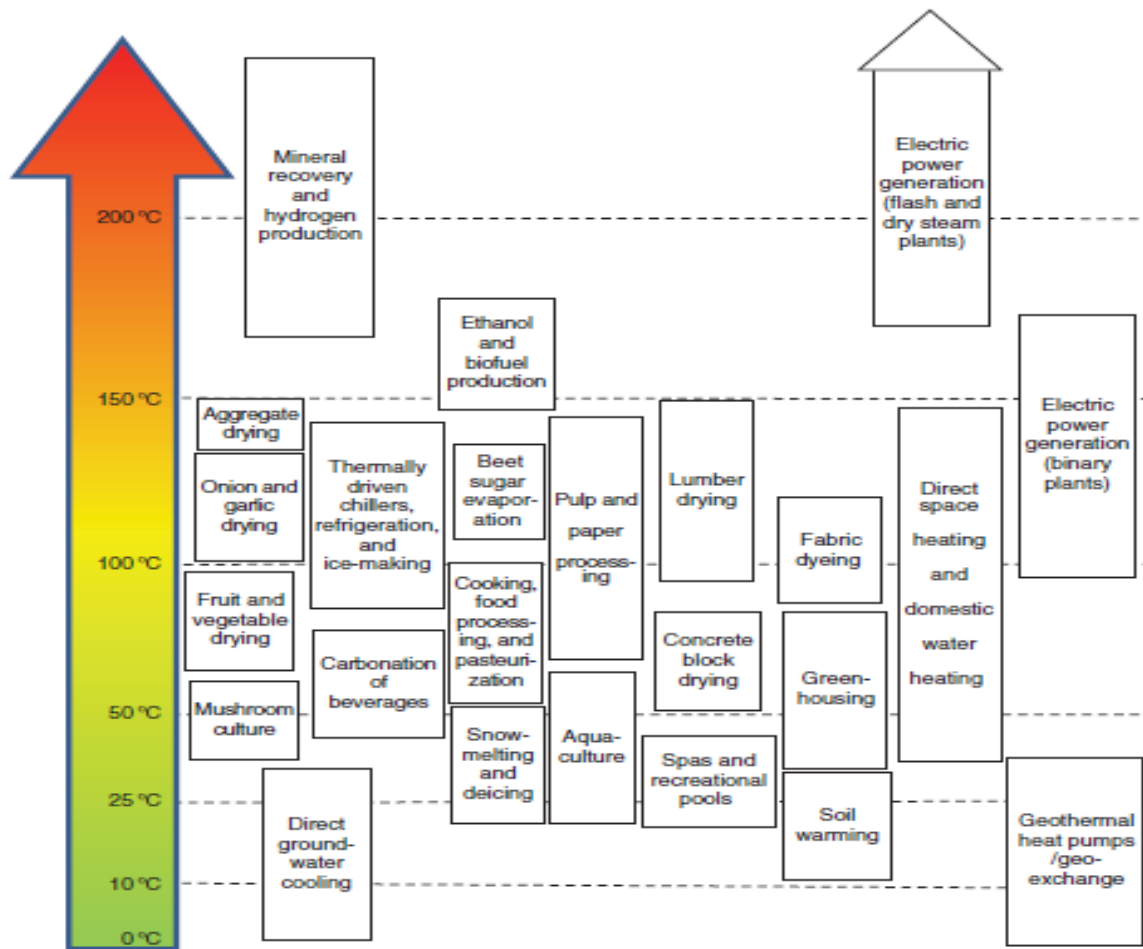


Figure 2-3 Geothermal energy applications based on the resource temperature [32,p. 6].

### 2.6 History of the Heat Pump

In 1748, the demonstration of artificial refrigeration given by William Cullen provided the grounds for the scientific principle behind the heat pump. In 1852, Lord Kelvin further explained the scientific concept of the heat pump. The first ever heat pump system was made by Peter Rittinger between 1855 to 1857. In the late 1940s, the first ground source direct exchange heat pump was developed by Robert C. Webber while he was experimenting with his deep freezer [33].

In 1948, J.D. Krockner built the first successful commercial project in the Commonwealth Building situated in Portland, Oregon. After the first oil crisis of the world in 1970, detailed work on GSHP



started in Europe and North America with suitable focus being laid on investigation-based experiments. In the 1980s, geothermal energy started to gain popularity, along with the use of GSHPs which reduced the cost of cooling and heating [34]. In the two subsequent decades, concerted efforts were applied for the development, design, and installation of the vertical borehole system. Nowadays, GSHP technology has gained worldwide popularity and, especially, in cold climatic conditions. Between 2006 and 2011, in the case of the new detached homes in Finland, the geothermal heat pump was the most preferred heating system and had a market share of more than 40%. Similarly, in the US the number of such installed units reached 80,000 per year [35].

### **2.6.1 Heat Pump and Refrigerators**

**Heat pump:** Heat energy is naturally transferred from higher to lower temperatures, but the reverse transfer of energy, from lower to higher temperatures, requires external work. A heat pump is a device that is designed to transfer thermal energy from a cold to a hot reservoir. Furthermore, it absorbs the external work done while transferring heat energy through the aforementioned path Figure 2.4.a. Both refrigerators and air conditioners are examples of heat pump technology.

**Refrigerator:** A refrigerator uses the same working principle as a heat pump, but its purpose and objective are different. It removes heat from a low temperature reservoir or a cold space, see Figure 2.4.b. Both heat pumps and refrigerators are cyclic devices and the latter mostly follows a vapor-compression refrigeration cycle.

The main purpose of a heat pump is to produce the heating effect while that of a refrigerator is to produce the cooling effect. In the heat pump, a condenser performs the main function while in the refrigerator, an evaporator does the same [36].

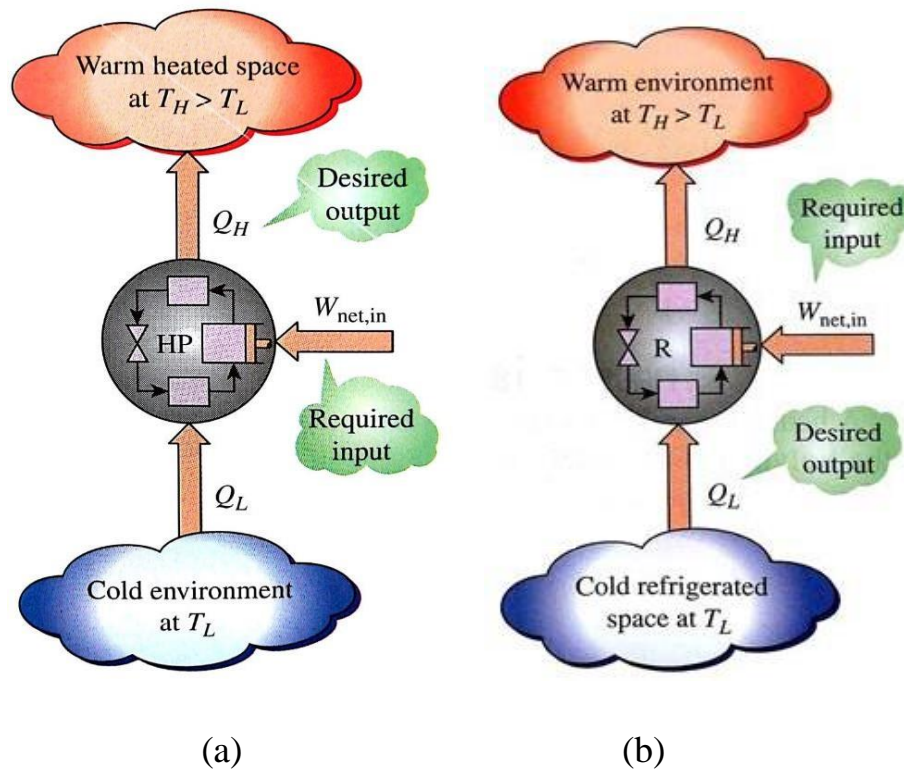


Figure 2-4 (a) The objective of a heat pump is to supply the heat  $Q_H$  into the warmer space. (b) The objective of a refrigerator is to remove the heat  $Q_L$  from the cold place [36, pp. 284-285].

### 2.6.2 Heat pump components

A heat pump consists of four main components, namely compressor, condenser, expansion valve, evaporator, and refrigerant [36]. Figure 2.5 shows the basic vapor-compression cycle for a heat pump which consists of the following parts:

**Compressor:** This is the most important part of a heat pump. When the compressor starts, it absorbs the refrigerant from the evaporator at a low temperature and pressure, raises its temperature and pressure by compressing it, and finally pushes it through the exhaust valve, in a vapor form and at a high pressure and temperature, into the condenser.

**Condenser:** This is an important component of the heat pump that produces the heating effect and is used to deliver the heat to the desired location. The condenser cools the refrigerant by transferring the heat to a warm space—a hot temperature reservoir. It consists of copper coils.

**Expansion valve:** This is a pressure control device which rapidly reduces the refrigerant pressure coming from the condenser. As a result, the temperature rapidly reduces.

**Evaporator:** This is used to absorb the heat from a cold space. The refrigerant, which has a smaller temperature than the cold space in the evaporator, absorbs the heat energy and transforms it into a gaseous state before it enters the compressor. It consists of copper coils.

**Refrigerant:** This is usually a liquid or gaseous substance used in the heat pumps. It is the same as the refrigerant which is used in an air conditioner. It carries the heat from the evaporator, which is at a low temperature, and delivers it to the condenser, which is at a high temperature.

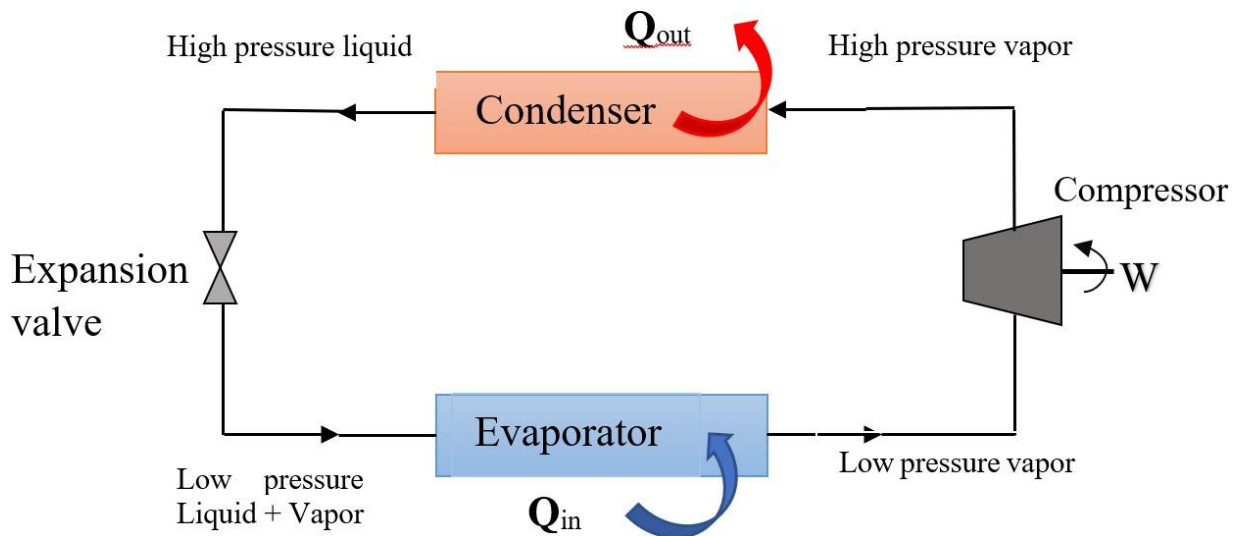


Figure 2-5 Schematic of the basic vapour-compression cycle.

### 2.6.3 Basic heat pump cycle

Figure 2.6 shows the basic thermodynamic cycle for a heat pump, where the refrigerant, as saturated vapor, enters the compressor at point 1. From point 1 to point 2, the compressor compresses the vapor that goes to the condenser (at constant entropy) with the rise in the enthalpy of the vapor. The vapor leaves the compressor at a very high pressure and temperature—a superheated vapor—at point 2. From point 2 to point 3, the condenser cools down the refrigerant and removes the superheat by cooling the vapor. The process of de-superheating as well as condensation of vapor follows the constant pressure process and enthalpy of vapor falls during these entire processes. Between point 3 and point 4, the vapor travels through the remainder of the condenser wherein the heat is transferred to a warm space and vapor gets converted to saturated liquid refrigerant at point 4.

After leaving the condenser at point 4, the refrigerant enters a capillary tube or an expansion valve, between points 4 and 5, in order to reduce the pressure created due to the process of throttling which is isenthalpic in nature. Due to the sudden decrease in pressure, there is a rapid decrease in temperature to about  $-10^{\circ}\text{C}$ . At point 5, this low-pressure refrigerant liquid enters the evaporator. Between points 5 and 1, the cold and partially vapourized refrigerant travels through the coil, which absorbs the heat energy and transforms it into a gaseous state, and enters the compressor at point 1. Enthalpy of the vapour increases during this process of evaporation. This cycle is repeated in order to produce the cooling or heating.[36],[37]. Enthalpy exchange at the terminal points represents work and heat interaction of heat pump cycle.  $Q_H$ ,  $Q_L$  and  $W_{NET}$  mentioned in equation 2.1 and 2.2 are representing enthalpy difference of  $h_2-h_4$ ,  $h_1-h_5$  and  $h_2-h_1$  respectively.

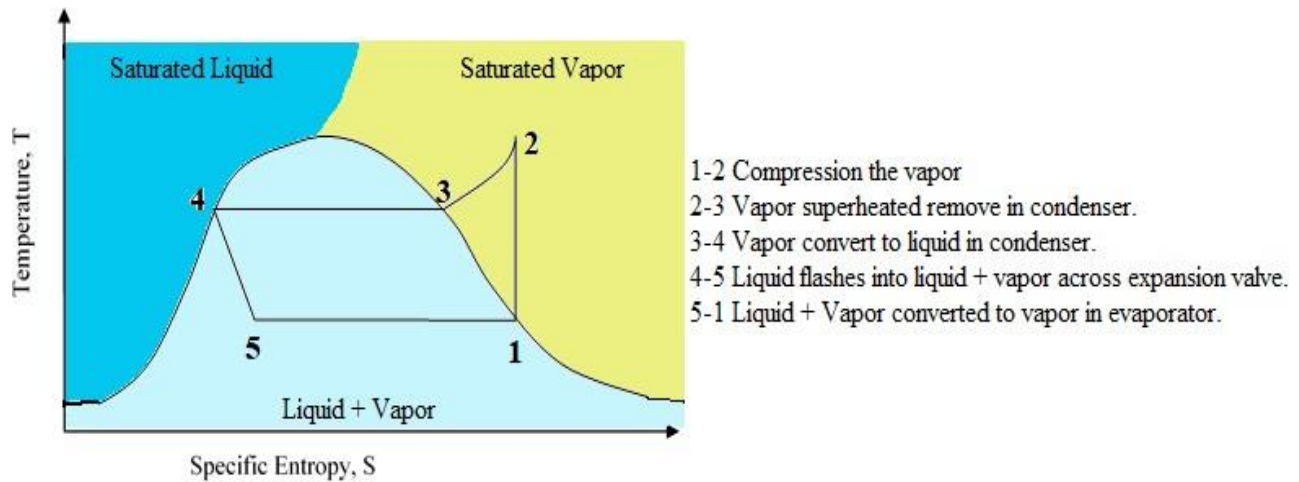


Figure 2-6 Schematic of the basic thermodynamic heat pump cycle

### 2.6.4 Performance of the heat pump

The heat pump provides heating or cooling to the space and its performance is expressed in terms of a coefficient of performance (COP). This is defined as the ratio between the power of the compressor (input power) and the amount of useful heating or cooling (output) done at the evaporator on cooling mode or at the condenser on heating mode. The COP for each mode can be expressed as follows:

$$COP_{cooling} = \frac{\text{Desired output}}{\text{Required input}} = \frac{Q_L}{W_{net}} = \frac{Q_L}{Q_H - Q_L} \quad (2.1)$$

$$COP_{heating} = \frac{\text{Desired output}}{\text{Required input}} = \frac{Q_H}{W_{net}} = \frac{Q_H}{Q_H - Q_L} \quad (2.2)$$

Where  $Q_L$  is the heat removed from the refrigerated space and  $Q_H$  is the heat reject to the environment. Thus, the higher COP the more efficient the system. For example, in the cooling mode, if the COP = 4 means the heat pump need 1 kW of electricity to extract 4 kW of heat. Heat rejection in the condenser is more than the heat absorbed in the evaporator section and thereby, it needs to work harder when in warmer conditions and less hard in cooler conditions. Thus, the COP varies on a daily basis. This is why it can be efficiently measured by a Seasonal Performance Factor (SPF), which is defined as the

ratio of the heat rejected by the heat pump to the workdone by the compressor over the heating season [32].

Moreover, the COP varies along with the types of heat pumps, i.e. air source and ground source heat pumps. An ASHP absorbs heat from the air while the GSHP absorb heat from the ground. To evaluate the seasonal performance of the heat pump in hot/dry regions, the term used is called the SPF or Seasonal Performance Factor, which is the ratio of seasonal heat generated to the seasonal electricity consumed by the heat pump. During summer, the SPF of the ASHP is less than 2.5 due to the reduced heat capacity of outdoor air, but in the winter, it may be as high as 4. For ground source heatpumps, the SPF is always about 4. Thus, ground source heat pumps are much more efficient for the heating season.

In the past, CFCs were used as refrigerants in heat pump, which eventually wee phased out due to major damage to the ozone layer when released into the atmosphere and they were replaced with hydrocarbons, such as R 134a and R410a with similar thermodynamic properties with insignificant ozone depletion potential but they had a problematic global warming potential. Recent refrigerants used are difluoromethane R32 and isobutane R600A, which do not deplete the ozone and are also far less harmful to the environment.

## **2.7 Ground Source Heat Pump Technology**

The ground source heat pump (GSHP) technology is based on the natural differences between the external temperature of the air and the underground temperature. The temperature below the ground surface, at a depth of more than 10-15 m, is relatively constant. Subsequently, the temperature increases by about 3 °C per 100 m of depth, depending on the geographical location[38]. Thus, the ground temperature is warmer than the air in winter and colder in summer. Temperature as a function of depth is shown in figure 2.7

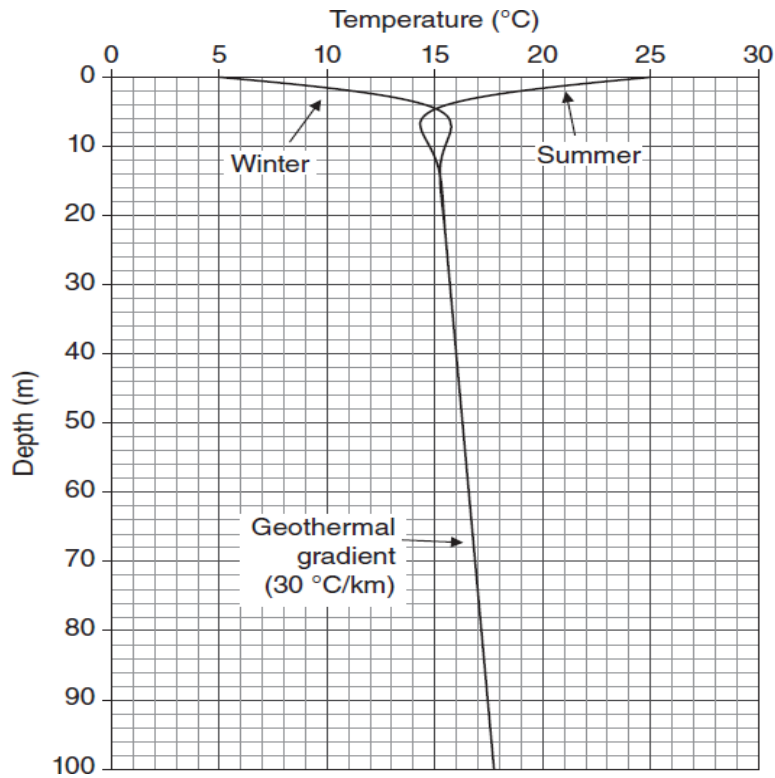


Figure 2-7 Temperature as a function of depth (0–100m) below the Earth’s surface [32,p. 65].

## 2.8 Principle of Operation of GSHPs

Ground Source Heat Pumps (GSHPs) are systems that consist of the following three major elements:

(a) the ground loop is contained in the HP which is known as the ground heat exchanger, GHX. (b) a heat pump unit, and (c) the heat distribution system. Figure 2.8 shows a schematic representation of the operation of a GSHP system.

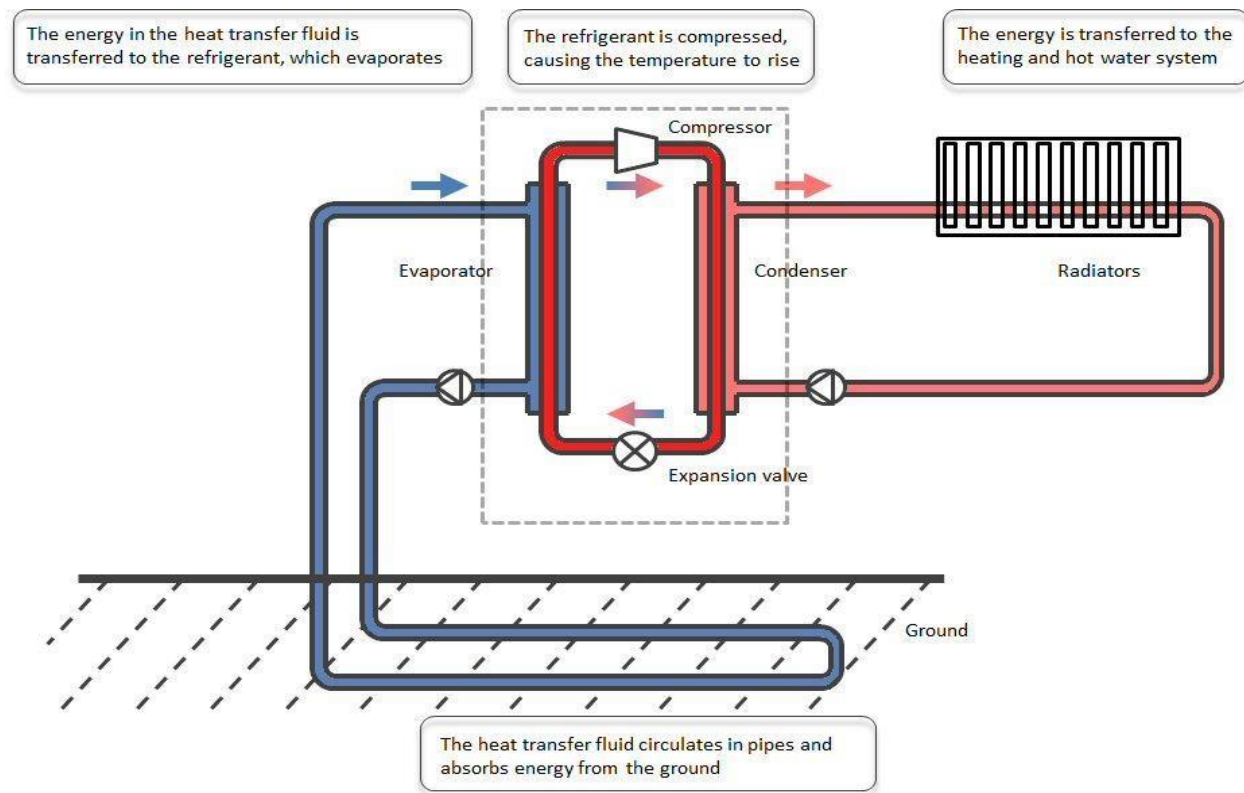


Figure 2-8 Schematic of the basic ground source heat pump system components [39].

### 2.8.1 Ground loop of GSHP

The ground loop is formed by the connection of a network of pipes which are located either underground or underwater. The entire setup of the ground loop is always located outside the building footprint. The main function of a ground loop is collection or rejection of heat from the ground. This is accomplished when the circulating fluid is circulated through the pipes [40]. There are several types of ground loops, e.g. closed loops, open loops, and vertical or horizontal loops. Section 2.10 provides a comprehensive explanation of the types of ground loops.

### 2.8.2 Heat pump of the GSHP

A heat pump is an electrical device that extracts heat from one place and transfers it to another. It transfers heat from a fluid with low temperature and passes it to another fluid at a very high temperature. As an example, one can consider using a heat pump to heat a swimming pool. Heat, collected in the



ground, is transferred to the swimming pool using a refrigerating medium where the ground is used as the heat source. The discharged heat is transferred from the swimming pool to the ground in the cooling mode.

### **2.8.3 Distribution system of the GSHP**

The major function of the distribution system is to distribute heat within the application as well as remove heat from the application. Distribution systems can have forced the air system or radiant heating system and in either case, it has a number of important components, e.g. Ducts, Plenums, and Fans. Moreover, the efficiency of the HVAC system is affected by the design quality of the distribution system.

## **2.9 Factors Affecting GSHP Operations**

Two prominent scientists, Eskilson (1987) and Hellstrom (1991) [32], gave a comprehensive explanation of the thermal analysis of Ground Heat Exchanger (GHX) and provided essential benchmarks regarding their performance. According to Chiasson [32], the five essential parameters are:

- i. Thermal conductivity of the soil or rock
- ii. Undisturbed temperature of the earth
- iii. The mass flow rate of carrying the heat liquid
- iv. Thermal resistance of the borehole
- v. The extraction and rejection rate of heat

The thermal conductivity is directly proportional to the thermal performance of the GHX, with granite being a better thermal conductor than the clay soil. For the last 20 years or so, research is being postponed with the aim of determining the thermal conductivity of the Earth which can be used for

simulation and design tools.

Borehole thermal resistance provides another parameter for measuring the performance of GHX. A number of components are used for describing the borehole thermal resistance, such as the rate of heat transfer of the liquid and its composition, the diameter, the material used in the heat exchange pipe, the material of the grout, and the structure of the flow channel. Length of ground heat exchanger is decided by the thermal resistance. As the thermal resistance decreases, the rate of heat transfer between the conducting fluid and soil increases and the length of the heat exchanger decreases and thus minimum thermal resistance leads to cost reduction and efficient operation.

The undisturbed temperature of the Earth is another parameter in the performance measurement. The rejection and extraction of heat is quite opposite to that on the Earth's surface and the borehole depth is directly proportional to the difference between the temperature of the Earth and the temperature of the design heat pump.

The nature of the heat rejection and extraction is also a parameter for measuring the performance of GHX. At low temperature, the efficiency of the heat pump gets affected because the performance of the heat pump degrades with a fall in atmospheric temperature as less heat is available for the heat pump to boost. This method is described with regard to a residential system in International Ground Source Heat Pump Association (IGSHPA) standard [41]. In the case of a commercial system, at the lowest cost, the design tools take the monthly and hourly load apart from the yearly load into consideration, for a period ranging between 10 to 20 years. This method is discussed in further details in the ASHRAE handbook [42].

The last parameter in the performance measurement of GHX is the bulk flow rate of the heat exchange liquid. This is mainly used in the calculation of the borehole thermal resistance. The rate of the flow should be maximized and the flow is turbulent so that it supports a smooth flow of energy. The heat

transfers the liquid as natural water. However, in cold climates, the liquid comprises of propylene glycol or methanol, which is an aqueous solution of antifreeze nature. The bulk flow rate has to balance well with the pumping power of the heat pump and the optimization is required between the point of maximum system performance in terms of the COP and pumping power. As per the ASHRE 2015 benchmark, the recommended value of the pumping power is less than 0.05hp/ton of thermal load or  $0.01\text{kWe/kW}_{\text{ton}}$ .

## **2.10 Types of Geothermal Heat Pump Systems**

There is a wide range of available GSHPs which are suitable for different applications. GSHPs are mainly classified as being either closed loop or open loop.

### **2.10.1 Closed loop system**

Heat transfer in the closed loop systems do not have any direct contact with the ground and the loop fluid for the heat transfer is enclosed. Furthermore, there is direct contact of the closed loop system with the ground. It is only through the installed pipes that the heat transfer occurs [43]. The closed loop is broadly classified into different types—one is a vertically closed loop and the other is a horizontally closed loop. Slinky or spiral closed loops, in addition to closed pond loops, are some other types of closed loop systems. For each of these closed loop systems, the configuration of the system, the space requirement, and the installation depths vary.

#### **2.10.1.1 Vertical closed loop**

For the installation of a vertical closed loop, ground boreholes have to be constructed as they contain vertically oriented heat exchange pipes. For residential applications, a borehole, ranging from 45 to 100 meters in depth, is usually required. And for industrial application, a 150-meter- deep borehole is usually constructed [44]. Thermal contact has to be maintained between the heat exchanger and the borehole wall. The entire gap in the borehole, between the pipes and the ground, can be filled with

grouting material that has a high thermal conductivity. In the heat exchanger, the fluid is circulated and transfers the heat from the ground to the heat pump and back to the ground again. This process leads to the exchange of heat between the bore hole and the ground surface. Based on the type of the heat exchanger and grouting material that is employed, the thermal efficiency of the BHE varies. Table 2.1 represents the different grouting material and their conductivity [32]. Properties required from the grouting material is that it should protect the groundwater contamination, enhance heat transfer, easy to use and have an affordable cost.

Table 2.1 Thermal conductivity of different grouting material [32]

Material	Thermal Conductivity W/mK
Bentonite (20- 30% Solids)	0.73-0.75
20 % Bentonite 80 % Silica sand	1.47-1.64
15 % Bentonite 85 % Silica sand	1.00-1.10
30 % Bentonite 70 % Silica sand	2.08-2.42
Graphite – Bentonite mixture	2.10-2.77

Moreover, the performance of the GHE is based on the initial ground temperature. The hydraulic and ground properties also impact on its performance. In general, the vertical loop system is more advantageous for larger applications but it has the major disadvantage of a large installation cost, which is higher than the cost of the horizontal closed loop.

### 2.10.1.2 Horizontal closed loop

The heat exchange well contains a horizontally installed loop of piping. It has to be installed 15 feet below the ground surface due to a lot of heat generated underneath which is transferred through the pipes to the surface for heating process. A horizontal closed loop is considerably the most cost-effective and cheaper than a vertical closed loop and its installation reduces the cost by up to 30% [45]. Several factors impact on the reduction in the cost of the horizontal closed loop:

- i. Poor geology: larger collector field is required.

- ii. Horizontal collector protection: The horizontal collector has to be protected from sharp stones. And underground features that can damage it.
- iii. The amount of time spent for excavating trenches has to be considered.
- iv. Landscaping, such as leveling the land, is also one of the key factors.

These aforementioned factors affect the cost of a horizontal closed loop. However, the exact cost can be calculated only after its installation.

### **2.10.1.3 Slinky closed loop**

Slinky closed loops, or spiral loops, are horizontally oriented loops installed within shallow trenches. Hence, it resembles a conventional horizontal loop. Piping in the slinky closed loop is laid out in the form of circular loops. These loops require a smaller area as compared to a horizontal closed loop. Moreover, at the end of a slinky closed loop, a return pipe is attached to the heat pump. However, it requires a huge amount of piping in order to carry the heat. Further, Spiral GHX can be fixed vertically as well as horizontally. Another disadvantage of a spiral GHX is that the heat transfer is low. However, slinky loop supports high pumping due to the added pipe length and this is the main advantage of its use [46].

### **2.10.1.4 Closed pond loop**

The geothermal long pipe is defined as a closed pond loop. It is attached and placed inside a lake or a similar waterbody, since it has to be completely immersed in water. Pond loops have to be installed in such a way that they must have eight feet of water above it. Only ponds or lakes which have a larger volume can be used for its installation. Coils of the pond loop are connected to the skid to facilitate heating process and installed underwater to prevent them from freezing. The exposed pipe is buried by digging a trench and placing the pipe within it.

### 2.10.2 Open loop systems

For large commercial applications, an open loop system is frequently used. This system directly interacts with the ground. Under groundwater or surface water is used as a direct medium for the heat transfer in open loop systems. Moreover, it requires a huge amount of groundwater for its operation; as a result, it is not suitable for all kinds of locations. The water from the lake or groundwater is directly extracted and sent to the heat exchange pipe. After the heat exchange, water is discharged to its source through a separate pipe. The only key factor regarding the installation of an open loop system is the sufficient availability of groundwater. Hence, its installation cost is very low. Open loop systems have a high coefficient of performance. And, moreover, they are environment friendly as the heat carrier medium is in direct contact with the ground.

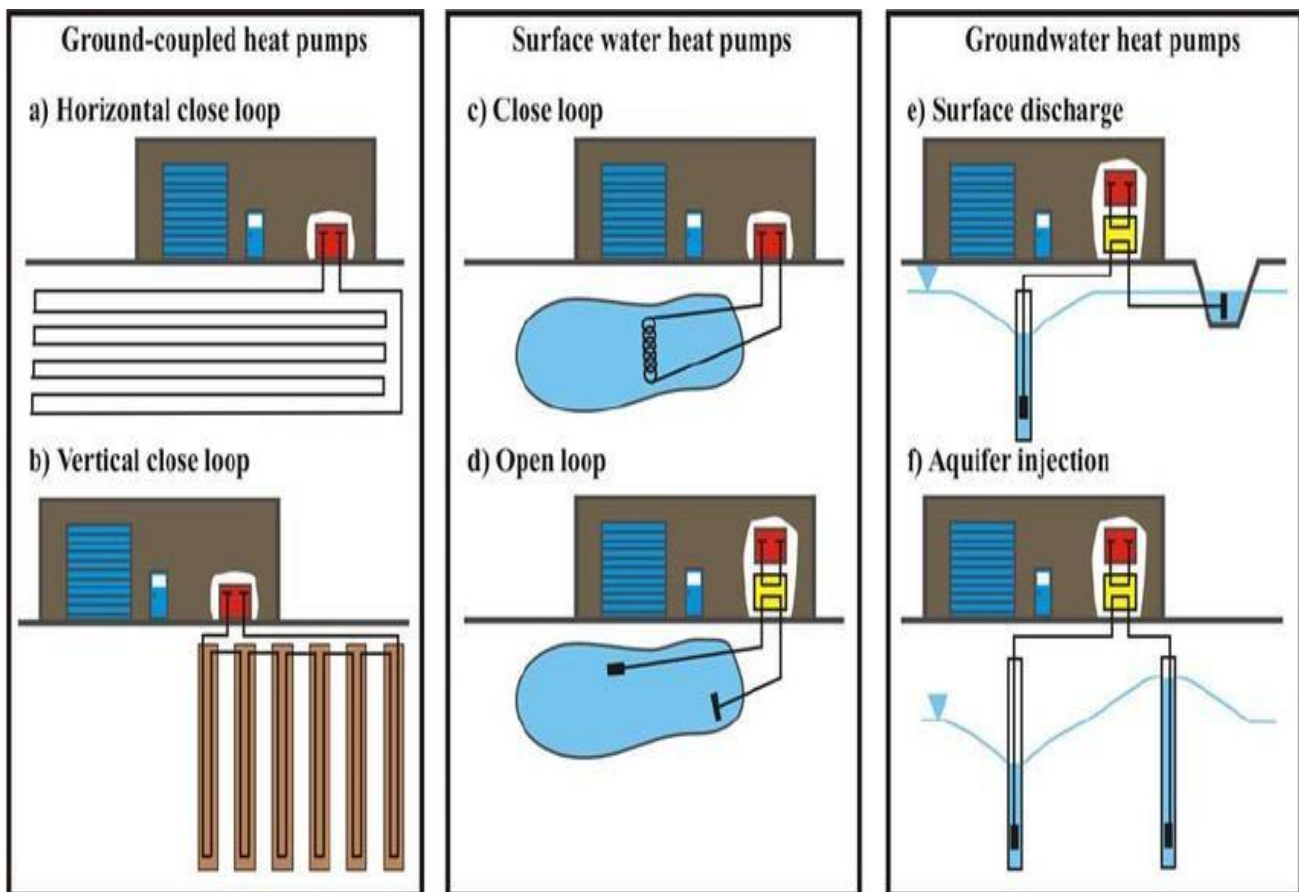


Figure 2-9 Schematic of the different types of geothermal heat pump systems [40].

## **2.11 Ground Source Heat Pumps in Hot and Dry Climates**

Geothermal energy has various applications with regard to power generation, heating and cooling, along with industrial and agricultural applications [32]. Geothermal power can be classified into three categories - low depth, intermediate depth, and shallow depth -depending on the resource temperature and regardless of its distance from the Earth's surface. The geothermal heat pump (which pertains to shallow depth) has limited application in the Middle East and North Africa (MENA) countries and therefore the following studies have evaluated the heat exchange process in MENA countries and different hot regions like Arizona, USA.

### **2.11.1 Saudi Arabia**

Said et al. [47], investigated whether ground-based condensers might be used to support air-conditioning systems in the Kingdom of Saudi Arabia. This was done by running thermal response tests and as an outcome the effective thermal resistance and thermal conductivity were calculated using the line source model. The study found that there were significant differences between the ground temperatures and the ambient temperature with 12°C being recorded and this temperature difference is constant below 30m depth which is a favorable factor for the performance of the GHX. Also, a cost analysis was undertaken, which indicated that the use of ground source heat pumps in Saudi Arabia would result in about 28% energy savings. However, this was deemed to be not economically viable due to the low electricity prices prevalent in the country due to government subsidies and high drilling costs.

### **2.11.2 Erbil, Iraq**

Due to the wide and varied climatic and soil conditions encountered in Saudi Arabia, a literature review of these conditions in Erbil, Iraq was performed. Erbil has more northern latitude than Saudi Arabia but it closely resembles the dry mountainous region of Hejaz which forms a natural barrier running

parallel to the Saudi coastline from Yemen in the south to Jordan in the North. Amin [48], investigated the energy storage technology used to save energy for a school building in Erbil, Iraq. The assessment covered a borehole thermal energy storage system in an underground structure for large quantities of heat and stored energy in the soil and rocks. The Earth Energy Design 2.0 PC-Program was used for the borehole design and the test building consisted of six class rooms within the school with a total build area of about 1200 m<sup>2</sup>, the height of the room was 3 m and a total volume of 3600 m<sup>3</sup>. The annual mean temperature was calculated to be 20.95 °C and the method that determine the temperature variation after on hour was used to calculate the energy demand above the base temperature 17 °C for heating and 20 °C for cooling. The required maximum power demand for heating was calculated at 158.4 kW and the maximum power demand for cooling the building was 211.2 kW based on the climatic yearly extremes experienced in Erbil. The months from November until April were used for calculating the total heating demand for the school building, and this was calculated to be 254,52 MWh. The months of May until September were used for calculating the total cooling demand for the building, and it was calculated to be 10MWh. The month of October had a mild climate and therefore required no heating or cooling. This study found that the borehole depth and borehole spacing were the main factors that affect the performance of the borehole thermal energy storage system.

### **2.11.3 Tunisia**

Naili et al. [49] conducted the first evaluation of the potential for geothermal energy in Tunisia, which featured the evaluation of a horizontal ground heat exchanger, in Bork Cedria, in the north of the country. A heat transfer coefficient was derived based on temperature readings taken at different locations below the surface. The loss of pressure at each length of the heat exchanger was determined based on the calculated mass flow rates. Using a room with a surface area 12 m<sup>2</sup>, it was established that a GHX system consisting of 25 m of pipeline located a meter underground could account for 38%



of the cooling required for that room. From this, it was concluded that a GHX could provide a novel cooling mechanism for buildings, thus demonstrating the scope that existed for Tunisia to become a leader in the development of geothermal heat pumps.

#### **2.11.4 Qatar**

Kharseh et al. [50], analyze the effect of global climate change on ground source heat pump systems in a different climate by considering thermal quality of the building envelope (TQBE) on the thermal performance of GSHP. Two buildings that were modelled in three cities with three different climates and these were taken as references. One building was in Stockholm, Sweden in a cold climate, the second was in Doha, Qatar in a hot climate, and the third city was in Istanbul,

Turkey in the mild climate. The two buildings were modelled according to the climate experienced in the area. In general, a 144 m<sup>2</sup> modelled house has a lifespan of about 50 years or more. In the study, the weather information in 2014 was used and the data for 2050 was predicted by using the Meteonorm software. The cooling and heating loads were estimated using the HAP software, and the Earth Energy Designer (EED) software was used to design the borehole heat exchanger. In the study, by the year 2050, the mean temperature will increase in each city. The temperature will rise by 1.3 °C in Stockholm, 0.9 °C in Doha, and 1.8 °C in Istanbul and the annual energy consumption of GSHP systems have a significant impact in the cold and hot climate.

The projected calculation shows that the impact of the warming on the heating load will be reduction by 10 % in cold climates and 55 % in hot climates and the effect on the cooling load will be increased by 10 % in cold climates and 34 % in mild climates by the year 2050. It is anticipated that change in annual energy consumption of the GSHP system ranges from -8.5 % in cold climates to +18.7 % in hot climates by the year 2050

### **2.11.5 Egypt**

An experimental study into the thermal performance of an Earth-Air Heat Exchanger (EAHE) system was used in Egypt by Serageldin et al. [51] and experimental data was employed to validate the simulations using the ANSYS Fluent and MATLAB codes. In that study, investigations were carried out into five parameters for the pipes that were used, and these were diameter, length, spacing, materials used and fluid flow velocity. The following results emerged:

- Increases in pipe diameter caused a decrease in outlet air temperature.
- Increases in fluid velocity caused a gradual decrease in outlet air temperature.

For ground source heat pumps to be used with confidence in hot/dry climates, certain critical design factors have to be achieved. If the underground heat exchanger (in this case an earth—air exchanger (EAHE)), can reduce the temperature of the incoming air to that of the surrounding soil at the selected depth, then the temperature difference between the ambient outside air in the hottest months and the air being returned will be suitable to allow a GSHP to be used.

### **2.11.6 Palestine and Jordan**

The first GSHP system was installed in Palestine in the city of Ramallah - Mediterranean climate zones with a 23 kW cooling/heating capacity and 10 boreholes with 70m depth [52]. This pilot project achieved a COP of 4.2 in heating and 14.5 EER in cooling. However, it is important to note that the main design conditions for this project were the outside temperature in the summertime, which was 31°C, and the soil temperature was 18.3 °C. This project proved the feasibility of the GSHP system, which reduces the operating costs by 67% compared to conventional boilers for heating and air-source split units for cooling, and the payback period was 4.2 years. Likewise, in Jordan [53], the American University of Madaba has installed a large GSHP system with an approximate capacity of 1.7 MW and 1.4 MW for cooling and heating, respectively, and it serves an educational building. 11 422 boreholes

of depth 100m were connected to 26 heat pumps units to meet the building demand for the cooling and heating where the operation hours are from 7 am to 5pm for approximately 330 days per year. The results show that the University saved 200,000 kWh electricity and 100,000 litres of diesel fuel per year. The system COP were 6 and 4.5 for the heating and cooling, respectively.

### **2.11.7 Algerian**

Belatrache et al. [54] investigated the effect of the length of the buried pipe and the air flow rate of the horizontal Earth-Air Heat Exchanger (EAHE). The model and experiment on the EAHE contain primarily a PVC pipe of length 45m and at a depth 5m, and the simulations used climatic conditions of the Algerian Sahara. In the study, the air temperature inside the EAHE drops significantly at a depth 5m from 46 °C until it achieves the soil temperature at about 25 °C and the maximum temperature difference in July between the ambient temperature and the buried pipe temperature is about 20.7 °C. This indicates the possibility of using the GSHP in such conditions.

### **2.11.8 Florida and Arizona, USA**

Despite the increasing use of GSHPs in cold regions in the USA, GSHPs are a relatively unfamiliar technology in hot and humid climates, such as Arizona and Florida. Zhu et al. [55] investigated the feasibility of using GSHPs in Florida. In this study, a commercial building in Pensacola, FL with GSHPs that have been in operation since 2010 and thus was used as the case study. Actual data has been collected to determine the life-cycle cost, comparing a deterministic life cycle costing method with a probabilistic life cycle costing method for GSHP and conventional systems. The study has shown that installing GSHP to be more feasible than using a conventional system, from a life cycle perspective.

On the other hand, Tambe [56] investigated the feasibility of using GSHPs for a small office building in Phoenix, Arizona. This master's dissertation presented a critical review, as well as a detailed

evaluation, of the energy performance and technical feasibility of both a vertical and a horizontal closed loop heat pump in Phoenix. The study showed approximately 40% energy savings from the GSHP system, compared to the ASHPs. In addition, there was a significant difference between the dry soil and saturated soil condition. The saturated soil decreased the length of the GHX by 26% and 25% for the horizontal and vertical ground source heat pumps, respectively. However, the payback periods were found to be 2.3 – 4.7 years for the horizontal system and over 25 years for the vertical system, implying that the option of the vertical system would not be economical.

## **2.12 GSHPs in Cold Climates**

GSHP systems are mostly used in a heating mode in residential and commercial buildings. The use of GSHP systems in cold climates such as those of North America, Scandinavian countries and China has been discussed for decades, to use GSHP in many countries needs more data about weather and geological zones. For example, in China, Zhihua et al. [57], investigated the feasibility of using GSHP in an office building in five different climate zones based on the COP value. The e-QUEST and TRNSYS were employed in this study, and the results show that in the very cold and cold cities the GSHP is applicable. In contrast, in the hot and warm cities, such as Guangzhou, the GSHP system is not feasible due to the thermal imbalance between the cooling and heating seasons.

However, the underground thermal imbalance issue is clearly demonstrated in a region with a harsh climate, such as Alaska, when more heat is extracted from the ground, or in Arizona, when used in a cooling mode, with more heat being rejected to the ground. The thermal imbalance issue may lead to a system failure after long-term running. Several studies have investigated the thermal imbalance issue, in order to increase the performance of GSHP. You et al. [58] proposed a solution for performance degradation of a ground-coupled heat pump system (GHCP) in cold regions due to the imbalance in heat exchange between the ground and the ambient environment. This work describes the use of a heat

compensation unit with a thermosyphon (HCUT) for compensating the decrease in soil temperature during the winter by rejecting the appropriate amount of heat, which is extracted from the ambient air during the summer season. DeST software was used to simulate a heating and cooling load model of a ten-floor office building of 16,000 m<sup>2</sup> in Harbin, China. Then, the performance of the HCUT-GCHP system developed was measured by simulation using TRNSYS. The developed system, while consuming some energy for pumping heat to the ground, provided a 15% energy saving as compared to a traditional boiler and split air-conditioner, and could be used to balance the heat in the ground [59].

On the other hand, a study by Eslami-nejad & Bernier [60] showed the effect of frozen ground in thermal boreholes. The study described the problem and developed a 1-D model, with some assumptions to account for the multiple layers of ground and phase change of ice covered by the use of effective capacity. The results from this model were compared with the experimental set-up outcome, and no significant difference was found. Based on the newly proposed model for the borehole, a different configuration was made, and the results were noted. It was found that the configuration using saturated sand rings provided a promising steady borehole wall temperature of 0°C for several days, even with a maximum heating setup without a saturated ring. The use of solar energy in melting the ice and recharging the saturated rings reduced the borehole length by 38% of small thermal conductivity ground [60].

Research by Garber-Slaght [61] studied the effect of ice formation, freezing ground and cold weather on a ground heat pump system in places such as Alaska, where the cooling load is estimated to be 400 hours per year, while heating hours per year is 7509. The paper covers a study period of over ten years, and features ground with permafrost, so that the causes behind the performance degradation of GSHPs can be found, and future designs can be refined so that they are suitable for such cold environments. With the help of a numerical simulation of the finite-element model and the pseudo-heat capacity

method, over a finite number of the years, within a small range of temperatures below 0 °C, a simulation over ten years was produced. An analysis of three years' data indicated a 14% decline in COP in the system; further analysis suggested that five years would be required to level out the decline, with COP not falling below 3.4.

The paper by Tu et al. [62] presents a refined resistance capacitance RC model for calculating the effect of freezing soil and ice cover on a ground heat pump system. In this work, a thermal resistance and capacity model was used to validate the effectiveness and authenticity of the model. The RC model was used to model the soil and the borehole, and to generate a nodal equation for the borehole. In addition to consideration of effective heat capacity and latent heat capacity, a module was developed to describe freezing conditions over a range of temperatures. Finally, the results obtained showed that 30% of the heat rise was solely due to the phase change in the soil, which could reach up to 75-80 W/m.

A study by Wu et al. [63] featured different heating system solutions in cold regions. The work comparatively analyzed the two major types of ground source heating pumps (GSHPs) - a Ground Source Absorption Heat Pump (GSAHP) and a Ground Source Electrical Heat Pump (GSEHP) - in the coldest cities, such as Harbin. The study provided solutions regarding energy efficiency, the imbalance ratio (which is the ratio of heat rejected to the ground to heat absorbed) and soil temperature (Wu et al., 2013). GSAHP, when used for both heating and cooling, was found to be more appropriate and energy efficient, in the long run, in the coldest cities, but when used for heating only, the soil temperature was found to increase by 4-6 °C in 10 years than that of using GSEHP.

Similarly, a paper by Slaght et al. [64] identified the major problems regarding the use of a ground heat pump system in cold regions such as Alaska, and, in addition, set some of the criteria needed to produce the most accurate and applicable outcome. The document focused particularly on two issues: the need for better data on the effectiveness of GSHPs, and the need for better information on the installation cost

of GSHPs. The work was carried out in Fairbanks, Alaska, and the findings were presented under three categories: heat delivery system, site considerations and costs. The work concluded that GSHP can be an efficient heating system, yet the long-term effects remained to be studied; the use of a baseboard heat delivery system was not suitable when using GSHP; the site must be such that there is sufficient solar energy; the cost of electricity and of heating fuel impacts on the cost-effectiveness of the GSHPs.

Present work is for Saudi Arabia and this does not resemble cold climate conditions presented in this section, however exhaustive parametric investigations have been performed in the cold climatic conditions and this is useful to decide the appropriate parameters and work methodology. Also, to demonstrate that the system can work in extreme climates.

### 2.13 Large-scale GSHPs

Over the years, the use of the large pump system for heating and cooling purposes has spread in several countries, especially in Europe and North America, where the cold climate is the prevailing climate. The operating principle for large scale commercial GSHP systems is exactly the same as that of the small GSHP systems. The main difference between the two systems is the vast land area required to operate large systems, which hinders its use in a narrow area. So far, there is no agreement on classifying the size of large and small systems. The classification of the size of large systems varies from one organization/institution to another. The Massachusetts Department of Energy Resources (DOER) for example, classifies the size of GSHPs based on system capacity as shown in Table 2.2 [65].

Table 2.2 Size classification of ground source heat pumps

Technology	Small	Intermediate	Large
Ground source heat pump	Output capacity less than or equal to 134,000 Btu per hour ( $\approx 11$ ton)	Output capacity between 134,000 and 1,000,000 Btu per hour ( $\approx 83$ ton)	Output capacity greater than or equal to 1,000,000 Btu per hour ( $\approx 85$ ton)

Another industry organization such as ASHRAE has standard built on many factors to ensure the adequate design of GSHP meet accurate, performance expectations and decrease the maintenance issues. One of these factors is Equipment Eligibility whereas the rated operating COP and EER of the heat pump unit must be not less than 3.6 and 17.1 respectively. Table 2.3 Illustrate the minimum COP and EER heat pump unit requirements for a small GSHP system [65].

Table 2.3 Minimum COP and EER requirements for a small GSHP system.

Type	Cooling EER	Heating COP
Closed Loop Water to Air	17.1	3.6
Open Loop Water to Air	21.1	4.1
Closed Loop Water to Water	16.1	3.1
Open Loop Water to Water	20.1	3.5

In general, the factors that affect the performance of small GSHP (the subject of chapter 6 in this thesis) are the same as those that affect large GSHP, such as the thermal conductivity of the soil and the soil temperature. Many monitoring studies have been implemented to evaluate the performance and installations of large GSHP system to Increased knowledge in GSHP technology. Rees et al [66] used one-year data collected from a large educational building at De Montfort University Leicester, UK. This building has 15,607m<sup>2</sup> required 360 kW and 330 kW for cooling and heating load, respectively. The GHX consisted of 56 boreholes and 100 meters depth, and the ground thermal conductivity was estimated to be 3.1-3.3 W/mK. High-quality data collected from monitoring the GSHP system for one year showed high COPs range from 3 to 6 based on the time of the year. Jingyang Han et al [67] investigated the thermal performance of a GSHP system compared to Solar energy coupled ground source heat pump system (SGSHP) for the large Library building located at Hebei University of Science & Technology, Hebei, Shijiazhuang, China. This building consists of eight floors with a total area of 49,000 m<sup>2</sup>. For the purposes of this analysis, three large heat pump units join to 1200 borehole with 100 m depth. The results show that the GSHP is more cost-effective for long-running compared to



SGSHP for the large building. Furthermore, in term of energy saving, it has revealed that 1131 metric tons of standard coal and 4641 metric tons of CO<sub>2</sub> emission can be saved.

Zhai and Yang [68] investigated the efficiency of GSHP compared with ASHP system operating in cooling dominates the region in Shanghai, China. Two large heat pump unit with a total cooling capacity of 500 kW installed under the university archives building joint to 280 boreholes with 80m depth to meet the cooling demand of 8000m<sup>2</sup>. It was deduced that the average COP under the typical weather condition of Shanghai for cooling and heating are 5.4 and 5.2, respectively.

## **2.14 Conclusion**

This chapter has provided an overview of the literature regarding ground source heat pump systems (GSHPs). An overall history of energy, the demand of renewable energy, types of geothermal energy, and the existing GSHP technology has been reviewed, and the various aspects of GSHP have been discussed. Also, this chapter reviews the performance of GSHP, and the use of this system in cold and hot/dry climates. Finally, at the end of the chapter several case studies for large scale GSHP systems are presented showing the advantages and ability of using GSHP systems.

From the above review, it can be seen that the use of ground source heat pump (GSHP) systems in cold climates, such as those in parts of North America, Scandinavian countries and China has been discussed for decades. However, hot and dry climates are encountered in vast regions across the globe but, unfortunately, not much research has taken place in the use of GSHP systems in hot and dry regions. This thesis aims to investigate the feasibility of using GSHP systems in hot and dry regions, and Saudi Arabia is an example. Therefore, we are now in a good position to conduct such an investigation as there is now good data on the climate and importantly on the underground temperature in this region. This thesis now uses this to examine the engineering and economic viability of these systems compared to the ASHP predictions in these conditions.

## Chapter 3: Ground Source Heat Pump Modelling

---

### 3.1 Introduction

A 'model' can be defined as a physical or a mathematical representation of an actual system. A model may help to explain a system and to study the effects of different components, and to make predictions about system behaviour. A numerical model is the best way to break everything down to an elemental level, with a view to reconstruct and predict how the system would behave under different conditions. One of the fundamental tasks in the design of a reliable GSHP system is the proper sizing of the GHX length. Over the past two decades many research efforts have produced several methods and commercially available design software tools for this purpose [69]. This chapter aims to briefly summarize the development and application of GSHP modelling in terms of methods and software.

### 3.2 Vertical Ground Source Heat Pump System Modelling

Over the years, many analytical and numerical models have been developed to estimate the heat transfer capacity of GSHP system. All of these models are based on the principles of heat conduction and rely on some estimate of the ground thermal conductivity and volumetric specific heat. These parameters are perhaps the most critical in the system design, yet adequately determining them is often the most difficult task in the design phase.


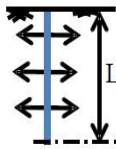
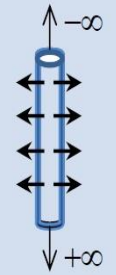
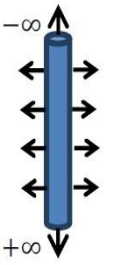
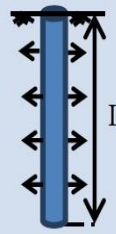
The effectiveness of the GSHP system is dependent on the size of GHX loop which is considered as the most expensive component of the GSHP system [70]. Undersized GHX lead to system failure due to accumulative heat in the soil around the heat exchanger. In contrast, oversized heat exchangers lead to high initial installation cost affecting the GSHP system's competitiveness with other traditional systems. Hence, for the mitigation of the cost of the GSHP system for the installation and optimum design, along with the reducing of the length of the GHX, it is essential to do further research

about the performance of GHXs [71]. In order to determine the temperature of the carrier fluid, a mathematical model is essential. This calculation helps to determine the circulation between the heating pumps and the GHX for different operational conditions. It also helps to determine the evaluation of different GSHP systems [72].

Two different zones are used in the analysis of the heat transfer process of GHXs. One of them is outside of the GHX, which is surrounding area such as rock or soil, and the other is the inside zone of the GHX, which includes grout material, U-tub pipes and fluids circulating inside the pipe [73]. Many mathematical calculations have been implemented in order to determine the transfer of the transient heat from the outside zone of the GHX [72]. The classification of the models can be done in two ways - numerical models and analytical models. The analytical model is generally based on cylindrical heat source theory and infinite line sources theory [74]. From the simulation point of view, analytical models are based on the line source model (LSM) and cylindrical source model (CSM), which are widely used to determine the thermal disturbance resulting from liquid circulation in the GHX. Table 3.1 showed the development in analytical models over the years [75].

In recent decades, numerous researchers monitored and simulated the ground source heat pump performance to investigate the elements that affect the heat transfer in the ground heat exchanger. These modelling approaches are beyond the scope of this thesis because this work emphasises simulating the GSHP system using the TRNSYS and GLD software, and not using mathematical/ analytical models' approach such as the 3D heat transport model or the finite element matrix assembly technique. Therefore, in this chapter, it will be sufficient to mention the main methods used in the design of GSHP. The various analytical models are described below.

Table 3.1 The main analytical models' approach for GHX.[75].

Heat source models		Analytical solution
Infinite line (Ingersoll et al. 1954)		$\Delta T(r, t) = -\frac{q_l}{4\pi k} Ei\left(\frac{-r^2}{4\alpha t}\right)$ $Ei(z) = \int_{-\infty}^z \frac{e^u}{u} du$
Finite line (Zeng et al. 2002)		$\Delta T(r, z, t) = \frac{q_l}{4\pi k} \int_0^L \left\{ \frac{\operatorname{erfc}\left(\frac{\sqrt{r^2 + (z-z')^2}}{2\sqrt{\alpha t}}\right)}{\sqrt{r^2 + (z-z')^2}} - \frac{\operatorname{erfc}\left(\frac{\sqrt{r^2 + (z+z')^2}}{2\sqrt{\alpha t}}\right)}{\sqrt{r^2 + (z+z')^2}} \right\} dz'$
Infinite hollow cylinder (Carslaw and Jaeger 1947)		$\Delta T(r, t) = \frac{q_l}{\pi^2 k r_b} \left[ \int_0^\infty (e^{-\alpha u^2 t} - 1) \frac{J_0(ur) Y_1(ur_b) - Y_0(ur) J_1(ur_b)}{u^2 [J_1^2(ur_b) + Y_1^2(ur_b)]} du \right]$
Infinite solid cylinder (Man et al. 2010)		$\Delta T(r, t) = -\frac{q_l}{4\pi k} \int_0^\pi \frac{1}{\pi} Ei\left(-\frac{r^2 + r_0^2 - 2rr_0 \cos\varphi}{4\alpha t}\right) d\varphi$
Finite solid cylinder (Man et al. 2010)		$\Delta T(r, z, t) = -\frac{q_l}{\rho c} \int_0^t \int_0^L \frac{1}{8 \left[ \sqrt{\pi \alpha (t-t')} \right]^3} I_0 \left[ \frac{rr_0}{2\alpha(t-t')} \right]$ $\cdot \left\{ \exp \left[ -\frac{r^2 + r_0^2 + (z'-z)^2}{4\alpha(t-t')} \right] - \exp \left[ -\frac{r^2 + r_0^2 - (z'+z)^2}{4\alpha(t-t')} \right] \right\} dz' dt'$

### **3.2.1 The line source model**

The line source model was developed based on Kelvin's line source theory (Kelvin, 1882). The line source model is usually used to describe the heat transfer process in long-term responses (days, months, years). The fluid temperature inlet and outlet of the GHX are determined to ensure that the temperature is within the design limits of the heat pump unit. In the line source model, the borehole is considered to be infinitely long, so that the heat flow is always radial and normal to the borehole the temperature of the ground surrounding the borehole at any radius and at any point at any time can be obtained. The heat flux at the source point is considered as the constant radial heat flow normal to the length of the source, and it transfers the heat from the line source to an infinite homogenous medium surrounding it. In the line source model, the geometry of the borehole is necessarily ignored, along with the thermal capacities of the fluid, pipes and grout material within the borehole. Consequently, the model is not suitable for short timescale applications where the dynamic response within the borehole should be considered [76].

Despite its limitations, the line source model has been widely used in the analysis of in situ thermal response test data, due to its simplicity and efficiency in terms of computing. Moreover, more sophisticated analytical models of GHXs have been developed, and contributions have been made to improve such models in recent decades [71].

### **3.2.2 Cylinder source model**

The cylindrical source model estimates the temperature difference between the outer cylinder surface and the surrounding soil for short operating periods of less than six hours. This short-term response is important for energy analysis and hybrid systems design. For example, the heat transfer inside the GHX constantly changes as a result of changes in the building load requirement over a short period.

The cylinder source solution assumes the borehole to be infinitely long and the ground to be homogeneous along the depth [69]. The geometry and the thermal properties of the materials inside the borehole, including the thermal mass of the fluid, were ignored and the cylinder source solution can be used to calculate the temperature distribution of the infinite ground with the initial temperature surrounding the borehole at any time. As a result of the heat transfer below the borehole, this model is not suitable for multi-annual simulations: for example, over 20 years, where the end effect becomes important and cannot be neglected.

In short, analytical models have been developed by making a number of simplifying assumptions and applying them to both the design of GHXs and the analysis of in situ test data. Both the theories (line source model and cylindrical source model) allow us to assume infinite length in infinite homogeneous medium in the case of the vertical GHX.

### **3.3 Numerical Methods**

Although analytical solutions require less computing effort, they are less suited to design and simulation tasks where one would like to take into account the varying time of heat transfer rates and the influence of the surrounding boreholes on long timescales. The complexity of the numerical models is high and is implemented through computer tools. Both analytical solutions (Cylindrical source models and line source models) are widely used in engineering applications software's [77]. The reasons for using these two models are for their simplicity and accuracy to estimate the heat transfer capacity of GHXs.

#### **3.3.1 G-function model**

Numerical modelling of GSHP considers the borehole geometry and thermal data in detail. The g-function model considers the highest development numerical solution of GHX used in many design tools for BHX, such as GLD, EED, and GLHEPRO [78],[79]. A G-function considers the temperature

change of the ground at the edge of the borehole, resulting in a heat pulse in a two-dimensional (axial-vertical) per unit length. In other words, the G-function solve the problem relating to the heat conduction in a homogenous medium by describing the relationship of temperature changes and heat fluxes of GHX fields/arrays. Basically, the G-function is hybrid approach combining analytical and numerical methods to derive response functions for pre-defined configurations of BHEs. Response factor models have been proved to be highly efficient and have been implemented in both design and simulation software. More details on the model and g-function can be found in [80], [81]. Currently, there are three popular methods for calculating the optimum length of the heat exchanger. The first method is rule-of-thumb which calculation based on experience or experimental but the output not strictly accurate. In this method, the peak cooling/heating load is the main factor in sizing the GHX. The second method is based on the ASHRAE standard, which considers the most widely used methods simplifying the calculation of GHX length. The last method is based on a computer simulation of the ground heat exchanger [74], which gave the best results and is compatible with experiential studies.

### **3.4 Simulation Software**

Variety of simulation tools are currently available in evaluating the design of the GSHP system. Design GSHPs are defined as complex objects that require a high level of expertise and knowledge in order to investigate the elements that affect the ground heat exchanger, heat pump unit and building envelope to simulate HVAC systems to achieve economic viability and comfort for the users. Building energy simulation is a powerful method for studying energy performance of buildings and for evaluating architectural design decisions as well as choices for construction materials and methods. Thus, the correct simulation software tool should be selected to simulate GSHP system interaction with their immediate surroundings to provide a comfortable working environment in various circumstances [82].

### **3.4.1 System simulation using TRNSYS**

The software package known as Transient Systems Simulation (TRNSYS) was originally developed at the University of Wisconsin and has been commercially available since 1975, following which it has now become a point of reference on a global scale for researchers, designers and engineers [83]. The software has been, and still is, primarily used in the fields of renewable energy engineering and building simulations and its main advantage is that it has a modular structure that gives the programme enormous flexibility. This flexibility enables the modeling of a variety of energy systems to different levels of complexity where users are able to describe the system components and the manner in which they are connected. TRNSYS consists of several programmes (TRNSYS Simulation Studio, TRNSYS3d, TRNFLOW, TRNLizard and TRNBuild for multi-zone buildings). The software meets the requirements of the European Standard for solar thermal systems ENV-12977-2 and the building model included in the software, known as 'Type 56', complies with the requirements of ANSI/ASHRAE standards 140-2001, the American Standard Method of Test for the Evaluation of Building Energy Computer Programmes and the Building Energy Simulation Test (BESTEST). In addition, it meets the requirements of the European Directive on the Energy Performance of Buildings [84].

Due to inherent advantages, such as robust, intuitive, have user friendly graphical front end, output of one component can be graphically connected to inputs of another, great flexibility in integrating, printing and reporting output values and easy to view plots of the of parameters such as temperature, flow rate, heat transfer etc. is used in the present work.

### **3.4.2 Ground loop design software, GLD:**

The GLD software is a monthly, and hourly analysis program tool which has been employed in this study in order to estimate the GHX length. GLD has been used worldwide in more than sixty three countries and is available in 14 languages. For example, it is recommended by the Ministry of



Knowledge Economy in Korea [85]. The GLD software can deal with three types of shallow geothermal systems: vertical, horizontal, and surface water, and GLD enables designers to import or export data for building load, heat pump unit, and system layout from other programs [86]. GLD able to upload the building load data which can be imported simply from different energy simulation software such as Carrier HAP and TRANE Trace on an Excel file [87]. In addition, GLD features include but are not limited to: English/metric unit convergent, CFD simulation, building piping system, lifecycle cost analyses, CO<sub>2</sub> reports, and bills of material [88]. Thus, features of GLD such as the flexible user interface, “what if” modelling facility, international standing, international pipe size, built-in fiancé and lifecycle costing, multiple design approach etc. makes it promising simulation modelling tool for present task.

### **3.5 Conclusion**

GHX modelling has been described in this chapter. The study shows that the solutions inside the borehole stay in a steady state. The transient effect outside the borehole should be taken into account. In most cases, the thermal therapy outside the borehole has not been taken into account for most of the analytical models. Instead of that, it is assumed that the length of the borehole is infinite. However, this process is still used in most of the cases for designing of GHXs of short computation time. In addition, following the literature review of the various models available, it was decided that a discretised three-dimensional model for GHXs fully captures all the requirements and would help to accurately predict thermal response of GHXs.

A simulation software model shall be developed to provide the following objectives:

- i. Assist in investigating the effects of the dynamics of the fluid transport along the pipe loop;
- ii. Assist in the study of three-dimensional characteristics of heat transfer around a GHX;

- iii. help examine the significance of applying a dynamic GHX model in domestic GSHP systems.
- iv. Investigate the thermal interferences of multiple GHX with different configuration.

Finally, in this study, the TRNSYS program was chosen to simulate the system because of its characteristics that enable the designer to study the thermal loads of the building and link them with the GSHP and ASHP. Also, the GLD program was also chosen to perform the sensitivity analysis, as it is quick and easy to use, while covering all the factors affecting the efficiency the ground heat exchanger.

## Chapter 4: The GSHP Potential in Saudi Arabia

---

### 4.1 Introduction

Throughout the world there has been - and will continue to be for the foreseeable future - a movement to the use of renewable energy. In hot dry climates an untapped form of renewable energy is from the ground. To demonstrate this idea we will use, as an approximation, a building in Saudi Arabia to investigate and test the performance of vertical ground source heat pumps as a new facet of renewable and sustainable energy in hot/dry climates, which predominate in Saudi Arabia, in order to reduce costs and CO<sub>2</sub> emissions from HVAC systems, along with saving energy.

In order to investigate the feasibility of using vertical GSHPs in Saudi Arabia, a techno-economic analysis is introduced to evaluate the use of GSHPs compared to the ASHP systems in this type of climate. The most important parameters that must be considered are the climate conditions, local geological conditions, initial costs and electricity tariffs. Based on the data found in relation to these aspects, the size of the GSHP will be calculated and a basic cost analysis that will be compared to conventional cooling systems will be determined. The following section provides information about these parameters before determining the ground heat exchanger size.

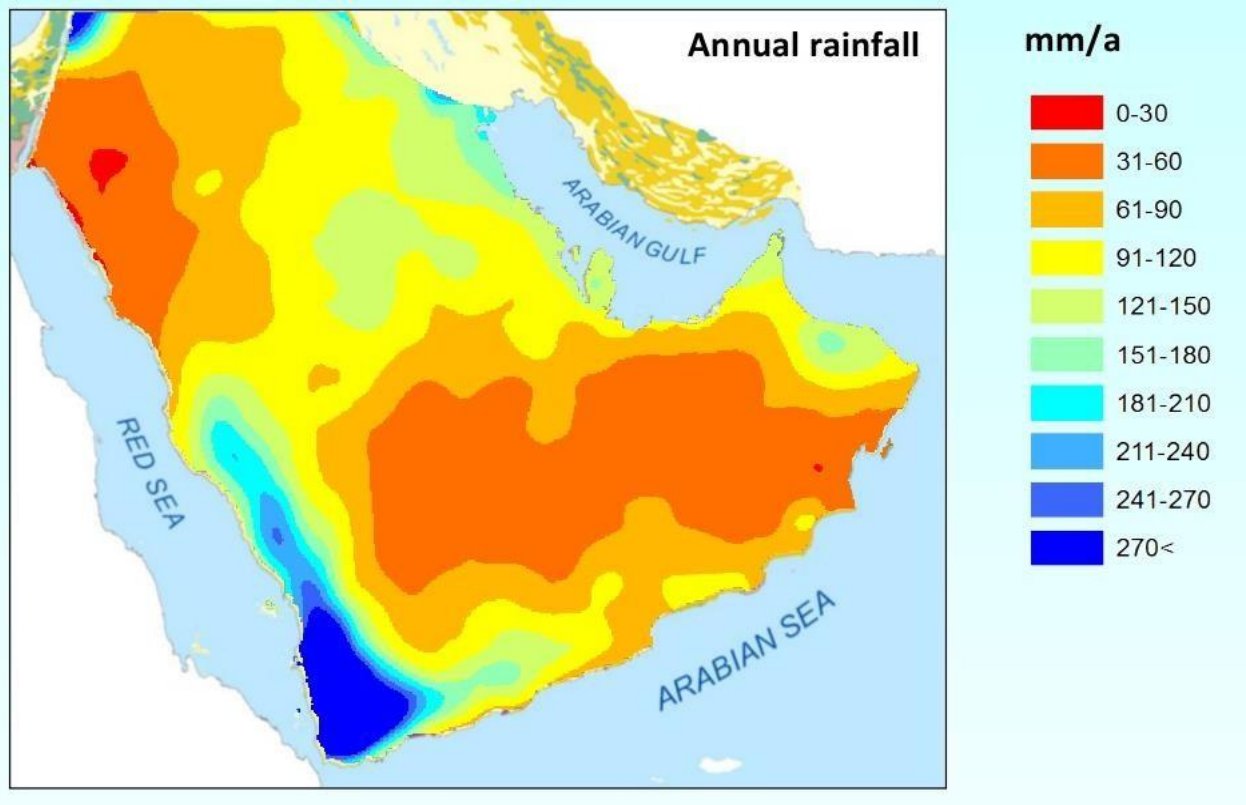
### 4.2 Climate Conditions in Saudi Arabia

Saudi Arabia is located at a longitude 37-52°E and its latitude lies between 16°N and 32°N with vast areas 2,000,000 km<sup>2</sup>. As a result, Saudi Arabia tends to be one of the hottest countries in the world with complex topographical surface and it has the largest continuous expanse of sand desert in the world [89]. The country is classified as a desert climatic (arid and semi-arid) pattern in all except the south-west provinces (Asir), which is a mountainous region [90]. For example, the Asir Province is the location of Sawda mountain, which is the highest peak in Saudi Arabia with 3000m above sea level. The climate

in Saudi Arabia also varies from one province to another. In the summer months the average temperature varies from 27 °C to 45 °C within the inland regions, while the coastal region experiences a temperature within the range of 27 °C to 38 °C but with high level of humidity. On the other hand, the average temperature in Saudi Arabia during the winter season usually ranges from 8 °C to 20 °C in regions such as Riyadh, while in locations such as Jeddah, which is located on the coast of the Red Sea, the temperature ranges from 19 °C to 29 °C [91]. In general, winter is mild in most regions of Saudi Arabia. However, this is not the situation in the mountainous regions located in the south-western part where, during winter, the temperature sometimes drops to 0°C and the prevalence of a high chill wind give to rise to a cold atmosphere [92]. Also, there might be snowfall in the north regions where the temperature reaches below zero due a cold wave gripping the region.

### **4.3 Precipitation**

Although seas surround Saudi Arabia from approximately three sides, evaporation from the sea surface does not add significant value to the amount of precipitation or the reduction in ambient temperature due to the small size of these water bodies in the Red Sea and the Arabian Gulf. Saudi Arabia classified as one of the poorest nations in terms of water resources such as rainfall, rivers and lakes. The arid regions are characterized by deficient annual rainfall. As shown in Figure 4.1, the amount of rainfall varies between 100 in the north region up to 300 mm on the mountain's areas in the southwestern highlands. It is important to note that the rate of rainfall directly affects the performance of GSHP because it affects the rate of soil moisture, the amount of groundwater and the ambient temperature, all of which are considered factors in the design of GSHPs.[93].



*Figure 4-1 Average annual precipitation for Saudi Arabia.*

#### **4.4 Climatic Zones in Saudi Arabia**

Knowledge of the climatic zone is one of the basic steps required to examine the application of the potential for renewable energy, to determine green home design, zero energy designs and energy consumption. Alrashed and Asif [94] evaluated the climatic zones in Saudi Arabia by dividing the country into five inhabited regions, including the following major cities: Dhahran, Quraiat, Riyadh, Jeddah and Khamis Mushait, see Figure. 4.2. Also, this study compared these five sites with the 18 global sites on the basis of four main parameters that affect the energy performance of zero energy homes (ZEH): air temperature, relative humidity, wind speed and solar radiation. The IES-VE software was used to model a virtual house for all the relevant locations. The findings of the sensitivity analysis indicated that the Saudi climate is not an obstacle to the application of ZEHs in the country. Also, the locations were compared with their corresponding Saudi locations, as shown in Table 4.1.

Table 4.1 The climatic parameters for the identified and represented locations [14].

Location	Temperature, °C		
	Min.	Max	Mean
Dhahran, SA	5	45.7	25.8
Borrego Springs, California, US	2.3	48.4	24.7
Quraiat, SA	-3.3	43.9	19.8
Tucson, Arizona, US	-2.1	43.2	20.4
Riyadh, SA	2.2	43.7	25.1
Phoenix, Arizona, US	-2.8	46.1	22.5
Jeddah, AS	13.9	41.7	27.9
Lake Bennett, Australia	15.6	35.8	27.7
Khamis Mushait, AS Cupertion , California, US	2.7	34.3	18.9
	-0.2	37.2	16.6

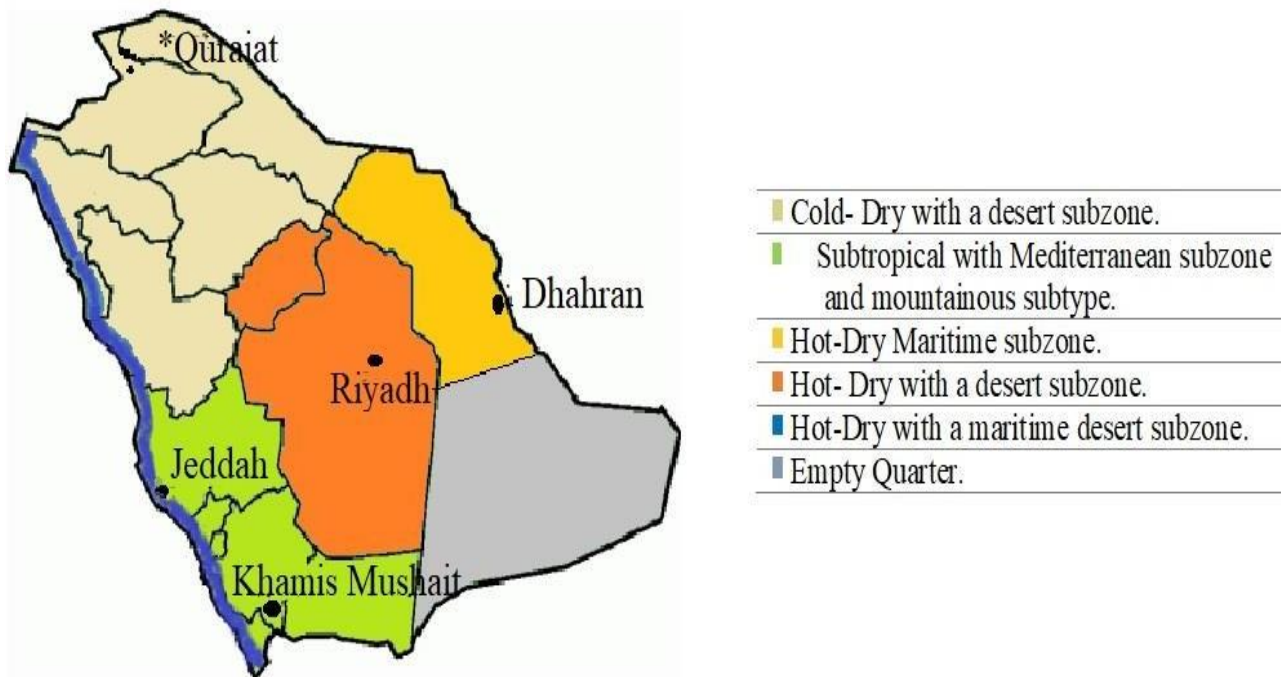


Figure 4-2 The climatic zones in Saudi Arabia, adopted from [94].

#### 4.5 Geothermal Conditions in Saudi Arabia

The geology of Saudi Arabia consists of two main parts, the Arabian Shield, which is located in the west of Saudi Arabia, and the Arabian Plate, which extends from the centre of Saudi Arabia to the east coast. These two parts contain different geological characteristics of the soil and rocks Figure 4.3. In the last two decades, several studies have identified the deep geothermal resources in Saudi Arabia; most of these studies have focused on exploring the location where geothermal power is generally stored [95]. Volcanic regions and hot spring waters are considered by researchers when understanding the capacity for geothermal power. Deep geothermal resources, however, are beyond the scope of this thesis but, regarding the exploitation of shallow geothermal energy using GSHP, there is a lack of research that addresses this issue in Saudi Arabia.

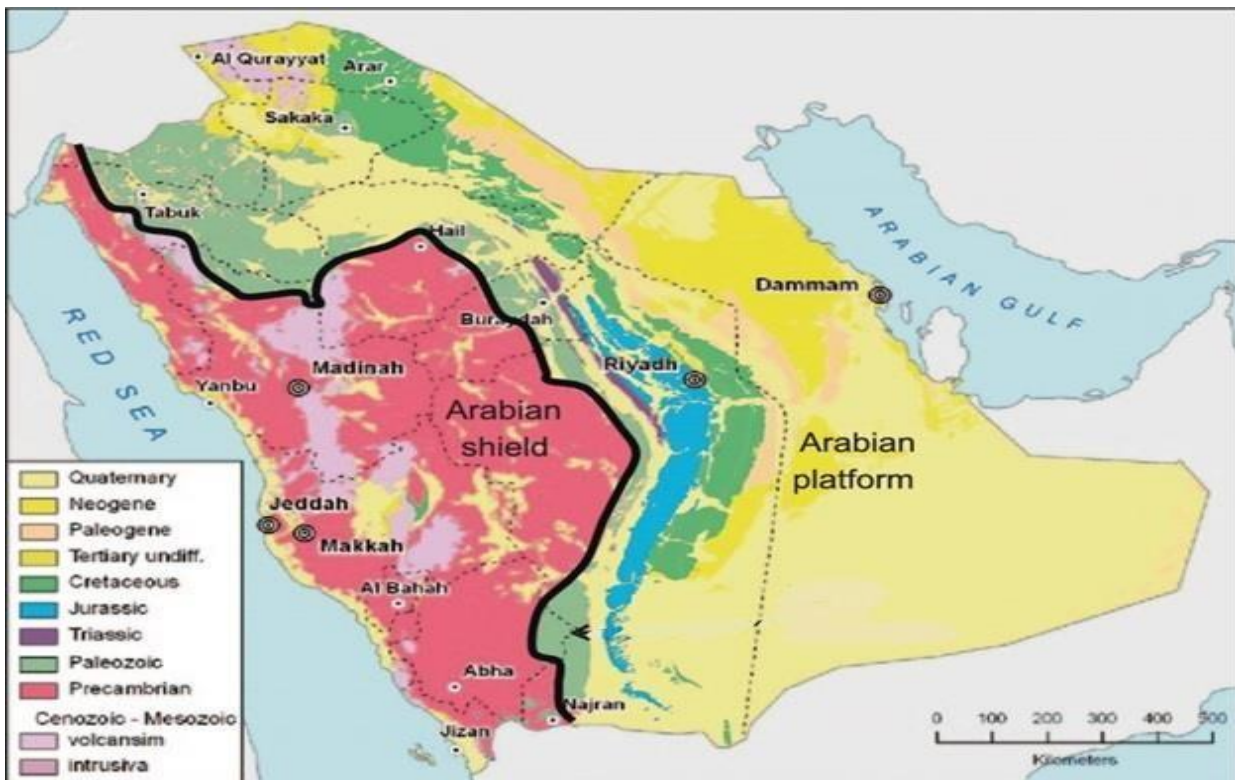


Figure 4-3 Map of Saudi Arabia, showing the two main parts, the Arabian Shield and the Arabian Plate

The feasibility of using ground-coupled condensers for air-conditioning (A/C) systems in Saudi Arabia was investigated by Said et al. [47] where the temperatures and soil properties required for the performance analysis of one of these condensers was determined experimentally. The measurements undertaken as part of the investigation revealed a significant difference between the ambient air and ground temperatures, which resulted in an increase in the coefficient of performance and a reduction in the energy consumption of an A/C unit using a vertical ground

heat exchanger rather than an air-cooled condenser, the latter of which is the current norm in the country. A maximum difference in temperature of about 12 °C was observed between the ground temperature and the dry bulb temperature of the ambient air as shown in Figure 4.4. A steady-state value of 32.5 °C was reached for the mean borehole temperature. Also, cost analysis was undertaken, which indicated that the use of ground-source heat pumps in Saudi Arabia would result in about 28% energy savings if ground coupled heat pumps were utilized over the ambient air. However, this was deemed to not be economically viable due to the low electricity prices prevalent in the country due to government subsidies and high drilling costs. The study by Said et al. [47] highlighted a few salient aspects as follows:

- There is a significant temperature difference between the ambient air and the ground that will favour the performance of GHXs over that of air-cooled condensers.
- The ground temperature in the KSA does not change significantly about 30m below the surface throughout the year.
- Performance analysis indicated an increase in the COP and a reduction in the energy consumption of an A/C unit when using a vertical GHX instead of an air-cooled condenser; this resulted in energy savings of about 28%.



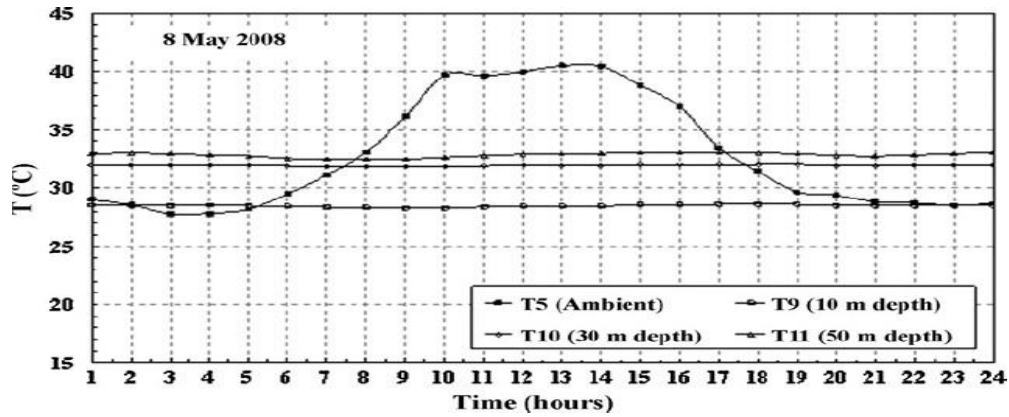


Figure 4-4 Difference between the ambient air and the ground at different depths in May 2008 [47]

Another study, by Sharqawy et al. [96], deals with the in situ experimental determination of the thermal properties of the underground soil for use in the design of borehole heat exchangers as shown in Figure 4.5. The approach is based on recording the unsteady thermal response of a GHX and this was, for the first time, installed in Saudi Arabia. In this approach, the temperature of the circulating fluid was recorded at the inlet and outlet sections of the GHX with time. The recorded thermal responses, together with the development of a simple line source theory, were used to determine the thermal conductivity, thermal diffusivity and the steady-state equivalent thermal resistance of the underground soil. From the results obtained, as detailed in the report, the following conclusions were drawn:

- For the selected site, the flow rate, power consumption and the inlet and outlet temperatures (T2 and T3 in Figure. 4.6) were recorded until the circulating fluid attained thermal equilibrium. The average fluid temperature was 32.5 °C and the maximum circulated outlet fluid temperature was 36.5 °C after 6 days of operation. This temperature difference is very important as it helps to select the flow rate of circulating fluid for a given fluid and capacity of heat pump.
- For the selected site, the underground temperature was recorded every 1m along the depth of the borehole (Figure. 4.6), and the average temperature of the ground ( $T_g$ ) was 32.6 °C.

- For the selected site, the GHX effective values of 2.154 (W/m K),  $6.252 \times 10^{-6}$  ( $\text{m}^2/\text{s}$ ) and 0.315 (m K/W) were determined for the soil thermal conductivity, thermal diffusivity and thermal resistance, respectively.

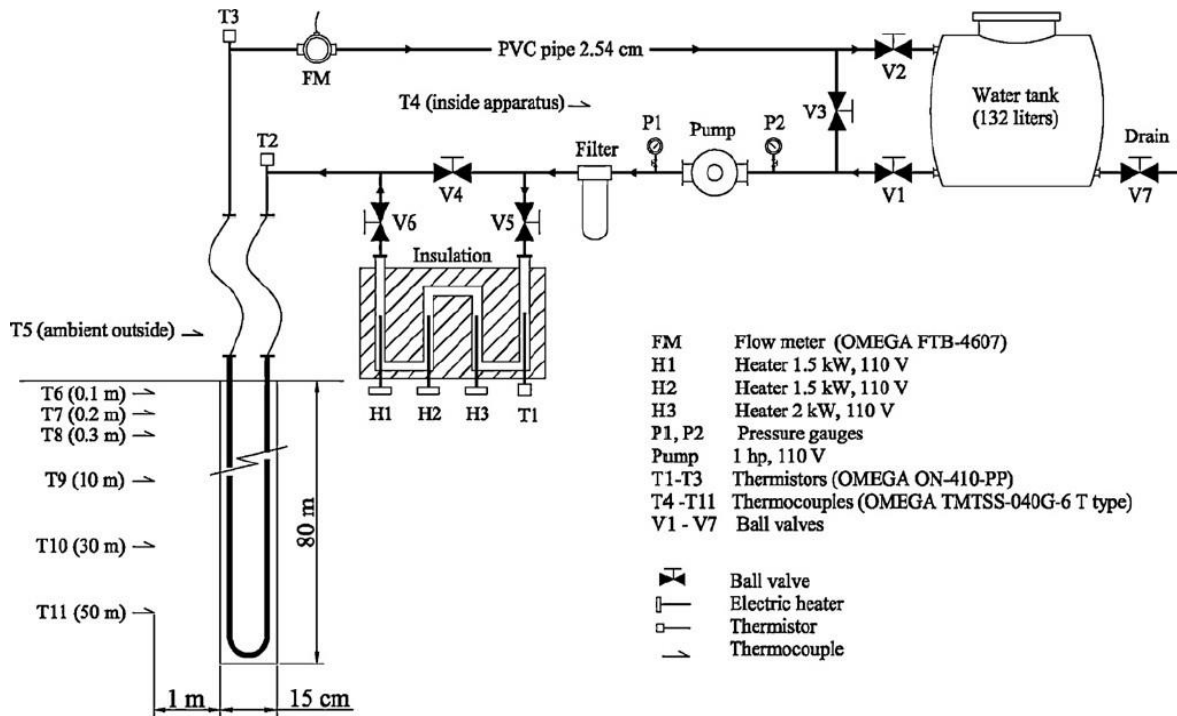


Figure 4-5 Layout of the first thermal response test in Saudi Arabia [96].

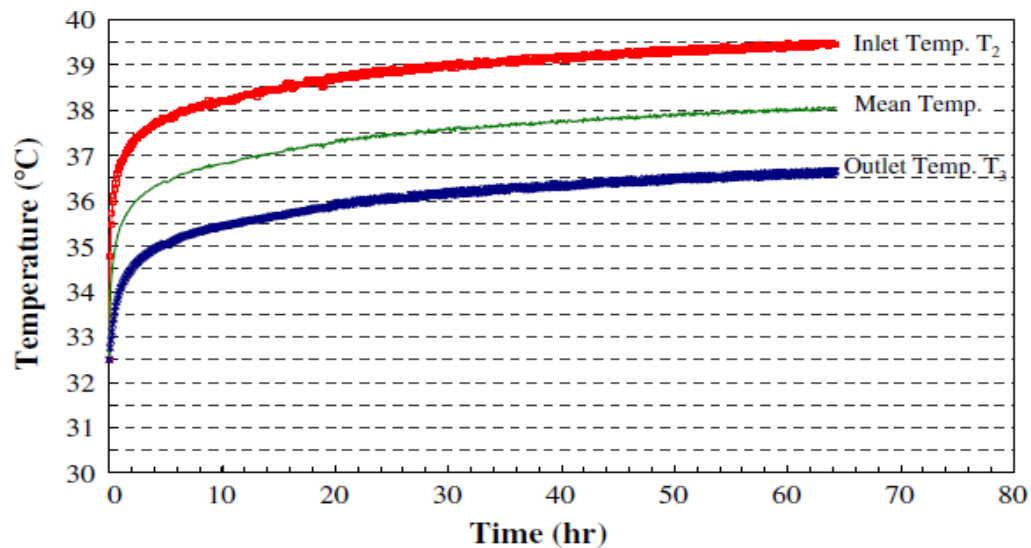


Figure 4-6 Inlet, outlet and mean fluid temperatures during the thermal response test [96].

In 1978, a detailed cooperative study between the Ministry of Petroleum and Mineral Resources in Saudi Arabia and the US Geological Survey investigated the heat-flow measurements. Five sites were selected in the region between the Riyadh provinces in the direction towards the southwest and the Farasan Islands [97]. Each site was mapped and sampled in detail. At each site, 15–20 wells were drilled with an average depth of 60 m; the distance between each site was approximately 200 km, see Figure 4.7.



*Figure 4-7 The location of the five sites that were selected for the drilling of the boreholes by the Ministry of Petroleum and Mineral Resources in Saudi Arabia and the US Geological Survey to investigate the heat-flow measurements adopted from [97].*

The thermal conductivity and underground temperature were computed in all boreholes. Table 4.2 summarizes some of the most important information regarding this building and its environment. The most important information from this study relates to the GSHP design was the average thermal conductivity for site 1 is 2.6 W/mK and the average underground temperature at 60m depth is 28.5 °C.

Table 4.2 Heat flow and thermal conductivity estimates from the five sites selected [97].

Shot point	Altitude (m)	Depth (m)	Thermal conductivity W/m·K
1	692	70	2.62
2	887	69	3.26
3	946	62	2.60
4	1144	58	3
5	179	58	4.22

Despite the lack of studies on shallow geothermal in Saudi Arabia. Data collected from these three studies related to the GSHP design was the average underground temperature, the fluid temperature from the borehole and the thermal resistance as summarized in Table 4.3. The maximum difference in temperature of about 12 °C was observed between the ground temperature and the dry bulk temperature of the ambient air and the outlet temperature from the ground loop was 36.5 °C. All these values will be used to estimate the ground heat exchanger length based on ASHRAE standard.

Table 4.3 Geological and soil properties conditions of the ground heat exchangers.

Average thermal conductivity for shot point (1)	2.6
Thermal diffusivity	$6.252 \times 10^{-6}$ (m <sup>2</sup> /s)
The main fluid temperature from the borehole	32.5°C
thermal resistance	0.315 (m K/W)
The average underground temperature at 60m depth for shot point (1)	28.5°C

Finally, ASHRAE standards and many simulation programs, such as TRNSYS use Eq. (4.1) as developed by Kasuda [98] to calculate the underground temperature at different depths. Figure 4.8 show the underground temperature for Riyadh city at different depths based on the daily weather data collected for Riyadh city, 2018.

$$T_{soil(D,t_{year})} = T_{mean} - T_{amp} \exp\left(-D \sqrt{\frac{\pi}{365 * a}}\right) \cos\left(\frac{2\pi}{365}\left(t_{year} - T_{shift} - \frac{D}{2} \sqrt{\frac{365}{\pi * a}}\right)\right) \quad (4.1)$$

$T_{soil(D,t_{year})}$  = soil temperature at depth D and time of year.

$T_{mean}$  = mean surface temperature (average air temperature). The temperature of the ground at an infinite depth will be at this temperature

$T_{amp}$  = amplitude of surface temperature [(maximum air temperature - minimum air temperature)/2] D = depth below the surface (surface=0)

$\alpha$  = thermal diffusivity of the ground (soil)  $t_{year}$  = current time (day)

$t_{shift}$  = day of the year of the minimum surface temperature

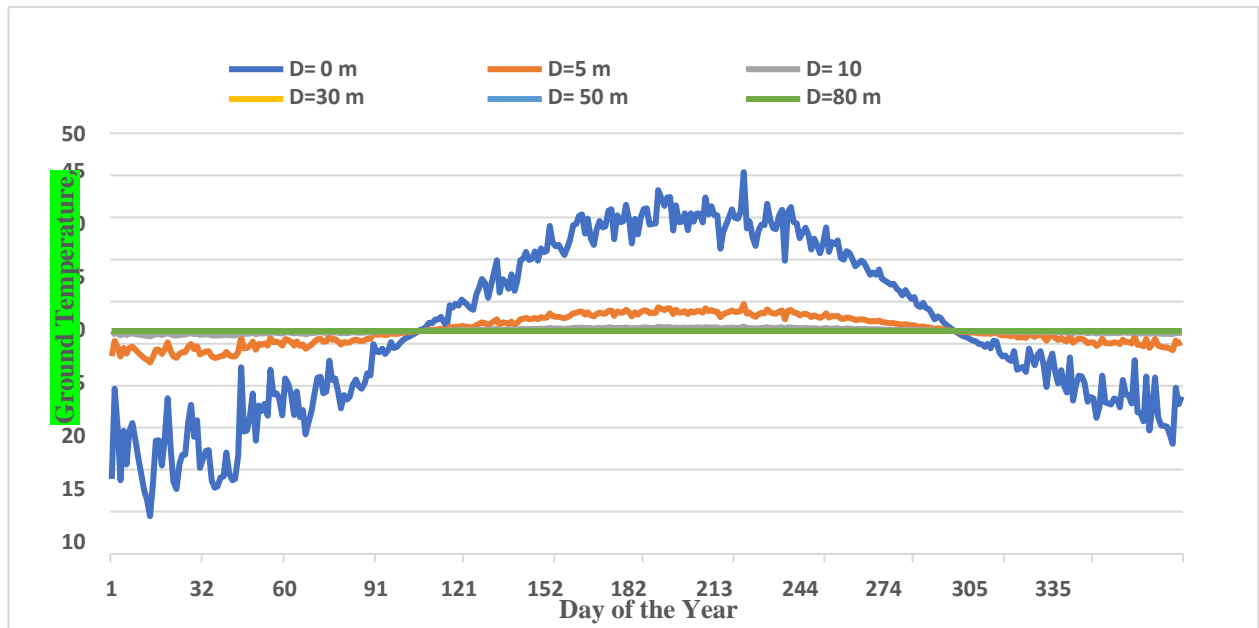


Figure 4-8 Underground temperature for Riyadh city at different depths

#### 4.6 Sizing a Geothermal Heat Pump in Saudi Arabia

The performance and initial cost of the geothermal pump depends on the calculation of the GHX. In North America, it is estimated that, on average 10%–30% of the GHXs are oversized [81]. The high initial cost of a vertical GSHP is linked to its oversized nature. The design of GHXs depends on many factors (cooling/heating load, soil type and climate conditions) that are more or less controllable by the

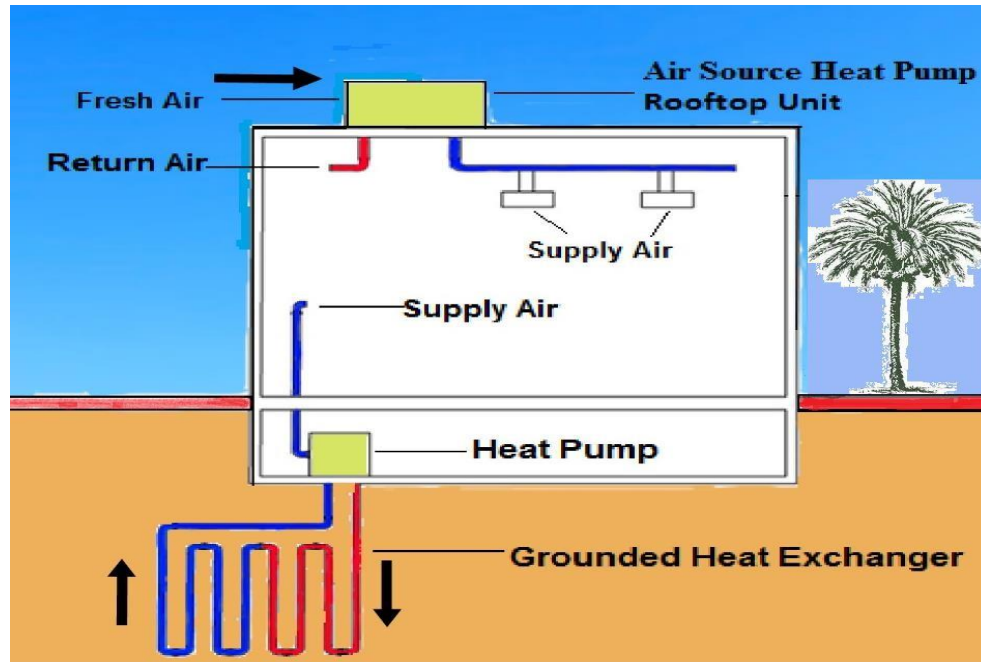
designer; for example, the heat transfer through the GHX and surrounding soil or rock, which is difficult to quantify. Thus, sizing a geothermal heat pump is a complex process, and therefore it is important for the accurate sizing of the vertical GSHP before making any decisions. Therefore, in order to make GSHPs economically feasible it is very important that there is a good estimation of its size so that the amount of drilling can be limited and there are fewer operational problems.

#### **4.7 Methods of Calculating the Length of a Vertical GHX**

Generally, various factors affect the design of GSHPs including but not limited to, peak heating/cooling load, characteristics of the heat pump, ground parameters and climate conditions. Thus, there are many methods that can be applied to estimate the length of a vertical GHX; the ASHRAE standards, based on the work of Carslaw and Jaeger (1947), is the most widely used. This method is also known as the cylinder source solution, which assumes that the borehole is infinitely long, and the ground is homogeneous along its depth. The geometry and the thermal properties of the materials inside the borehole are ignored, including the thermal mass of the fluid. This approach was developed and evaluated initially by Ingersoll and Zobel (1954) in steady-state mode, then Kavanaugh and Rafferty (1997) developed method to calculate the equivalent thermal resistance for three different heat pulses [69]. For example, in a 20-year pulse, a one-month pulse, and a six-hour pulse. This method became ASHRAE standards to estimate the size of GHX.

In order to determine the feasibility of using GSHPs versus ASHPs in Saudi Arabia as shown in Figure 4.9, the following steps are performed:

- (i) Calculate the length of the GHX based on the ASHRAE handbook ASHRAE (2017).
- (ii) Perform a basic cost analysis compared to a conventional cooling system ASHP.



*Figure 4-9 Schematics of ground and air source heat pump systems for a typical house in Saudi Arabia.*

#### **4.7.1 Description of generic model**

To perform a basic cost analysis, Table 4.4 and 4.5 shows the data that has been collected from the literature review and from the actual project for the bank building located in Riyadh Saudi Arabia as follows:

- The soil properties (thermal conductivity and underground temperature) collected from the report prepared for the Ministry of Petroleum and Mineral Resources in Saudi Arabia and the US Geological Survey to investigate the heat-flow measurements [97].
- The cooling and heating load collected from the actual project for the bank building located in Riyadh Saudi Arabia performed by an engineering consultant [99] attached in Appendix 1.
- The costs of the heating pump unit were estimated by the Water Furnace Company [100].

Construction and the installation cost (drilling, pipe and labour) is estimated based on the

average price of three local contractors that we have been in contact with (see attached in Appendix 2).

- The liquid temperature at the heat pump inlet/outlet, thermal resistance of the bore and pipe properties were collected from Sharqawy et al. [96].

Table 4.4 The data collected for the design calculation for the length of the GHX.

Parameters	Value
Average Thermal conductivity for the soil, W/mK	2.6
Underground temperature at 60 m of depth, °C	29
Outside Temperature, °C	45
Average Annual Temperature (ASHRAE Handbook-2013), °C	26.5
Liquid temperature at heat pump inlet, °C	32.8
Liquid temperature at heat pump outlet, °C	39.5
Thermal diffusivity, m <sup>2</sup> /day	0.54
Total cooling load (Actual data), kW	196
Total heating load (Actual data), kW	38

Table 4.5 The design conditions for the estimation of the cooling and heating loads.

Parameters	Value
Building Area, m <sup>2</sup>	584
Total cooling load, kW	196.2
Total heating load, kW	38.1
Riyadh cooling degree days	5688
Riyadh Heating degree days	291
Outdoor temperature, F	115 (46.1 °C)
Indoor temperature, F	73 (22.78 °C)

Also, in terms of the estimated total borehole length, by use of the sizing Eq. (4.2), all the variables or factors have been obtained from the ASHREA hand-book (2017), HVAC Application: Chapter 34. And, in case of the city of Riyadh the climatic parameters will be compared to the city of Phoenix, Arizona, US.



#### 4.7.2 Calculation of the length of the GHX based on the ASHRAE standards

In this work, the equations employed to estimate the length of the GSHP systems are based on the ASHRAE standards (2017) Handbook –HVAC Application: Chapter 34.

The length to satisfy the cooling loads was calculated using the following relation:

$$L_c = \frac{q_a R_{ga} + (q_{lc} - 3.41 W_c)(R_b + P:F_m R_{gm} + R_{gd} F_{sd})}{t_g - \frac{t_{wi} + t_{wo}}{2} - t_p} \quad (4.2)$$

Where:

$F_{sc}$	=	short-circuit heat loss factor
$L_c$	=	required bore length for cooling, ft
$L_h$	=	required bore length for heating, ft
$PLF_m$	=	part-load factor during design month
$Q_a$	=	net annual average heat transfer to ground, Btu/h
$R_{ga}$	=	effective thermal resistance of ground (annual pulse), ft · h · °F/Btu
$R_{gst}$	=	effective thermal resistance of ground (peak short term) 1 to 6 hours recommended, ft · h · °F/Btu
$R_{gd}$	=	effective thermal resistance of ground (peak daily pulse: 1 h minimum, 4 to 6 h recommended), ft · h · °F/Btu
$R_{gm}$	=	effective thermal resistance of ground (monthly pulse), ft · h · °F/Btu
$R_b$	=	thermal resistance of bore, ft · h · °F/Btu
$t_g$	=	undisturbed ground temperature, °F
$t_p$	=	temperature penalty for interference of adjacent bores, °F
$t_{wi}$	=	liquid temperature at heat pump inlet, °F
$t_{wo}$	=	liquid temperature at heat pump outlet, °F
$W_c$	=	system power input at design cooling load, W
$W_h$	=	system power input at design heating load, W

To determine the total borehole length by use the sizing equation (4.2), the cooling load 196.2 kW and the heating load 38.1 kW for the building, were calculated by used the HAP software as design tool for the bank building located in Riyadh Saudi Arabia, convert from power units (kW) to British Thermal Units (BTU) can be calculated as follows:

$$1 \text{ kW} = 3,412.14 \text{ Btu/h} \quad (4.3)$$

Thus:

Cooling load,  $Q_{lc} = 196.2 \text{ kW} * 3412.142 = 669,462 \text{ Btu/h}$

Heating load,  $Q_{lh} = 38.1 \text{ kW} * 3412.142 = 130,002 \text{ Btu/h}$

In the cooling mode, the condenser rejects heat to the surrounding soil, and the evaporator extracts heat from the load. For that, cooling rates are assumed to be negative in the cooling mode. The heat rejected at the condenser is determined from

$$q_{cond} = q_{lc} \times \frac{ERR+3.412}{EER} \quad (4.4)$$

$$= 669.462 \text{ Btu/h} * (14.9 + 3.412)/14.9 = -822.765 \text{ Btu/h}$$

And the heat extracted at the evaporator is determined from

$$q_{evap} = q_{lh} \times \frac{COP-1}{COP} \quad (4.5)$$

$$= 130.002 * (4.4-1)/4.4 = 100456 \text{ Btu/h}$$

Where EER=14.9 and COP= 4.4 was selected based on the heat pump catalogue.

The net annual average heat transfer to the ground,  $q_a$  is as follows

$$q_a = \frac{q_{cond} \times EFLH_c + q_{evap} \times EFLH_h}{8760h} \quad (4.6)$$

$$= (-822,765 \text{ Btu/h}) (985h) + (100,456 \text{ Btu/h}) (87.5h) / 8760$$

$$= -91,510 \text{ Btu/h}$$

Where EFLH is Equivalent Full-Load Hours (EFLH) for different building types and climates. were

determined from Table 8 and location is city of Phoenix, Arizona, US. (ASHRAE Handbook,2017).

Other factor must be determined to solve the Eq. (4.2) is the effective ground thermal resistances ( $R_{ga}$ ,  $R_{gm}$ ,  $R_{gd}$ ) which depend on soil properties, boreholes diameter, and reference “heat pulse” duration.

The three ground heat pulses,  $q_a$ ,  $q_m$  and  $q_h$ , are applied over time periods which are typically equal to 10 years ( $q_a$ ), 1month ( $q_m$ ), and 4 or 6 hours ( $q_h$ ), respectively. And  $\tau$  is the time of operation.

$$q_a = 10 \text{ year (3650 day)} \Rightarrow \tau_1 = 3650 \text{ days.}$$

$$q_m = 1 \text{ month (30 day)} \Rightarrow \tau_2 = 3650 + 30 = 3680$$

$$q_h = 4 \text{ hours (0.167 day)} \Rightarrow \tau_f = 3650 + 30 + 0.167 = 3680.167 \text{ days}$$

Therefore, Fourier number ( $F_o$ ) is then computed for each period of time with the following values:

$$F_{of} = \frac{4a\tau_f}{d_b^2} \quad (4.7)$$

Where:

$\alpha$  = thermal diffusivity,

$\tau$  = the time of operation and  $d$  is bore diameter.

$\alpha_g$  = thermal soil diffusivity (for Table 4 in the stander limestone =  $1.15\text{ft}^2 / \text{day}$ )

$d_b$  = boreholes diameter (5 in)

Therefore, the Fourier number each reference period of time

$$\begin{aligned} \tau_1 &= 3680.167 \text{ days} \\ F_{o2} &= \frac{4a\tau_f}{d_b^2} \\ &= 84,000 \end{aligned}$$

$$\begin{aligned} \tau_1 &= 3650 \text{ days} \\ F_{o2} &= \frac{4a(\tau_f - \tau_2)}{d_b^2} \\ &= 695 \end{aligned}$$

$$\begin{aligned} \tau_2 &= 3650 + 30 = 3680 \\ F_{o2} &= \frac{4a(\tau_f - \tau_2)}{d_b^2} \\ &= 3.25 \end{aligned}$$

G-factor which is then determined from Figure16 (ASHRAE Handbook, 2017) For each Fourier value.

$$G_f = 0.96$$

$$G_1 = 0.58$$

$$G_2 = 0.21$$

G-factor is obtained through the infinite cylindrical heat source model. More information about G-factor ( $G_f$ ,  $G_1$  and  $G_2$ ) can be obtained from ASHRAE standards (2017) online Handbook – HVAC application, chapter 34. From Figure 15,16 and Table 6.

Also, In the ASHRAE standards of sizing method, the infinite cylinder solution is used as the thermal responsefactor. Thus,  $R_{ga}$ ,  $R_{gm}$ ,  $R_{gd}$  are given by:

$$R_{ga} = \frac{G_f - G_1}{K_g} \quad (4.8a)$$

$$R_{gm} = \frac{G_1 - G_2}{K_g} \quad (4.8b)$$

$$R_{gst} = \frac{G_2}{K_g} \quad (4.8c)$$

Where:

$R_{ga}$ ,  $R_{gm}$  and  $R_{gst}$ , are annual, monthly and daily pulse respectively.  $k_g$  = ground conductivity = 2.6 Btu/h/f<sub>t</sub> (given)

$$R_{ga} = (0.96 - 0.58) / 2.6 = 0.271 \text{ h f}_t \text{ F / Btu.}$$

$$R_{gm} = (G_1 - G_2) / k_g = (.58 - .21) / 1.4 = 0.264 \text{ h f}_t \text{ F / Btu.}$$

$$R_{gst} = G_2 / k_g = 0.21 / 2.6 = 0.15 \text{ h f}_t \text{ F / Btu.}$$

In addition, to determine the required length to satisfy cooling loads, some factors can be found in ASHRAE sizing standard (2017) Handbook – HVAC application, chapter 34.

$$R_b = 0.185 \text{ ft h F / Btu} \quad (\text{thermal resistance of bore - table 6})$$

$PLF_m = 0.28$  (part load factor during the heating/cooling design months)>

$F_{sc} = 1.05$  (short circuit heat loss factor - table 7)

Ground temperature is a key value to know the length of the GHX. In our case there are two value which are 26 °C based on Eq.(4.1) and 29 °C based on experimental study [97].

Thus, based on Eq. (4.2) and the data in Tables 4.4 and 4.5, the collection of data from the previous studies and the actual project for the bank building located in Riyadh Saudi Arabia, the required length of the GHX in order to satisfy the cooling loads was estimate as follows:

GHX length at underground temperature 26 °C,  $L_c = 4082\text{m}$

GHX length at underground temperature 29 °C,  $L_c = 5831\text{m}$

Thus, 3 °C rise in underground temperature (the difference between the two values) reduces the GHX length by 1749 m, which is approximately 42 % of the GHX length.

Despite the wide use of Eq. (4.2), three studies have focused on the ASHRAE standards Handbook length method by comparing the total length to the results obtained using the simulation tool or actual project. Cullin et al. [47] made a performance assessment of a GSHP, using a simulation tool for four cities, namely Valencia, Leicester, Atlanta and Stillwater, suggested that, while the simulation-based design tool predicted the borehole length to within  $\pm 6\%$  in all cases, the ASHRAE standards design equation yielded systems with errors ranging from  $-21\%$  to  $167\%$ . Ruan & Horton [81], on the other hand, estimated that, in North America, on average,  $10\% \sim 30\%$  of the GHXs were oversized. Another study [101] compared two methods, namely the ASHRAE standard analytical method of Kavanaugh & Rafferty and the GLHEPRO commercial tool, based on the g-functions method by Eskilson. The comparative analysis of the two methods showed that the ASHRAE standards tends to overestimate BHE size by up to  $27\%$ , as compared to GLHEPRO.

Based on the above three studies, it is possible that the ground loop length calculated using the ASHRAE standards handbook results in oversizing by about 20%, which, if factored in, would result in reduced bore lengths, thereby resulting in decreased boring costs.

## 4.8 Cost Analysis

### 4.8.1 Savings on the power consumption

The cooling and heating load collected from the actual project for the bank building located in Riyadh Saudi Arabia was performed by engineering consultants [99]. Table 6 shows the design conditions for the estimation of the cooling and heating load. These input data were used to select the ASHP as a conventional cooling system and the HAP software was used as the design tool to calculate the heating/cooling load.

The results were obtained for the total cooling load 196 kW and the total heating load 38 kW and from the Carrier catalogue, this building requires 3×20 TR package A/C units. As per catalogue, each unit has a power consumption of 28 kW at a maximum ambient temperature 46 °C. In addition, the calculation of the annual cooling power consumption and the cost based on a constant speed compressor (conventional A/C unit).

The electrical energy consumption for the cooling is determined as follows:

$$P = \frac{Q_{cooling} \times 3412 \times 24 \text{ hours} \times CDD}{EER \times 1000 \times (T_{out} - T_{in})} \quad (4.9)$$

where  $Q_c$  is the cooling load, CDD is the cooling degree days and EER the energy efficiency ratio. The equation (4.9) becomes:

$$P = 196 \times 3412 \times 24 \times 5688 / (9.76 \times 1000 \times (115 - 73))$$

$$= 222,935 \text{ kWh per year}$$

The cooling electricity cost per year is determined as follows:

$$\text{cost per year} = \text{power (kWh)} \times \text{electricity tariff} \quad (4.10)$$

Saudi electricity cost: SR 0.32 per kWh

$$\begin{aligned} \text{Cooling electricity cost} &= 222,935 \times \text{SR } 0.32 \text{ per kWh} \\ &= \text{SR } 71,340 \text{ per year} \end{aligned}$$

The electrical energy consumption for the heating is determined as:

$$P = \frac{Q_{cooling} \times 3412 \times 24h \times HDD}{1000 \times (T_{out} - T_{in})} \quad (4.11)$$

$$P_h = 38.1 \times 3412 \times 24 \times 291 / 1 \times 1000 \times 76 - 31 = 20,175 \text{ kWh per year}$$

From equation (4.10),

$$\begin{aligned} \text{Heating electricity cost} &= 20,175 \text{ kWh/y} \times \text{SR } 0.32 / \text{kWh} \\ &= \text{SR } 6,456 \text{ per year.} \end{aligned}$$

Differences in the annual primary energy consumption and the annual electrical cost between ASHP and GSHP are presented in Table 4.6. It is seen that thenet savings in the power consumption for heating and cooling is 97,098 kWh/year, which is equivalent to SR 31,066.

Table 4.6 The annual primary power consumption for the ASHP and the GSHP.

	ASHP	GSHP
Cooling block load, kW	196	196
Heating block load, kW	38	38
COP for the system	2.3	4.4
EER	9.76	14.9
Power consumption, cooling kWh per year	222,953	146,030
Power consumption, heating kWh per year	20,175	0 (free heating)
Cost of power consumption cooling mood SR per year	71,339	46,729
Cost of power consumption heating mood SR per year	6,456	0 (free heating)
Total cost, SR	77,795	46,729
Net saving on power consumption. SR per year		31,066

It is important to note that the heating period in most regions in Saudi Arabia is short. For example, Riyadh heating degree days is 291 hours compared to 5688 hours cooling degree days. This short period represents 9% of the total annual energy consumption. However, due to the high underground temperature, typically 29°C, which is above the indoor design temperature 26 °C in winter, then Thus, the heating load can obtained by blowing the air through the warm circulating water only and without the need to run the compressor, which consumes the most significant amount of energy compared to the fan. Also, GSHPs can produce hot water without separate boiler unit, thus leading to the saving in costs for domestic hot water equipment.

Another potential factor related to the use of GSHPs in Saudi Arabia is the reduction in CO<sub>2</sub> emissions. For the next decade, the emissions of CO<sub>2</sub> are estimated to increase rapidly. In G-20 (the Group of Twenty countries), Saudi Arabia has the second highest per capita emissions in CO<sub>2</sub> in the last two decades where the CO<sub>2</sub> has increased by about 75% [102]. Liu et al. [103] compared the ASHP produced CO<sub>2</sub> to three alternative systems (wall-hanging gas boiler, direct electric heating and coal-fired boiler) used in heating mode in China. Their results showed that there is significant energy efficiency and cost effect to use ASHP. In addition, the GSHP is more energy efficient than ASHP and also a further reduction in CO<sub>2</sub> release rate is anticipated.

To estimate the annual CO<sub>2</sub> emissions then we multiply the power consumption in kilowatt hours (kWh) by the Emissions Factor (EF) for the state. In Saudi Arabia 1 kWh = 0.7 kg CO<sub>2</sub>. As a result, when the GSHPs saving is 97,000 kWh /year then this leads to a saving of 67,900 Kg CO<sub>2</sub>/year. Approximately 40%.



#### **4.8.2 Initial cost analysis**

The initial cost price is fundamental in determining the HVAC system. Song et al. [104] investigated the techno-economic on operation performance of using ASHPs. From Table 8, it can be seen that the unit price for GSHP is about twice the ASHP. However, this price is variable depending on the manufacturing company, taxes and location. In addition, the initial installation cost for the GSHP leads to an increase in the investment costs of GSHP because of the extra expensive drilling costs. However, over a period (22 years) then it is predicted that the GSHP will be more feasibly.

The life expectancy of the heat pump is different from one region to another; based on the Air Conditioning, Heating & Refrigeration Institute (AHRI), the average lifespan of ASHP is 15 years in the ideal conditions such as average weather and regular maintenance. From Table 4.7, it can be observed that the life expectancy of the ASHPs is rather limited in Saudi Arabia, due to the high ambient temperatures, dust and the saline coastal environment, and in the cities near the sea, which rapidly corrodes the aluminum heat transfer fins, and this leads to a shorter life span. The typical life-span of an ASHP is 10-15 years; for the current assessment, a lifetime of 11 years has been assumed because of the harsh climate. However, the GSHP does not have the corrosion problems that are generally encountered with the ASHP. This is due to the fact that the heat pump unit is located indoors, and the loop pipes are buried in the ground and therefore the plant is not exposed to the ambient air. Thus, GSHPs have a typical life-span of 25 years and beyond, but for this study a lifetime of a GSHP has been assumed to be 22 years, namely twice the life-span of an ASHP.

Table 4.7 The initial cost analysis for the ASHP and the GSHP.

	ASHP	GSHP		Notes
Ground Temp. °C	-----	26.5	29	26.5 °C from equ (1)
GHX Loop length, m	-----	4082	5831	@29 °C from experimental [13].
Unit price, SR	160,000	240,000		
Drilling cost, SR	-----	326,560	466,480	SR80/m } Ground SR2.6/m } loop cost Estimated }
Pipe price, SR	-----	10,613	15,160	
Installation GHX, SR	-----	8,000	10,000	
Total initial cost, SR	160,000	585,173	731,640	
Power consumption cost, SR /22 y From equ.3 (cooling)	71,339*22 =1,569,462	46,729*22 =1,028,038		Life cycle for the unit Estimated 11 years for ASHP and 22 years for GSHP. We assumed the cost of installing the two systems is equal.
Power consumption cost, SR /22 y From equ.3 (heating)	6,456*22 =142,000	0 (free heating)		
Total Cost, SR /22 y	1,711,500	1,613,211	1,759,678	
Power saving, SR /22 y	0	31,066*22= 683,460		
Net total cost /22 y	1,712,000	929,750	1,076,217	
<b>Saving % /22y</b>	<b>0</b>	<b>45.67 %</b>	<b>37.11 %</b>	

### 4.8.3 Simple payback periods

The payback period (PBP) is the easy way to determine the time required to cover the costs. The PBP is the ratio between the differences in the total cost to the difference in the operation cost. The cost and energy performance are the only two parameters considered in the PBP. The Department of Energy, USA (DOE) does not consider PBP as a cost-effectiveness tool because it does not include the long-term factors such as the replacement costs and the time value of money. The simple payback period [56] can be summarized in the following equation:

$$PBP = \frac{K_2 - K_1}{(E+M)_1 - (E+M)_2} \quad (4.12)$$

where,

PBP = payback time, years. K = capital investment.

E = annual energy cost.

M = annual maintenance cost.

1 = system under consideration (ASHP). 2 = alternative system (GSHP).

The annual maintenance cost, M, is given by

$$M = \frac{0.5 * K}{\text{year of life cycle}} \quad (4.13)$$

$$M_2 = (0.5 * 240000) / 22 = 5454$$

where we have assumed that the maintenance cost for ASHP  $M_1$  is double  $M_2$ .

From Tables 7 and 8, equation (4.13) becomes:

$$\begin{aligned} PBP &= \frac{731,640 - 16000}{(77795 + 10909)_1 - (46729 + 5454)_2} \\ &= 15.7 \text{ years.} \end{aligned}$$

#### 4.9 Underground Thermal Imbalance

For the GSHP to operate effectively and efficiently there has to be a balance in the underground thermal conditions. This balance means that heat released into the ground by heat exchangers on an annual basis should equal that extracted from the ground. This stability, however, can easily be disrupted by climatic conditions surrounding the buildings. In a cold climate, more heat will be taken from the ground to keep the buildings warm and less will be replaced [105]. In a hotter climate, where internal cooling is the priority, the reverse will take place. If these fluctuations are not properly controlled, then

a thermal imbalance will occur in the soil due to reductions or increases in the ground temperature. This in turn will cause deterioration in the performance of the heat exchangers and heat pumps, leading eventually to failure of the systems. In addition, groundwater and soil type play an important role in the thermal load imbalance rate [105].

Ignoring the lack of thermal balance in the design stage leads to low system efficiency [106]. The imbalance ratio (IR) is defined as:

$$IR = \frac{Q_{inj} - Q_{ext}}{\max(Q_{inj}, Q_{ext})} * 100\% \quad (4.14)$$

where  $Q_{inj}$  is the accumulated heat rejected to the soil in the cooling seasons and  $Q_{ext}$  is the accumulated heat extracted from the soil in the heating seasons.

To determine the accumulated heat for the GSHP the COP and EER for the GSHP is assumed to be 4.4 and 14.9 respectively based on the catalogue and the ground load is determined as follows:

$$\text{Cooling load, } Q_{lc} = 196.2 \text{ kW} * 3412.142 = 669,462 \text{ Btu/h}$$

$$\text{Heating load, } Q_{lh} = 38.1 \text{ kW} * 3412.142 = 130,002 \text{ Btu/h}$$

In the cooling mode, the condenser rejects heat to the ground heat exchanger, and the evaporator extracts heat from the load. The heat rejected at the condenser is given by

$$\begin{aligned} Q_{cond} &= Q_{lc} ((EER + 3.412) / EER) \\ &= 669,462 \text{ Btu/h} * (14.9 + 3.412) / 14.9 \\ &= 882,762 \text{ Btu/h} \end{aligned}$$

The heat extracted at the evaporator is given by

$$\begin{aligned}Q_{\text{evap}} &= Q_{\text{lh}} * (\text{COP} - 1)/\text{COP} \\ &= 130002 * (4.4 - 1)/4.4 \\ &= 100,456 \text{ Btu/h}\end{aligned}$$

Thus, the thermal imbalance ratio is given by

$$IR = \frac{100456 - 882762}{882765} \times 100\% = 88\%$$

The negative IR indicates that the heat transfer to the soil is more than the heat extraction which normally occurs in cooling dominated situations. A lower IR means a smaller difference between the heating and cooling loads. However, the thermal balance is the subject of our further investigations where we are attempting to simulate the whole system by using TRNSYS, but this is a very challenging and novel approach.

#### **4.10 Discussion of the Results of this Saudi Arabi Application**

The data for this example on the viability of GCHPs for small commercial buildings in a hot/dry climate, exemplified by Saudi Arabia gives a useful comparison of the energy consumption between ASHPs and GSHPs and indicates the relative effectiveness of both systems. The ASHRAE standards were used to determine the length of the GHX and from the results detailed above the following can be drawn:

- The thermal properties of the soil and climate conditions have been analysed and this study shows that the soil temperature is 29°C and the average thermal conductivity of the soil is 2.6 W/mK.

- Accurate soil temperatures and thermal conductivity would result in savings of 20-30 % in the bore lengths and a 3°C increase in the soil temperature from 26°C to 29°C would lead to an increase of 42% in the length of the GHX from 4082 m to 5831 m.
- In the heating season, the GSHPs are able to heat the building as free heating (passive heating) due to the high temperature of the ground.
- The total cost savings of 22 years were determined for 45% and 37% at underground temperatures 26°C and 29°C, respectively.
- The total annual cost of the power consumption for the GSHP is less than for the ASHP by 34.6%.
- The payback period would exceed 15.6 years when compared to the ASHP system. This may be due to the high initial cost required for the installation of GSHPs.
- One of the key challenges of GSHP systems in hot dry climates is the thermal imbalance.

#### **4.11 Conclusion**

In this study, comparison between GSHP and ASHP systems shows that GSHPs are technically feasible to use for air conditioning systems in hot dry region due to the significant temperature difference between the ambient air and the ground. However, the underground temperature is the most important factor in determining the GHX length which led to the lengthy payback period and increase in the initial cost.

This study also clearly shows that with the GSHP approach to cooling and heating, there will be a reduction in the energy consumption in buildings in Saudi Arabia and hence the cost. It will also help to minimize the CO<sub>2</sub> emissions in the region. The same result may be applicable to similar environmental conditions both in the Middle East and in other hot, dry climates with cool periods.

# **Chapter 5: Modelling of Ground and Air Source Heat Pumps in a Hot and Dry Climate**

---

## **5.1 Introduction**

After the encouraging results of the numerical analysis of GSHP in the fourth chapter, the simulation and evaluation of the performance of GSHPs compared with systems employing ASHPs are described in detail in this chapter. Both systems were comprehensively modelled and simulated using the Transient System Simulation (TRNSYS). Also, the Ground Loop Design (GLD) software was used to design the length of the ground loop heat exchanger. In order to assess this configuration, an evaluation of a model of a single-storey office building, based on the climatic conditions and geological characteristics that occur in the city of Riyadh in Saudi Arabia, was investigated. The period of evaluation was twenty years, in order to determine the COP, energy efficiency ratio (EER) and powerconsumption.

## **5.2 Literature Review**

Over time, ASHP have become the most popular and commonly used systems for cooling and heating. These use outside air for both climate seasons, one for the heat source and the other for the heat sink [107]. External temperature variations can cause a drop in performance in either season if, for example, the summers are too hot or the winters too cold.

On the other hand, GSHPs are considered the most efficient HVAC technology [108],[109] because the underground temperature remains almost constant all year-round. This means that theeffect of the ambient temperature is limited and the difference in temperature between what is considered desirable (inside the building), and the surrounding medium (underground soil) is small compared to the outside temperature. This is due to the fact that the underground temperature relates favourably to the annual average air temperature, particularly at ten metres in depth whereit remains almost constant.

However, despite GSHPs being well established in cold regions worldwide, their use remains limited in hot and dry regions, such as in the MENA countries. Unfortunately, very few studies are available concerning the use of geothermal heat pumps in hot climate regions.

In contrast, in a harsh cold climate where there is a high demand for heating, such as Canada and the Scandinavia countries, GSHP has proven its ability to produce highly efficient results. For example, Healy and Ugursal [110] compare the economic feasibility between GSHP and three conventional heating systems, including (electric resistance heat, oil-fired furnace and ASHP) for a residential house in Nova Scotia, Canada where the required heating load was 22,800 kWh compared to 2,300 kWh for cooling. The study illustrated that the GSHP system is the most economic system for the fifteen-year life period.

In moderate Mediterranean climate zones, such as Cyprus, Paul et al. [111] investigated the feasibility of using GSHPs compared to ASHP based on experimental data and a CFD model. The study showed that the long payback period of the GSHP and the nowadays high efficiency of ASHP systems reduced the chances for the economic success of GSHP.

A representative experimental investigation was carried out to assess energy savings on a comparative basis between GSHP's and ASHP's, has been performed in Arizona, US. The data emerged as a result of an initial feasibility study [56] into the use of a GSHP system for a small office building in the capital, Phoenix. The results showed that a 40% saving in energy could be achieved by using the GSHP, compared to the ASHP. However, an important variable emerged.

Safa et al. [112] in their study monitors and simulates the performance of GSHPs compared to ASHPs based on Canadian climate. Both these systems were installed at Twin Houses - sustainable housing- in Ontario, Canada. The ambient temperature is very from (-19 °C ~ 9 °C) in wintertime and from (16 °C ~ 33 °C) in the summertime. Both Heat pump performance was monitored for 23 days in summer and winter. The experimental results from 23 days of monitoring in the summer



and winter showed that the performance of GSHPs is better than ASHPs. The COP value in the hottest time was 4.9 for GSHP compared to 4.7 for the ASHP. At the highest heating demand (-19°C), the COP was 3.05 and 1.79 for GSHP and ASHP, respectively.

Likewise, Abdel-Salam and Zaidi [113] conducted two-part research to determine the performance of GSHPs in the winter and summer seasons in two single-family detached houses in Canada. COP and total power consumption were monitored, analysed and evaluated over one cooling and heating season. The experiment results show the GSHP able to meet the peak heating load with sufficient COP above 4. Furthermore, the total power consumption of GSHPs is less compared to ASHPs by 66% and 46% for cooling and heating seasons, respectively.

From the short literary reviews above, it is clear the performance of the GSHP achieving a very high COP with a long-term analysis in very cold areas, where there is a significant difference between the outside temperature and the ground temperature. These results encourage the study of GSHP in very hot regions such as Saudi Arabia and finding the most critical factors affecting GSHP performance in such claimant.

Furthermore, the acceptability of a new system depends on its efficiency and cost-effectiveness. The purpose of this chapter is to increase the accuracy by analysing the behaviour, performance and technical feasibility of a GSHP compared to the equivalent ASHP in a very harsh hot climate, such as Saudi Arabia. The industry standard modelling tool [83] TRNSYS was used to developed and model both systems under the climate and geological characteristics of the city of Riyadh in Saudi Arabia.

### **5.3 System Simulation Using TRNSYS.**

#### **5.3.1 Building envelope model**

In this chapter, an exemplar building has been selected for the comparison. The design of the building envelope represents a typical house or small commercial building in a city. As shown in

Figure 5.1, a single storey office building has been considered for the purposes of this simulations. With the simplifications that have been introduced, the model is not intended to be architecturally realistic, but this does not affect the general results.

Despite the building envelope being outside the scope of this research, the scientific approach used here is a general one, which other users could apply to real designs. In this case, the selection of envelope elements would lead to accurate energy predictions and would also be a useful guide to select the most appropriate size for an HVAC system. Therefore, in most cases, the building's envelope and orientation would have a significant impact on the simulation results.

The total building surface area is about 120 m<sup>2</sup>, the height is 3m with a gross volume of 360 m<sup>3</sup>. There are windows on three sides of the building and the fourth side has a main door. There are no sun shading devices and the sun affects all sides of the building. This means that the cooling loads will be much higher than normal.

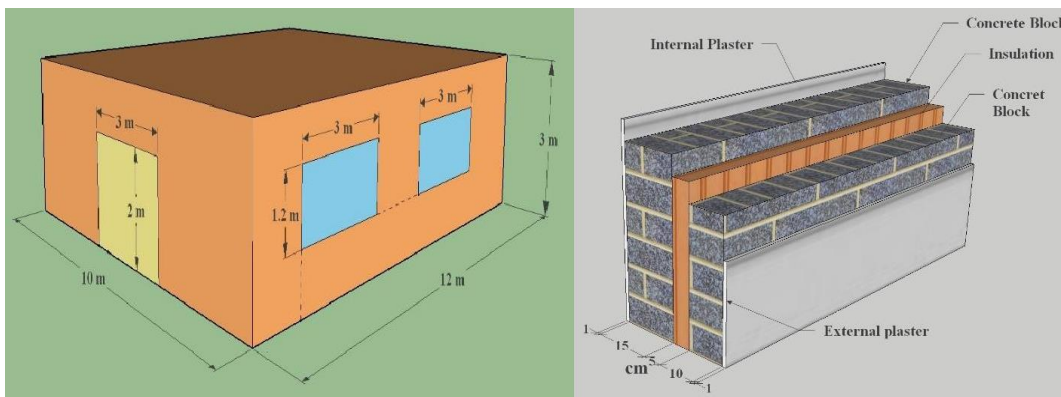


Figure 5-1 (a) Schematic of the single-storey office building investigated. (b) Walls Construction

### Details

TRNSYS (TRNSYS3d and TRNBuild) were used to simulate the thermal performance of this building. The main thermal compulsory characteristics of the building envelope, such as being thermally insulated, meant that the U-values for walls, roof and windows were chosen, based on the Saudi Building Code 2018 [114] the minimum requirements shown in this code, based on the building location zones (See Figure.5.2) are set out in Table 5.1. This model will be used in

comparison to both systems. Despite the lower the U-value being the best, the wall, roof, windows and door U-value were defined as 0.24, 0.20, 2.80 and 2.60 W/ m<sup>2</sup> K, respectively.

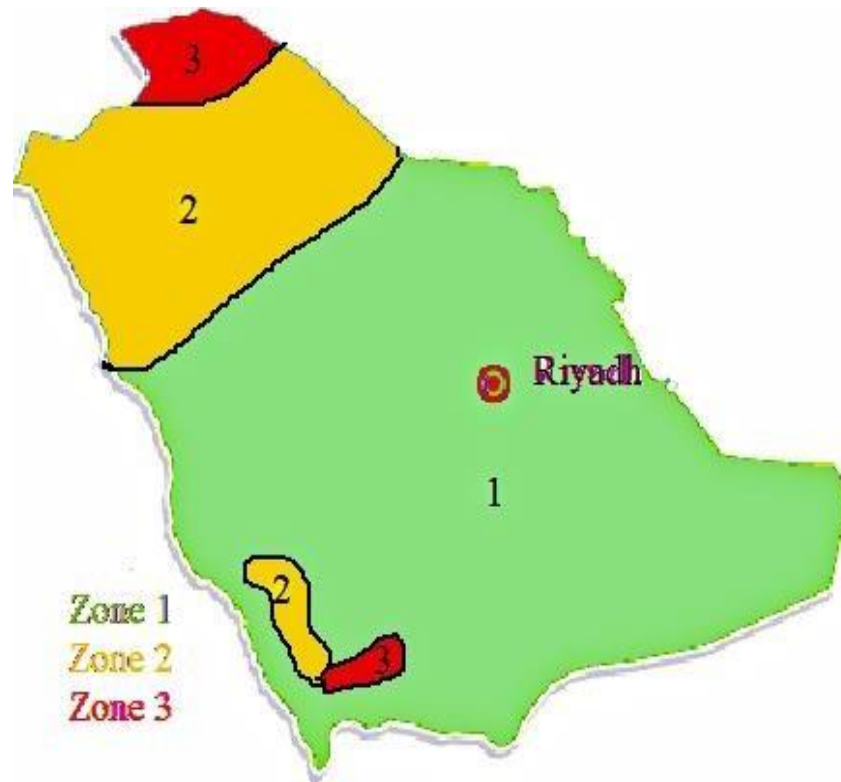


Figure 5-2 Saudi Arabia Climate Zones based on the Saudi Building Code [16].

Table 5.1 The U-Values for low-rise / residential buildings [16].

Opaque Elements (W/ m <sup>2</sup> K)	Zone 1	Zone 2	Zone 3
Roofs	0.20	0.24	0.27
Walls	0.34	0.4	0.45
Opaque Doors –All Assemblies	2.84	2.84	2.84
Vertical Glazing - 25% of wall All Assemblies	2.67	2.67	2.67
Skylight with Curb Glass	4.26	4.26	4.26
% of Roof % -3% All Types			

### 5.3.2 Building load estimation

Saudi Arabia is a large country with different climate zones and different geological characteristics from one region to another. More information about the natural environment of Saudi Arabia can be found in section 4.2 [94]. The capital city of Riyadh has been selected to be the location for this study. The city has a very hot and dry climate in summer with generally mild weather in winter, with little rainfall and low relative humidity.

In order to investigate the energy use, TRNSYS software has been employed to estimate the cooling and heating loads. The size of a heating or cooling system for a building is determined on the basis of the desired indoor conditions that must be maintained, based on the outdoor conditions that exist at that location. Table 5.2 shows the design conditions for the building, based on the climate in Riyadh and the ASHRAE standard. For example, the building of the ventilation rate use was based on the ANSI/ASHRAE Standard 62.1-2010 (Ventilation for Acceptable Indoor Air Quality).

Table 5.2 Design conditions for the building investigated: summer period.

Outside conditions	44 °C RH 45% - August
Inside conditions	24 °C RH 50%
Area	120m <sup>2</sup> with suspended ceiling, 3m Height
Located	24.4 N
Operation hours	8:00 am to 6:00 pm weekdays.
People	Assumed 12
Equipment	Assumed 12 W/m <sup>2</sup>
Lighting	Assumed 20 W / m <sup>2</sup>
Ventilation / person	Assumed 8.5 l / sec

Based on the design conditions shown in Table 5.2, the cooling and heating loads were computed by employing TRNSYS for all months, as shown in Table 5.3 and Figure.5.3. Based on the local climatic and design conditions, the maximum cooling and heating loads were 14 kW and 10 kW, respectively. It will be seen that the annual equivalent full load hours (AEFLH) were to be 2,552 and 374, respectively.

Table 5.3 Estimated cooling and heating loads for the building investigated.

M	Cooling load		Heating load	
	kWh	Peak (kW)	kWh	Peak (kW)
Jan	3	1	1,701	10
Feb	96	5	896	7
Mar	789	7	121	4
Apr	2,230	10	1	1
May	4,952	13	0	0
Jun	5,793	14	0	0
Jul	6,587	14	0	0
Aug	6,631	14	0	0
Sep	4,854	12	0	0
Oct	2,916	10	0	0
Nov	606	6	137	4
Dec	27	2	1159	7
	cumulative	max. peak	cumulative	max. peak
	35,484	14	4,014	10

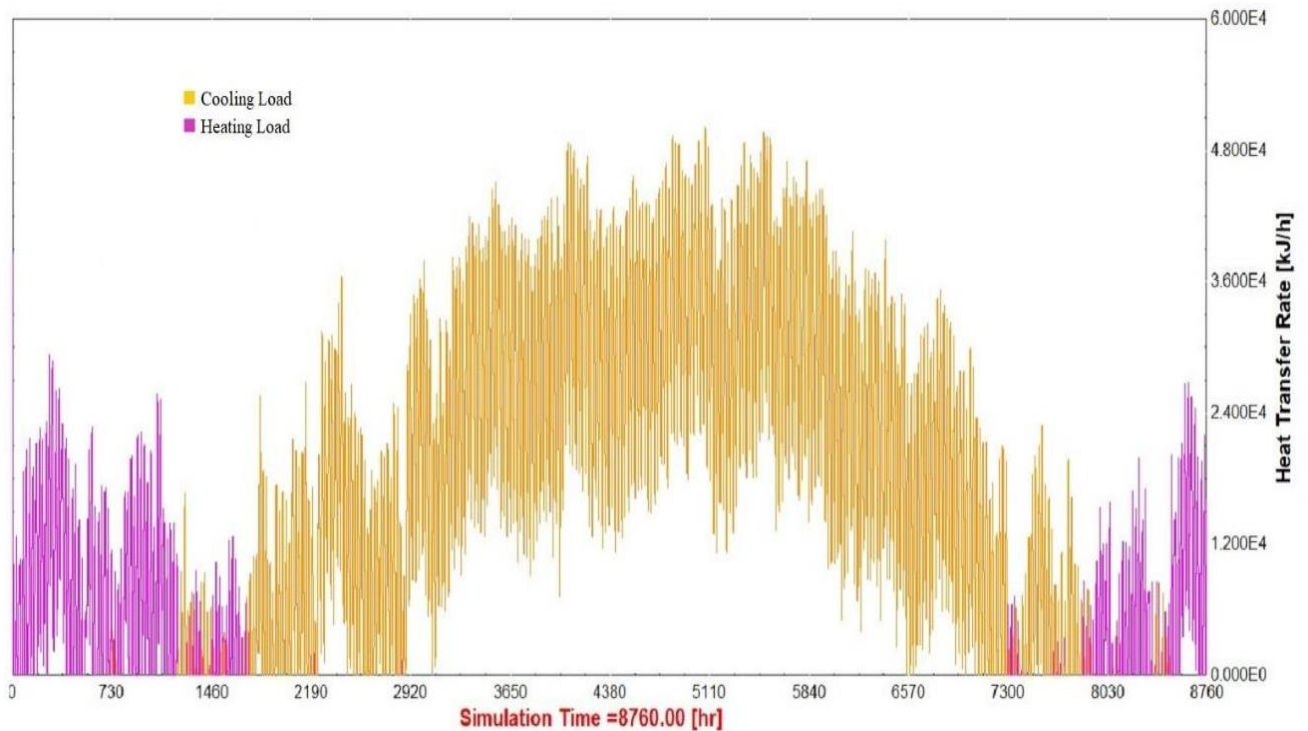


Figure 5-3 Cooling and heating loads for the building created by TRNSYS.

### **5.3.3 Heat pump simulation**

The main advantage of a heat pump is the ability to transfer more energy than it consumes. As mentioned in Section 2.6.4, COP and EER describe the performance of the heat pump, and in prevailing discussion the COP term is used to describe the performance of the heat pump.

In fact, there are several unconventional ways to increase the efficiency of the heat pump, for example, Johnson controls [115] is one case where the wastewater from the bathroom increases the efficiency of the heat pump in cold climates, where the efficiency increases by 55%. Likewise, Afshari [116] investigated experimentally and numerically the effect of the implementation of a thermoelectric cooler on the heat pump COP of air-to-water and air-to-air thermoelectric coolers. The results show that a 30–50% higher COP could be achieved from an air-to-water rather than an air-to-air system. Both these research are helpful to further improve performance of GSHP and ASHP systems.

In addition, it is known that the refrigerant type affects the COP of the system. However, the effect of the refrigerant type is beyond the scope of this paper. Therefore, the same coolant R-410a was used for both ASHP and GSHP so that performance of both can be easily compared. Furthermore, R-410a is selected as refrigerant because it is conventionally used refrigerant in Saudi Arabia as well as worldwide and their properties are very promising and have minimum environmental effect.

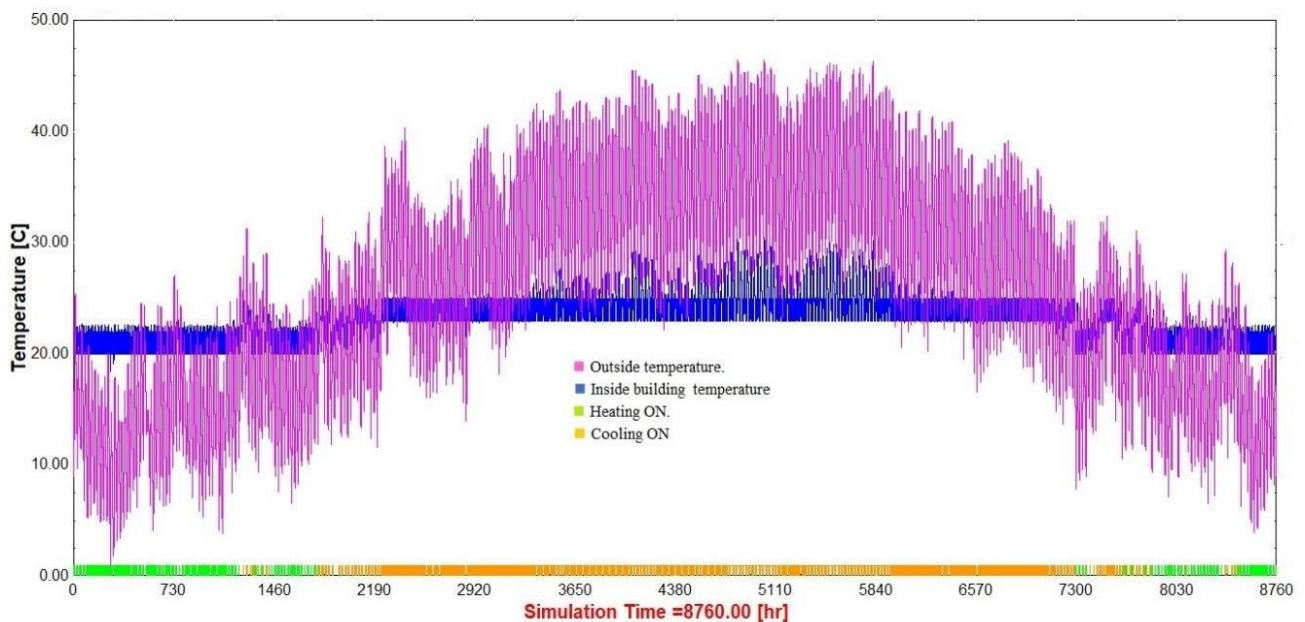
#### **5.3.3.1 Air source heat pump.**

The ASHP system is the traditional system used for refrigeration and air conditioning in residential buildings and small business buildings in Saudi Arabia.

For simulation purposes with this modelling package, an air-to-air heat pump, type 119 was selected; this was the rooftop unit YORK ZE/EN series [117]. The data in the manufacturer's catalogue was used to model the ASHP (attached in Appendix 4). The capacity of the pump selected was 10.5 kW and 17.5 kW for the heating and cooling, respectively. While this is higher

than the value given in Table 5.3 it is a safety factor to account for extreme events.

The simulation runs for a full-year period based on the TMY2 (typical meteorological years) data and the input data for TRNSYS attached in Appendix 3. During the test period, the ambient temperature varied from 0 °C to 45 °C. Figure 5.4 shows the outside temperature and inside set temperature (21 °C in the winter and 24 °C in the summer) when the ASHP was operating, and the model time step was 0.02/ hour (1 minute, 12 seconds). In addition, Figure 5.4 shows the operation period for the ASHP in both cooling and heating (heating on and cooling on). It is clear that the cooling remained dominant most of the year with 8 months when there is a large difference between the indoor and outdoor temperature, this is up to 21 °C in the summertime which requires substantial work from the compressor, which adversely affects the performance of the system.

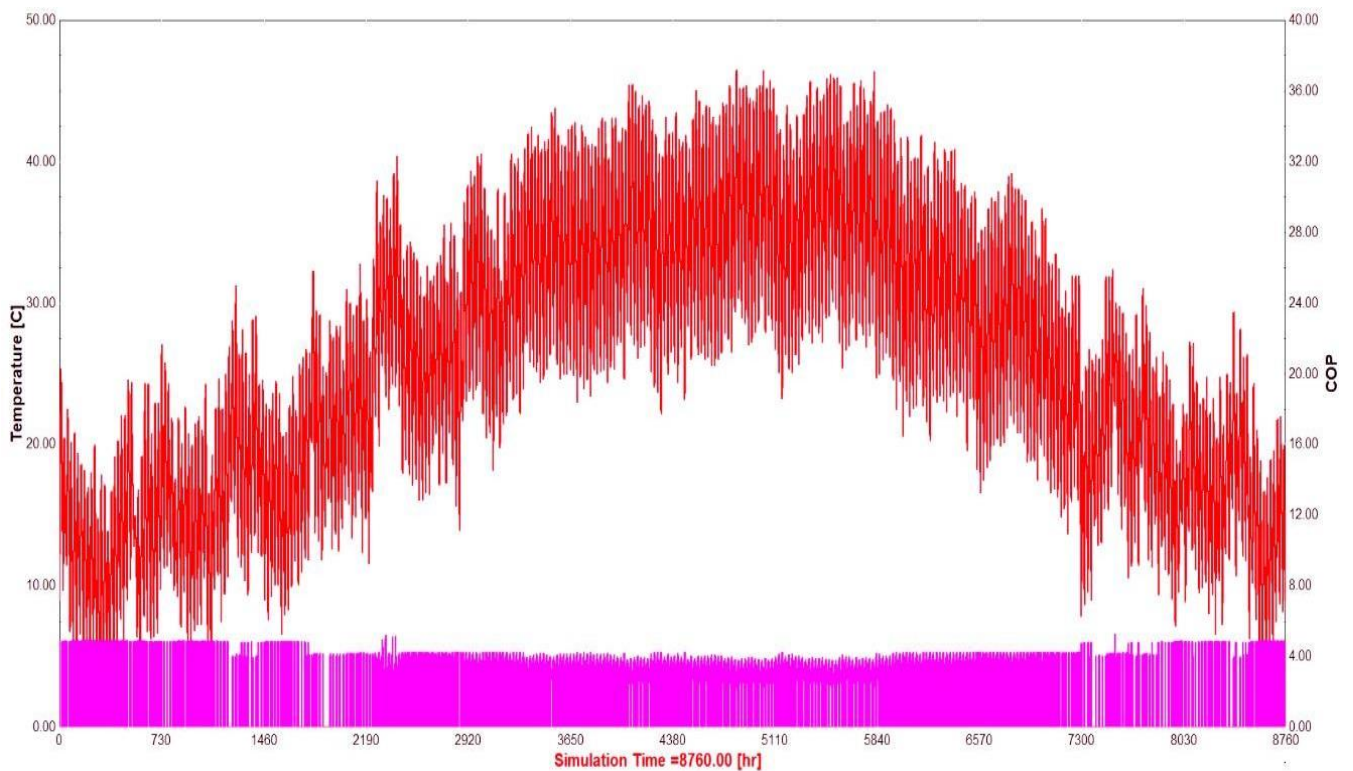


*Figure 5-4 Outside and inside building temperature during the simulation period.*

In these regions, the hottest months provide a challenge for ASHP systems as the ambient temperature can reach 50 °C. Thus, we must place a greater emphasis on the hottest months when calculating the COP and EER. Figure 5.5 shows the COP for the ASHP during the simulation period and Table 5.4 shows the average monthly COP and power consumption during the simulation

period that starts at midnight on 1<sup>st</sup> January until midnight on the 31<sup>st</sup> December (8,760 calendar hours).

In this chapter, the ASHP unit has been selected and this is similar to the GSHP unit in terms of characteristics and specifications (such as the source of power, refrigeration type, compressor type, unit efficiency and the cooling/ heating capacity) in order to make a fair comparison between the two systems.



*Figure 5-5 COP for the ASHP unit.*



Table 5.4 The annual COP and power consumption of the ASHP and GSHP units.

M	Overall power consumption kWh			Overall COP	
	GSHP	ASHP	% Saving	ASHP	GSHP
Jan	362	684	47	4.71	5.32
Feb	170	290	41	4.68	5.32
Mar	148	210	29	4.29	4.21
Apr	686	963	29	3.55	4.03
May	1,379	2,210	38	3.36	3.80
Jun	1,693	2,806	40	3.22	3.59
Jul	2,025	3,271	38	3.15	3.47
Aug	2,116	3,366	37	3.14	3.37
Sep	1,490	2,244	34	3.36	3.42
Oct	797	1,069	25	3.60	3.56
Nov	144	179	20	4.16	3.82
Dec	174	312	44	4.73	5.40
Overall	11,183	17,602	36	3.83	4.11

### 5.3.3.2 Ground source heat pump modelling

The GSHP can be seen to be more efficient than the ASHPs and, incidentally, it is also classified as a renewable energy system because GSHP uses the heat from the underground as a source of energy. Generally, GSHPs consists of three main parts: a heat pump, a distribution system and the GHX. Thus, understanding the geology and hydrogeology of the underground soil (ground layer) is an essential element in the design process for a GHX. Additional information on the geothermal conditions in Saudi Arabia can be found in section 4.5 [47]. For the purposes of this study, two elements must be carefully calculated to obtain the optimum length of the GHX, namely the thermal conductivity and the underground temperature.

#### 5.3.3.2.1 Thermal conductivity

For the purposes of this study, variable geological characteristics were obtained from the report prepared for the Ministry of Petroleum and Mineral Resources in Saudi Arabia and the US Geological Survey [97] so as to be able to investigate the heat-flow measurements. The soil in Riyadh consists of clay, silt, sand and gravel in different proportions. However, the thermal geological characteristics of the soil [47],[97] can be summarized as follows:

- Average thermal conductivity is 2.6 W/mK.

- Thermal diffusivity is  $6.252 \times 10^6 \text{ m}^2/\text{s}$ .
- Thermal resistance is  $0.315 \text{ mK/W}$ .

### 5.3.3.2.2 Underground temperature

ASHRAE standards and many simulation programs, such as TRNSYS, use equation (4.1) to calculate the underground temperature at different depths. Figure 5.6. shows the underground temperature for Riyadh city at different depths based on the daily weather data collected for Riyadh city, 2018. It is clear that the underground temperature for Riyadh city at a depth of over 10 m is assumed to be  $26.5 \text{ }^\circ\text{C}$ . However, in this work, the value of  $29 \text{ }^\circ\text{C}$  was used in the TRNSYS simulation, based on the experimental studies [97] that have been performed at five different locations in Saudi Arabia. This investigation is therefore a pessimistic scenario.

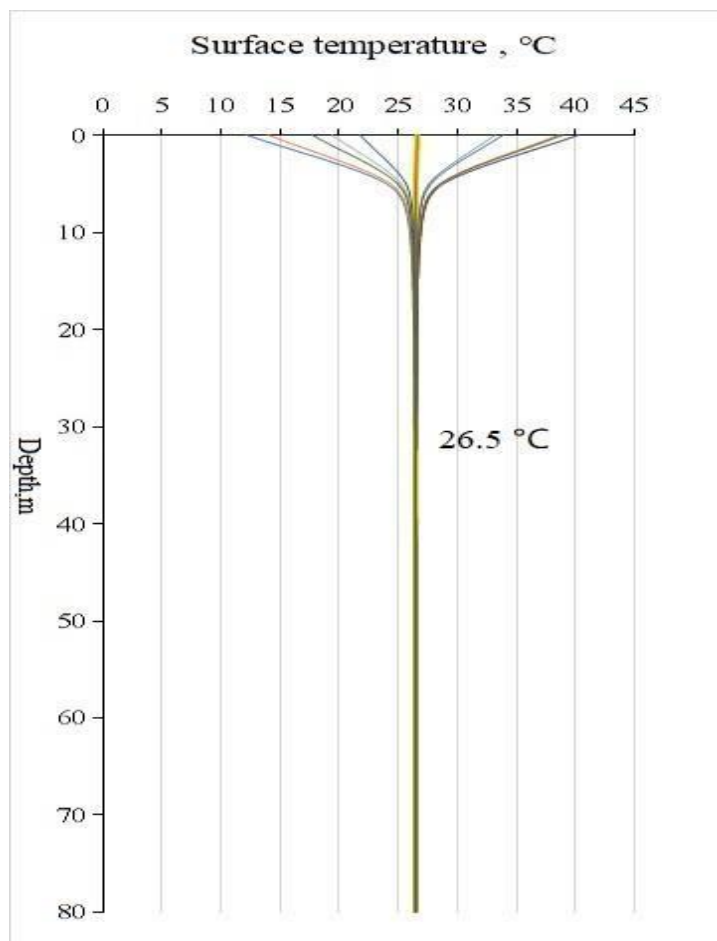


Figure 5-6 Underground temperature for Riyadh city at different depths.

## 5.4 Sizing of the GHX

Correctly determining the length of the heat exchanger significantly determines the economic feasibility of using GSHP. The initial cost of the geothermal pump related to the cost of implementing the geothermal heat exchanger and geological studies for the region.

Based on the thermal conductivity and underground temperature as calculated above (2.6 W/mK and 29 °C, respectively) two methods have been applied to estimate the size of the GHX as follows:

- i. ASHREA method as before in chapter 4 section 4.7.2.
- ii. Ground loop design software, GLD [86].

Both methods are based on the monthly and peak loads in Table 5.3. A single borehole with a diameter of 128 mm and 6 m spacing between pipes was employed and the borehole characteristics and considerations are shown in Table 5.5.

Table 5.5 Design input data of the GHSP.

Design input data	Specification
Borehole diameter	128mm
Pipe type	HDPE, SDR11
Pipe thermal conductivity	0.38 W/mK
Inside diameter	34.5 mm
Outside diameter	42.2 mm
Fluid type	Water
Soil thermal conductivity	2.6 W/mK
underground temperature at 60m depth	29 °C
Prediction time	22 Years

### 5.4.1 ASHREA standards method

The use of the ASHRAE standards equation to calculate the length of GHX is widely used to give preliminary results of the total well length [69]. The length ( $L_c$ ) to satisfy the cooling loads can be expressed based on Eq. (4.2) which obtained from the ASHRAE (2017) online Handbook –HVAC application, Chapter 34. Based on the data calculated above the required length of the GHX in order to satisfy the cooling loads was estimate as follows:

$L_c = 400$  m is the total length for the heat exchanger loop at 29 °C.

### 5.4.2 Ground loop design software, GLD

The GLD software is a monthly, and hourly analysis program tool [87] which has been employed in this study in order to estimate the GHX length. The length obtained from this simulation was found to be 400 m. Thus, in this simulation, the result obtained from the GLD, which was 400m total length is used in the TRNSYS analyses. Furthermore, the inlet and the outlet water temperatures were 39.4 °C and 45.6 °C, respectively. Figure 5.7 shows the average entering water temperature to the GSHP unit for a 22-year period.

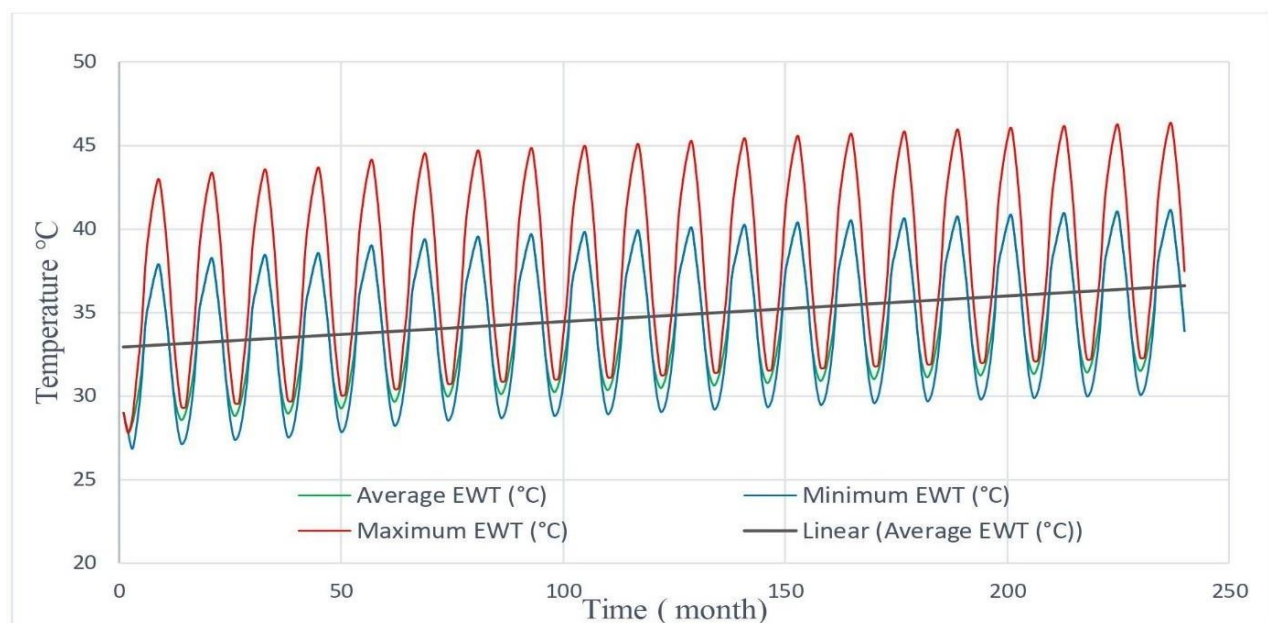


Figure 5-7 Average entering water temperature to the GSHP unit for a 22 year period by the GLD.

## 5.5 Ground Source Heat Pump Simulation

To provide the literature with information on the use of a GSHP in a hot/dry climate, TRNSYS has been used to simulate the whole system. Similar to ASHP, for simulation purposes with this modelling package, a water to air heat pump, type 919 was selected. The data in the manufacturer's catalogue (ClimateMaster – Tranquility 30 Digital (TE) Series – (attached in Appendix 4) was used to model the ground source heat pump. The capacity of the pump selected was again 3 and 5 ton for heating and cooling, respectively. This is higher than the value presented in Table 5.3 in order to include a safety factor. The office building was modelled in TRNSYS v. 18 using the multizone building component (Type 56a). The TRNSYS model shown in Figure 5.8.

The simulation was run for a twenty-year period based on the TMY2 (typical meteorological years) data. In the TRNSYS model, the characteristics and considerations of the borehole are the same as those used in sizing the GHX in Table 5.5. The simulation results' emphasis is on the amount of energy conservation and liquid flow temperature that leads to the identification of the properties of the surrounding ground. Figure 5.9 shows the COP for the GSHP during the simulation period, and Table 5.4 shows the COP and monthly power consumption during the simulation period, as well as the savings rate for both systems.

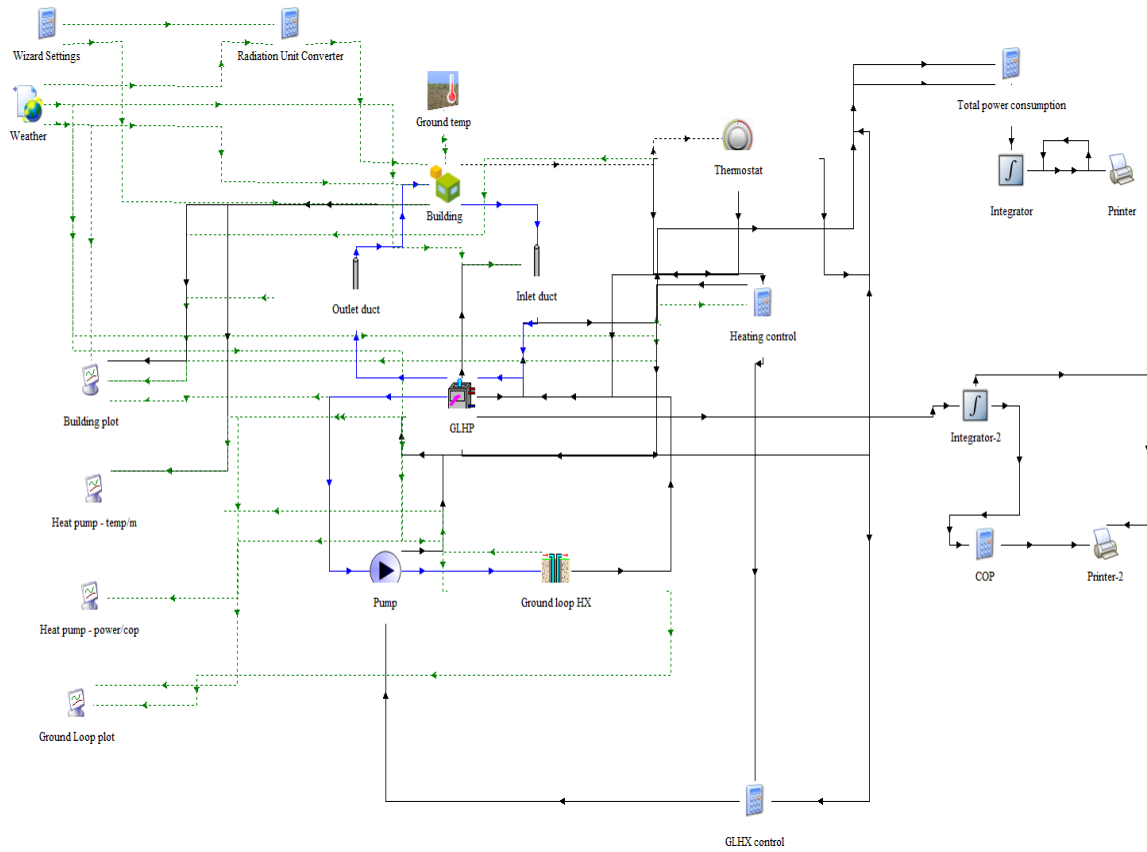


Figure 5-8 The TRNSYS model.

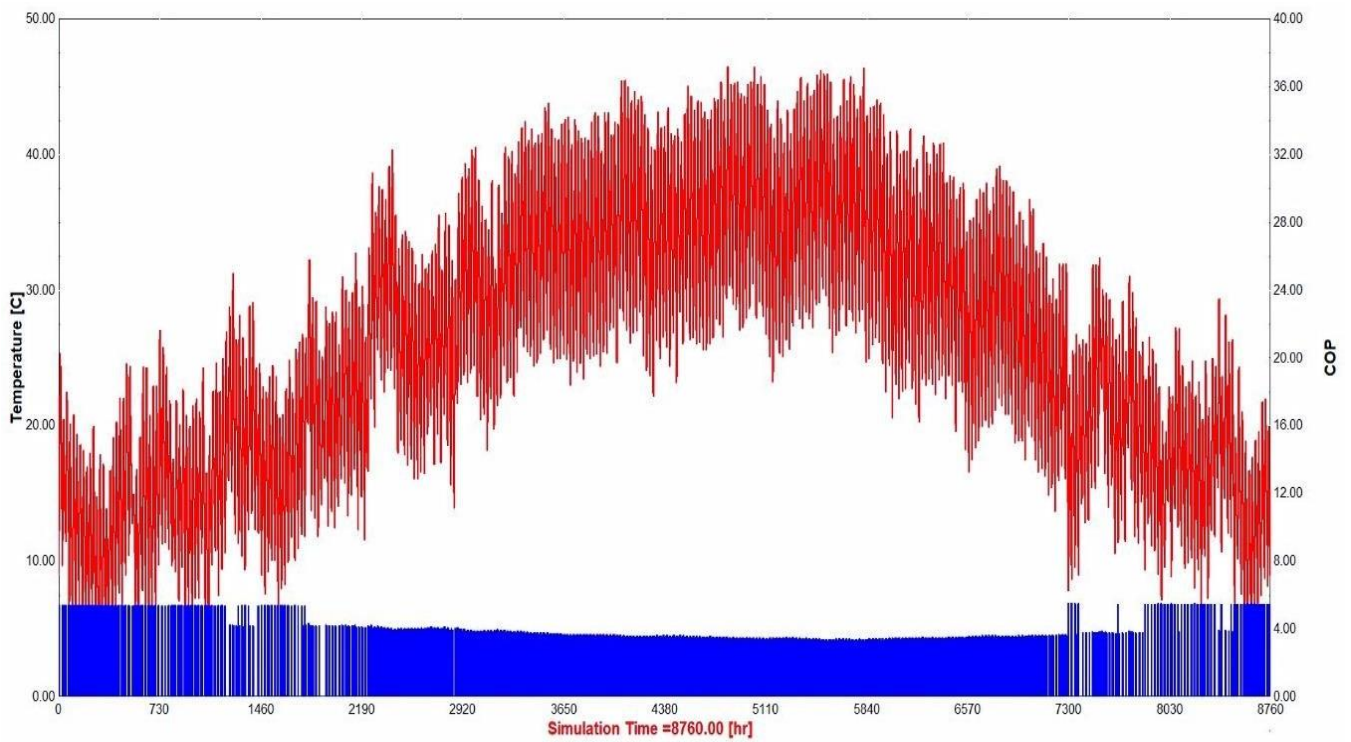


Figure 5-9 COP for the GSHP unit.

## 5.6 Results

### 5.6.1 Savings on the power consumption

Energy consumption is an essential factor that determines the efficiency of the system. The monthly energy consumption of the GSHP and ASHP systems are compared in detail in Table

5.4 and Figure 5.10. It is shown that in the hottest months (June - September) the power consumption using the GSHP is approximately 37% less than that from ASHP. In addition, in the winter season, the monthly consumption value of electricity remains less than the summer in the two systems, with the GSHP system reducing the electricity use by approximately 44%. Figure 5.11 shows the comparison of the COP for the GSHP and the ASHP.

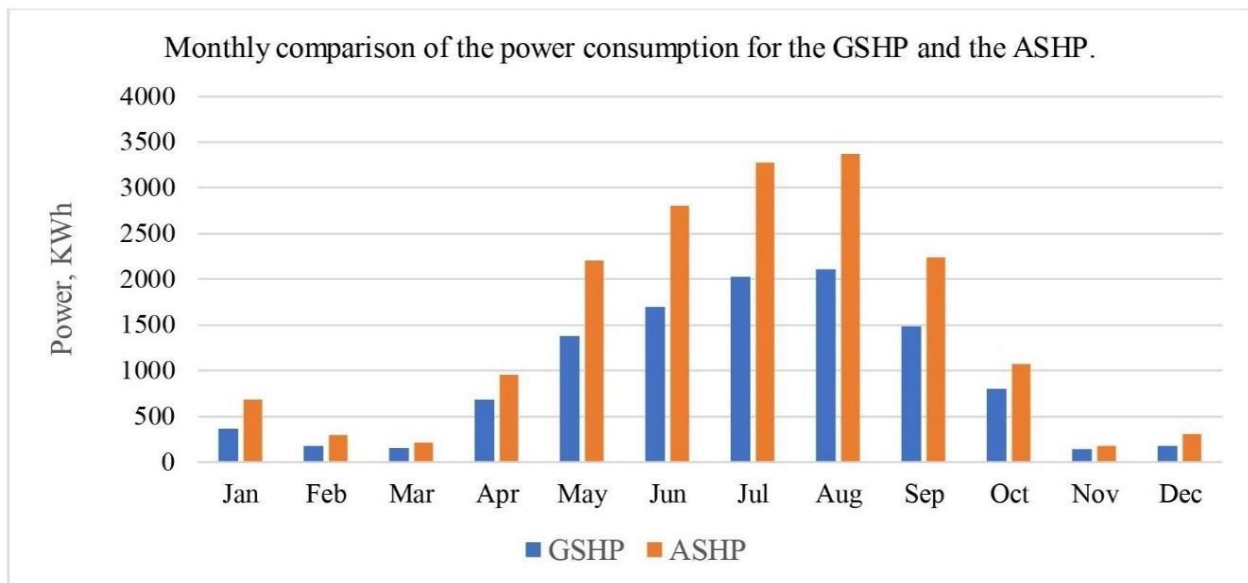


Figure 5-10 Comparison of the power consumption for the GSHP and the ASHP.

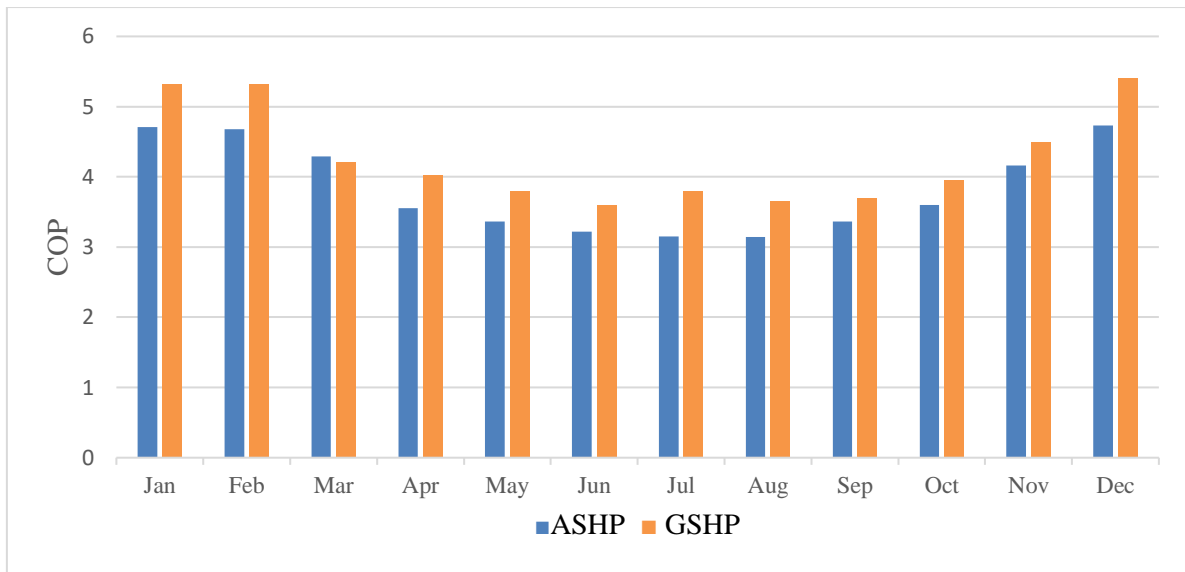


Figure 5-11 Comparison of the COP for the GSHP and the ASHP

From Table 5.4, it is observed that the total energy required is 11,183 kWh per year and 17,602 kWh per year for the GSHP and ASHP respectively. Saudi electricity cost (SR 0.32) per kWh, and from Eq. (4.10) the annual electricity cost is determined as follows:

$$\begin{aligned} \text{For GSHP electricity cost} &= 11,183 \text{ kWh} \times \text{SR } 0.32 \text{ per kWh} \\ &= \text{SR } 3,579 \text{ per year} \end{aligned}$$

$$\begin{aligned} \text{For ASHP electricity cost} &= 17,602 \text{ kWh} \times \text{SR } 0.32 \text{ per kWh} \\ &= \text{SR } 5,632 \text{ per year} \end{aligned}$$

$$\text{Annual cost saving} = 5,632 - 3,579 = \text{SR } 2,053$$

A total reduction of approximately 36% in the annual of electricity can be obtained by using a GSHP system. This saving does not include the cost of the power to produce the hot water that can again be produced by the GSHP. On the other hand, the energy consumption by the circulating pump is not included in the total electricity consumption.

Therefore, using the GSHP not only reduces the total power consumption but also reduces the overall CO<sub>2</sub> emissions. For the purposes of calculating the annual rate of the CO<sub>2</sub> emissions, CO<sub>2</sub>



emission can be expressed as follows:

$$\text{CO}_2 \text{ emissions} = \text{Emissions Factor (EF)} \times \text{power Consumption kWh} \quad (5.7)$$

Based on the Carbon Footprint Ltd. [118] the EF for Saudi Arabia is estimate as 0.7176 KgCO<sub>2</sub> /kWh. As a result, from Table 5 the GSHPs saving is 6,419 kWh/year and this leads to a saving of 4,606 kg CO<sub>2</sub>/year.

### 5.6.2 Initial cost analysis

When comparing the two air condition systems, two cost factors play a crucial role in determining the feasibility of using the new system, namely the initial cost and the life-spancest. Table 5.6 shows the total cost over a 22-year period and the parameters that effect theinitial value for both systems.

Table 5.6 The cost analysis for the ASHP and GSHP for 22 years.

	ASHP	GSHP
GHX Loop length, m	-	400
Unit price	20,000	10,000
Drilling cost, SR	-	40,000
GHX Pipe price, SR	-	1,000
Installation GHX, SR	-	6,000
Total initial cost, SR	20,000	57,000
Maintenance /22 y	56,980	28,490
Power consumption cost, SR/ y	5,632	3,579
Power consumption cost, SR/22y	5632×22 =123,904	3,579×22 = 78,738
Total cost for 22 years	200,884	164,228
Total saving	18.24 %	

It is important to note that the unit life-span of the GSHP is assumed to be double that of theASHP. The typical life-span of the ASHP is 10–15 years but in harsh climates, such as SaudiArabia, the ASHP is exposed to very high ambient temperatures, corrosion in the coastal region and dust. Due to this, the lifetime of the ASHP is assumed to be 11 years. On the other hand, the GSHP system is located indoors and is not exposed to external factors and atypical life-span is 20-25 years; thus 22 years is assumed as the lifetime of the GSHP.

Furthermore, the hot water production is a positive point for GSHPs. Since the GSHP is installed in the basement, the boiler to produce hot water can be combined with the GSHP easily compared

to ASHP, which is usually located outdoor (most of the time on the top of the roof), and thus exposed to external factors such as rain or dust, which is an unsuitable environment for the boilers. In new and well insulated residential buildings, power consumption by hot water is maybe 3.5 times higher than the heating demand [119]. This energy demand saving by employing GSHP needs many more investigations in a hot climate and in particular as to what extent it affects the efficiency of the system.

### 5.6.3 Simple payback periods

Generally, in renewable energy systems, the high initial cost of installation of the system is usually reclaimed by energy savings. Therefore, there are several ways to evaluate the feasibilities in the investments of the new system, such as the payback period (PBP), life-

cycle cost analysis (LCCA), net present value (NPV) and return on investment (ROI).

Despite the fact that PBP does not consider a cost-effectiveness tool because it does not include the long-term factors. From the cost analysis in Table 6.5 we have assumed that the maintenance cost for the ASHP  $M_1$  is double that of the  $M_2$ . Thus  $M_1 = 2590$ .

From table 5.6 and Eq. (4.12) the simple payback period can be expressed as follows:

$$PBP = \frac{57,000 - 20,000}{(5,632 + 2590)_1 - (3,579 + 1,295)_2} = 11 \text{ years}$$

### 5.6.4 Underground thermal imbalance

The thermal imbalance is considered one of the most challenging elements that can be calculated due to a large number of factors related to the operating conditions such as climatic conditions and the length of each season in the year, the time and duration of the system operation, soil characteristics and type of system. In hot dry climate regions, as is clear from figure 5.12, GSHP operates in the cooling mode most of the time and this causes heat accumulation in the soil (more heat is rejected into the soil more than is extracted) this may lead to a system failure in the long run

[58]. In cold regions, Tian et al. [59], discussed the most critical factors that lead to thermal imbalance and ways to reduce its impact, such as increasing the area of the well, increasing the depth of the well and improving the soil properties. For that, the thermal imbalance should be taken into account in the initial stages in the design to avoid system failure or low efficiency. The imbalance ratio (IR) was defined in (4.14).

To determine the accumulated heat for the GSHP, the average COP and EER for the GSHP is determined from Figure 5.9 to be 4.1 and 13 respectively.

So, based on the TRNSYS simulation and from Eq. (4.3) the ground load is determined as follows:

$$\text{Cooling load, } Q_c = 14 \times 3,412.142 = 47,768 \text{ Btu/h}$$

$$\text{Heating load, } Q_h = 10 \times 3,412.142 = 34,120 \text{ Btu/h}$$

In the cooling mode, the condenser rejects heat to the ground heat exchanger, and the evaporator extracts heat from the load. The heat rejected at the condenser is given by

$$\begin{aligned} Q_{\text{cond}} &= Q_c \left( \frac{\text{EER} + 3.412}{\text{EER}} \right) \\ &= 47,768 \text{ Btu/h} \times \left( \frac{13 + 3.412}{13} \right) \\ &= 60,305 \text{ Btu/h} \end{aligned}$$

The heat extracted at the evaporator is given by

$$\begin{aligned} Q_{\text{evap}} &= Q_h \times \frac{\text{COP} - 1}{\text{COP}} \\ &= 34,120 \times \frac{4.1 - 1}{4.1} \\ &= 25,798 \text{ Btu/h} \end{aligned}$$

Thus, from Eq. (4.14) the thermal imbalance ratio is given by

$$IR = \frac{25,798 - 60,305}{60,305} \times 100\% = -57\%$$

In contrast, the monthly-accumulated heat obtained from TRNSYS is presented in Table And, From Table 5.7, it is observed that the total accumulated heat rejected to the soil is 37,094 kWh compared to 4,148 kWh extracted from the soil in the heating seasons. Figure 5.12 represents the heat exchanged per month of the heat exchanger; it is clear that in the summer months, more heat is rejected to the soil. And based on Eq (4.14) the imbalance ratio (IR) is defined as follows:

$$IR = \frac{4148 - 37094}{37049} \times 100\% = -88.8\%$$

Table 5.7 Monthly accumulated heat to the soil

Month	Monthly accumulated heat	
	Heating (kWh)	Cooling (kWh)
Jan	1,963	-
Feb	814	81
Mar	297	393
Apr	-	2,760
May	-	5,228
Jun	-	6,067
Jul	-	7,032
Aug	-	7,131
Sep	-	5,097
Oct	-	2,839
Nov	158	439
Dec	917	27
Overall	4,148	37,094

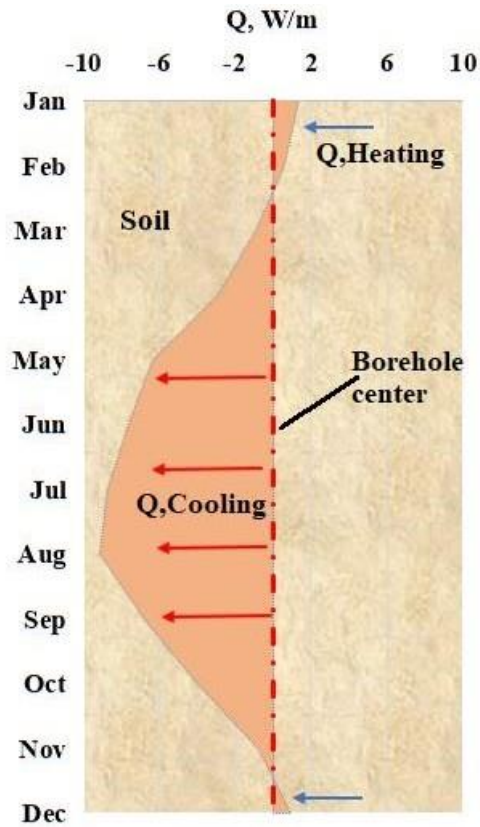


Figure 5-12 Total heat rejected and extracted from/to the soil.

The negative IR indicates that the heat transfer to the soil is more than the heat extraction, which normally occurs in cooling dominated situations, and such a high IR rate must be taken into account to maintain the efficiency of the system. In addition, a lower IR means a smaller difference between the heating and cooling loads.

### 5.7 Discussion of the Results

In this work, TRNSYS software has been used to provide a fully comprehensive simulation for the ASHP and GSHP in terms of the operating efficiency. Despite the simulation results showing that the GSHP is applicable for hot and dry climate regions, the lack of accurate data on the main governing parameters may affect, negatively or positively, the efficiency and therefore performance of a real system. The study has a number of limitations, for example, the lack of information on the groundwater and soil layers, which have different thermal conductivity. In particular, it has been assumed that there is only one soil layer and no groundwater effects. These could significantly

increase or decrease the GHX size and thus lead to a major effect on the initial system cost. In addition, domestic hot water produced by the GSHP is not considered in this analysis.

On considering the long-term running of the system, the results of the study have shown that the rate of the simulation of the underground thermal imbalance is approximately 88% compared to 66% as obtained theoretically. This could be due to the effect of the parameters considered for each method. The COP and EER are determined based on the catalogue only (limited input) in the theoretical calculation. In contrast, the IR is estimated based on the COP and the EER resulting from the simulation, which is affected by the main factors such as the thermal conductivity, underground temperature, soil humidity, liquid flow and pipe diameter. It can be observed that the IR value is influenced by the GHX geometry and underground properties. In addition, the function and type of the building will have an effect on the thermal imbalance and the GSHP performance. For example, when a school building is closed in the summer, this will lead to a reduction in the heat entering to the soil. Likewise, health clubs with swimming pools can use the GSHPs to heat the water and maintain a thermal balance. In addition, the geological characteristics present in one region will be different in another region, for example aquifers. When the velocity of groundwater exists, the rate of heat transfer increases and thus, the length of the GHX decreases, which has an impact on the initial and operational cost [120].

Even though there are many input data in the analysis, the use of the industry-standard software, TRNSYS, gives credibility to this work. This all reinforces the fundamental point of this work, that the implementation of GSHP is a far more viable approach, both in terms of primary energy and cost, than the ASHP system currently universally employed in the Middle East. It is particularly important to note that much of the wealth of Saudi Arabia is based on drilling holes for energy extraction. It would be advantageous for this expertise to be used to save energy for drilling vertical loops for GSHP systems.

## 5.8 Conclusion

In this chapter, for the first time, the more accurate and industrial standard TRNSYS has been used in an annual simulation of the GSHP system compared to the ASHP system in a hot and dry climate. The COP, EER and Initial cost were investigated. The ASHRAE standards and the GLD software were used to determine the length of the GHX from the results detailed above the following can be drawn:

- The soil thermal conductivity is high with an average 2.6 W/mK. in contrast; the underground temperature is high, and this leads to a reduction in the GSHP efficiency
- The total cost savings over a 22-year period were found to be 18%.
- The thermal imbalance ratio was 88.5%.
- The payback period exceeds 11 years when compared to the ASHP system.
- Despite the higher underground temperature, the inlet and outlet fluid temperatures remaining in the design range for most manufacturing companies.
- Despite these positive results of the GSHP efficiency, the high rate of the underground thermal imbalance (88%) could lead to a system failure in the long term.

Adding to the studies conducted in different climatic regions; this work fulfils the knowledge gap of performance and examines, using accurate modelling techniques the feasibility of GSHP in a hot dry climate when the very high soil temperature acts as a negative effect and the high thermal conductivity of the ground as a positive effect.

# Chapter 6: Sensitivity Analysis of GSHP Systems in a Hot Dry

## Climate

---

### 6.1 Introduction

In Chapter 5, the TRNSYS model was developed to investigate the performance of GSHPs compared to ASHPs, based on the local weather and geological characteristics of the city of Riyadh. The purpose of this chapter is to address the most important parameters that influence the design and operation of ground source heat pumps. For that, a rigorous sensitivity analysis method has been applied to analyze 12 parameters that most affect the performance of the system, most of which relate to GHX. It also describes the near-optimum design of a GSHP system in the city of Riyadh in Saudi Arabia. The temperature of the water entering the heat pump is a variable parameter that determines the performance of a GSHP unit. Because of the coefficient of performance of the heat pump, it can also be measured by the value of the entering water temperature. Thus, the entering water temperature (EWT) was selected to be the performance measure of the system, as all the heat transfer processed between the ground heat exchanger components and the surrounding soil is manifested in the entering water temperature.

### 6.2 Literature Reviews for the Sensitivity Analysis

Adoption of a ground source heat pump (GSHP) as a source of renewable energy can lead to a significant reduction in the energy consumption and long-term sustainability of cooling and heating systems. Therefore, in order to fully assess the advantages arising from the use of such a system in an arid climate, a sensitivity analysis is a positive and enlightening way to ensure its effectiveness.

However, many studies have covered various aspects of using GSHPs in different climates; the correct interpretation of such results assists in the analysis of the heat pump performance in dry areas.

The ideal design of GSHPs, for instance, is heavily influenced by the GHX length. Zhu et al. [121] applied both a sensitivity analysis and 3-dimensional transient numerical methods to study the most



critical factors affecting the operation of a borehole thermal energy storage system (BTES). *Four key components* were evaluated, namely:

- i. Total quantity of injected heat (IH)
- ii. Storage efficiency (SE)
- iii. Percentage of heat loss (HLP)
- iv. Energy density (ED).

It was found that the borehole depth and heat changing temperature were positive components responsible for the 95% changes observed in the injected heat. Likewise, the borehole heat changing temperature affected the results, showing changes in the energy density by up to 90%. In addition, the borehole spacing and the thermal conductivity of the soil were the key parameters that affected the storage efficiency and heat loss. Likewise, the study carried out by Ilisei et al. [122] focused on the link between the performance of the ground source heat pump and the length of the heat exchanger. Both Design Builder and Earth Energy Designer software were used for a number of simulations to evaluate the greatest number of parameters affecting the COP of the system. In contrast, the ASHRAE standards were used to determine the length of the heat exchanger. This study showed that a well-designed borehole length would lead to a saving in energy of up to 22%. The estimation of borehole length is actually the principal consideration in deciding the GSHPs' economic viability in comparison to different conventional methods.

Biao et al. [123] addressed the absence of the groundwater impact on the thermal response test (TRT) result over the long-term performance. A three-dimensional mathematical model has been proposed to analyse the thermal behaviour of TRT with and without groundwater effect. The result shows very little difference in the heat transfer for the short-term operation. In contrast, the heat transfer (when including the effect of groundwater over the period of ten years) was 3.07% higher than that of the normal TRT.

Gunawan et al. [124] carried out a study to discuss the alternative heating systems that are suitable for use in the remote northern regions of Canada. In this paper, a techno-economic analysis method was used to evaluate the use of a ground-coupled heat pump system instead of a traditional heating system powered by a diesel-fired furnace. It was found that the heating costs generated by the use of a GSHP system, coupled with solar photovoltaic panels, were CAD\$ 179,000, compared to CAD\$ 277,000 when operating a diesel-fired system. This confirmed that such a system would also be suitable for use in other sub-Arctic regions of Canada and in similar climatic conditions throughout the world.

Sakellariou et al.[125] developed a TRNSYS model to investigate the effect of coupling a (Photovoltaic and Thermal Collector) (PVT) system with a ground source heat pump for regions where heating was the primary requirement. Heating loads were estimated based on the demands for a single-family home and weather data for the city of Birmingham, UK. The sensitivity analysis evaluated data from the following:

- i. Pairing of the PVT
- ii. Flowrate of the PVT
- iii. Inclination angle of the PVT
- iv. Effectiveness of the plate heat exchanger
- v. Overall storage capacity
- vi. BHE ground thermal conductivity.

Results from this study indicated that the storage capacity and the performance of the plate heat exchanger were the two factors that most affected the heat productivity.

Han and Yu [126] applied a 3-dimensional finite element model in an attempt to improve the performance of the GHX system. The three parameters evaluated in the sensitivity analysis

covered data from the geological findings, design criteria, and operational conditions. The results obtained from the thermal conductivity of the soil and specific heat of the grout material were the most important factors from the geological aspect, whilst the fluid flow rate velocity was the key factor as far as the design was concerned. On the operational side, an intermittent operation achieved a higher coefficient of performance than when the system was operated continuously.

Woloszyn and Golaś [127] examined the coefficient of performance for a horizontal ground heat exchanger using the finite element method, and investigated the influence of the thermal conductivity, mass flow, and dynamic fluid viscosity. The results obtained showed that the heat pump COP was greatly hindered by the thermal conductivity of the soil, but not substantially by any of the other factors.

Hong et al. [128] conducted six scenarios to identify the most important factors that would impact upon the performance of a GSHP system. These factors were classified into three categories: regional, system, and design. The subject for the analysis was a medium-sized building at the University of Seoul, South Korea. The sensitivity analysis was applied to investigate the effect of these factors on the structure of the GSHP, having regard for the energy generation and environmental impact, based upon the life cycle assessment method. The results showed that the most significant factors affecting the system's COP were the borehole length, diameter and spacing, thermal conductivity, and U-pipe's diameter. In contrast, the borehole length was again considered to have the greatest number of factors affecting the environment, and the U-pipe spacing was determined to be the factor that had the least effect on both the COP and the environment.

Likewise, the research directed by Casasso and Sethi [129] investigated the factors affecting the double U-pipe within a borehole heat exchanger. Both the finite-element modelling and FEFLOW software were applied to verify the influence of the geometrical components and surrounding geological conditions on the performance of the GHX as regards the long-term operation. The performed sensitivity analysis confirmed that despite all parameters having a significant impact on

the GHX performance, the borehole length and thermal conductivity of the soil were the major modelling parameters. The authors specified that using actual site data led to a more accurate design, as opposed to relying on estimated values for the governing parameters.

Christopher et al. [130] experimentally compared the effect of a ground heat exchanger on the GSHP's coefficient of performance. In this study, two types were investigated: the *U*-tube and the Coaxial Borehole models. Values obtained experimentally showed that, despite the lower pressure drop in the *coaxial* borehole, *this type* needs much more power to reach the turbulence flow rate required to extract the heat from the ground. In addition, the results showed that the coaxial loop was less costly and easier to install. However, these benefits did not add enough comparative values to gain an advantage over the U-tube pipe type of heat exchanger.

It is clear from previous literature reviews that determining the most important elements affecting the performance of a GSHP is both difficult and variable from one location to another. In addition, the methods used in the analysis very much affect the results. In this work, novel and comprehensive sensitivity analysis on the most important parameters affecting the cost and performance of a GSHP has been conducted. It should also be pointed out that this was achieved against the background of a considerable lack of information concerning the properties of the underground soil in the city of Riyadh, Saudi Arabia. In this study, twelve important parameters have been considered in order to provide an optimal design for a GSHP under these geological and climatic conditions.

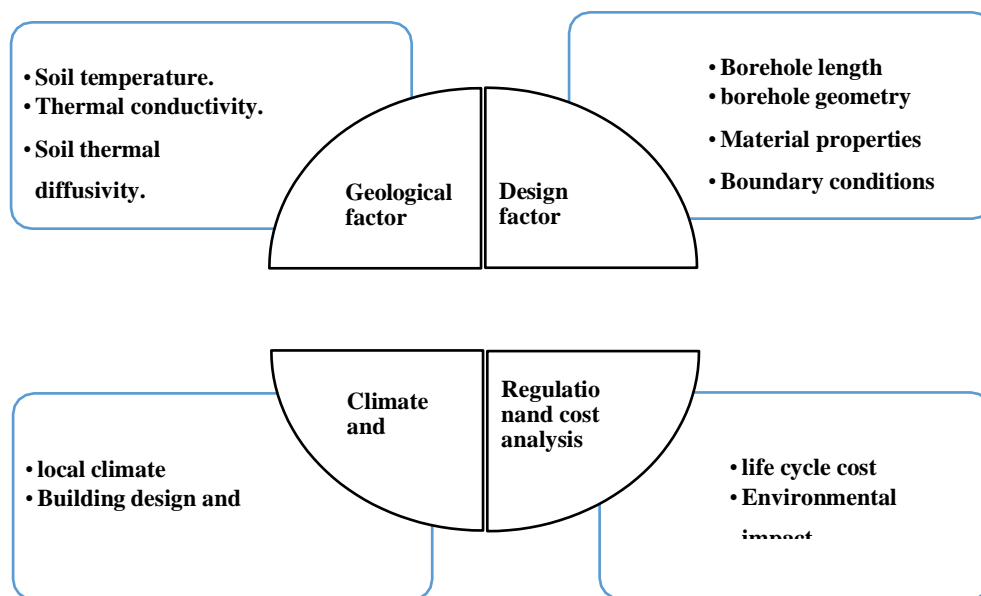
### **6.3 Parameters Affecting the Design of the GSHP**

Numerous studies have been performed relating to the GSHP design and performance. Some of this research has focused on the use of ground heat exchangers (GHX) as the main source of the initial cost [131-133]. Alternatively, some studies have focused on the heat pump itself, its distribution system and the building's design [134-135]. In addition, the combined implementation of a hybrid GSHP system with renewable energy, such as solar energy, has been investigated widely [136-138].

In general, GSHPs consist of three main components:

- i. Ground loop heat exchanger, GHX.
- ii. Heat pump unit.
- iii. Distribution system.

Each component has various features that affect the design of a GSHP up to a different extent and therefore Figure 6.1 illustrates the most important of these parameters. A detailed literature study also indicates that the soil temperature, ground thermal conductivity and the ‘entering-water’ temperature, play an important role in the efficiency of the pump [127].



*Figure 6-1 The most important parameters that affect the GSHP design and operations.*

In this chapter, the 12 most important parameters that affect the efficiency of the GSHP system have been investigated and a sensitivity analysis based on the hot/dry climate as shown in Figure 6.2. It is clear that most of the parameters that have been considered are related to the use of the GHX. The reason for this is that the heat of rejection/extraction and temperature distribution are related to the underground geological conditions, and these are the parts of the system that are mostly unknown and which directly affect the GSHPs design, efficiency and initial cost.

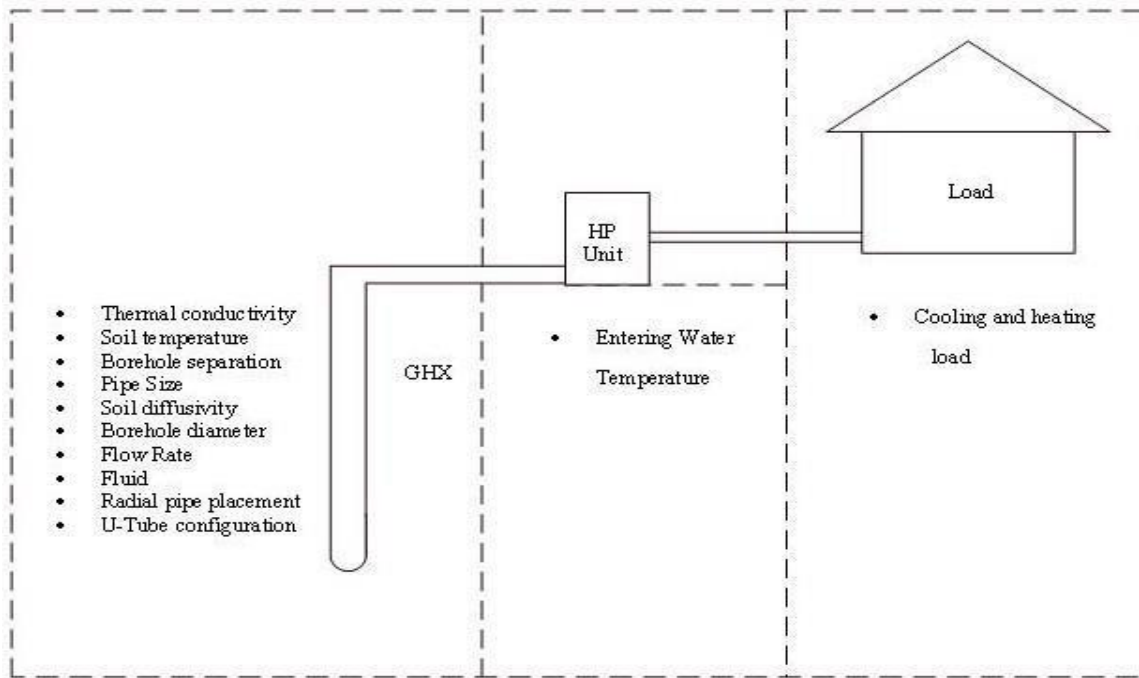


Figure 6-2 Illustration of the most important parameters employed in the sensitivity analysis

## 6.4 Modelling of the GSHP System Using GLD

### 6.4.1 Sizing the GHX using GLD

The purpose of this chapter is to address the most important parameters that influence the design and operation of ground source heat pumps. Building upon the chapter 5 section 5.3.1, an office building was designed to enable an investigation into their viability in hot and dry climates, such as in the city of Riyadh. The building envelope, weather data, cooling and heating loads, and sizing of the GHX were simulated by the use of TRNSYS. The designer of the GSHP aims to calculate the return water temperature from the GHX to the heat pump that is sufficient to operate the heat pump unit, depending on the thermal and geological characteristics of the site. In the GLD software, the designer can easily connect the load module, heat pump module, and the ground heat exchanger module, as shown in Figure 6. 3. The first step is to upload the building load data, which can be imported simply from different energy simulation software packages such as Carrier HAP and TRANE Trace in an Excel file. The designer can choose between two different load modules,

namely the average block load used to size the GHX quickly, and the zone load used when heating and cooling differently from one zone to another.

Secondly, the characteristics and capacity of the heat pump unit can be selected automatically from the program library, based on building load data, or manually, re-entered based on the designer's suggestions. The last step is the combined selection of the heat pump and building load profile within the GHX simulation studio. In the GHX design module, the designer can select between two methods: fixed length of the borehole or fixed by the heat pump entry water temperature. In the fixed length mode, the program will calculate: the number of boreholes, EWT value, and COP for the heat pump unit. In the EWT mode, where the designer has fixed the desired temperature of the water entering the heat pump, the GLD will calculate the borehole length based on the borehole number inputted by the designer, and other information such as soil temperature, soil thermal conductivity, soil moisture, and borehole geometry.

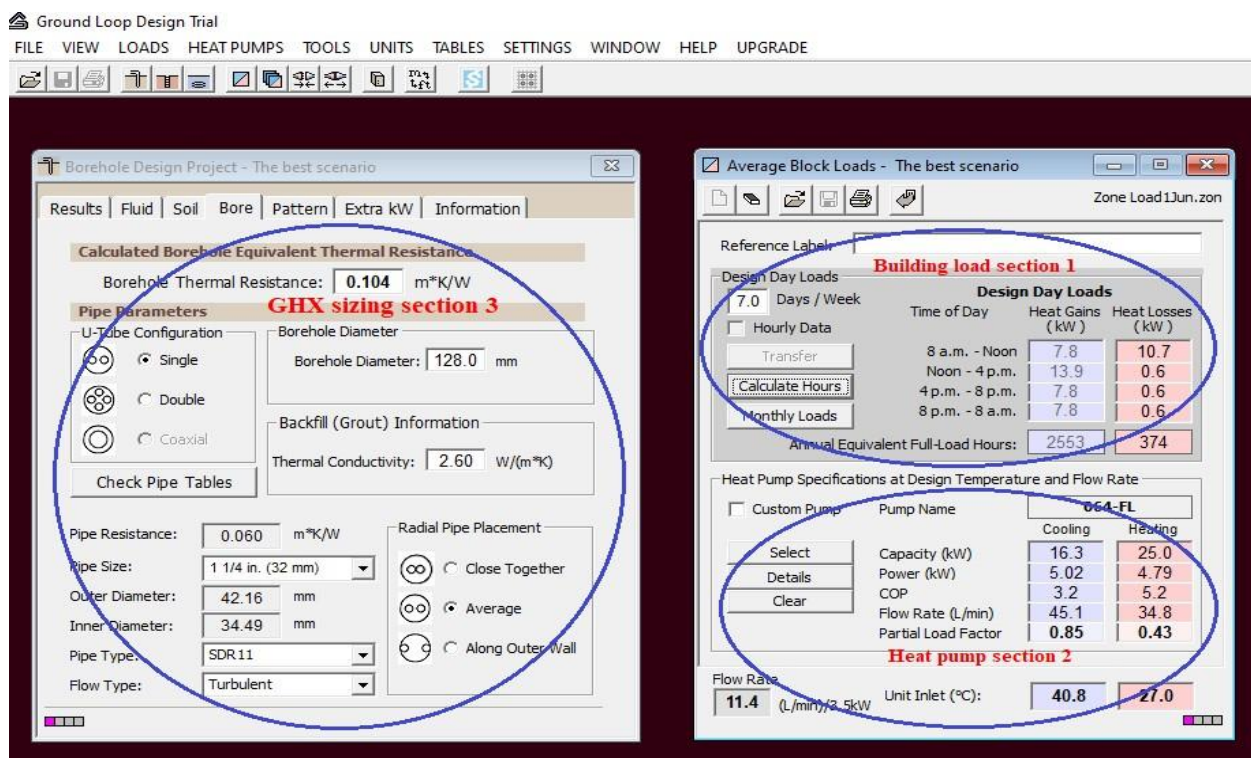


Figure 6-3 A typical model of a vertical GSHP system developed in GLD.

## 6.4.2 Methodology and baseline model

The proposed baseline system was modelled on the design conditions present in the city of Riyadh. From chapter 5, an office building having a floor area of 120m<sup>2</sup> was created in TRNSYS, and the maximum cooling and heating loads were computed as 14 kW and 10 kW respectively. The total length of the GHX was determined to be 400m (four boreholes, each of 100m length) according to the ASHRAE standards. The baseline characteristics used for the modelling are shown in Table 6.1, whilst Table 6.2 clarifies the simulation results for one year's operation by GLD.

Table 6.1 The baseline parameters' values.

Parameters	Value
Thermal conductivity, W/mK	2.6
Soil temperature, °C	29
HP Entering water temperature, °C	39.4
Circulated fluid type	Water
Pipe size, mm	32 (1.25 in)
Soil thermal diffusivity, m <sup>2</sup> /day	0.070
Borehole separation, m	10
Borehole diameters, m	0.128
Borehole length, m	100

Table 6.2 GLD output of 1-year modelling for the GSHP system.

M	Q, W.m-1	Power kWh	Power-Cooling, kWh	Power-Heating, kWh	T Borewell, °C	Tf, °C	Average Exit WT, °C	Average EWT, °C	Min. EWT, °C	Max. EWT, °C
1	1.41	325	0.7	324	29	29	29	29	29	29
2	0.62	194	22	172	28	27	27	28	28	28
3	-0.9	207	184	23	28	28	28	28	27	29
4	-2.84	539	539	0.13	30	30	30	30	29	31
5	-6.36	1261	1,261	0	31	32	32	31	31	33
6	-7.59	1621	1,621	0	34	36	37	35	34	37
7	-8.72	1923	1,923	0	35	38	39	36	36	39
8	-9.15	2010	2,010	0	36	39	41	37	37	40
9	-7	1501	1,501	0	37	40	42	38	38	41
10	-4	854	854	0	35	37	39	36	36	39
11	-0.7	191	166	25	33	35	35	34	34	36
12	0.93	225	6.66	218	31	3	31	31	31	33



To explore how the parameters have affected the GSHP's design, based on the heat pump features and cooling and heating loads, a closed-loop U-pipe process to size the GHX has been developed by the GLD software. Figure 6.4 depicts a schematic flow chart of this paper's methodology. The following steps were used: Determination of the baseline parameter values, as shown in Table 6.1:

- The independent individual parameters were altered by  $\pm 5$ ,  $\pm 10$  and  $\pm 15\%$  and assessed against the borehole length and power consumption. This was because initial investment costs are generally related to the cost of drilling and the lifetime costs are those from operations, such as the COP, monthly use of electricity, and the payback period due to energy use.
- Determination of the most significant factors affecting the design of the GSHP to meet the cooling demand.
- For these most significant factors it was found that individually, the changes are very small and may be neglected or vary almost linearly with the GHX length.
- For the parameters that show the biggest changes, then a combination of them produces changes that are simply additive. This shows the validity of the approach.
- Conclusions on the best and worst scenarios of the changes in the four most important parameters that have a significant impact on the GSHP design in a hot and arid climate.
- Estimation of the best/worst-case scenarios to determine the optimal design of the GSHP under these geological and climate conditions.

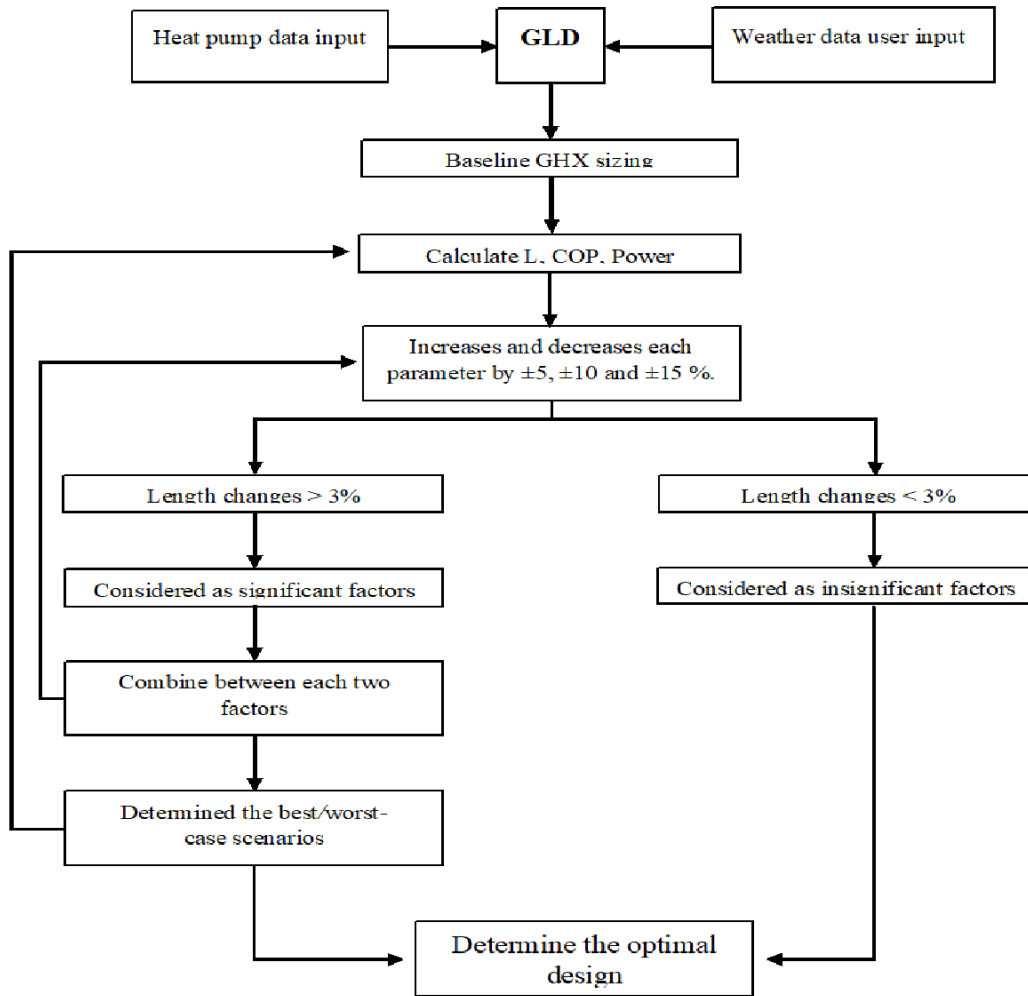


Figure 6-4 Flowchart of the proposed methodology.

## 6.5 System Simulation and Validation

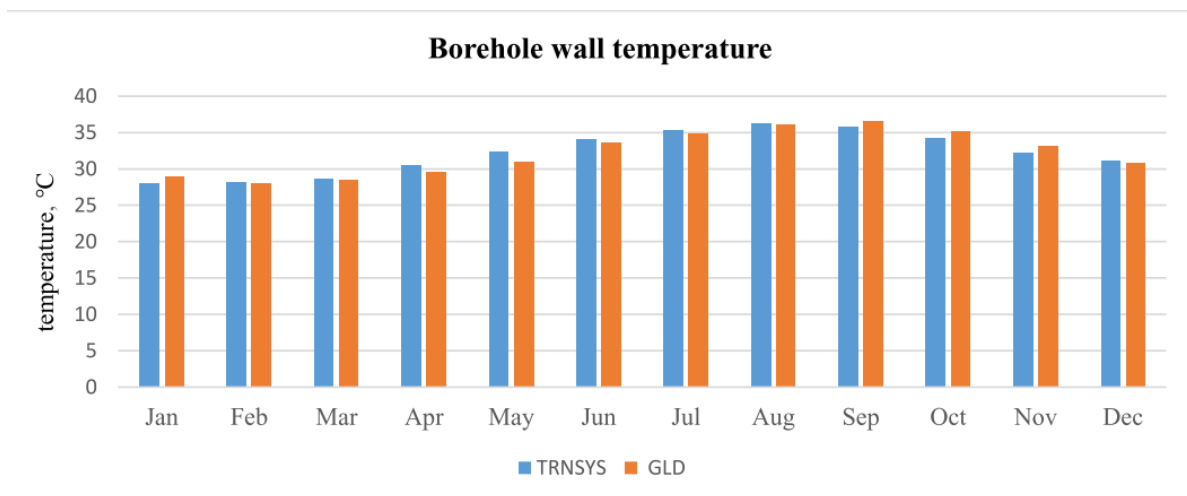
### 6.5.1 System validation

While the baseline parameter values were modelled in TRNSYS, parallel GLD software was developed to investigate the effect of the parameters on the GSHP's design. This was based on the cooling and heating loads calculated by TRNSYS and the same values shown in Table 6.1.

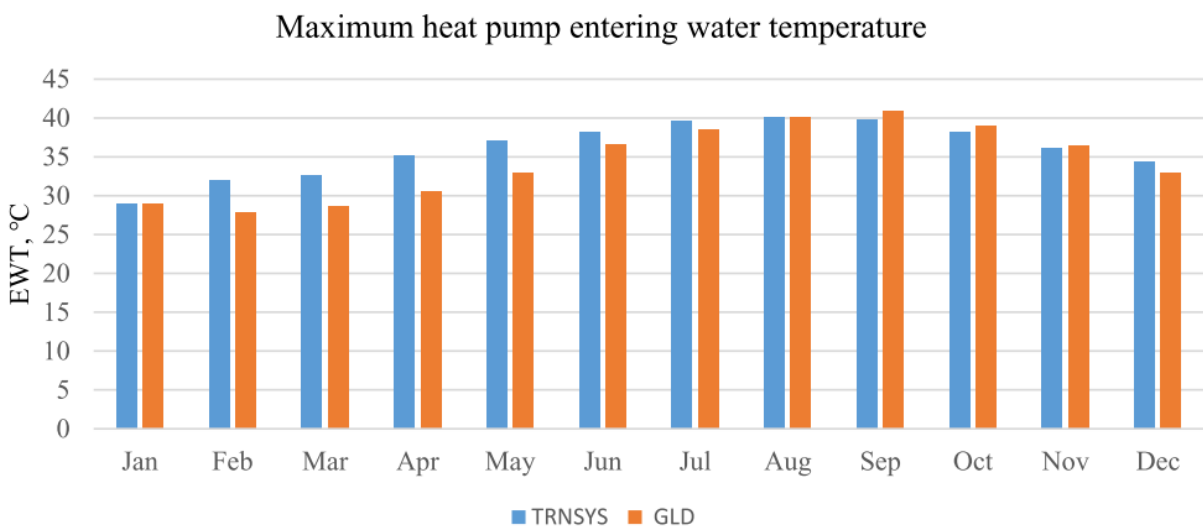
Despite TRNSYS being the main software for the simulation, GLD was used in the sensitivity analysis for several reasons:

- Comprehensiveness of the variables and the flexibility of their changes.

- Programme outputs cover all aspects that enable the designer to determine the optimum design for the GHX as shown in Table 2. Also, the availability in different languages.
- The simulation results indicate that there is a relationship between the GLD and TRNSYS.
- The software contains a range of heat pump modules from various manufacturers, full piping design system, lifecycle cost and CO2 reports, thermal conductivity report and computational fluid dynamics reports.



(a)



(b)

Figure 6-5 Comparison between the predicted TRNSYS and GLD as regards (a) Borehole wall temperatures and (b) entering water temperatures.

## **6.6 Sensitivity Analysis Results**

The optimization of GSHPs in specified locations requires full knowledge of the weather and geological characteristics; each parameter must be analysed in order to determine its effect on the performance and cost. In this section, the effect of the changes in each of the most important parameter behaviours was investigated separately against the baseline case by an increase and decrease in each individual parameter value by  $\pm 5$ ,  $\pm 10$ , and  $\pm 15$  % respectively. Table 6.3 shows all the parameters analysed against the length and power. In contrast, Table 6.4 shows the analysed parameters employed in the study based on the parameter type, such as the fluid type and U-Tube configuration. In addition to the above information, the characteristics of the heat pump unit must match the actual entering water temperature. All these aspects are explained in detail in the next section.

Table 6.3 Parameters analysed against the length of the GHX and energy consumption of the GSHPunit.

S	Parameter	% change	Parameter value	Length change		Power change	
				L,m	%	kWh	%
a	Thermal conductivity W/mK	-15	2.21	111	11	10853	-0.06
		-10	2.34	107	7	10877	0.23
		-5	2.47	103	3	10868	0.15
		Baseline	2.6	100	0	10852	0
		5	2.73	97	-3	10856	0.03
		10	2.86	94	-6	10850	-0.01
		15	2.99	91	-9	10843	-0.08
b	Soil temperature °C	-15	24.65	75	-25	10314	-5
		-10	26.1	82	-18	10493	-3.3
		-5	27.55	90	-10	10675	-1.6
		Baseline	29	100	0	10852	0
		5	30.45	112	12	11053	1.85
		10	31.9	127	27	11246	3.63
		15	33.35	148	48	11444	5.5
c	Entering water temperature °C	-15	33.49	175	75	9910	-8.68
		-10	35.46	139	39	10225	-5.78
		-5	37.43	116	16	10530	-2.97
		Baseline	39.4	100	0	10852	0.00
		5	41.37	88	-12	11203	3.23
		10	43.34	79	-21	11530	6.25
		15	45.31	71	-29	11883	9.50
d	Soil diffusivity m <sup>2</sup> /s	-15	0.0595	98	-2	10867	0.14
		-10	0.063	99	-1	10864	0.11
		-5	0.0665	99	-1	10864	0.11
		Baseline	0.07	100	0	10852	0.00
		5	0.0735	100	0	10861	0.08
		10	0.077	101	1	10859	0.06
		15	0.0805	101	1	10859	0.06
e	Borehole separation m	-15	8.5	96	-4	10960	1.00
		-10	9	100	0	10857	0.05
		-5	9.5	100	0	10860	0.07
		Baseline	10	100	0	10852	0.00
		5	10.5	99	-1	10867	0.14
		10	11	99	-1	10866	0.13
		15	11.5	99	-1	10866	0.13
f	Borehole diameters m	-15	108.8	104	4	10794	-0.53
		-10	115.2	101	1	10862	0.09
		-5	121.6	100	0	10861	0.08
		Baseline	128	100	0	10852	0.00
		5	134.4	99	-1	10863	0.10
		10	140.8	99	-1	10862	0.09
		15	147.2	98	-2	10864	0.11
g	U-pipes size inch	0.17	5/8	106	6	10842	-0.1
		0.20	3/4	104	4	10845	-0.1
		0.25	1	102	2	10856	0.0
		Baseline	1 1/4	100	0	10852	0.0
		40	1 1/2	98	-2	10866	0.1
		50	2	97	-3	10874	0.2
		65	2 1/2	Not fit with borehole diameter			
h	Fluid flowrate L/m	-15	9.69	95	-5	10860	0.07
		-10	10.26	97	-3	10861	0.08
		-5	10.83	97	-3	10861	0.08
		Baseline	11.4	100	0	10852	0.00
		5	11.97	99	-1	10856	0.04
		10	12.54	100	0	10868	0.15
		15	13.11	100	0	10869	0.16
i	Building	-15	12.33	85	-15	9219	-15.05
		-10	13.1	90	-10	9767	-10.00
		-5	13.8	95	-5	10314	-4.96
		Baseline	14.0	100	0	10852	0.00
		5	15.2	104	4	11412	5.16
		10	16.0	109	9	11960	10.21
		15	16.7	114	14	12510	15.28

Table 6.4 Parameters analysed against the length and power consumption of the GSHP based on the parameter type.

S	Parameter	Parameter type	Length change		Power change	
			L,m	%	kWh	%
a	Circulation fluid type	Water	100	0	10852	-1.33
		Methanol-15	98	-2	10869	-1.17
		Ethanol	100	0	10861	-1.25
		Ethylene Glycol-3.89	98	-2	10866	-1.20
		Propylene Glycol-3.89	99	-1	10856	-1.29
		Calcium Chloride	97	-3	10873	-1.14
b	U-Tube configuration	Single	100	0	10852	0.00
		Double	90	-10	10900	-0.44
		Coaxial	106	6	10840	-0.11
c	Radial pipe placement	Close together	104	4	10848	-1.36
		Average	100	0	10852	0.00
		Along outer wall	98	-2	10855	-1.30

### 6.6.1 Soil thermal conductivity

The thermal conductivity is a property that plays a key role in the geothermal heat pump application and the ground thermal conductivity indicates that the heat transfer capacity between the GHX and surrounding soil. In fact, the thermal conductivity of the soil is affected by the soil texture. Soil texture is decided by proportion of sand, silt, clay and amount of water it can hold. Therefore, the thermal conductivity has a direct influence on the borehole wall temperature, resistance and circulated fluid temperature. On the other hand, for engineering geological investigations, the main geological formation of the study region

– Riyadh city- is mainly made up of limestone, dolomite and sandstone which has a very good thermal conductivity that lies in the range 1.4-6.2, 1.6-6.2 and 2.1-3.5 W/mK, respectively. Figure 6.6 shows the geological profile of the soil layers

and contains information on the thickness of the layer and soil types in Al-Jubail which is located

in thenorth of the city of Riyadh. [139]

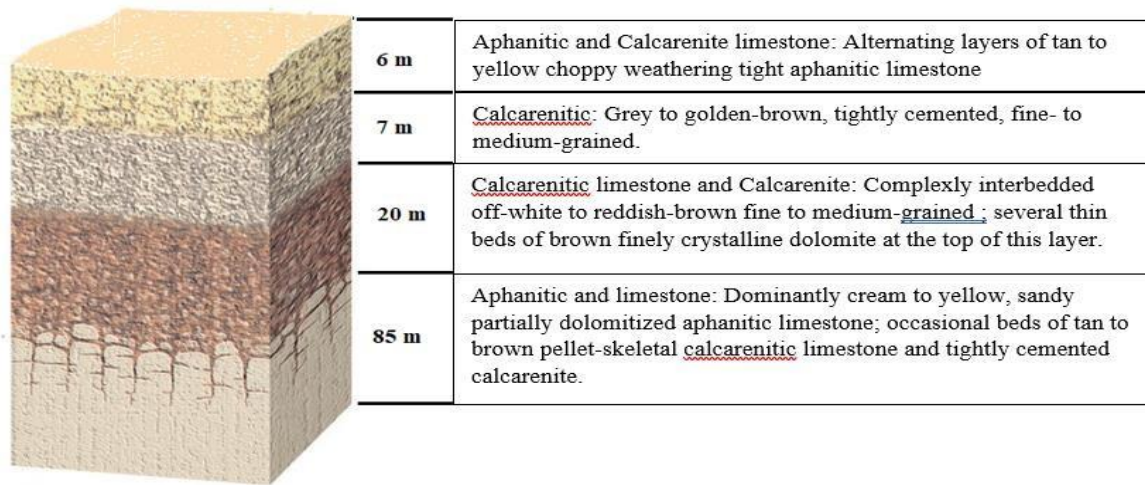


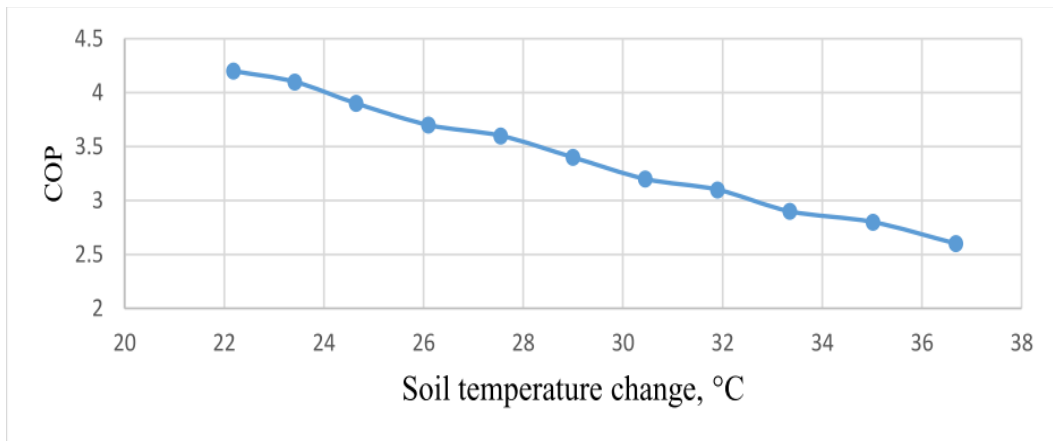
Figure 6-6 Composition of Soil and types for the Al-Jubaila area - city of Riyadh [31].

It is important to note that the thermal conductivity of the ground is considered to be a fixed factor because it is an external parameter related to the specific location [128]. In this paper, the thermal conductivity baseline value was selected to be 2.6 W/mK, based on the measurements extracted from [97]. From Table 3(a), a  $\pm 5\%$  change in the thermal conductivity has a significant effect on the borehole length, with changes being approximately  $\pm 3\%$ , whereas there is virtually no effect on the power consumption. Likewise,  $\pm 15\%$  changes in the thermal conductivity led to a  $\pm 10\%$  length change with an almost linear trend on power consumption.

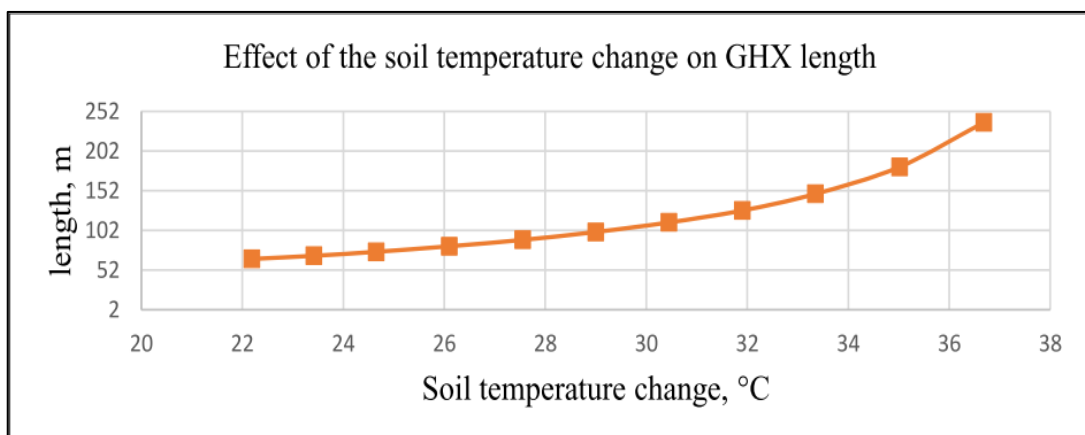
### 6.6.2 Soil temperature

Similar to the thermal conductivity, the soil temperature is also considered as non-adjustable factor that has a major impact on the GHX. In this study, the soil temperature was determined to be 29 °C, based on the results of the field measurements [97]. However, it should be pointed out that the soil temperature is assumed to be 26.5 °C after a depth of 10m, according to the ASHRAE standards and many simulation calculations, such as in TRNSYS [69]. There are *extensive studies* on the influence of the soil temperature on GSHP efficiency, because the accumulated soil temperature over time can lead to system failure. From Table (3b), it can be seen that the reduction in the soil

temperature by 5% and 15% leads to a decrease in the length by 10% and 25% respectively. Also, the energy consumption decreases by 2% and 5% respectively. This change in length significantly affects the initial cost of the GSHP and system viability. Furthermore, such changes in the soil temperature affect the entering water temperature and the COP of the heat pump. Figures 6.7 (a), (b), and (c) shows the effect of the soil temperature change on the other design elements - COP, length, and WET, respectively. In addition, it is important to note that based on the GLD simulation, if the soil temperature reaches 36 °C under the same values for the baseline parameters, system failure can occur because of the EWT being outof range for the selected heat pump.

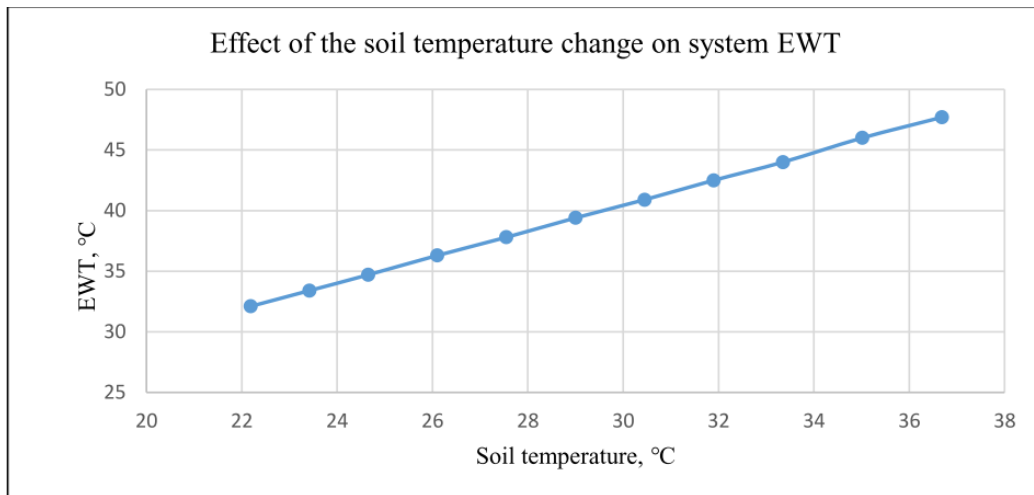


(a)



(b)





(c)

Figure 6-7 The effect of the soil temperature change on the (a) COP, (b) GHX length, and (c) WET.

### 6.6.3 Entering water temperature

The sizing of the ground loop is key to the successful operation of a heat pump system. The temperature of the water entering the heat pump unit determines the performance coefficients of the heat pump, since the unit capacity is directly related to the EWT, which is a variable parameter that depends on the geological characteristics and the quality of the design of the geothermal exchanger. Practically, the EWT value should remain in the heat pump unit capacity limit over the lifetime period of the heat pump (usually 20-25 years) because of the 35-50% COP value, depending on the EWT [140]. For that purpose, the ClimateMaster (Tranquility-30) water to air heat pump was selected [141]. According to this heat pump data, the operating range of the EWT in cooling mode is -1.11 to 48.89 °C.

In this study, the simulation results for the EWT remains within the capacity limits of the heat pump and Figure 6.8 illustrates the maximum EWT for the three periods of 1, 20, and 40 years; these were 39.4 °C, 44.1 °C, and 44.9 °C respectively. As observed in Figure.6, the maximum EWT increases by 11% in the first 20 years, while it remains almost constant in the next 20 years, with only a 1.8%

increase over this later period. This EWT value indicates the viability of implementing the GSHP system not only for 20 years, but for 40 years and maybe longer.

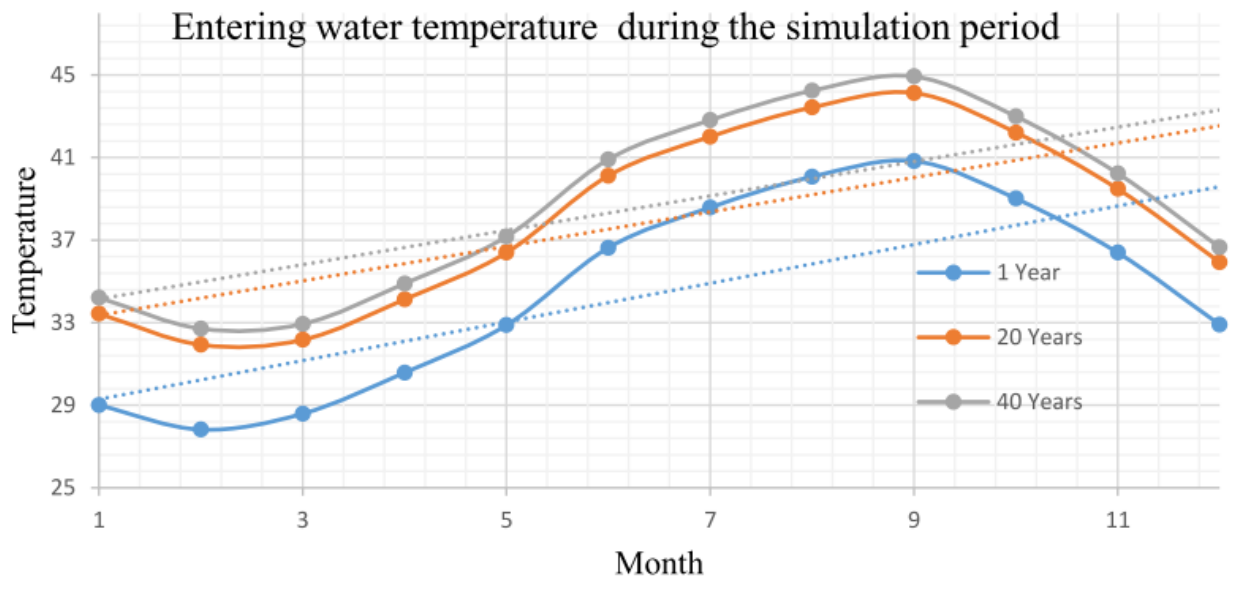


Figure 6-8 The maximum EWT for the periods of 1, 20, and 40 years.

#### 6.6.4 Soil diffusivity

The thermal diffusivity is the factor that describes how fast the heat transfer works in the soil [36], and it is a function of the soil thermal conductivity divided by the heat storage (density and specific heat) of the soil. This relation can be determined as follows:

$$a = \frac{k}{\rho c_p}$$

Where  $\alpha$  is the thermal diffusivity,  $k$  is the thermal conductivity,  $\rho$  is the density, and  $c_p$  is the specific heat. Thus, the higher the thermal conductivity, the faster the heat diffuses into the surrounding medium. Based on the GLD library, the values of the thermal diffusivity of the limestone, dolomite, and sandstone range from 0.093-0.13, 0.1-0.21, and 0.065-0.11 m<sup>2</sup>/day, respectively. However, in this chapter, the value of the thermal diffusivity was selected to be 0.070

m<sup>2</sup>/day, based on [96].

Table 3(d) shows that the effect of the thermal diffusivity on the length of the GHX was limited to a  $\pm 1$ m change. Similarly, the effect of the thermal diffusivity on the heat pump power consumption is less than 1%. Thus, in our case, the thermal diffusivity may be considered as a negligible design factor in this sensitivity analysis. so, in the steady state, the result will be neglectable too.

### **6.6.5 Borehole geometry**

The borehole geometry consists of a number of the adjustable factors that the designer can specify. In this paper, the layout of the boreholes was set to be next to each other in one row. The parameters were selected by simulation using GLD, and the results are presented in the following sections.

#### **6.6.5.1 Borehole separation**

The borehole separation refers to the centre-to-centre distance of the GHX boreholes. The distance between the wells is determined based on the available area of the project without affecting the required bore length. In general, 6 to 10 m between the wells may be considered to be a sufficient distance in order to maintain a balance between the thermal interference and the project area [69]. From Table (3e), it can be seen that the borehole separation was selected to be 10m, and this led to a decrease in the length by 1% when the separation increase was within 5-15%; thus it may be concluded that there is no significant effect from the separation on the borehole length and power consumption. However, when the distance between the wells is short, a thermal imbalance occurs; Figure 6.9 shows the effect of the distance between the wells on the thermal diffusion from both sides of the well.

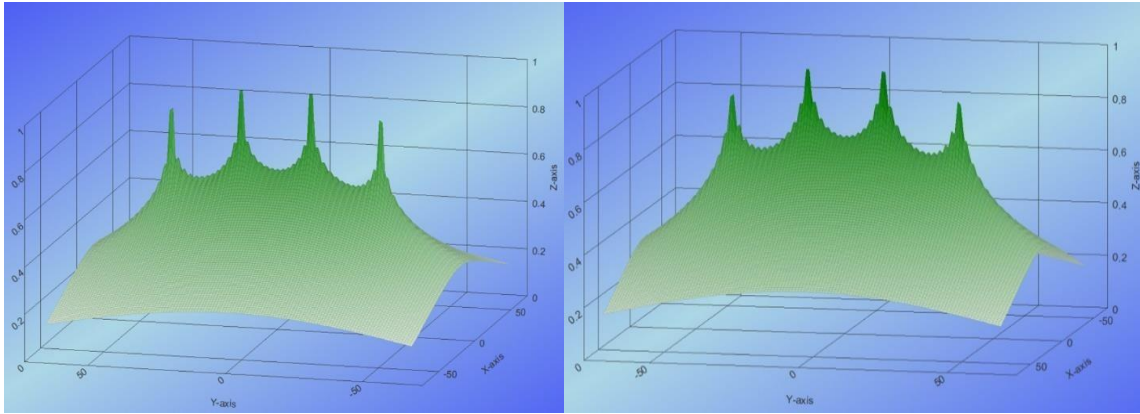


Figure 6-9 The *g*-function 3D map for the borehole separation: (a) 3m separation, and (b) 10m separation.

### 6.6.5.2 Borehole diameters

The borehole diameters play a key role in the GHX design as adjustable elements by the designer. Wider borehole diameters lead to increases in the GHX resistance, and this reduces the thermal transfer between the fluid and the soil. Furthermore, extra initial costs occur, such as the volume of the grout and drilling materials. For example, Kavanaugh [69] estimated that the volume of the filling material is 970L, compared to 1379L at a depth of 100m with a 32 mm U-pipe. In practice, the minimum borehole diameter is determined based on the GHX pipe size. In contrast, the maximum borehole diameter should be no more than 200 mm, based on the UK standard [142]. In Germany, Luo et al. [143] investigated the effect of the borehole diameters on the GHX thermal efficiency. Three different borehole diameters were selected, namely 121, 165, and 180 mm in order to compare the thermal performance. The results showed that the larger borehole diameter (180mm) has a 6.7%, 2.16% better thermal performance, compared to the 121mm and 165mm borehole diameters respectively.

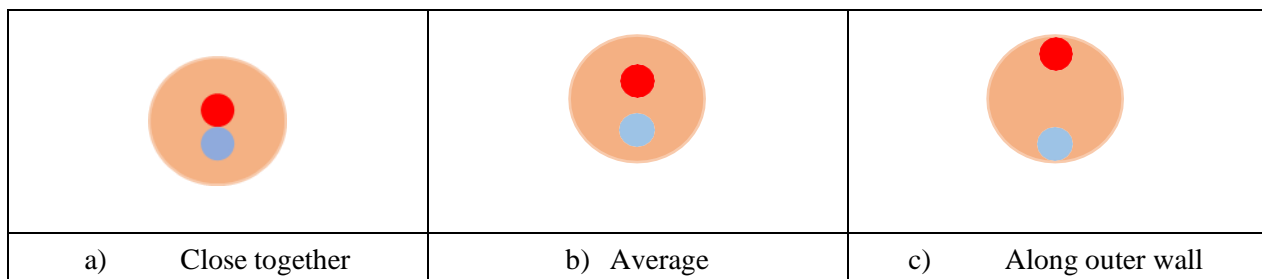
From Table (3f), it is seen that the effect of the borehole diameter is limited in this work too. When the diameter increases by 15%, the length decreases by 2%, compared to 4% when the diameter decreases by 15%, but it has almost no effect for the smaller diameter changes on the length of the borehole and power consumption. Therefore, the borehole diameters have limited effect on the length but not on the initial cost for grout.

### 6.6.5.3 Radial pipe placement

The heat transfer between the U-pipe legs and surrounding soil as a result of the variation in the fluid temperature along the pipe depends on its location and depth [144]. Figure 6.10 shows a U-pipe shape inside the borehole based on the ASHRAE standard [69] and the GLD software as follows:

- a) Close together: the position of the U-pipe legs is close together, with a 4mm average distance between the pipes.
- b) Average: the position of the U-pipe legs – the pipes are centred at a point halfway between the wall and the centre line of the borehole.
- c) Along the outer wall: the GHX pipes are placed along the outer wall of the well.

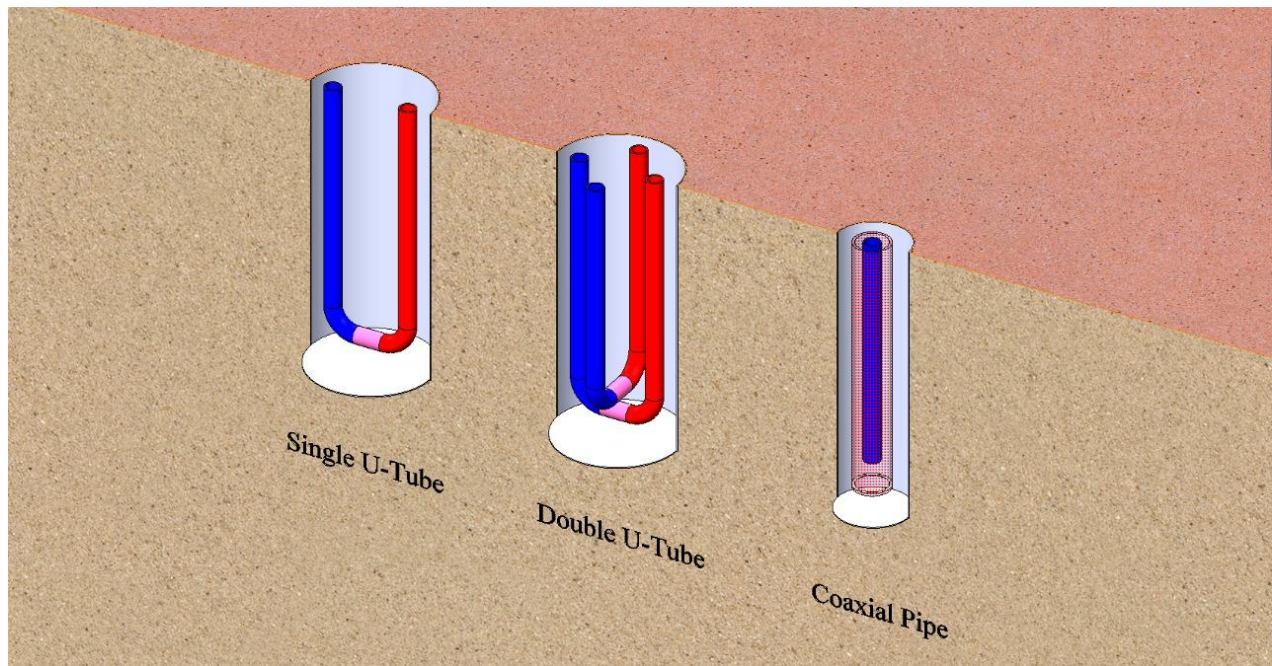
The U-pipe position is a design factor that may be adjusted. As can be seen in Table (4c), there is a 4% increase in the GHX length when the pipes are located close to each other, while the GHX length will decrease by 2% when the U-pipe legs are located along the outer wall.



*Figure 6-10 The position of the U-pipe legs inside the borehole.*

### 6.6.5.4 U-Tube configuration

The U-Tube configuration includes both adjustable and design parameters that have a major effect on the borehole length, with the adjustable parameters being able to be selected by the designer. There are three commonly used shapes for the GHX U-tube heat exchangers, and these are shown in Figure 6.11.



*Figure 6-11 The three commonly used shapes for the GHX: (A) single U-tube, (B) double U-tube, and (C) coaxial.*

Angelo et al. [145] investigated the heat transfer for both the double U-tube and coaxial GHX versions, within a short time-frame, by developing an analytical and finite-element numerical model. The results showed that the coaxial heat exchanger had a thermal responsetime six times better when compared with the double U-tube duo, thus showing lower thermal resistance and the ability to carry fluids at higher temperatures. However, the highercost of the coaxial GHX, when compared to the double U-tube, remains an obstacle to the coaxial system being adopted. Wood et al. [130], however, carried out an experimental studyon the performance of a coaxial GSHP when compared to a single U-tube GSHP. This studyshowed that the COP of the single U-tube proved to be more beneficial than that of the coaxial system duo, and this was due to the turbulent flow.

As can be seen from Table 4(b), the U-tube configuration had no significant effect on the heat pump's power consumption. On the other hand, with the GHX length being 10% less than the baseline length, when applied to the double U-tube shape, a positive effect resulted.In contrast, the GHX length was increased by 6% when the coaxial system was adopted. Inaddition, the borehole

thermal resistance was found to be 0.076, 0.104, and 0.121 m/ KW for the double U-tube, single U-tube, and coaxial GHX systems, respectively. It was also observed that the double U-tube configuration of the GXH was more cost-effective in terms of the initial cost, but, very importantly, care needs to be taken to monitor for possible thermal imbalance problems over the long-term [146]. U-pipe size U-pipe sizes for the GHX affect the performance of a ground source heat pump in two ways: power consumption and heat flux [147]. In practical terms, the high - density polyethylene (HDPE) proved to be the most common pipe material used in GHX installations because of its

- i. Flexibility
- ii. Durability
- iii. Ease of use
- iv. Ability to withstand high pressure at different depths and temperatures
- v. Resistance to corrosion
- vi. Long-life duration, expected to be 50-100 years.

Moreover, HDPE meets the requirements of the manufacturing standards, codes, and most local regulations of the GSHP industry. However, the pipes are only available in a range of diameters. Table 6.5, the most appropriate diameters suitable for the GHX are SDR 11 (25,32, and 40 mm) [148]. In addition, the correct specification and installation according to the industry and manufacturing guidelines are crucial to reach the life-span, which is expected to be a minimum of fifty years.

The pipe size has a direct effect on the borehole diameter in the fluid pressure and velocity. Therefore, pipes should be selected so that the diameter is such that the power required for pumping is kept to a minimum, and yet they should be small enough enable turbulent flow in the pipe.

Table 6.5 The most popular pipe sizes of the HDPE used in GSHP installations.

Nominal diameter (in.)	SDR 9	SDR 11	SDR 17
	OD/ID (mm)	OD/ID (mm)	OD/ID (mm)
3/4 (20 mm)	26.7 / 20.8	26.7 / 21.8	26.7 / 23.6
1 (25 mm)	33.4 / 26.0	33.4 / 27.4	33.4 / 29.5
1 1/4 (32 mm)	42.2 / 32.8	42.2 / 34.5	42.2 / 37.1
1 1/2 (40 mm)	48.2 / 37.5	48.2 / 39.4	48.2 / 42.7
2 (50 mm)	60.3 / 46.9	60.3 / 49.3	60.3 / 53.3
3 (75 mm)	88.9 / 69.1	88.9 / 72.6	88.9 / 78.5

The evidence presented in Table (3g), shows that the selected pipe size has little effect on the power consumption. In contrast, a change of 4% in the length has little impact, particularly when the baseline diameter changes from -5 % to +5%. Furthermore, the designer should take into account the risk of the grout material pressure on the structure of the pipe, at different depths, to avoid any collapse in the pipe. Figure 6.12 represents the relation between the pipe diameter and the borehole thermal resistance. This reduction in thermal resistance as a result of an increase in the pipe surface area leads to a greater heat flux.

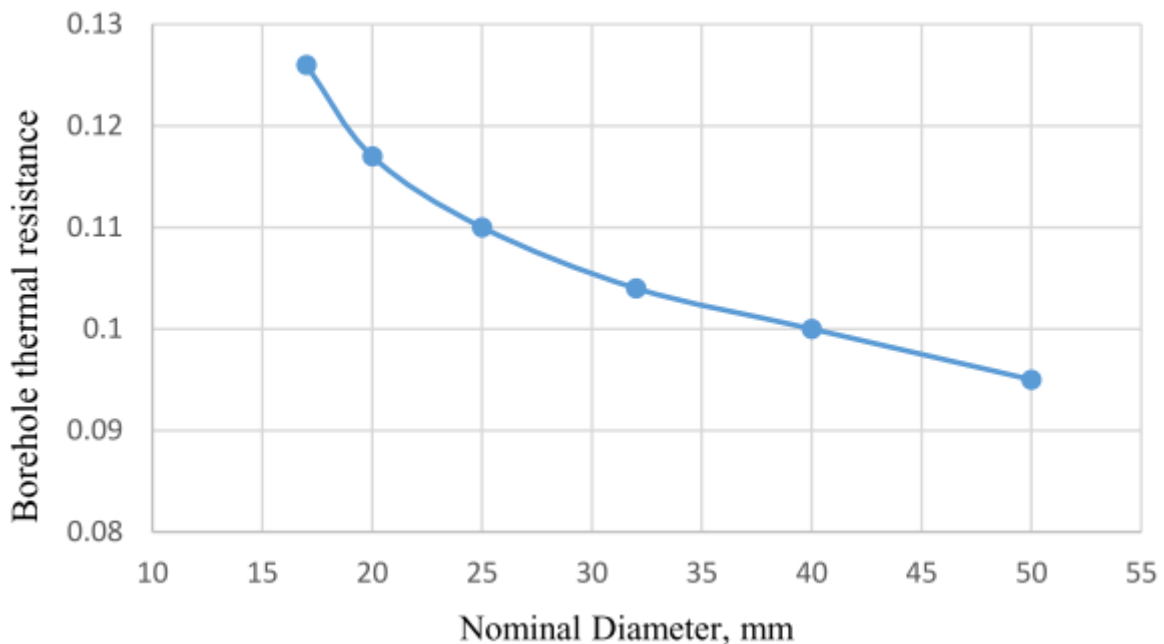


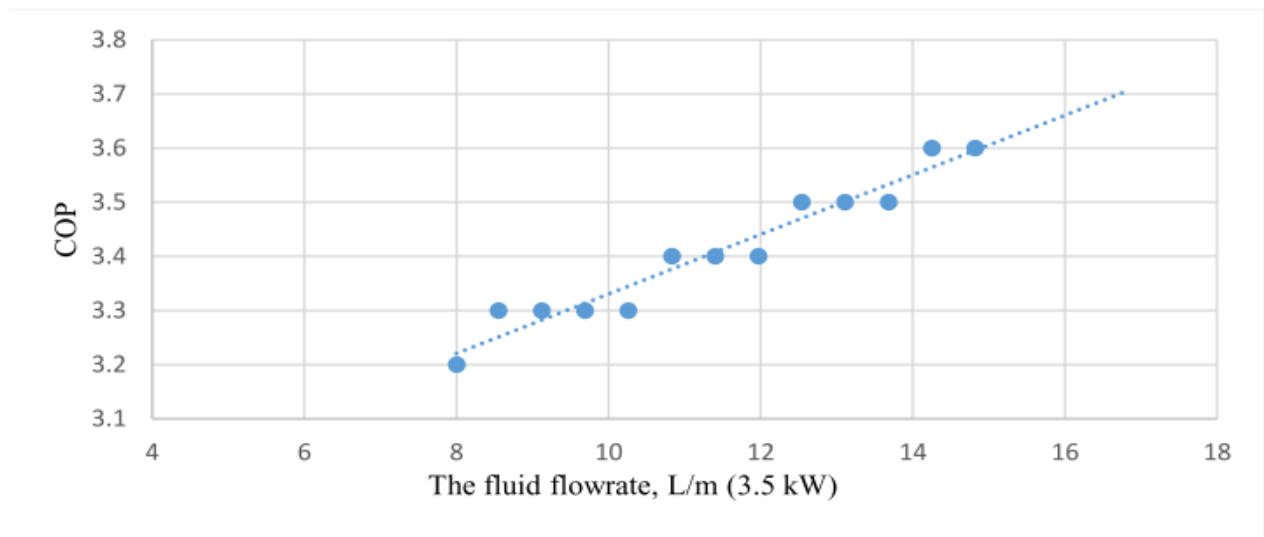
Figure 6-12 The effect of the pipe size on the borehole thermal resistance.



#### **6.6.5.6 The fluid flowrate**

The fluid flowrate is classified as an adjustable factor (design factor) that plays an important role in a system's power consumption and the amount of heat extracted from the region surrounding the heat exchanger [127]. To achieve the maximum heat exchange between the fluid and the pipe wall, the fluid flow must be turbulent and not laminar. As shown in Figure 6. 3, the GLD program allows the determination of the type of fluid and its flow method (turbulent/laminar) and the increase or decrease in the flow rate. In this study, the GLD automatically calculates the flow rate (11.4 L/m) and the Reynolds numbers based on the peak cooling/heating load, the heat pump size, and system characteristics. In addition, the GLD automatic purging flow rate calculations keep the water flow turbulent, which helps to transfer more heat in the regime.

In this study, it can be seen from Table 3h that the effect of the fluid flowrate on the length of the heat exchanger (GHX) is considered to be relatively small; a 5% decrease in the flowrate results in a decrease of 1% in the borehole length. Also, the effect on energy consumption is virtually non-existent, not exceeding 0.02 % in any operational condition. It is important to note that the coefficient of performance changes significantly when the fluid flowrate decreases by 5% causing the COP to decrease by 3.3%. This can be seen from the data presented in Figure 6.13. This change in the COP could be due to the alteration in the borehole length and the increase in the flow velocity, thereby causing a greater heat exchange between the fluid and the pipe.



*Figure 6-13 The effect of the fluid flowrate on the COP of the GSHP.*

### 6.6.6 Circulated fluid type

The circulated fluid used in the GHX depends on the geographical location and climatic conditions. Although water is the most common fluid in cold regions, an anti-freeze solution is used to prevent the liquid freezing inside the pipes. Table 4a contains a summary of the best-known types of circulating fluid and, in general, the antifreeze solution added prevents freezing down to  $-10^{\circ}\text{C}$ . Due to the high soil temperature used in this study, water is the fluid water without anti-freeze solution is adequate. As seen from Table (4a), 1-2% can be saved in the length of the GHX and GSHP power consumption when the anti-freeze solution is used. However, this saving is not commensurate with the anti-freeze initial cost.

### 6.6.7 Cooling and heating loads

The annual thermal loads within a building have a direct impact on the performance of ground source heat pumps, both in terms of the amount of heat rejection and the amount of extraction from the ground, which affects the thermal balance of a GHX system. In regions of extreme climatic heat, such as that experienced in the city of Riyadh, the proper design of the building envelope plays a major role in the amount of energy consumed. For example, Matthieu [149] investigated the most important design factors of a building envelope that affect energy savings, based on the climatic

conditions for two major Saudi cities (Riyadh),

hot/dry, and Jeddah, hot/humid). The results showed that improvements in the thermal resistance of the walls and windows led to savings of up to 52% in energy, and general improvements in the building envelope design led to savings of 78%. Air conditioning loads have a direct impact on the energy consumption, causing a change in the heat pump size and the length of the GHX. As shown in Table (3i), only  $\pm 5\%$  in variable thermal loads led to  $\pm 5\%$  in the total energy demand. Likewise, for thermal loads, change by  $\pm 5\%$  led to 5% change in the length of the GHX. The cooling and heating load are the most significant parameters that affect both the GHX length and heat pump power consumption.

### 6.7 Parameter Evaluation

The aim of this sensitivity analysis is to determine how to target the variables (borehole length and power consumption) that are most affected by independent changes in the design parameters. Figure 6.14 and Figure 6.15 show the effect of a parameter change of 5% on the borehole length and power consumption respectively.

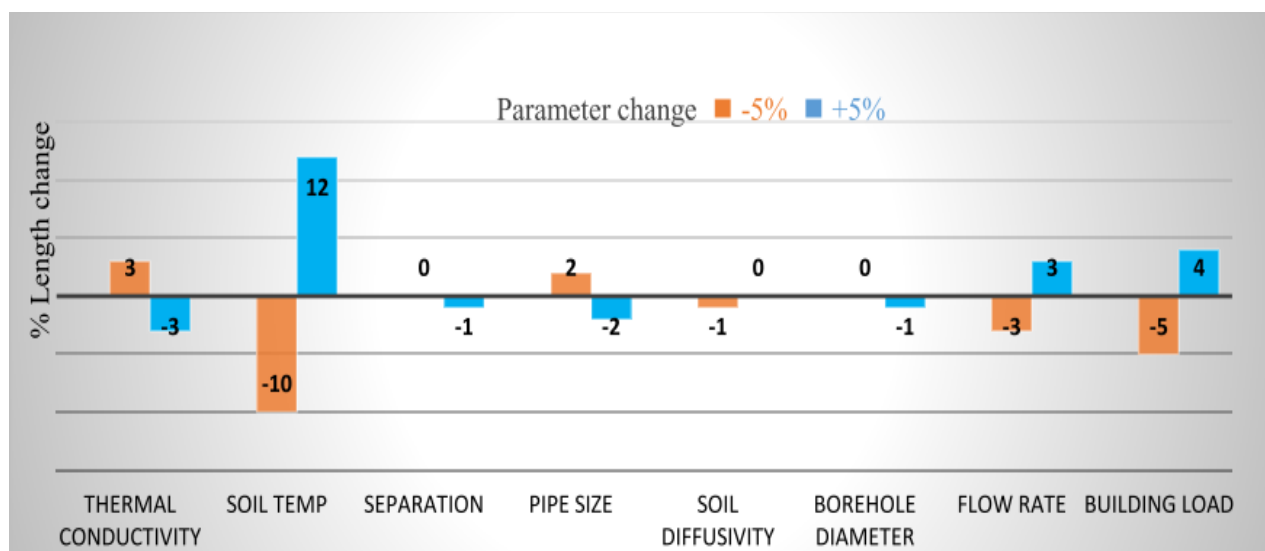


Figure 6-14 The effect of the parameter changes by  $\pm 5\%$  on the borehole length.

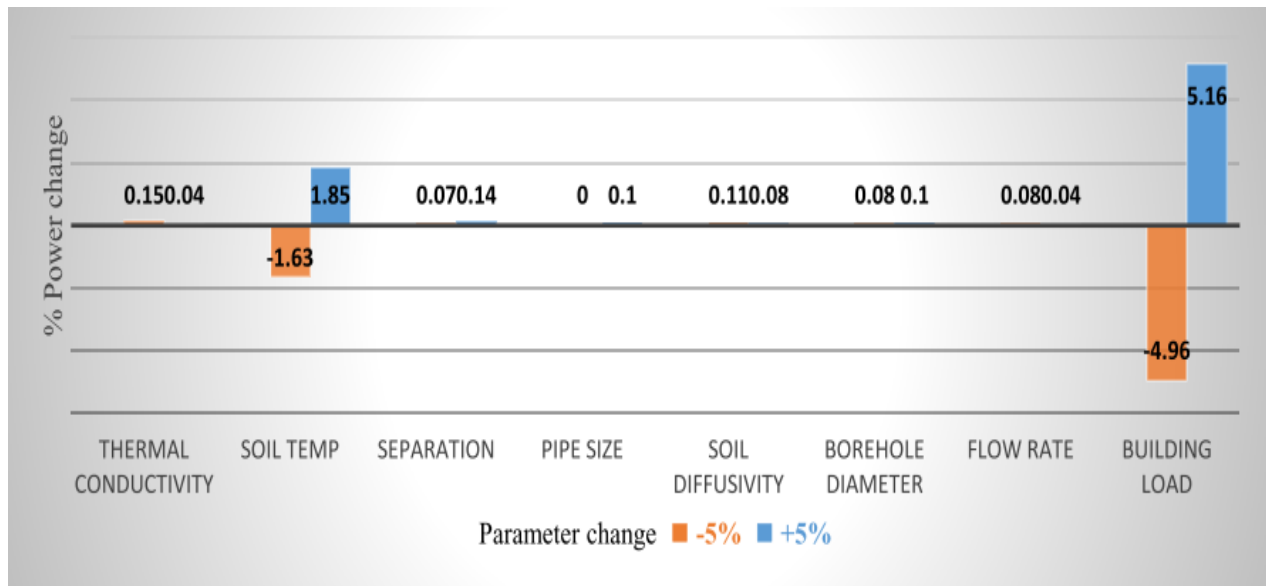


Figure 6-15 The effect of a parameter change by  $\pm 5\%$  on the power consumption.

It is clear from Figures 6.14 and 6.15 that the most important parameters that affect the length of the borehole are the thermal conductivity, soil temperature, fluid flowrate, and building load. In addition, the most important parameters that affect the power consumption are the soil temperature and building load.

Generally, all these independent variables change simultaneously, some of them with a negative and others with a positive impact. Therefore, determining the exact impact of each parameter and the exact relationship between the components is extremely difficult. Despite the fact that the length of the GHX determines the initial cost, the EWT will be the parameter used to measure the applicability of the system. This is because the EWT describes the final state of the temperature of the fluid after going through the heat exchange process, regardless of the effect of each of the parameters. If the EWT value is within the pump design limits, then the system can be applied and re-applied. This value must be tested over the system's lifespan of 25 years. In order to enrich the sensitivity analysis, the additive value technique and the best/worst-case scenarios have been used to measure this sensitivity analysis.

## 6.8 Additive Value Technique

In order to evaluate the results presented in Section 6.7, the additive value technique is applied to determine whether the most influential parameters produce variations in the most important quantities in a linear manner or not. Based on Table 6.3 and Figure 6.12, the fourmost critical parameters that influence the length of the borehole were the thermal conductivity, soil temperature, building load and fluid flowrate, given by the symbols A, B,C and D, respectively, as shown in Table 6.6. Now suppose that two random parameters are both changed by the same percentage  $\pm 5$ ,  $\pm 10$  and  $\pm 15\%$  and all the other parameters are fixed at the base case to determine whether or not the length and EWT changes additively. This is repeated for all combination of the 2 parameters against the length and EWT. Regarding the length of the borehole, Table 6.7 shows the percentage changes due to the changes in these 2 parameters against the baseline length, which is 100m. In addition, Figure 6.16 shows the negative and positive effects of combining these two parameters on the borehole length. It is clear that the two most significant parameters that affect the length of a borehole are the soil temperature and the air-conditioning load of the building, and changes by  $\pm 5\%$  led to approximately a  $\pm 15\%$  change in the length of the GHX. Likewise, in the second most important parameters, the combination of soil temperature and fluid flowrate affects the length of the borehole by  $\pm 12\%$  when the parameters change by  $\pm 5\%$ .

Table 6.6 The notation for the four most important parameters influencing the length of the borehole.

Symbol	Parameter
A	Thermal conductivity
B	Soil temperature
C	Building load
D	Fluid flowrate

Table 6.7 The impact of combination of the two different parameters on the borehole length(baseline, 100m).

%	A		B		C		D		A+B		A+D		A+C		B+C		B+D		C+D	
	L	%	L	%	L	%	L	%	L	%	L	%	L	%	L	%	L	%	L	%
-15	111	11	75	-25	85	-15	91	-9	83	-17	106	6	94	-6	64	-36	73	-27	83	-17
-10	107	7	82	-18	90	-10	94	-6	88	-12	105	5	97	-3	74	-26	81	-19	88	-12
-5	103	3	90	-10	95	-5	97	-3	93	-7	102	2	98	-2	86	-14	89	-11	94	-6
0	100		100		100		100		100		100		100		100		100		100	
5	97	-3	112	12	104	4	103	3	108	8	97	-3	101	1	117	17	113	13	105	5
10	94	-6	127	27	109	9	105	5	120	20	95	-5	103	3	140	40	130	30	111	11
15	91	-9	148	48	114	14	107	7	136	36	93	-7	104	4	170	70	154	54	116	16

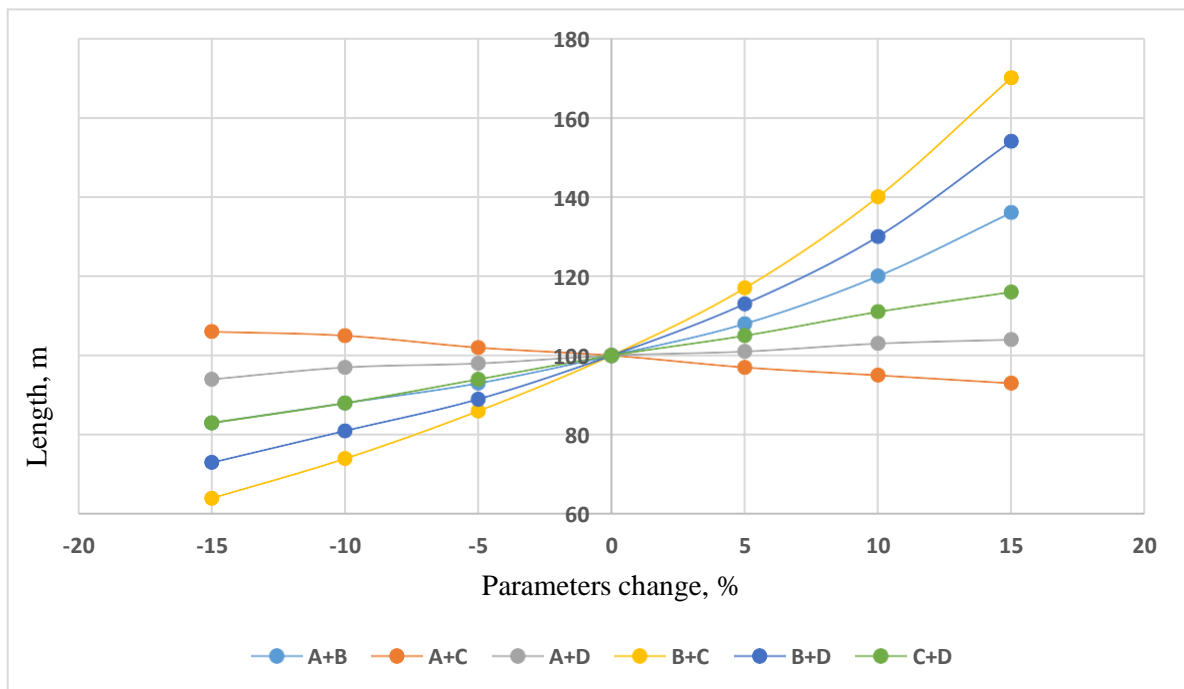


Figure 6-16 The effect of the combination of two different parameters on the borehole length.

Likewise, the additive value technique was applied against the EWT to determine whether or not the EWT temperature changes additively. Table 6.8 and Figure 6.17 shows the percentage changes due to the changes in these 2 parameters against the baseline EWT, which is 39.4°C. The value of the EWT generated by the combination of soil temperature and building load had the most influence on the GSHP system. When the soil temperature and the air conditioning load changes by

5%, the EWT changes by 6%.

In fact, all the heat transfer process between the GHX components and the surrounding soil manifest in the EWT. Therefore, the value of the EWT is the most critical measured parameter that determines the applicability of the GSHP regardless of other factors and their effect.

Table 6.8 The impact of the combination of the two different parameters on the EWT (baseline, 39.4°C).

	A		B		C		D		A+B		A+C		A+D		B+C		B+D		C+D	
	°C	%	°C	%	°C	%	°C	%	°C	%	°C	%	°C	%	°C	%	°C	%	°C	%
-15	40.9	4	34.7	-12	37.3	-5	38.9	-1	36.3	-8	38.7	-2	40.5	3	32.8	-17	34.3	-13	36.9	-6
-10	40.3	2	36.2	-8	38	-4	39.1	-1	37.3	-5	38.9	-1	40.1	2	35	-11	36	-9	37.7	-4
-5	39.8	1	37.8	-4	38.7	-2	39.2	-1	38.3	-3	39.1	-1	39.7	1	37.1	-6	37.7	-4	38.5	-2
0	39.4		39.4		39.4		39.4		39.4		39.4		39.4		39.4		39.4		39.4	
5	39.1	-1	40.9	4	40	2	39.5	0	40.5	3	39.6	1	39	-1	41.6	6	41	4	40.1	2
10	38.5	-2	42.4	8	40.7	3	39.6	1	41.6	6	39.8	1	38.7	-2	43.9	11	42.7	8	40.8	4
15	38.2	-3	44	12	41.4	5	39.6	1	42.8	9	39.9	1	38.4	-3	46.1	17	44.3	12	41.6	6

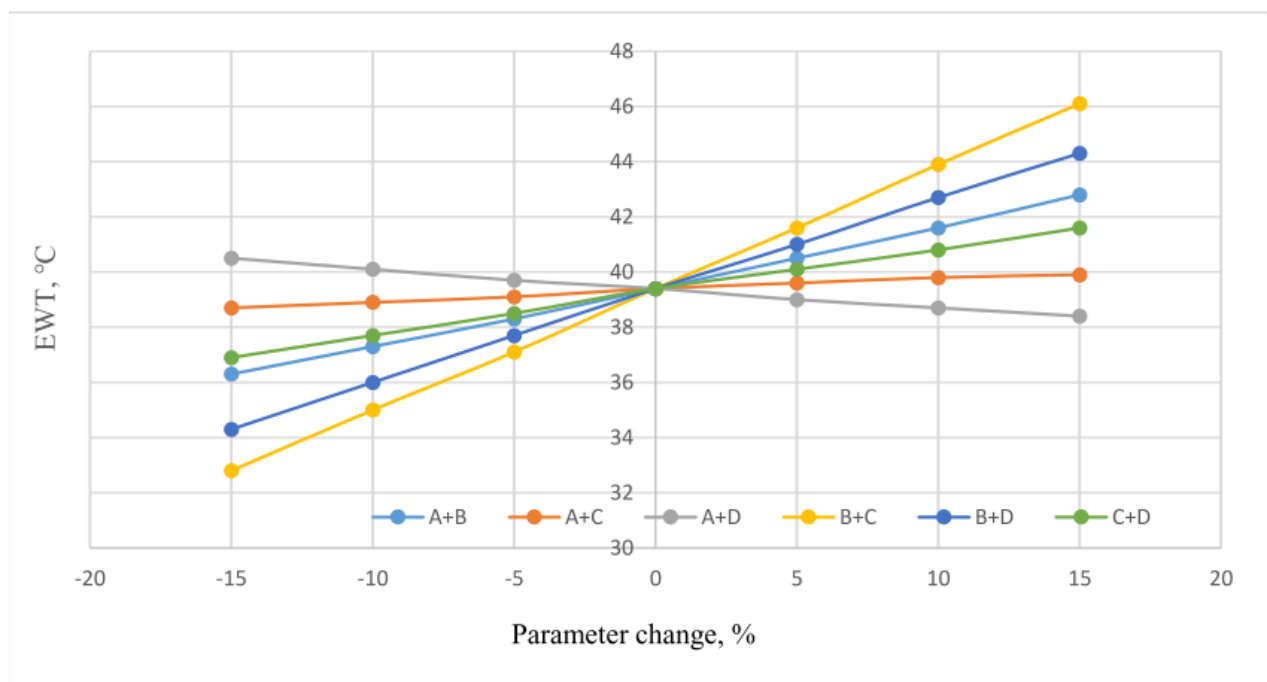


Figure 6-17 The effect of the combination of two different parameters on the EWT.

The aim of using the additive value technique is to be confident that a combination of any changes in the most important and influential parameters can be adequately approximated by the sum of the effect of the sum of the changes for each parameter, i.e., the changes vary both linearly and independently. Based on the results presented in Figure.16 and 17, it may be concluded, with confidence, that the most important and influential parameters satisfy this criterion of additive and linear variations over changes of up to 15%, and therefore it is not necessary to perform any further calculations. Thus, this sensitivity analysis shows that a good estimate of the effect of changing any of the parameters by up to 15% can be calculated based on the present results. Therefore, it is only necessary to investigate the best/worst case scenarios.

### 6.9 The Best/worst-case Scenarios

The best/worst-case scenarios have to be estimated, in order to determine the optimal design for the GSHP. In order to examine the best-case scenarios, all the parameters having a positive effect have been increased by +5% and all the parameters that have a negative effect have been decreased by 5%. Conversely, in order to examine the worst-case scenario, the opposite investigation was performed so that the value of each component having a positive effect was reduced by 5%, and the value of each component having a negative effect was increased by 5%. Table 6.9 shows the parameter values and the geometrical configuration for both the best and worst-case scenarios.

Table 6.9 The best/worst-case scenarios for the parameters which change by  $\pm 5\%$ .

S	Parameter	The best scenario		The worst scenario	
		%	Value	%	Value
1	Thermal conductivity	+5	2.73	-5	2.47
2	Soil Temp	-5	27.55	5	30.45
3	Separation	+5	-1%	-5	0
4	Pipe Size	+5	1.5 in	-5	1 in
5	Soil diffusivity	-5	0.0665	5	0.0735
6	Borehole diameter	+5	134.4	-5	121.6
7	Flow Rate	-5	10.8	+5	11.97
8	Building load	-5	13.8	+5	15.2
9	Fluid	water			
10	Radial pipe placement	Along outer wall		close together	
11	U Tube configuration	Double U-Tube		Coaxial	



To investigate the effect that these new parameters have then the values of the  $\pm 5\%$  changes are presented in Table 6.10, and the GSHP was re-modelled in order to ensure that the EWT, GHX length and power consumption provided the desired indoor thermal comfort that is compatible with the initial cost. It can be seen in Table 6.10 that in the worst scenario the EWT was  $44^{\circ}\text{C}$  after 20 years of operation, which is within the acceptable range of a heat pump unit design. This result indicates that the GSHP system is applicable despite the high temperature of the entering water of the heat pump.

Table 6.10 The comparison of the results for the best/worst-case scenarios in comparison to the baseline case.

Design Output	Baseline	Best scenarios	% Change	Worst scenarios	% Change
EWT $^{\circ}\text{C}$ , 1 year	39.4	37	-6	42.4	+7.6
Depth, m	100	90	-10	100	0
Power, kWh / year	10852	9800	-9.7	12183	12.26
EWT $^{\circ}\text{C}$ , 20 years	40.7	38.4	-5.6	44.1	8.35

In the best scenarios a 10 % in the initial cost and 6% in the operation cost can be saved. On the other hand, there is no increase in the initial cost in the worst-case scenario, and only an 8% increase in the operation cost which is acceptable.

### 6.10 Re-designing the System Using the Sensitivity Analysis

The third step in the evaluation of this sensitivity analysis is to redesign the system based on the results obtained from the additive value technique and the best/worst-case scenarios. The values employed in the new model are estimated based on previous studies or the designer's experience. In this section, the value of the EWT was fixed to be  $39.4^{\circ}\text{C}$  for both the baseline and the proposed design systems, and for the system COP, the GHX length and power consumption were measured.

Table 6.11 shows a comparison between the baseline and the proposed design parameters values.

	Thermal conductivity (W/mK)	Soil Temp. °C	Fluid	Pipe Size, mm	Soil Thermal diffusivity, m <sup>2</sup> /day	Separation, m	Borehole D,mm	Heat pump size, kW
Baseline	2.6	29	Water	32 (1.25 in)	0.07	10	128	18.75
Proposed design	2.73	28	Water	32 (1.25 in)	0.07	10	134	14.4
% change	5	-3.45	-	-	-	-	4.7	-23

The GSHP was re-modelled to ensure that the EWT remained within the acceptable range of the heat pump unit, and the GHX length and power consumption provided the desired indoor thermal comfort that is compatible with the initial cost. As shown in Table 6.11, the heat pump size reduces due to the favourable changes in the system parameters.

Table 6.12 shows the comparison results between the baseline and the proposed design. Significant saving in the initial cost of the proposed design is shown by the decrease in the GHX length from 100 m to 85m and the heat pump size reduced to 14.4 kW instead of 18.75 kW. Further, the power consumption slightly decreases from 10852 to 10730 kWh, (by 1.12% compared to the baseline system).

Table 6.12 The comparison between the baseline and the proposed design parameters values.

	Length, m	Power consumption, kWh	COP
Baseline	100	10852	3.4
Proposed design	85	10730	3.4
% change	15	1.12	-

It can be summarized based on study performed including additive value technique, the best/worst-case scenarios analysis and system redesign that compared to conventionally used chiller based heating and cooling system or ASHP, GSHP system is more beneficial specially for Saudi Arabia location.

## 6.11 Conclusions

This chapter presents a detailed evaluation of the most important parameters that affect the design of the GSHP system in the city of Riyadh in Saudi Arabia and other arid regions where the underground temperature is very high and the GSHP system operates in a cooling mode for most of the year. The modelling and sensitive analysis presented in this chapter provides a very valuable better understanding on the GSHP application in hot/dry regions and it can be concluded that:

As in the case of cold regions, the soil temperature, soil thermal conductivity, and air conditioning load are the most important factors that determine the efficiency of the GSHP in hot/dry regions.

The soil temperature is the most critical parameter that affects the length of the borehole and thus the cost of the installation. When the soil temperature change by  $\pm 5\%$  the length and power change by approximately 10 and 2%, respectively.

Regardless of what are the most important factors affecting the GSHP design and performance, the EWT is the parameter that determines the applicability of the GSHP system. When the value of EWT is within the heat pump unit design range then the GSHP system considered to be applicable. In this study the EWT after 20 and 40 years of operation were 44.1 and 44.9 °C, respectively, which remains within the capacity limits of the heat pump unit based on the manufacturing catalogue. However, the soil thermal imbalance needs to be calculated in order to avoid system failure.

The importance of some of the governing parameters varies from one region to another, for example, the circulated fluid type does not have any significant effects in hot regions, while in cold regions an antifreeze solution should be added to avoid freezing and the resulting system failure.

In general, this is the first attempt to analyse the performance of GSHPs in an arid region and in particular in Saudi Arabia. The result from the sensitivity analysis confirms that the implementation of the GSHP system in hot/dry regions has great potential. In addition, this result can be used to

evaluate the optimal design and initial cost for the GSHP system in Saudi Arabia and other arid regions. Finally, the proposed method assists and leads to the production of important guidelines for the application of GSHPs in hot/dry regions.

## **Chapter 7: Discussion, Conclusion and Future WorkClimate**

---

### **7.1 Discussion**

#### **7.1.1 Research background**

The government of the Kingdom of Saudi Arabia has developed a long-term plan to diversify the economy and reduce their nation's dependency on oil; this plan is known as Vision 2030. One of the most important pillars of this vision is to substantially improve the investment in the renewable energy sector and to quickly move forward in the implementation of new energy efficiency standards in key sectors and the end-uses being linked to their energy saving potential. Thus, the first wind farm has been built in the north of Saudi Arabia and construction of an 8 MW solar power plant has been started to service domestic energy consumption, which is predicted to increase by 10% annually. In addition, the government has stopped subsidising the electricity tariff, and this has led to an increase in the cost of electricity by as much as 200% for residential and commercial buildings (see Figure 1.4). All of these factors have driven researchers to find alternative and sustainable solutions for conventional systems in order to reduce fuel consumption and carbon emissions.

#### **7.1.2 Aim and main findings of the thesis**

In hot and dry countries such as in Saudi Arabia, air-conditioning systems consume about seventy per cent of the total electrical energy used. Therefore, it is essential to reduce this demand, and conventional air-conditioning technology should be replaced by more efficient renewable energy systems. These should be compared to the current standard systems, which use ASHP, but these have a poor performance when the air temperature is high. In Saudi Arabia, this temperature can be as much as 50 °C. Therefore, an attempt is made in this thesis to simulate and evaluate the performance of ground source heat pumps (GSHPs) compared to systems employing ASHPs. For the first time, both the systems have been very comprehensively modelled and simulated using the Transient System Simulation (TRNSYS) technology for Saudi Arabia location. In addition, the new

Ground Loop Design (GLD) software has been used to design the length of the ground loop heat exchanger. In order to assess this configuration, an evaluation of a model of a single-storey office building, based on the climatic conditions and geological characteristics that occur in the city of Riyadh in Saudi Arabia, has been investigated. The period of evaluation used to determine the coefficient of performance (COP), energy-efficiency ratio (EER) and power consumption was twenty years. The simulation results show that the GSHP system has a very high performance when compared to ASHP. The average annual COP and EER were

4.1 and 15.5 for the GSHP, compared to 3.8 and 11 for the ASHP; the GSHP is a feasible alternative to ASHP, with a very encouraging 11-year payback period, with a very cost-effective 18% total cost saving over the simulation period and a 36% lower annual energy consumption.

These very encouraging results were the motivation to search for the most important factors affecting the GSHP system. Because of the success of GSHPs in some cold regions, this does mean that it will have the same effect in other regions, such as in arid regions. Thus, for the first time in such a hot/dry climate, a rigorous sensitivity analysis approach has been employed to analyse 12 parameters that most affect the behaviour of the system where cooling demands dominate over most of the year. It is concluded that the most important four design parameters are thermal conductivity, soil temperature, building load and fluid flow rate, and on increasing these values then they have opposing effects on the arid environmental conditions, such as those found in the city of Riyadh in Saudi Arabia.

In addition, in Chapter 6 the results of the additive value technique and the sensitivity analysis evaluation, the best/worst-case scenarios, were found. The initial cost analysis for the ASHP and GSHP, and the system redesign, leads us to conclude that a GSHP system is highly competitive with conventional cooling and heating systems; based on this scenario then the GSHP system is a very feasible cost-effective alternative system to be employed in such climates.

Although the energy consumption for the heating and cooling in a hot climate is important, very few studies have been performed on the potential of applying GSHPs in arid regions. Kharseh et al [150] investigated the feasibility of using GSHPs in Qatar. The results obtained from this study illustrate the possibility of implementing the GSHP system in Qatar. Table 7.1 shows the main input parameters that were used for both the studies in Riyadh and Qatar, and Table 7.2 shows the main simulation result, namely the GSHP results for the total length of the borehole, payback period and COP. It is clear that there is excellent agreement between the two systems in terms of the COP and PBP, where the COP was 2.8 and 2.7 and the PBP was 11 and 9 years in Riyadh and Qatar respectively. Despite these results, the length of the GHX in Qatar is less than the GHX in Riyadh by approximately 30%, and this means that the initial cost is 30% less in Qatar than in Riyadh. This may be because the weather in Qatar is more humid than - and not as dry as - in Riyadh. Alternatively, it may be because the groundwater in Qatar is only a few metres under the ground [151], and this leads to increasing the soil moisture, which assists in the faster conduction of heat, since Qatar is surrounded by water on three sides and is only spread over a small region. This phenomenon will reduce the effect of the higher soil temperature warming and maintain the system stability. However, the likely differences in the results obtained in Qatar and Riyadh are probably a combination of the above two aspects.

Table 7.1 The baseline parameter values for the simulation of GSHPs in Riyadh and Qatar.

Parameters		Value	
		GSHPs in Riyadh	GSHPs in Qatar
1	Building area, m <sup>2</sup>	120	144
2	Max. cooling capacity, kW	14	11.2
3	Thermal conductivity (W/mK)	2.6	2.63
4	Soil temperature, °C	29	29
5	Circulated fluid type	water	water
6	Pipe size, mm	32 (1.25 in)	32 (1.25 in)
7	Borehole diameter, m	0.128	0.11
8	Borehole separation, m	10	17
9	Simulation software	TRNSYS	EED

Table 7.2 The main results for the simulation of GSHPs in Riyadh and Qatar.

S	Parameters	Value	
		GSHPs in Riyadh	GSHPs in Qatar
1	Total borehole length, m	400	285
2	Payback period	11	9
3	COP	3.37	2.7

In addition, this study has found that, in general, the evaluation of the GSHP behaviour overlong periods of time are significant in at least two major respects. Firstly, the full picture for this research is important because it presents new and novel results that have not been identified in any other research works to date for hot/dry climates. Secondly, this much deeper understanding of the optimum design of the system determines the most important governing factors that must be studied very carefully. This evaluation found that the results obtained from the sensitivity analysis evaluation in Chapter 6 from the additive value technique constituted the best/worst-case scenarios analysis. The initial cost analysis for the ASHP and GSHP, together with the system redesign, leads us to conclude that a GSHP system is highly competitive with conventional cooling and heating systems; based on this scenario, then, the GSHP system is feasible and cost-effective.



Although there are many types of GSHPs (see Figure.2.5), the vertical GSHP system was chosen instead of other systems, such as the horizontal and open loop GSHP, for several reasons; these include: the soil temperature over the long depth of the borehole remains reasonably consistent and this leads to the heat transfer between the borehole and the surrounding area being suitable. This gives more stability to the heat exchanger and the vertical system is suitable for narrow areas, which is a viable option for the project with limited land. For example, the soil temperature at depths less than ten metres is very variable, and this is strongly affected by the seasonal ambient temperature, thus the horizontal GSHP system has not been studied in this thesis, because it has not been considered to be a successful and reliable approach for the cooling process. Likewise, the open loop system has not been addressed in this thesis due to the lack of available water resources such as lakes, rivers, and groundwater in sufficient quantity to operate the open loop system.

On returning to the GSHP system, the system consists of three main parts: the building load, the heat pump unit, and the ground heat exchanger. Each part has a direct and important impact on the system efficiency, design, and initial cost. Each part consists of many factors, and these may be considered to be either adjustable or non-adjustable factors. For example, the underground temperature and thermal conductivity are classified as being non-adjustable factors because they depend on the climatic conditions and the geological characteristics of the site, while the borehole geometry is an adjustable factor. Therefore, each component has a different weight when investigating the effect on the efficiency of the GSHP system.

### **7.1.3 Buildings and loads**

Despite the building envelope being outside the scope of this research, the building load (demand) plays a very important role in choosing the heat pump size, and this has a direct effect on the initial costs and running costs. For example, Wahl [152] investigated the effect of the elements' building envelope on the energy savings for buildings in the city of Riyadh. The results that she obtained show that 27% of the energy required can be saved when changing the type of window employed from

single clear glass to double glass, and the amount of energy consumed can also be reduced by 78% when changing the insulation in other elements, such as the exterior walls, roof, and doors. Thus, the selection of the envelope elements would lead to further substantial reductions in the energy required, and this would also be a useful guide when selecting the most appropriate size for an HVAC system.

The analysis of the building load is important for determining the HVAC system equipment's and size. In this work, the building is a cooling dominated building and the monthly cooling load ratio, the CLR, is defined by Fan *et al.* [153] as follows:

$$CLR = \frac{Q_m}{Q_{m,max}} \times 100 \quad (7.1)$$

where  $Q_m$  is the monthly cooling load, and  $Q_{m, max}$ , is the maximum cooling load. From Figure 7.1 it is observed that for seven months of the year the cooling capacity is less than 70% of the total maximum load. Thus, for this building, it is possible to install two GSHP units with a total capacity of 15kW to work alternately, instead of one big unit with 15kW. Thus, when the cooling load is less than 70%, the system does not have to work at full capacity, so operating one unit is sufficient to cover cooling demand, which leads to the

long life of the system, saves energy consumption, decreases the carbon footprint and results in less thermal accumulation in the borehole.

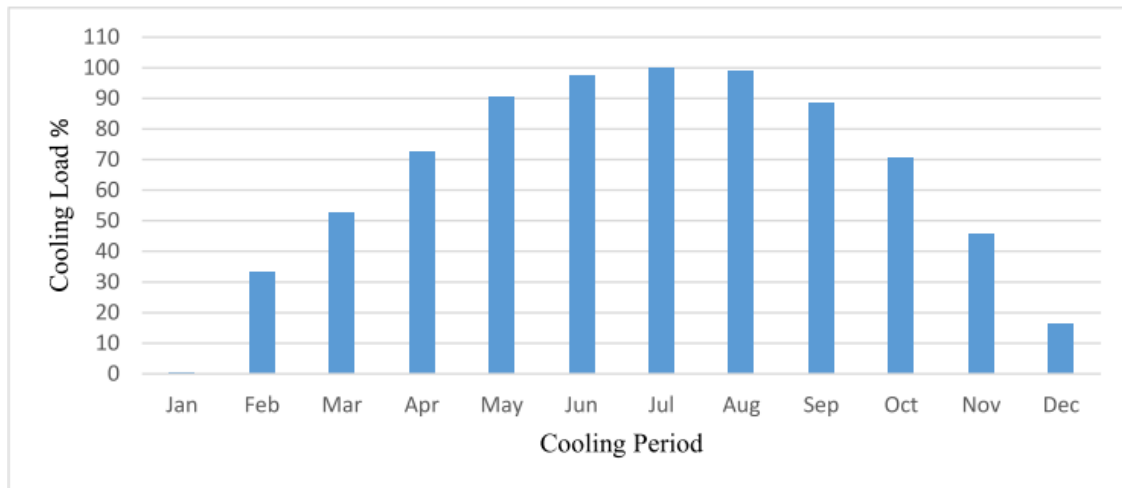


Figure 7-1 The percentage of monthly cooling load compared to the maximum cooling load for the office building in the city of Riyadh.

In addition to the building load and envelope, the function and type of the building have a significant effect on the performance of GSHPs. For example, school buildings are closed in the summer, and in Saudi Arabia the summer holidays are approximately 80 days and include the months of July and August. From Table 5 it is observed that the summer holiday period represents approximately 54% of the total cooling load, which leads to a reduction in the heat ejected to the soil, which leads to less cumulative heat; this alleviates the problem of thermal imbalance. Figure 7.2 shows a comparison between the amount of cooling heat ejected to the soil for office and school buildings.

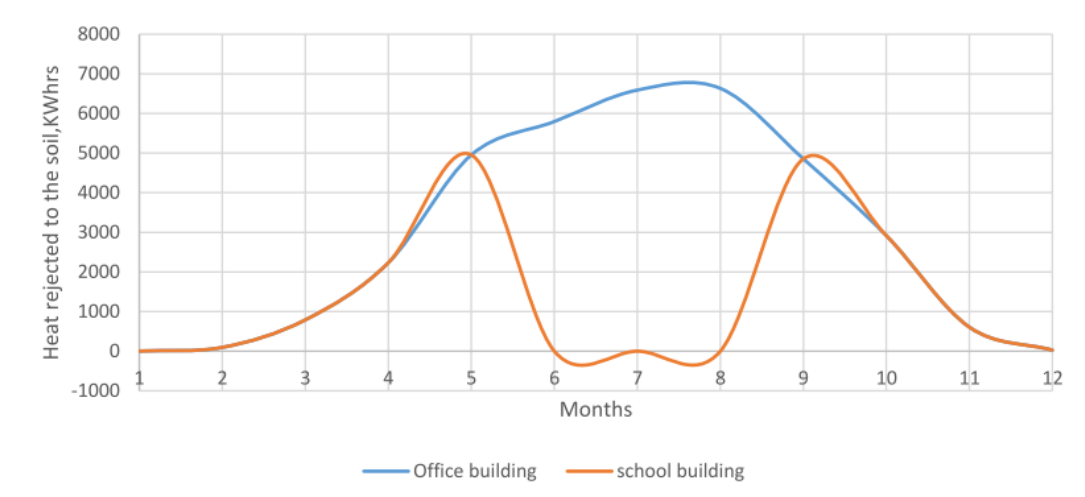


Figure 7-2 The amount of cooling heat ejected to the soil for office and school buildings in Riyadh.

Because the GSHP has not as yet operated in harsh hot/dry climates, then the thermal imbalance issues have now been investigated in conditions such as those found in countries like Saudi Arabia. Therefore, comparisons between countries such as Saudi Arabia and extreme cold regions, such as in Alaska, USA, where the thermal equilibrium almost does not exist (the worst-case scenario), could produce a much better understanding and give a reasonable explanation of the results and the ways to reduce the negative effect for the thermal imbalance issues which vary from place to place [154]. Although GSHPs have been operating for many years in cold regions, the topic of underground thermal imbalance that is estimated based on theoretical analyses still needs a substantial amount of real field data and experimental investigations. Several projects related to GSHPs have now been started in cold climates, such as in Sweden, Canada, China and Alaska, USA. In China, Mingyang et al. [155] investigated the thermal imbalance issues based on real field data obtained from many Chinese residential buildings. The results obtained show that the distribution system substantially affects the thermal imbalance, and that GSHP systems with only a radiant floor for heating lead to the most severe thermal imbalances, while GSHP systems with fan coil units or radiant ceilings for cooling and/or heating have achieved a much better thermal balance. Similarly, Wu et al. [58] investigated the effect of the type of heat pump on the ground thermal imbalance. The result shows that higher soil thermal balances and system efficiency are obtained from ground source absorption heat pumps (GSAHPs) compared to ground source electrical heat pumps (GSEHPs).

In Alaska, the Cold Climate Housing Research Centre (CCHRC) monitored the performance of GSHPs in six communities in wintertime over a period of six years [157]. The results show that the efficiency of the GSHP system can be reduced over a period of six years, in which the average COP drops from 3.65 to 3.2, but this value remains excellent and competitive with other systems. It is clear that the issues of thermal imbalance can be solved in more than one way; some of them relate to the demand load and some of them relate to the design of the GHX. However, the issue of thermal



imbalance needs many more studies based on site characteristics.

#### **7.1.4 Heat pump units**

In a hot and dry climate, the heat pump unit that is normally selected is based on the maximum cooling load capacity, with an increase of 10-20% as a safety factor. In this work, the ASHP unit has been selected, and this is similar to the GSHP unit in terms of its characteristics and specifications (such as the source of power, refrigeration type, compressor type, unit efficiency and the cooling/heating capacity), in order to make a fair comparison between the two systems. For example, the same coolant R-410a was used for both the ASHP and GSHP in order to avoid any effect on the comparison in the system efficiency. In addition, the coolant R-410a was used because it is now the most common type used in Saudi Arabia and in the world; this is due to its characteristics, such as its environmentally friendly qualities and a high cooling capacity.

In fact, there are several ways to increase the efficiency of the heat pump unit, and it is known that the refrigerant type affects the COP of the system. For example, Shuxue et al. [157] experimentally studied the effect of four different kinds of refrigerant on the system COP. As can be seen in Figure 7.3, the R32 and R410A yield the highest heating capacity and also the heating COP. Among the four kinds of refrigerants investigated, the heating COP value of the R32 is about 1.3–2.2% higher than that of the R134a.

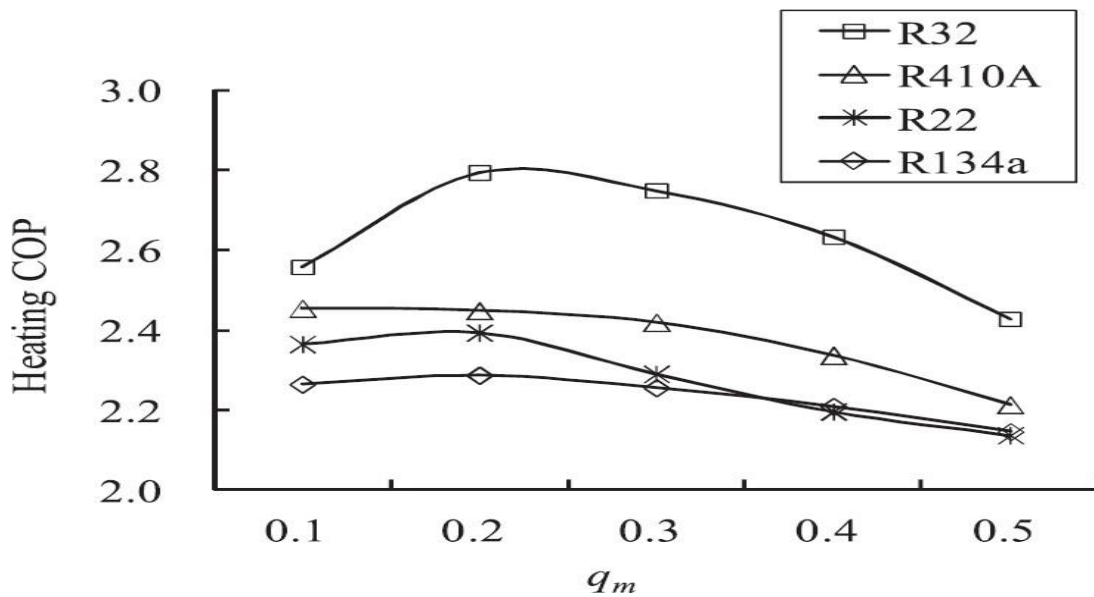


Figure 7-3 The relationship between the coolant type and system COP [157]

Moreover, many factors have significant impacts on the heat pump unit performance and efficiency. For instance, system technologies such as the VRF technology (variable refrigerant flow) deliver very attractive benefits associated with this technology, as they include improved comfort at a lower operating cost because the system can control the cooling/heating required for each zone separately. Other factors that play an important role, but are integral to the work presented in this thesis, include the following:

- 1- Heat pump type (water to water or water to air).
- 2- The heat pump compressor type (scroll compressors, rotary compressor, and screw compressor).

Normally, all these factors are taken into account at the design stage, and are based on many other factors such as the cost, operation purpose, unit size, site and weather.

### 7.1.5 Ground loop heat exchangers

The performance of the GSHP system is affected by the efficiency of the borehole heat exchangers design. The GHX length is a major component that may play a vital role in the determination of the feasibility of the system. One of the most striking results to emerge from the data is the relationship

between the two most important elements that affect the GHX length (soil temperature and soil thermal conductivity) when each element has an adverse effect on the heat transfer in the heat exchanger. When changing the soil temperature value by 5%, then the length of the heat exchanger is reduced by 10%, compared to 3% for thermal conductivity.

It is important that the designers take into account the difference between the lifetimes of the GHX elements (which should be expected to yield around 50+ years of usage) and the heat pump unit installations in the utility room of the building. Therefore, on the technical side, a high system performance is achieved by maintaining as small a temperature difference between the heat source and the heat load as possible, and by minimizing all possible losses, including energy, pressure, and temperature. Unfortunately, the thermal balance is the most difficult to achieve; this is mainly due to a couple of reasons, which include, but are not limited to, the very high soil temperature and the length of the summer period.

### **7.1.6 Grout material**

In this work, the thermal conductivity of the filling material was assumed to have the same high value for the soil thermal conductivity (2.6 W/mK). Grout with high thermal conductivity significantly reduces the borehole resistance. As the total temperature difference between the heat carrier fluid and the undisturbed ground depends on the combined borehole and ground thermal resistance, it has been found that the greatest reduction in the required borehole length of the ground loop occurred with higher ground thermal conductivity values. Where grout and ground thermal conductivities are similar, the borehole diameter is not a critical factor in the performance of the borehole heat exchanger. If the ground thermal conductivity is higher than the grout thermal conductivity, a greater borehole diameter will yield a higher combined borehole and ground thermal resistance. Smaller boreholes require less grout and have a lower total resistance, which indicates that the borehole diameter has an economic impact. Determining the optimum grout for a given project will require actual costs for the grout, pipes, and drilling.

### 7.1.7 Thermal imbalance

In a similar manner, the thermal imbalance is considered to be one of the most challenging elements that affect the system's feasibility. In hot dry climate regions, GSHPs operate in cooling mode most of the time, and this causes heat accumulation in the soil (more heat is ejected into the soil than is extracted) and this high rate in the underground thermal imbalance (87.5%) could lead to a system failure in the long term. Therefore, it is important to focus on finding technical solutions that assist in the reduction of heat accumulation in the soil. One of the proposed solutions is to add a fan that cools the water when it leaves the heat pump and before it enters the ground loop heat exchanger, this hybrid solution reduces size of GHX and thermal imbalance. For example, when the entering water temperature to the ground loop is reduced by 5%, then the length of the GHX will be reduced by approximately 10%; this leads to a 10% reduction in the initial cost. Figure 7.4 shows the proposed idea and how to install it.



*Figure 7-4 The proposed new fan and how it should be installed*

Although GSHPs have been operating for many years in cold regions, and many different types of research have been performed in order to solve the thermal imbalance problems, this issue still requires a substantial amount of more experimental studies. Unfortunately, some of the solutions proposed in cold regions are not suitable for application in hot regions, due to the difference in the goal of adding or removing heat from the soil. For instance, YuJin et al. [158] proposed that the GSHP assisted by solar thermal energy can effectively maintain the soil temperature balance, but



such a system does not work in hot environments when it is required to remove heat from the soil.

### 7.1.8 Soil thermal conductivity

The value of the thermal conductivity of the soil employed in this thesis was considered to be 2.6 W/mK. Nevertheless, it is important to note that most soil layers for the city of Riyadh consist of limestone and dolomite, which have a value of thermal conductivity that varies in the range 1.6 to 6.2 W/mK, which means that there is a possibility that the actual thermal conductivity of the soil is twice the value suggested in this thesis; this would lead to an even much more compelling reason to employ a GSHP system in such a region.

### 7.1.9 Site characteristics

A problem that may not appear elsewhere is the existence of caves and sinkholes that appear in the Riyadh limestone bedrock. Samir [159] investigated the cavities problems on a construction project in three locations in Saudi Arabia and Egypt. Figure 7.5 shows the size of the holes found in the project land in the city of Riyadh, Saudi Arabia. The lack of knowledge concerning this phenomenon could significantly affect the GHX performance in terms of the heat transfer, and this results in the installation having a more complex initial cost. For this reason, it is very important to ensure that the land employed for the new proposed system is free of these properties.



*Figure 7-5 The caves that appear in the limestone bedrock in Saudi Arabia [159]*

### **7.1.10 Limitations in installing and sizing GSHPs in Saudi Arabia**

Due to the nature of the GSHP system, where there are a large number of climate and geological factors that influence the performance and design method of the GSHP, then this makes it difficult to cover them all in one study. This PhD study has several limitations: for example, the lack of information about the groundwater and soil layers that have different thermal conductivities; we have assumed only one soil layer with no groundwater effect. However, these issues could significantly increase or decrease the GHX size, and this would lead to an effect on the system's initial cost. Also, the domestic hot water produced by the GSHP is not taken into account in this analysis, which is a big advantage in the life-cycle cost analysis. In addition, there is a lack of information about the price of GSHPs in the Saudi market, which makes it difficult to make a very good comparison between GSHP units and conventional systems such as the ASHP. Therefore, the value of the simple payback period requires much more accurate estimates in order to determine the viability of the GSHP system.

### **7.1.11 Legislation as a limiting factor**

Government legislation plays a major role in the adoption and use of renewable energy technologies by beneficiaries who own small projects or homes, as the foundational cost of renewable energy applications generally represents a hindrance to the adoption of the technology by either citizens or investors in small and medium buildings. To support the spread of this technology, governments must take motivational measures that encourage citizens to accept the idea of applying this system. Among the most important methods leading to the spread of this technology are direct financial support, training and exemption or reduction of some government fees, such as taxes. For example, in Saudi Arabia, the Saudi Energy Efficiency Centre (SEEC) [160] adopted an initiative to motivate citizens to replace old air conditioners with high-efficiency units (min. EER 13.5) by supporting the applicant with an amount of 900 Riyals (240 USD) for each old air conditioner that was replaced. This initiative reduced the annual consumption rate of air conditioner units by 40%. Figure. 7.6

shows the effect of increasing the energy-efficiency ratio (EER) from 7.5 in 2013 to 13.5 in 2020 on the annual power consumption rate for air conditioning units. To date, there is no direct support from government agencies in Saudi Arabia to apply GSHP technologies to small projects such as homes and small commercial buildings, but this kind of government subsidy has encouraged citizens to use and adapt clean and renewable energy applications.

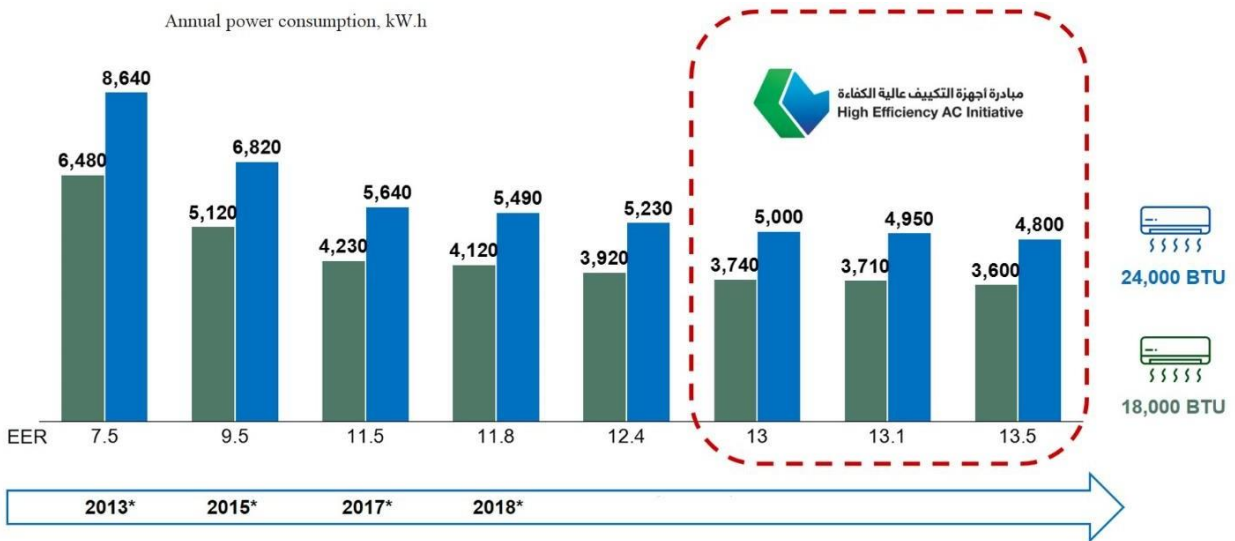


Figure 7-6 The effect of increasing the energy-efficiency ratio (EER) on power consumption for air conditioning units.

### 7.2 Conclusion

In hot regions, air conditioning and refrigeration systems are among the most important parts of a building that the designer focuses on to reduce energy consumption. Indeed, GSHP systems achieve this goal as a result of the higher performance of GSHPs, compared to conventional systems such as ASHPs. In arid regions such as Saudi Arabia, the potential benefits of energy savings from GSHPs face as many difficulties as elsewhere in the world.

- It is concluded that GSHPs are feasible, albeit with a long payback period, depending on the conditions, set-up and predictions. Also, it can be seen that there is a saving in CO2

emissions and there may be a substantial decrease in the total costs of using GSHP compared to ASHP.

- The underground temperature and thermal conductivity are the most important factors in determining the GHX length, while high underground temperatures can lead to a lengthy payback period and a subsequent increase in the initial cost.

Conducive soil temperatures and thermal conductivity would result in boreholes of shorter length, producing savings of 20–30%.

- The total cost savings over a 22-year period were found to be 18%.
- The thermal imbalance ratio was 88.5%, which is very high and has a negative impact on the system efficiency and operation.
- The payback period of GSHPs exceeds 11 years when compared to the ASHP system.
- Building types and operational hours - such as the hours involved in school building use - could solve the soil thermal imbalance problem resulting from the difference in the duration between cooling and heating.
- Although the efficiency of the GSHP is high compared to conventional systems, one of the *many challenges* of adapting the GSHP in Saudi Arabia is the larger initial investment.
- Climatic and weather information is covered and is easily accessible in Saudi Arabia compared to geological information; in particular, the data of the thermal properties of soils at shallow depths are absent, so this point needs further research and field studies.
- Site characteristics could have geological phenomena that significantly affect the GHX performance, such as caves and sinkholes that appear in various regions in Saudi Arabia.
- The impact of the government's adoption of a new policy for using renewable energy technology, namely by subsidising and encouraging residents to use alternative energy

conservation methods such as solar, wind, and geothermal energy, accelerates the process of adopting these systems.

### **7.3 Future Work**

To solve the issue of the lack of information about the benefits, possible risks, potential, and operation of shallow geothermal energy systems in hot/dry regions, several issues could be investigated in the future in order to fill these gaps in the literature:

- The GSHP has not yet been operated in harsh hot/dry climates and the thermal imbalance issue has not as yet been investigated in conditions in countries such as Saudi Arabia. Therefore, much more research is required to fully identify the thermal imbalance and the best way to reduce the high percentage of the new accumulative heat in the ground.
- The depth of the heat exchanger should be much more precisely determined in the sort of geological conditions that occur in Saudi Arabia. The COP, initial cost, and system performance are affected directly by the depth of the heat exchanger. In cold regions, as the depth of the heat exchanger increases, the efficiency of the system increases, due to the increase in soil temperature. This phenomenon may have an adverse effect in hot regions, and it is very important to determine the best depth to be employed by considering the balance between the cost and performance.
- It is also recommended that the impact of the government's adoption of a new policy for using renewable energy technology, namely by subsidising and encouraging residents to use alternative energy conservation methods, such as solar, wind, and geothermal energy, is considered. For example, by 2020 the British government's target was to produce 15% of energy from renewable sources, which meant that approximately 12% of the heating sources had to be from renewable energy. Such policies pushed investors to adopt new renewable

energy projects, but at the same time, they needed studies that showed the strengths and weaknesses of each field of renewable energy.

- The use of GSHP systems is very rare in hot regions, and therefore future studies should emphasize a comprehensive economic analysis of GSHPs in hot/dry regions and the government's role in promoting adoption of GSHP systems. In addition, a comprehensive method is required in order to estimate the feasibilities of the investments, such as the life-cycle cost analysis.
- Extensive studies have been made on solar-assisted GSHP system. Saudi Arabia is considered to be potentially one of the largest solar energy producers because of its geographic location, with it being in the sunbelt and receiving very strong levels of solar energy throughout the year. Therefore, the advantage of solar energy should be investigated in a hybrid system, with the employment of the proposed geothermal heat pump system.
- Saudi Arabia has a 2600 km coastline, on which there are many major cities.

Therefore, there are many great opportunities to investigate the possibilities of employing the open-loop GSHP benefits, using sea water as the cooling source. It should be noted that open-loop systems have greater efficiency and cost-effective installations if three basic criteria are adhered to, namely: (i) The quality of the water must be sufficient. Hard water can cause scaling in the system and reduce efficiency;

- water sources must be sufficient and renewable; and (iii) some open loop systems affect and contaminate groundwater, so it is necessary to know the compatibility of the open-loop GSHP system with the legislation of environmental agencies.

## References

---

- [1]"General Authority for Statistics", *General Authority for Statistics*, 2021. [Online]. Available: <https://www.stats.gov.sa/en>. [Accessed: 09- Jul- 2018].
- [2]R. Sultana and N. Nasrollahi, "Evaluation of remote sensing precipitation estimates over Saudi Arabia", *Journal of Arid Environments*, vol. 151, pp. 90-103, 2018. Available: 10.1016/j.jaridenv.2017.11.002.
- [3]A. Alshehry and M. Belloumi, "Energy consumption, carbon dioxide emissions and economic growth: The case of Saudi Arabia", *Renewable and Sustainable Energy Reviews*, vol. 41, pp. 237-247, 2015. Available: 10.1016/j.rser.2014.08.004.
- [4]G. Lahn and P. Stevens, "Burning Oil to Keep Cool The Hidden Energy Crisis in Saudi Arabia", The Royal Institute of International Affairs, London, 2011.
- [5]R. Obaid and A. Mufti, "Present State, Challenges, and Future of Power Generation in Saudi Arabia", in *IEEE Energy2030*, Atlanta, GA USA, 2008. Available: [10.1109/ENERGY.2008.4781073](https://doi.org/10.1109/ENERGY.2008.4781073)
- [6]M. Ramli, A. Hiendro, K. Sedraoui and S. Twaha, "Optimal sizing of grid-connected photovoltaic energy system in Saudi Arabia", *Renewable Energy*, vol. 75, pp. 489-495, 2015. Available: 10.1016/j.renene.2014.10.028.
- [7]D. Gately, N. Al-Yousef and H. Al-Sheikh, "The rapid growth of domestic oil consumption in Saudi Arabia and the opportunity cost of oil exports foregone", *Energy Policy*, vol. 47, pp. 57-68, 2012. Available: 10.1016/j.enpol.2012.04.011.
- [8]F. Alrashed and M. Asif, "Saudi Building Industry's Views on Sustainability in Buildings: Questionnaire Survey", *Energy Procedia*, vol. 62, pp. 382-390, 2014. Available: 10.1016/j.egypro.2014.12.400.
- [9]M. Salam and S. Khan, "Transition towards sustainable energy production – A review of the progress for solar energy in Saudi Arabia", *Energy Exploration & Exploitation*, vol. 36, no. 1, pp. 3-27, 2017. Available: 10.1177/0144598717737442.
- [10]M. Surf and L. Mostafa, "Will the Saudi's 2030 Vision Raise the Public Awareness of Sustainable Practices?", *Procedia Environmental Sciences*, vol. 37, pp. 514-527, 2017. Available: 10.1016/j.proenv.2017.03.026.
- [11]M. Saleem and M. Ali, "Sustainable Energy Measures in Saudi Arabia Based on Renewable Energy Sources: Present Actions and Future Plan", in *4th International Conference on Energy, Environment and Sustainable Development*, Mehran UET, Jamshoro, 2016.
- [12]M. Surf and L. Mostafa, "Will the Saudi's 2030 Vision Raise the Public Awareness of Sustainable Practices?", *Procedia Environmental Sciences*, vol. 37, pp. 514-527, 2017. Available: 10.1016/j.proenv.2017.03.026.
- [13] "Saudi Electricity Company", *Se.com.sa*, 2018. [Online]. Available: <https://www.se.com.sa/en-us/Pages/home.aspx>. [Accessed: 27- Jul- 2018].
- [14]A. Flint, *On the Source of Muscular Power. Arguments and Conclusions Drawn from Observations Upon the Human Subject, Under Conditions of Rest and of Muscular Exercise*. Palala Press, 2016.
- [15]M. Mackay, *Solar energy*. Oxford: Oxford University Press, 2015.
- [16]International Correspondence Schools, *Steam engine design & mechanism*. Rough Draft Printing, 2012.
- [17]"History NaturalGas.org", *Naturalgas.org*, 2013. [Online]. Available: <http://naturalgas.org/overview/history/>. [Accessed: 27- May- 2018].
- [18]D. Strohl, "How Henry Ford And Thomas Edison Killed The Electric Car", *Jalopnik*, 2021. [Online]. Available: <https://jalopnik.com/how-henry-ford-and-thomas-edison-killed-the-electric-ca-5564999>. [Accessed: 11 - Apr- 2017].

- [19]G. Boyle, *Renewable energy*, 3rd ed. Oxford: Oxford University Press, 2012.
- [20]A. Pierce, *The Industrial Revolution*. Edina, Minn.: Abdo Pub., 2005.
- [21]R. Hinrichs and M. Kleinbach, *Energy*. [Pacific Grove, California]: Brooks/Cole, Cengage Learning, 2013.
- [22]C. Hardy, *Atomic rise and fall*. Peakhurst, N.S.W.: Glen Haven, 1999.
- [23]"History of Nuclear Energy - World Nuclear Association", *World-nuclear.org*, 2021. [Online]. Available: <https://world-nuclear.org/information-library/current-and-future-generation/outline-history-of-nuclear-energy.aspx>. [Accessed: 27- May- 2017].
- [24]J. Shere, *Renewable: The World-Changing Power of Alternative Energy*, 1st ed. New York: St. Martin's Press, 2013.
- [25]"Healthy Forests Initiative - Sierra Forest Legacy", *Sierraforestlegacy.org*, 2021. [Online]. Available: [https://www.sierraforestlegacy.org/FC\\_LawsPolicyRegulations/KFSP\\_HealthyForests.php](https://www.sierraforestlegacy.org/FC_LawsPolicyRegulations/KFSP_HealthyForests.php). [Accessed: 16-Jan- 2017].
- [26]S. Bartoletto, "Patterns of Energy Transitions", *Past and Present Energy Societies*, pp. 305-330, 2012. Available: 10.14361/transcript.9783839419649.305.
- [27]S. Wang and B. Chen, "Energy–water nexus of urban agglomeration based on multiregional input–output tables and ecological network analysis: A case study of the Beijing–Tianjin–Hebei region", *Applied Energy*, vol. 178, pp. 773-783, 2016. Available: 10.1016/j.apenergy.2016.06.112.
- [28]P. Malanima, *Energy consumption in Italy in the 19th and 20th centuries*. [Napoli]: Consiglio nazionale delle ricerche, 2006.
- [29]J. Gittler, "Energy and Society: The Relation Between Energy, Social Change, and Economic Development.Fred Cottrell", *American Journal of Sociology*, vol. 62, no. 1, pp. 117-118, 1956. Available: 10.1086/221930 [Accessed 03 Feb 2018].
- [30]Renewable Energy Policy Network for the 21st Century, "Renewables 2017 Global Status Report", REN21 Secretariat, Paris, 2017.
- [31]A. Toth and E. Bobok, *Flow and heat transfer in geothermal systems*. Amsterdam: Elsevier, 2017.
- [32]A. Chiasson, *Geothermal Heat Pump and Heat Engine Systems: Theory And Practice*. John Wiley & Sons, 2016.
- [33]M. Rosen and S. Koohi-Fayegh, *Geothermal Energy: Sustainable Heating and Cooling Using the Ground*. Malaysia: John Wiley & Sons, 2018.
- [34]M. Dickson and M. Fanelli, *Geothermal Energy: Utilization and Technology*. Paris, France: UNESCO, 2005.
- [35]T. Lim, "Geothermal Heat Pump System for U.S. Residential Houses: Barriers of Implementation and it's Environmental and Economic Benefits", Master's Thesis, University of Michigan: Ann Arbor 1-103., 2014.
- [36]Y. Çengel and M. Boles, *Thermodynamics: An Engineering Approach*, 8th ed. New York: McGraw-Hill Education, 2015.
- [37]A. Mota-Babiloni, "Analysis of low Global Warming Potential fluoride working fluids in vapour compression systems. Experimental evaluation of commercial refrigeration alternatives", PhD, The Polytechnic University of Valencia, 2016.
- [38]J. Andújar Márquez, M. Martínez Bohórquez and S. Gómez Melgar, "Ground Thermal Diffusivity Calculation by Direct Soil Temperature Measurement. Application to very Low Enthalpy Geothermal Energy Systems", *Sensors*, vol. 16, no. 3, p. 306, 2016. Available: 10.3390/s16030306.
- [39]J. Price, "Ground source heat pumps", *Isoenergy.co.uk*, 2018. [Online]. Available: <https://www.isoenergy.co.uk/ground-source-heat-pump>. [Accessed: 03-Jul- 2018].



- [40]J. Bonin, *Heat Pump Planning Handbook*. Hoboken: Taylor and Francis, 2015.
- [41] Residential and Light Commercial Design and Installation Standards, #21025,2017
- [42]ASHRAE., *ASHRAE HANDBOOK 2017*. [S.l.]: ASHRAE, 2017.
- [43]S. Rees, *Advances in ground-source heat pump systems*. Amsterdam: Woodhead Publishing, 2016.
- [44]H. Javadi, S. Mousavi Ajarostaghi, M. Rosen and M. Pourfallah, "Performance of ground heat exchangers: A comprehensive review of recent advances", *Energy*, vol. 178, pp. 207-233, 2019. Available: 10.1016/j.energy.2019.04.094.
- [45]M. Kim, S. Lee, S. Yoon and J. Jeon, "Evaluation of geometric factors influencing thermal performance of horizontal spiral-coil ground heat exchangers", *Applied Thermal Engineering*, vol. 144, pp. 788-796, 2018. Available: 10.1016/j.applthermaleng.2018.08.084 [Accessed 27 May 2021].
- [46]C. Chong, G. Gan, A. Verhoef, R. Garcia and P. Vidale, "Simulation of thermal performance of horizontal slinky-loop heat exchangers for ground source heat pumps", *Applied Energy*, vol. 104, pp. 603-610, 2013. Available: 10.1016/j.apenergy.2012.11.069 [Accessed 27 May 2021].
- [47]S. Said, M. Habib, E. Mokheimer and M. El-Sharqawi, "Feasibility of using ground-coupled condensers in A/C systems", *Geothermics*, vol. 39, no. 2, pp. 201-204, 2010. Available: 10.1016/j.geothermics.2010.02.001.
- [48]A. Amin, "Amin, A. (2016). Underground Thermal Energy Storage Application in Erbil City Kurdistan, Region-Iraq (Case Study).", *Journal of Environment and Earth Science*, vol. 6, pp. 83-92, 2016. [Accessed 28 May 2021].
- [49]N. Naili, I. Attar, M. Hazami and A. Farhat, "Experimental Analysis of Horizontal Ground Heat Exchanger for Northern Tunisia", *Journal of Electronics Cooling and Thermal Control*, vol. 02, no. 03, pp. 44-51, 2012. Available: 10.4236/jectc.2012.23005.
- [50]M. Kharseh, L. Altorkmany, M. Al-Khawaja and F. Hassani, "Analysis of the effect of global climate change on ground source heat pump systems in different climate categories", *Renewable Energy*, vol. 78, pp. 219-225, 2015. Available: 10.1016/j.renene.2015.01.017.
- [51]A. Serageldin, A. Abdelrahman and S. Ookawara, "Earth-Air Heat Exchanger thermal performance in Egyptian conditions: Experimental results, mathematical model, and Computational Fluid Dynamics simulation", *Energy Conversion and Management*, vol. 122, pp. 25-38, 2016. Available: 10.1016/j.enconman.2016.05.053.
- [52]K. Al Sabawi, "First geothermal system in Palestine", *eceee 2009 Summer Study on energy efficiency: Innovative buildings technologies*, vol. 7, pp. 1493-1498, 2009. Available: [https://www.eceee.org/static/media/uploads/site-2/library/conference\\_proceedings/eceee\\_Summer\\_Studies/2009/Panel\\_7/7.047/paper.pdf](https://www.eceee.org/static/media/uploads/site-2/library/conference_proceedings/eceee_Summer_Studies/2009/Panel_7/7.047/paper.pdf). [Accessed 28 May 2021].
- [53]B. Yasin and A. Alkhaldeh, "GROUND SOURCE HEAT PUMP SYSTEMS AND PUMP EXCHANGER SYSTEMS IN JORDAN", Dead Sea, Jordan, 2017.
- [54]D. Belatrache, S. Bentouba and M. Bourouis, "Numerical analysis of earth air heat exchangers at operating conditions in arid climates", *International Journal of Hydrogen Energy*, vol. 42, no. 13, pp. 8898-8904, 2017. Available: 10.1016/j.ijhydene.2016.08.221.
- [55]Y. Zhu, Y. Tao and R. Rayegan, "A comparison of deterministic and probabilistic life cycle cost analyses of ground source heat pump (GSHP) applications in hot and humid climate", *Energy and Buildings*, vol. 55, pp. 312-321, 2012. Available: 10.1016/j.enbuild.2012.08.039.
- [56] V. Tambe, "Feasibility Study of Ground Coupled Heat Pump Systems For Small Office Building Types in Phoenix, Arizona", Master of Science, ARIZONA STATE UNIVERSITY, 2014
- [57]Z. Zhou et al., "Feasibility of ground coupled heat pumps in office buildings: A China study", *Applied Energy*, vol. 162, pp. 266-277, 2016. Available: 10.1016/j.apenergy.2015.10.055.

- [58]W. Wu, B. Wang, T. You, W. Shi and X. Li, "A potential solution for thermal imbalance of ground source heat pump systems in cold regions: Ground source absorption heat pump", *Renewable Energy*, vol. 59, pp. 39-48, 2013. Available: 10.1016/j.renene.2013.03.020.
- [59]T. You, W. Wu, W. Shi, B. Wang and X. Li, "An overview of the problems and solutions of soil thermal imbalance of ground-coupled heat pumps in cold regions", *Applied Energy*, vol. 177, pp. 515-536, 2016. Available: 10.1016/j.apenergy.2016.05.115.
- [60]P. Eslami-nejad and M. Bernier, "Freezing of geothermal borehole surroundings: A numerical and experimental assessment with applications", *Applied Energy*, vol. 98, pp. 333-345, 2012. Available: 10.1016/j.apenergy.2012.03.047.
- [61]R. Garber-Slaght and R. Peterson, "Can Ground Source Heat Pumps Perform Well in Alaska?", *Proceedings of the IGSHPA Technical/Research Conference and Expo 2017*, 2017. Available: 10.22488/okstate.17.000525.
- [62]S. Tu, X. Zhang and X. Zhou, "A revised thermal resistance and capacity model for the ground heat exchanger under freezing soil conditions and thermal performance analysis", *Procedia Engineering*, vol. 205, pp. 19-26, 2017. Available: 10.1016/j.proeng.2017.09.929.
- [63]W. Wu, X. Li, T. You, B. Wang and W. Shi, "Combining ground source absorption heat pump with ground source electrical heat pump for thermal balance, higher efficiency and better economy in cold regions", *Renewable Energy*, vol. 84, pp. 74-88, 2015. Available: 10.1016/j.renene.2015.06.025
- [64]R. Garber-Slaght, R. Daanen and A. Roe, "Ground Source Heat Pump Efficiency in Cold Climates", in *In Proceedings of the Conference Paper Session-Ground Source Heat Pump System*, Seattle, WA, USA, 2014.
- [65]Commonwealth of Massachusetts Executive Office of Energy & Environmental Affairs, "the Guideline on Metering and Calculation the Useful Thermal Output of Eligible Renewable Thermal Generation Units. Part2", 2019.
- [66]S. Naicker and S. Rees, "Monitoring and Performance Analysis of Large Non-domestic Ground Source Heat Pump Installation", in *CIBSE Technical Symposium*, Leicester, UK, 2011.
- [67]J. Han, M. Cui, J. Chen and W. Lv, "Analysis of thermal performance and economy of ground source heat pump system: a case study of the large building", *Geothermics*, vol. 89, p. 101929, 2021. Available: 10.1016/j.geothermics.2020.101929.
- [68]X. Zhai and Y. Yang, "Experience on the application of a ground source heat pump system in an archives building", *Energy and Buildings*, vol. 43, no. 11, pp. 3263-3270, 2011. Available: 10.1016/j.enbuild.2011.08.029.
- [69] S. Kavanaugh and K. Rafferty, *Geothermal heating and cooling : design of ground-source heat pump systems*. Atlanta, GA: American Society of Heating, Refrigeration and Air-Conditioning Engineers (ASHRAE), 2014.
- [70]J. Luo, J. Rohn, M. Bayer, A. Priess, L. Wilkmann and W. Xiang, "Heating and cooling performance analysis of a ground source heat pump system in Southern Germany", *Geothermics*, vol. 53, pp. 57-66, 2015. Available: 10.1016/j.geothermics.2014.04.004.
- [71]S. Soni, M. Pandey and V. Bartaria, "Hybrid ground coupled heat exchanger systems for space heating/cooling applications: A review", *Renewable and Sustainable Energy Reviews*, vol. 60, pp. 724-738, 2016. Available: 10.1016/j.rser.2016.01.125.
- [72]T. Sivasakthivel, K. Murugesan and P. Sahoo, "Optimization of ground heat exchanger parameters of ground source heat pump system for space heating applications", *Energy*, vol. 78, pp. 573-586, 2014. Available: 10.1016/j.energy.2014.10.045 [Accessed 28 May 2021].
- [73]T. Sivasakthivel, M. Philippe, K. Murugesan, V. Verma and P. Hu, "Experimental thermal performance analysis of ground heat exchangers for space heating and cooling applications", *Renewable Energy*, vol. 113, pp. 1168-1181, 2017. Available: 10.1016/j.renene.2017.06.098 [Accessed 28 May 2021].

- [74]J. Cullin et al., "Validation of vertical ground heat exchanger design methodologies", *Science and Technology for the Built Environment*, vol. 21, no. 2, pp. 137-149, 2015. Available: 10.1080/10789669.2014.974478.
- [75]O. Fare and P. Basu, "An annular cylinder source model for heat transfer through energy piles", in *92nd Annual Meeting: Transportation Research Board (TRB)*, Washington, D.C., 2013.
- [76]Y. Zhao, Z. Ma and Z. Pang, "A Fast Simulation Approach to the Thermal Recovery Characteristics of Deep Borehole Heat Exchanger after Heat Extraction", *Sustainability*, vol. 12, no. 5, p. 2021, 2020. Available: 10.3390/su12052021 [Accessed 31 May 2021].
- [77]I. Sarbu and C. Sebarchievici, "Using Ground-Source Heat Pump Systems for Heating/Cooling of Buildings", *Advances in Geothermal Energy*, 2016. Available: 10.5772/61372.
- [78]M. Cimmino and M. Bernier, "A semi-analytical method to generate g-functions for geothermal bore fields", *International Journal of Heat and Mass Transfer*, vol. 70, pp. 641-650, 2014. Available: 10.1016/j.ijheatmasstransfer.2013.11.037.
- [79]F. Loveridge and W. Powrie, "Temperature response functions (G-functions) for single pile heat exchangers", *Energy*, vol. 57, pp. 554-564, 2013. Available: 10.1016/j.energy.2013.04.060 [Accessed 31 May 2021].
- [80]L. Lamarche, "g-function generation using a piecewise-linear profile applied to ground heat exchangers", *International Journal of Heat and Mass Transfer*, vol. 115, pp. 354-360, 2017. Available: 10.1016/j.ijheatmasstransfer.2017.08.051 [Accessed 31 May 2021].
- [81]W. Ruan and W. Horton, "Literature Review on the Calculation of Vertical Ground Heat Exchangers for Geothermal Heat Pump Systems", in *International High Performance Buildings Conference*, 2010
- [82]T. Persson, O. Stavset, R. Ramstad, M. Alonso and K. Lorenz, "Software for modelling and simulation of ground source heating and cooling systems", SINTEF Energy Research, Trondheim, Norway, 2016.
- [83]"TRNSYS - Official Website", *Sel.me.wisc.edu*, 2021. [Online]. Available: <https://sel.me.wisc.edu/trnsys/>. [Accessed: 04- Jun- 2021].
- [84] GmbH T. TRANSSOLAR Software, [https://www.trnsys.de/docs/trnsys3d/trnsys3d\\_uebersicht\\_de.htm](https://www.trnsys.de/docs/trnsys3d/trnsys3d_uebersicht_de.htm) (accessed 27 Jan 2019).
- [85]A. Zarrella, M. Scarpa and M. De Carli, "Short time step analysis of vertical ground-coupled heat exchangers: The approach of CaRM", *Renewable Energy*, vol. 36, no. 9, pp. 2357-2367, 2011. Available: 10.1016/j.renene.2011.01.032 [Accessed 4 June 2021].
- [86] [86] 24. Thermal Dynamics. GLD Software geothermal HVAC software design package, [www.groundloopdesign.com/](http://www.groundloopdesign.com/) (accessed 5 June 2018).
- [87]K. Mensah, Y. Jang and J. Choi, "Assessment of design strategies in a ground source heat pump system", *Energy and Buildings*, vol. 138, pp. 301-308, 2017. Available: 10.1016/j.enbuild.2016.12.055.
- [88]*The Ground Loop Design Premier Edition User's Manual*. USA: Celsia, LLC., 2019. Available: [www.groundloopdesign.com](http://www.groundloopdesign.com)
- [89]A. Alghamdi and T. Moore, "Analysis and Comparison of Trends in Extreme Temperature Indices in Riyadh City, Kingdom of Saudi Arabia, 1985–2010", *Journal of Climatology*, vol. 2014, pp. 1-10, 2014. Available: 10.1155/2014/560985.
- [90]H. Hasanean and M. Almazroui, "Rainfall: Features and Variations over Saudi Arabia, A Review", *Climate*, vol. 3, no. 3, pp. 578-626, 2015. Available: 10.3390/cli3030578
- [91]M. Almazroui, M. Islam, R. Dambul and P. Jones, "Trends of temperature extremes in Saudi Arabia", *International Journal of Climatology*, vol. 34, no. 3, pp. 808-826, 2013. Available: 10.1002/joc.3722.

- [92]M. Sharif, "Analysis of projected temperature changes over Saudi Arabia in the twenty-first century", *Arabian Journal of Geosciences*, vol. 8, no. 10, pp. 8795-8809, 2015. Available: 10.1007/s12517-015-1810-y.
- [93]E. DeNicola, O. Aburizaiza, A. Siddique, A. Siddique, H. Khwaja and D. Carpenter, "Climate Change and Water Scarcity: The Case of Saudi Arabia", *Annals of Global Health*, vol. 81, no. 3, p. 342, 2015. Available: 10.1016/j.aogh.2015.08.005.
- [94]F. Alrashed and M. Asif, "Analysis of critical climate related factors for the application of zero-energy homes in Saudi Arabia", *Renewable and Sustainable Energy Reviews*, vol. 41, pp. 1395-1403, 2015. Available: 10.1016/j.rser.2014.09.031 [Accessed 1 June 2021].
- [95]A. Lashin, D. Chandrasekharam, N. Al Arifi, A. Al Bassam and C. Varun, "Geothermal energy resources of wadi Al-Lith, Saudi Arabia", *Journal of African Earth Sciences*, vol. 97, pp. 357-367, 2014. Available: 10.1016/j.jafrearsci.2014.05.016.
- [96]M. Sharqawy, S. Said, E. Mokheimer, M. Habib, H. Badr and N. Al-Shayea, "First in situ determination of the ground thermal conductivity for borehole heat exchanger applications in Saudi Arabia", *Renewable Energy*, vol. 34, no. 10, pp. 2218-2223, 2009. Available: 10.1016/j.renene.2009.03.003.
- [97]M. Gettings, "Heat-flow measurements at shot points along the 1978 Saudi Arabian seismic deep-refraction line. Part 2. Discussion and interpretation", U.S. Geological Survey, Jeddah, 1982.
- [98]G. Florides and S. Kalogirou, "Annual ground temperature measurements at various depths", in *CLIMA, 8th RHEVA World Congress*, 9-12 October, Lausanne, Switzerland., 2005.
- [99] "The pillars of brooj engineering consultants in Saudi Arabia" Privet contact with engineering consultants in Saudi Arabia, The pillars of Brooj, Eng. Abdullah, office # 6 , 1<sup>st</sup> Floor, 7139 King Abdulaziz Rd. , Al Masif district,  
Riyadh 12467- 2372, Saudi Arabia
- [100]"WaterFurnace - Smarter From The Ground Up", *Waterfurnace.com*, 2018. [Online]. Available: <https://www.waterfurnace.com>. [Accessed: 4- Jun- 2018].
- [101]M. Staiti and A. Angelotti, "Design of Borehole Heat Exchangers for Ground Source Heat Pumps: A Comparison between Two Methods", *Energy Procedia*, vol. 78, pp. 1147-1152, 2015. Available: 10.1016/j.egypro.2015.11.078.
- [102]Climate-transparency.org, "Brown to green: G20 transition to a low carbon economy", 2016. Available: [https://www.climate-transparency.org/wp-content/uploads/2016/09/Saudi-Arabia\\_Country-Profile.pdf](https://www.climate-transparency.org/wp-content/uploads/2016/09/Saudi-Arabia_Country-Profile.pdf). [Accessed: 27- Jan- 2019].
- [103]S. Liu et al., "Energetic, economic and environmental analysis of air source transcritical CO<sub>2</sub> heat pump system for residential heating in China", *Applied Thermal Engineering*, vol. 148, pp. 1425-1439, 2019. Available: 10.1016/j.applthermaleng.2018.08.061.
- [104]M. Song, C. Tso, C. Chao and C. Wu, "Techno-economic analysis on frosting/defrosting operations for an air source heat pump unit with an optimized multi-circuit outdoor coil", *Energy and Buildings*, vol. 166, pp. 165-177, 2018. Available: 10.1016/j.enbuild.2018.01.060.
- [105]W. Wu, B. Wang, T. You, W. Shi and X. Li, "A potential solution for thermal imbalance of ground source heat pump systems in cold regions: Ground source absorption heat pump", *Renewable Energy*, vol. 59, pp. 39-48, 2013. Available: 10.1016/j.renene.2013.03.020 [Accessed 3 June 2021].
- [106] 27] B. Bozkaya, R. Li and W. Zeiler, "A dynamic building and aquifer co-simulation method for thermal imbalance investigation", *Applied Thermal Engineering*, vol. 144, pp. 681-694, 2018.
- [107]Y. Ding, Q. Chai, G. Ma and Y. Jiang, "Experimental study of an improved air source heat pump", *Energy Conversion and Management*, vol. 45, no. 15-16, pp. 2393-2403, 2004. Available: 10.1016/j.enconman.2003.11.021.

- [108]A. Michopoulos, V. Voulgari, A. Tsikaloudaki and T. Zachariadis, "Evaluation of ground source heat pump systems for residential buildings in warm Mediterranean regions: the example of Cyprus", *Energy Efficiency*, vol. 9, no. 6, pp. 1421-1436, 2016. Available: 10.1007/s12053-016-9431-1.
- [109]V. Vakiloroyaya, B. Samali, A. Fakhar and K. Pishghadam, "A review of different strategies for HVAC energy saving", *Energy Conversion and Management*, vol. 77, pp. 738-754, 2014. Available: 10.1016/j.enconman.2013.10.023.
- [110]P. Healy and V. Ugursal, "Performance and economic feasibility of ground source heat pumps in cold climate", *International Journal of Energy Research*, vol. 21, no. 10, pp. 857-870, 1997. Available: 10.1002/(sici)1099-114x(199708)21:10<857::aid-er279>3.0.co;2-1.
- [111]P. Christodoulides, L. Aresti and G. Florides, "Air-conditioning of a typical house in moderate climates with Ground Source Heat Pumps and cost comparison with Air Source Heat Pumps", *Applied Thermal Engineering*, vol. 158, p. 113772, 2019. Available: 10.1016/j.applthermaleng.2019.113772.
- [112]A. Safa, A. Fung and R. Kumar, "Comparative thermal performances of a ground source heat pump and a variable capacity air source heat pump systems for sustainable houses", *Applied Thermal Engineering*, vol. 81, pp. 279-287, 2015. Available: 10.1016/j.applthermaleng.2015.02.039 [Accessed 2 June 2021].
- [113]M. Abdel-Salam and A. Zaidi, "Field study of cooling performance of two ground-source heat pumps in Canadian single-family houses", *Applied Thermal Engineering*, vol. 184, p. 116294, 2021. Available: 10.1016/j.applthermaleng.2020.116294
- [114] Saudi Building Code- General, SBC 201,2018, [www.sbc.gov.sa/En/BuildingCode/Pages/SBC\\_2018.aspx](http://www.sbc.gov.sa/En/BuildingCode/Pages/SBC_2018.aspx) [Accessed 27 July 2018].
- [115]A. Khanlari, A. Sözen, B. Sahin, G. Di Nicola and F. Afshari, "Experimental investigation on using building shower drain water as a heat source for heat pump systems", *Energy Sources, Part A: Recovery, Utilization, and Environmental Effects*, pp. 1-13, 2020. Available: 10.1080/15567036.2020.1796845 [Accessed 2 June 2021].
- [116]F. Afshari, "Experimental and numerical investigation on thermoelectric coolers for comparing air-to-water to air-to-air refrigerators", *Journal of Thermal Analysis and Calorimetry*, vol. 144, no. 3, pp. 855-868, 2020. Available: 10.1007/s10973-020-09500-6
- [117] Johnson Controls. R-410A ZE/XN SERIES, <http://www.upgnet.com/PdfFileRedirect/5190086-YTG-D-0118.PDF> ,[Accessed 10 July 2019].
- [118]Carbon Footprint Ltd., "Country specific electricity grid greenhouse gas emission factors", Hampshire, UK, June 2020.
- [119]A. Bagdanavicius and N. Jenkins, "Power requirements of ground source heat pumps in a residential area", *Applied Energy*, vol. 102, pp. 591-600, 2013. Available: 10.1016/j.apenergy.2012.08.036.
- [120]A. Capozza, M. De Carli and A. Zarrella, "Investigations on the influence of aquifers on the ground temperature in ground-source heat pump operation", *Applied Energy*, vol. 107, pp. 350-363, 2013. Available: 10.1016/j.apenergy.2013.02.043.
- [121]L. Zhu, S. Chen, Y. Yang, W. Tian, Y. Sun and M. Lyu, "Global sensitivity analysis on borehole thermal energy storage performances under intermittent operation mode in the first charging phase", *Renewable Energy*, vol. 143, pp. 183-198, 2019. Available: 10.1016/j.renene.2019.05.010.
- [122]G. Ilisei, T. Catalina and R. Gavriluc, "Sensitivity analysis using simulations for a ground source heat pump – implementation on a solar passive house", *E3S Web of Conferences*, vol. 111, p. 01070, 2019. Available: 10.1051/e3sconf/201911101070 [Accessed 24 July 2020].
- [123]B. Li, Z. Han, C. Bai and H. Hu, "The influence of soil thermal properties on the operation performance on ground source heat pump system", *Renewable Energy*, vol. 141, pp. 903-913, 2019. Available: 10.1016/j.renene.2019.04.069 [Accessed 2 June 2021].
- [124]E. Gunawan, N. Giordano, P. Jensson, J. Newson and J. Raymond, "Alternative heating systems for northern remote communities: Techno-economic analysis of ground-coupled heat pumps in Kuujuaq,

- Nunavik, Canada", *Renewable Energy*, vol. 147, pp. 1540-1553, 2020. Available: 10.1016/j.renene.2019.09.039 [Accessed 2 June 2021].
- [125]E. Sakellariou, A. Wright, P. Axaopoulos and M. Oyinlola, "PVT based solar assisted ground source heat pump system: Modelling approach and sensitivity analyses", *Solar Energy*, vol. 193, pp. 37-50, 2019. Available: 10.1016/j.solener.2019.09.044 [Accessed 2 June 2021].
- [126]C. Han and X. Yu, "Sensitivity analysis of a vertical geothermal heat pump system", *Applied Energy*, vol. 170, pp. 148-160, 2016. Available: 10.1016/j.apenergy.2016.02.085 [Accessed 2 June 2021]
- [127]J. Woloszyn, "SENSITIVITY ANALYSIS OF GROUND SOURCE HEAT PUMP PERFORMANCE ON SELECTED SOIL AND OPERATING PARAMETERS", *15th International Multidisciplinary Scientific GeoConference SGEM2015, ENERGY AND CLEAN TECHNOLOGIES*, 2015. Available: 10.5593/sgem2015/b41/s17.066 [Accessed 2 June 2021].
- [128]T. Hong, J. Kim, M. Chae, J. Park, J. Jeong and M. Lee, "Sensitivity Analysis on the Impact Factors of the GSHP System Considering Energy Generation and Environmental Impact Using LCA", *Sustainability*, vol. 8, no. 4, p. 376, 2016. Available: 10.3390/su8040376 [Accessed 2 June 2021].
- [129]A. Casasso and R. Sethi, "Sensitivity Analysis on the Performance of a Ground Source Heat Pump Equipped with a Double U-pipe Borehole Heat Exchanger", *Energy Procedia*, vol. 59, pp. 301-308, 2014. Available: 10.1016/j.egypro.2014.10.381 [Accessed 2 June 2021].
- [130]C. Wood, H. Liu and S. Riffat, "Comparative performance of 'U-tube' and 'coaxial' loop designs for use with a ground source heat pump", *Applied Thermal Engineering*, vol. 37, pp. 190-195, 2012. Available: 10.1016/j.applthermaleng.2011.11.015 [Accessed 2 June 2021].
- [131]T. Sivasakthivel, K. Murugesan and H. Thomas, "Optimization of operating parameters of ground source heat pump system for space heating and cooling by Taguchi method and utility concept", *Applied Energy*, vol. 116, pp. 76-85, 2014. Available: 10.1016/j.apenergy.2013.10.065 [Accessed 2 June 2021].
- [132]Y. Liu, Y. Zhang, S. Gong, Z. Wang and H. Zhang, "Analysis on the Performance of Ground Heat Exchangers in Ground Source Heat Pump Systems based on Heat Transfer Enhancements", *Procedia Engineering*, vol. 121, pp. 19-26, 2015. Available: 10.1016/j.proeng.2015.08.1013 [Accessed 2 June 2021].
- [133]M. Li and A. Lai, "Review of analytical models for heat transfer by vertical ground heat exchangers (GHEs): A perspective of time and space scales", *Applied Energy*, vol. 151, pp. 178-191, 2015. Available: 10.1016/j.apenergy.2015.04.070 [Accessed 2 June 2021].
- [134]T. Sivasakthivel, K. Murugesan and H. Thomas, "Optimization of operating parameters of ground source heat pump system for space heating and cooling by Taguchi method and utility concept", *Applied Energy*, vol. 116, pp. 76-85, 2014. Available: 10.1016/j.apenergy.2013.10.065 [Accessed 2 June 2021].
- [135]W. Wu, H. Skye and P. Domanski, "Selecting HVAC systems to achieve comfortable and cost-effective residential net-zero energy buildings", *Applied Energy*, vol. 212, pp. 577-591, 2018. Available: 10.1016/j.apenergy.2017.12.046 [Accessed 2 June 2021].
- [136]G. Nouri, Y. Noorollahi and H. Yousefi, "Solar assisted ground source heat pump systems – A review", *Applied Thermal Engineering*, vol. 163, p. 114351, 2019. Available: 10.1016/j.applthermaleng.2019.114351 [Accessed 2 June 2021].
- [137]O. Ozgener and A. Hepbasli, "A review on the energy and exergy analysis of solar assisted heat pump systems", *Renewable and Sustainable Energy Reviews*, vol. 11, no. 3, pp. 482-496, 2007. Available: 10.1016/j.rser.2004.12.010 [Accessed 2 June 2021].
- [138]F. Rad, A. Fung and W. Leong, "Feasibility of combined solar thermal and ground source heat pump systems in cold climate, Canada", *Energy and Buildings*, vol. 61, pp. 224-232, 2013. Available: 10.1016/j.enbuild.2013.02.036 [Accessed 2 June 2021].
- [139]R. Powers, L. Ramirez, C. Redmond and E. Elberg, "Geology of the Arabian Peninsula; sedimentary geology of Saudi Arabia", *Professional Paper*, vol., no. 560, 1966. Available: 10.3133/pp560d [Accessed 2 June 2021].

[140]S. Bae, Y. Nam and B. Shim, "Feasibility Study of Ground Source Heat Pump System Considering Underground Thermal Properties", *Energies*, vol. 11, no. 7, p. 1786, 2018. Available: 10.3390/en11071786 [Accessed 2 June 2021].

[141] ClimateMaster (Tranquility-30) catalogue, Available: <https://files.climatemaster.com/rp1000-climate-master-residential-tranquility-30-digital-te-series-geothermal-heating-and-cooling-product-catalog.pdf> [Accessed 25 June 2019].

[142] Ground Source Heat Pump Association, Closed-loop Vertical Borehole Design, Installation & Materials Standard, National Energy Centre, Milton Keynes, 2011.

[143]J. Luo, J. Rohn, M. Bayer and A. Priess, "Thermal Efficiency Comparison of Borehole Heat Exchangers with Different Drillhole Diameters", *Energies*, vol. 6, no. 8, pp. 4187-4206, 2013. Available: 10.3390/en6084187 [Accessed 2 June 2021].

[144]D. O'Neal and Y. Gu, "Development of an equivalent diameter expression for vertical U-Tubes used in ground-coupled heat pumps", *ASHRAE Transactions*, vol. 104, pp. 347–355., 1998. [Accessed 22 June 2020].

[145]A. Zarrella, M. Scarpa and M. De Carli, "Short time step analysis of vertical ground-coupled heat exchangers: The approach of CaRM", *Renewable Energy*, vol. 36, no. 9, pp. 2357-2367, 2011. Available: 10.1016/j.renene.2011.01.032 [Accessed 2 June 2021].

[146]A. Zarrella, G. Emmi and M. De Carli, "A simulation-based analysis of variable flow pumping in ground source heat pump systems with different types of borehole heat exchangers: A case study", *Energy Conversion and Management*, vol. 131, pp. 135-150, 2017. Available: 10.1016/j.enconman.2016.10.061 [Accessed 2 June 2021].

[147]H. Zhang and Y. Yu, "Analysis of optimum U-tube diameter in ground source heat pump", in *the 2012 International Conference on Frontiers of Energy and Environment Engineering*, Hong Kong, 2020, pp. 354-357.

[148]W. Mazzotti, J. Acuña, A. Lazzarotto and B. Palm, "Deep Boreholes for Ground-Source Heat Pump", Swedish Energy Agency, Stockholm, Sweden., 2018.

[149]M. Maerten, "Cooling system for solar housing in the Middle East A design study based on a concept", Master, Chalmers University of Technology, 2011.

[150]M. Kharseh, M. Al-Khawaja and M. Suleiman, "Potential of ground source heat pump systems in cooling-dominated environments: Residential buildings", *Geothermics*, vol. 57, pp. 104-110, 2015. Available: 10.1016/j.geothermics.2015.06.009 [Accessed 2 June 2021].

[151]H. Baalousha, "Groundwater vulnerability mapping of Qatar aquifers", *Journal of African Earth Sciences*, vol. 124, pp. 75-93, 2016. Available: 10.1016/j.jafrearsci.2016.09.017 [Accessed 3 June 2021].

[152]E. Wahl, "Buildings in Arid Desert Climate: Improving Energy Efficiency with Measures on the Building Envelope", Ph.D, Luleå University of Technology, Department of Civil, Environmental and Natural Resources Engineering, 2017.

[153]B. Fan, X. Jin and Z. Du, "Optimal control strategies for multi-chiller system based on probability density distribution of cooling load ratio", *Energy and Buildings*, vol. 43, no. 10, pp. 2813-2821, 2011. Available: 10.1016/j.enbuild.2011.06.043 [Accessed 3 June 2021].

[154]D. Üрге-Vorsatz, L. Cabeza, S. Serrano, C. Barreneche and K. Petrichenko, "Heating and cooling energy trends and drivers in buildings", *Renewable and Sustainable Energy Reviews*, vol. 41, pp. 85-98, 2015. Available: 10.1016/j.rser.2014.08.039 [Accessed 3 June 2021].

[155]M. Qian, D. Yan, J. An, T. Hong and J. Spitler, "Evaluation of thermal imbalance of ground source heat pump systems in residential buildings in China", *Building Simulation*, vol. 13, no. 3, pp. 585-598, 2020. Available: 10.1007/s12273-020-0606-5 [Accessed 3 June 2021].

2021].



- [156]R. Garber-Slaght and R. Peterson, "Can Ground Source Heat Pumps Perform Well in Alaska?", *Proceedings of the IGSHPA Technical/Research Conference and Expo 2017*, 2017. Available: 10.22488/okstate.17.000525 [Accessed 3 June 2021].
- [157]X. Xu, Y. Hwang and R. Radermacher, "Performance comparison of R410A and R32 in vapor injection cycles", *International Journal of Refrigeration*, vol. 36, no. 3, pp. 892-903, 2013. Available: 10.1016/j.ijrefrig.2012.12.010 [Accessed 3 June 2021].
- [158]Y. Nam, X. Gao, S. Yoon and K. Lee, "Study on the Performance of a Ground Source Heat Pump System Assisted by Solar Thermal Storage", *Energies*, vol. 8, no. 12, pp. 13378-13394, 2015. Available: 10.3390/en81212365 [Accessed 3 June 2021].
- [159]S. El sayed, "Karst limestone foundation geotechnical problems, detection and treatment: Case studies from Egypt and Saudi Arabia", *International Journal of Scientific & Engineering Research*, vol. 4, no. 5, 2013. [Accessed 3 June 2021].
- [160]" Saudi Energy Efficiency Center , SEEC", *Seec.gov.sa*, 2021. [Online]. Available: <https://www.seec.gov.sa/en/>. [Accessed: 03- Jun- 2021].



## Appendix 1: Cooling and heating load calculation for the bank building in Riyadh

### a) Air System Sizing Summary for PACKAGE A/C UNIT

<b>Air System Information</b>		Number of zones ..... 1
Air System Name PACKAGE A/C UNIT		Floor Area ..... 584.7 m <sup>2</sup>
Equipment Class PKG ROOF		Location ..... Riyadh, Saudi Arabia
Air System Type .....SZCAV		
<b>Sizing Calculation Information</b>		Zone L/s Sizing ..... Sum of space airflow rates
Calculation Months ..... Jan to Dec		Space L/s Sizing ..... Individual peak space loads
Sizing Data ..... Calculated		
<b>Central Cooling Coil Sizing Data</b>		Load occurs at ..... Aug 1500
Total coil load ..... 196.2 kW		OA DB / WB ..... 46.0 / 21.0 °C
Sensible coil load ..... 196.2 kW		Entering DB / WB ..... 25.4 / 15.2 °C
Coil L/s at Aug 1500 ..... 14888 L/s		Leaving DB / WB ..... 13.6 / 10.6 °C
Max block L/s ..... 14888 L/s		Coil ADP ..... 12.3 °C
Sum of peak zone L/s ..... 14888 L/s		Bypass Factor ..... 0.100
Sensible heat ratio ..... 1.000		Resulting RH ..... 38 %
m <sup>2</sup> /kW ..... 3.0		Design supply temp. .... 13.0 °C
W/m <sup>2</sup> ..... 335.6		Zone T-stat Check ..... 1 of 1 OK
Water flow @ 5.6 °K rise ..... N/A		Max zone temperature deviation 0.0 °K
<b>Central Heating Coil Sizing Data</b>		Load occurs at ..... Des Htg
Max coil load ..... 38.1 kW		W/m <sup>2</sup> ..... 65.1
Coil L/s at Des Htg ..... 14888 L/s		Ent. DB / Lvg DB ..... 19.8 / 22.1 °C
Max coil L/s ..... 14888 L/s		
Water flow @ 11.1 °K drop ..... N/A		
<b>Supply Fan Sizing Data</b>		Fan motor BHP ..... 21.66
Actual max L/s ..... 14888 L/s		.....BHP
Standard L/s ..... 13840 L/s		Fan motor kW ..... 17.18 kW
Actual max L/(s-m <sup>2</sup> ) .....25.46 ...L/(s-m <sup>2</sup> )		Fan static ..... 750 Pa
<b>Outdoor Ventilation Air Data</b>		L/s/person .....16.21 L/s/person
Design airflow L/s 1200 ..... L/s		
L/(s-m <sup>2</sup> ) .....2.05 L/(s-m <sup>2</sup> )		

**b) Summary for design cooling heating load**

	DESIGN COOLING			DESIGN HEATING		
	COOLING DATA AT Aug 1500 COOLING OA DB / WB 46.0 °C / 21.0 °C			HEATING DATA AT DES HTG HEATING OA DB / WB 5.0 °C / 1.2 °C		
ZONE LOADS	Details	Sensible (W)	Latent (W)	Details	Sensible (W)	Latent (W)
Window & Skylight Solar Loads	627 m <sup>2</sup>	52254	-	627 m <sup>2</sup>	-	-
Wall Transmission	11 m <sup>2</sup>	139	-	11 m <sup>2</sup>	73	-
Roof Transmission	326 m <sup>2</sup>	5806	-	326 m <sup>2</sup>	2001	-
Window Transmission	627 m <sup>2</sup>	21842	-	627 m <sup>2</sup>	17173	-
Skylight Transmission	0 m <sup>2</sup>	0	-	0 m <sup>2</sup>	0	-
Door Loads	0 m <sup>2</sup>	0	-	0 m <sup>2</sup>	0	-
Floor Transmission	0 m <sup>2</sup>	0	-	0 m <sup>2</sup>	0	-
Partitions	79 m <sup>2</sup>	2395	-	79 m <sup>2</sup>	1802	-
Ceiling	0 m <sup>2</sup>	0	-	0 m <sup>2</sup>	0	-
Overhead Lighting	21353 W	21352	-	0	0	-
Task Lighting	0 W	0	-	0	0	-
Electric Equipment	14045 W	14044	-	0	0	-
People	74	5309	4070	0	0	0
Infiltration	-	13145	-1295	-	9208	0
Miscellaneous	-	0	0	-	0	0
Safety Factor	10% / 10%	13629	277	10%	3026	0
<b>&gt;&gt; Total Zone Loads</b>	-	<b>149916</b>	<b>3052</b>	-	<b>33282</b>	<b>0</b>
Zone Conditioning	-	148801	3052	-	33590	0
Plenum Wall Load	0%	0	-	0	0	-
Plenum Roof Load	0%	0	-	0	0	-
Plenum Lighting Load	0%	0	-	0	0	-
Return Fan Load	14888 L/s	0	-	14888 L/s	0	-
Ventilation Load	1200 L/s	30217	-3052	1200 L/s	21661	0
Supply Fan Load	14888 L/s	17180	-	14888 L/s	-17180	-
Space Fan Coil Fans	-	0	-	-	0	-
Duct Heat Gain / Loss	0%	0	-	0%	0	-
<b>&gt;&gt; Total System Loads</b>	-	<b>196198</b>	<b>0</b>	-	<b>38072</b>	<b>0</b>
Central Cooling Coil	-	196198	0	-	0	0
Central Heating Coil	-	0	-	-	38072	-
<b>&gt;&gt; Total Conditioning</b>	-	<b>196198</b>	<b>0</b>	-	<b>38072</b>	<b>0</b>
<b>Key:</b>	Positive values are clg loads Negative values are htg loads			Positive values are htg loads Negative values are clg loads		

**Appendix 2:** Three contractors bid for pipes and drilling for GSHP system installation.

a) Pipes Prices

5	Supplier	Unit price/ m	Total price for 4082 m
1	<b>AlMunif Pipes</b> Third Industrial City - Riyadh - Saudi Arabia Tel. +966 11 265 2111 - FAX. +966 11 265 1845	2.45	5100
2	<b>Advanced Piping Solutions</b> 2nd Industrial Area, Street No 39, Cross 150, PO Box 5794, Dammam 31432, KSA Tel: 9200 120 40 (Toll Free) Email: <a href="mailto:info@advancedpiping.com.sa">info@advancedpiping.com.sa</a>	2.60	10613
3	<b>Al-Jazera Factories For Steel Products Co.Ltd (JASCO)</b> Riyadh Branch P.O.Box 9984 Riadh 11423, Saudi Arabia +966 11 270 5511 +966 11 242 4270	2.75	11225
	<b>Average</b>	<b>2.6</b>	<b>10613</b>

b) Derailing Price

S	Supplier	Unit price(m)	Total price for 4082 m
1	<b>Al-Aboudi Corporation for Drilling Artesian Wells</b> <a href="tel:+966-50-143-5433">+966-50-143-5433</a> <a href="mailto:info@alabudi.com">info@alabudi.com</a>	70	285,740
2	<b>AL MUMAYAZ geotechnical engineering</b> Riyadh – Al Yarmouk – Al Najah Street Tel: 0114157461   E: <a href="mailto:info@almumayaz.sa">info@almumayaz.sa</a>	78	318,396
3	<b>TMNCO laboratory</b> Riyadh - King Abdulaziz Street PO Box 90229 - Riyadh – 11612 Tel.: :00966556691010	92	375,544
	<b>Average</b>	<b>80</b>	<b>643,360</b>

## APPENDIX 3. TRNSYS parameters and input data for modelling ASHP and GSHP.

### a) GSHP system

\* Model "Water–Air heat pump" (Type 919)  
parameters: Type 919

1	Storage Volume	4000	m <sup>3</sup>	The volume of the cylindrical shaped storage region which contains the boreholes. The boreholes will be placed uniformly within the storage volume. The properties of the ground within the storage volume are considered uniform while the properties of the ground outside the storage volume may be described for several vertical layers. If the spacing between boreholes is known, the storage volume can be calculated from the relationship: Storage Volume = $\pi * \text{Number of Boreholes} * \text{Borehole Depth} * (0.525 * \text{Borehole Spacing})^2$
2	Borehole Depth	100	m	The depth of one borehole (from the surface). This depth is also considered the height of the storage volume for determining the cross-sectional storage area. This value is also the length of one of the u-tube heat exchangers from the ground surface to the bottom of the u-tube bend.
3	Header Depth	1	m	The depth below the surface of the top of the u-tube ground heat exchangers. This value is also typically the depth below the surface of the horizontal header pipe which feeds the ground heat exchangers.
4	Number of Boreholes	2	-	The total number of boreholes within the storage volume. If each borehole contains one u-tube ground heat exchanger (which is the most common application in the U.S.) then this value is also the number of u-tube ground heat exchangers.
5	Borehole Radius	0.1016	m	The radius of one of the identical boreholes (the holes that were drilled for the heat exchangers).
6	Number of Boreholes in Series	1	-	The number of boreholes that are connected in series per parallel loop. The flowrate per heat exchanger is then the total flowrate times the number of boreholes in series divided by the total number of boreholes.
7	Number of Radial Regions	1	-	The number of radial subregions that the storage volume will be divided into for the calculation of the local solution. The number of radial subregions must be less than or equal to the number of boreholes connected in series.
8	Number of Vertical Regions	10	-	The number of vertical subregions of the storage volume for the computation of the local solution. The number of vertical subregions times the number of radial subregions must be less than 121 or an error will be generated.
9	Storage Thermal Conductivity	4.68	kJ/hr.m. K	The number of vertical subregions of the storage volume for the computation of the local solution. The number of vertical subregions times the number of radial subregions must be less than 121 or an error will be generated.
10	Storage Heat Capacity	2016	kJ/m <sup>3</sup> / K	The heat capacity (density*specific heat) of the ground comprising the storage volume. The properties of the soil within the storage volume are considered uniform. The properties of the soil past the boundary of the storage volume can be specified for vertical layers later in the parameter description.

11	Negative of U-Tubes/Bore	-1	-	The negative of the number of u-tube ground heat exchangers per borehole. For geothermal heat pump applications in the U.S., this value is typically 1.
12	Outer Radius of U-Tube Pipe	0.01664	m	The outer radius of the pipe comprising the u-tube ground heat exchanger.
13	Inner Radius of U-Tube Pipe	0.01372	m	The inner radius of the pipe comprising the u-tube ground heat exchanger.
14	Center-to-Center Half Distance	0.0254	m	One half of the horizontal distance from the center of the downward flowing u-tube pipe to the center of the upward flowing u-tube pipe (same borehole). This value is also called the half shank spacing.
15	Fill Thermal Conductivity	4.68	kJ/hr.m.K	The thermal conductivity of the material used to fill the borehole after the u-tube ground heat exchanger has been installed.
16	Pipe Thermal Conductivity	1.5122	kJ/hr.m.K	The thermal conductivity of the material comprising the u-tube ground heat exchanger pipes.
17	Gap Thermal Conductivity	5.04	kJ/hr.m.K	The thermal conductivity of the material in the gap between the u-tube pipes and the fill material. The gaps are usually air or water depending on the water table and other factors.
18	Gap Thickness	0	m	The thickness of the gap between the u-tube pipes and the fill material.
19	Reference Borehole Flowrate	613.04	kg/hr	The reference fluid flowrate per borehole for the calculation of the fluid to ground thermal resistance (borehole thermal resistance). This parameter is very important and should correspond to the expected borehole flow rate during operation.
20	Reference Temperature	30	C	The reference fluid temperature for the calculation of the fluid to ground thermal resistance.
21	Pipe-to-Pipe Heat Transfer	0	-	This parameter indicates to the general ground heat exchanger model whether the heat transfer between the upward and downward flowing fluid in the u-tube ground heat exchanger should be included: (0 = Do not account for heat transfer between the u-tube pipes, -1 = Account for the heat transfer between the u-tube pipes).
22	Fluid Specific Heat	4.19	kJ/kg.K	The specific heat of the fluid flowing through the ground heat exchanger pipes.
23	Fluid Density	1000	kg/m <sup>3</sup>	The density of the fluid flowing through the ground heat exchanger pipes.
24	Insulation Indicator	0	-	An indicator for the placement of thermal insulation on the boundaries of the storage volume: (0 = No insulation, 1 = Insulation on the upper side of the cylindrical storage volume. The upper user-specified fraction of the storage height (next parameter) is covered with thermal insulation, 2 = Insulation on the top of the storage volume that extends a user-specified fraction of the storage height (next parameter) beyond the boundary of the storage volume).
25	Insulation Height Fraction	0.5	-	The fraction of the height of the storage volume that is insulated (if previous parameter=1) or the fraction of the height of the storage volume that the insulation on top of the storage extends beyond the boundary of the storage volume (if previous parameter=2).
26	Insulation Thickness	0.0254	m	The thickness of the insulation on the top and sides of the storage volume (if specified).
27	Insulation Thermal Conductivity	1	kJ/hr.m.K	The thickness of the insulation on the top and sides of the storage volume (if specified).
28	Number of Simulation Years	1	-	The length in years of the simulation to be performed. This value should include the number of years of preheating used to heat up the

				surrounding ground. This parameter is used to determine the mesh extension for the finite difference calculations.
29	Maximum Storage Temperature	100	C	The maximum temperature of the fluid entering the ground heat exchangers.
30	Initial Surface Temperature of Storage Volume	20	C	The initial surface temperature of the storage volume
31	Initial Thermal Gradient of Storage Volume	0	any	The initial thermal gradient in the ground inside the storage volume.
32	Number of Preheating Years	0	-	The number of preheating years run before the simulation begins (0 = no preheating). During preheating, a sinusoidal yearly variation of the average storage volume temperature is used to heat up the ground surrounding the storage volume.
33	Maximum Preheat Temperature	30	C	The maximum temperature (average) of the storage volume ground for preheating calculations. This temperature is used in a sinusoidal calculation to preheat the soil surrounding the storage volume. This parameter is also used in the calculation to set the initial temperature of the storage volume ground at the beginning of the simulation. See the description of the phase delay parameter for more information on the initial storage temperature.
34	Minimum Preheat Temperature	10	C	The minimum temperature (average) of the storage volume ground for preheating calculations. This temperature is used in a sinusoidal calculation to preheat the ground surrounding the storage volume. This parameter is also used in the calculation to determine the initial temperature of the storage volume ground. Refer to the description of the preheating phase delay for more information on the initial storage volume temperature.
35	Preheat Phase Delay	90	day	<p>The phase delay in the preheating sinusoidal temperature curve. This phase delay is simply 90 minus the day of maximum storage temperature, or 270 minus the day of minimum storage temperature. For preheating, the storage temperature equation is:</p> $T_{store} = (T_{max,ph} + T_{min,ph})/2 + (T_{max,ph} - T_{min,ph})/2 * \sin(w(t + \theta))$ <p>where: <math>T_{store}</math> = storage temperature, <math>T_{max,ph}</math> = maximum storage temperature for preheating, <math>T_{min,ph}</math> = minimum storage temperature for preheating, <math>\theta</math> = this parameter, <math>t</math> = simulation time in days.</p> <p>The storage temperature at the beginning of the simulation is found from the above equation with <math>t=0</math>.</p>
36	Average Air Temperature - Preheat Years	20	C	The yearly average air temperature for preheating calculations. The average air temperature is used to calculate the air temperature as a function of time. The air temperature (and storage temperature) variation throughout the preheat years are used to calculate the temperature of the ground past the storage volume boundary at the beginning of the simulation.
37	Amplitude of Air	15	deltaC	The amplitude of the air temperature over the year. This parameter is used to calculate the air temperature as a function of time. The air

	Temperature - Preheat Years			temperature and the average storage temperature (both as a function of time) are used to calculate the temperature of the ground outside the storage volume boundary at the beginning of the simulation.
38	Air Temperature Phase Delay - Preheat Years	240	day	<p>The phase delay in air temperature for the preheating calculations. The delay can be simply calculated as the 90 minus the day of the maximum air temperature or 270 minus the day of minimum air temperature. The air temperature as a function of time is then:</p> <p>Air Temperature = Average Air Temperature + Amplitude*sin(w(t+delay))</p> <p>where: t = time in days, delay = phase delay (days), w = conversion constant</p>
39	Number of Ground Layers	5	-	The number of unique vertical soil layers that comprise the ground outside the boundary of the storage volume (the storage volume soil is assumed uniform). For each layer, the user must specify the thermal conductivity, heat capacity, and layer thickness.
40	Thermal Conductivity of Layer	4.68	kJ/hr.m. K	The thermal conductivity of the specified vertical layer at the outside boundary of the storage volume.
41	Heat Capacity of Layer	2016	kJ/m <sup>3</sup> / K	The volumetric heat capacitance of the specified vertical soil layer at the outside boundary of the storage volume.
42	Thickness of Layer	1000	m	The thickness of the specified vertical soil layer at the outside boundary of the storage volume.

### Input data:

1	Inlet Fluid Temperature	32	C	The temperature of the fluid entering the ground heat exchangers.
2	Inlet Flowrate (Total)	0	kg/hr	The flowrate of fluid (total, not per borehole) entering the ground heat exchangers.
3	Temperature on Top of Storage	20	C	The temperature of the air directly above the storage volume. In most cases this is the ambient temperature. In some cases (like the storage volume being located beneath an asphalt parking lot) this temperature must be calculated and passed to this model.
4	Air Temperature	45	C	The ambient temperature
5	Circulation Switch	1	-	This input determines how the fluid is circulated through the boreholes: (1 = Circulate from center to border of storage volume, -1 = Circulate from border to center). This input should only be used when multiple boreholes are connected in series and when the flow direction through the boreholes is changed depending on operation. For most geothermal applications this input should be set to a constant value of 1. If however, a radial stratification of the ground is desired (such as heat storage), the fluid should circulate from the center to the border in heat injection (=1) and from the border to the center during heat abstraction (= -1).

## b) ASHP system

\* Model "Air –Air heat pump" (Type 119)

parameters: Type 119

1	Humidity Mode	2		The humidity mode indicates which of the input humidity values will be used to calculate the inlet moist air state: 1= the inlet humidity ratio will be used, 2 = the inlet relative humidity (%) will be used.
2	Logical Unit for Cooling Data	32		The logical unit which is assigned to the data file which contains the heat pump cooling performance data.
3	Logical Unit for Heating Data	33		The logical unit which is assigned to the data file containing the heat pump heating performance data.
4	Logical Unit Number for Cooling Correction Data	34		The logical unit which is assigned to the data file which contains the cooling correction factors for off-design indoor air temperatures.
5	Logical Unit Number for Heating Correction Data	35		The logical unit which is assigned to the data file containing the heating correction factors for off-design indoor air temperatures.
6	Number of Water Flow Steps	3		The number of water flowrates for which data is provided in the performance data files.
7	Number of Water Temperatures - Cooling	4		The number of water temperatures for which cooling performance data is provided in the associated data files.
8	Number of Water Temperatures - Heating	4		The number of water temperatures for which heating data is provided in the associated heating performance data file.
9	Number of Wet Bulb Steps	6		The number of indoor wet bulb temperatures for which cooling correction factors are supplied in the associated data file.
10	Number of Dry Bulb Steps - Cooling	4		The number of indoor dry-bulb temperatures for which cooling correction factors are supplied in the associated data file.
11	Number of Dry Bulb Steps - Heating	6		The number of entering air dry bulb temperatures for which heating correction factor data is supplied in the associated data file.
12	Number of Airflow Steps - Cooling	2		The number of air flowrate steps for which cooling performance data will be supplied in the associated data file.
13	Number of Airflow Steps - Heating	2		The number of air flowrate steps for which heating performance data is supplied in the associated data file.
14	Density of Liquid Stream	1000.0	kg/m <sup>3</sup>	The density of the liquid stream entering the heat pump. The liquid stream is used for heat rejection when in cooling mode and for heat absorption when in heating mode.
15	Specific Heat of Liquid Stream	4.190	kJ/kg.K	The specific heat of the liquid stream entering the heat pump. The liquid stream is used for heat rejection when in cooling mode and for heat absorption when in heating mode.
16	Specific Heat of DHW Fluid	4.190	kJ/kg.K	The specific heat of the domestic hot water fluid which will be heated using the desuperheater of the heat pump.
17	Blower Power	671.1	kJ/hr	The power of the blower motor when the heat pump is operating. Typically, the entire heat pump package power (compressor + blower + controls) is given for the reported heat pump power in the catalog data. The blower and controller power will be subtracted from the calculated power in order to calculate the compressor power.



18	Controller Power	36.0	kJ/hr	The power of the controller in the packaged heat pump unit. Typically, the total packaged heat pump power (blower + controls + compressor) is reported for heat pump power in the catalog data. The blower and controller power will be subtracted from the total calculated heat pump power in order to get the compressor power.
19	Capacity of Stage-1 Auxiliary	0.0	kJ/hr	The heating capacity of the first-stage auxiliary heating device.
20	Capacity of Stage-2 Auxiliary	0.0	kJ/hr	The heating capacity of the 2nd-stage auxiliary heating device.
21	Total Air Flowrate	300.0	l/s	The flowrate on the air-side of the heat pump. This flowrate is the total flowrate (return plus outside air).
22	Rated Total Cooling Capacity	37980	kJ/hr	The total cooling capacity of the device at the rated conditions. Make sure that the external data file which provides off-rated multipliers is consistent with the provided rating conditions.
23	Rated Sensible Cooling Capacity	30384	kJ/hr	The sensible cooling capacity of the device at the rated conditions. Make sure that the external data file which provides off-rated multipliers is consistent with the provided rating conditions.
24	Rated Cooling Power	12660	kJ/hr	The power of the device at the rated conditions (including the blower). Make sure that the external data file which provides off-rated multipliers is consistent with the provided rating conditions.
25	Rated Heating Capacity	37980	kJ/hr	The heating capacity of the device at the rated conditions. Make sure that the external data file which provides off-rated multipliers is consistent with the provided rating conditions.
26	Rated Heating Power	12660	kJ/hr	The power of the device at the rated conditions (including the blower). Make sure that the external data file which provides off-rated multipliers is consistent with the provided rating conditions.
27	Rated Air Flowrate	300.0	l/s	The value of volumetric dry air flowrate at the rated conditions.
28	Rated Liquid Flowrate	0.28	l/s	The volumetric flowrate of liquid through the heat pump at its rated conditions.

### Input data:

1	Inlet Liquid Temperature	20.0	C	The temperature of the heat transfer fluid entering the heat pump. This is typically water from a ground-coupled heat exchanger.
2	Inlet Liquid Flowrate	1000.0	kg/hr	The flowrate of heat transfer fluid entering the heat pump.
3	Return Air Temperature	20.0	C	The temperature of the air returning to the heat pump from the zone. This is typically the room air temperature. This air will be mixed with a user-controlled amount of outside air before entering the heat pump.
4	Return Air Humidity Ratio	0.008	-	The absolute humidity ratio of the air returning to the heat pump from the zone. This air is typically at room air conditions. This return air will be mixed with a user-specified amount of outside air before entering the heat pump.
5	Return Air Relative Humidity	50.0	% (base 100)	The percent relative humidity of the air returning to the heat pump from the zone. This air is typically at room air conditions. This return air will be mixed with a user-specified amount of outside air before entering the heat pump.
6	Return Air Pressure	1.0	atm	The absolute pressure of the air returning to the heat pump from the zone. This air is typically at room air conditions. This return air will be mixed with a user-specified amount of outside air before entering the heat pump.

7	Return Air Damper Pressure Drop	0	atm	The pressure drop of the return air stream as it passes across the return air damper.
8	Fresh Air Temperature	20.0	C	The temperature of the fresh air available to the heat pump. The heat pump will mix a user-specified amount of fresh air with the return air before conditioning this air in the heat pump.
9	Fresh Air Humidity Ratio	0.008	-	The absolute humidity ratio of the fresh air available to the heat pump. The heat pump will mix a user-specified amount of fresh air with the return air before conditioning this air in the heat pump.
10	Fresh Air Relative Humidity	50.	% (base 100)	The percent relative humidity of the fresh air available to the heat pump. The heat pump will mix a user-specified amount of fresh air with the return air before conditioning this air in the heat pump.
11	Fresh Air Pressure	1.0	atm	The absolute pressure of the fresh air available to the heat pump. The heat pump will mix a user-specified amount of fresh air with the return air before conditioning this air in the heat pump.
12	Fresh Air Damper Pressure Drop	0	atm	The pressure drop of the fresh air stream as it passes across the outside air damper.
13	Inlet DHW Temperature	40.0	C	The temperature of the entering domestic hot water stream to be heated by the desuperheater.
14	Inlet DHW Flowrate	400.0	kg/hr	The flowrate of domestic hot water entering the heat pump to be heated by the desuperheater.
15	Cooling Control Signal	1.0	-	The control signal for cooling operation: ctrl < 0.5 : cooling mode is off, ctrl >= 0.5 : cooling mode is on.
16	Heating Control Signal	0	-	The control signal for heating operation: ctrl < 0.5 : heating mode is off, ctrl >= 0.5 : heating mode is on.
17	Stage 1 Auxiliary Signal	0.0	-	The control signal for the 1st stage auxiliary heater: ctrl < 0.5 : 1st stage auxiliary heater is off, ctrl >= 0.5 : 1st stage auxiliary heater is on.
18	Stage 2 Auxiliary Signal	0.0	-	The control signal for the operation of the 2nd-stage auxiliary heater: ctrl < 0.5 : 2nd stage auxiliary heater is off, ctrl >= 0.5 : 2nd stage auxiliary heater is on.
19	Fan Control Signal	0.0	-	The control signal for operation of the ventilation fan when the heat pump is not operating in heating or cooling mode: ctrl < 0.5 : fan is off if heat pump compressor is off, ctrl >= 0.5 : fan is on regardless of compressor operation.
20	Fraction of Outside Air	0.15	Fraction	The heat pump will mix this user-specified amount of fresh air with the remaining fraction of return air before conditioning this air in the heat pump.
21	Cooling Desuperheater Temperature	60.0	C	The temperature of the refrigerant in the heat pump desuperheater when the heat pump is operating in cooling mode. This temperature will be used to calculate the heat transfer to the domestic hot water flow stream.
22	Heating Desuperheater Temperature	55.0	C	The temperature of the refrigerant in the heat pump desuperheater when the heat pump is operating in heating mode. This temperature will be used to calculate the heat transfer to the domestic hot water flow stream.
23	Desuperheater UA - Cooling	1500.0	kJ/hr.K	The overall heat transfer coefficient from the heat pump to the desuperheater flow stream in cooling mode.
24	Desuperheater UA - Heating	1500.0	kJ/hr.K	The overall heat transfer coefficient between the heat pump and the desuperheater flow stream in heating mode.
25	Fraction of Rated Cooling Power	1.0	-	The fraction of rated catalog cooling power that will be used for this heat pump. The actual power will then be the power

				(interpolated from the data file based on the current conditions) multiplied by this parameter.
26	Fraction of Rated Cooling Capacity	1.0	-	The fraction of the catalog cooling capacity that will be used for this heat pump.
27	Fraction of Rated Heating Power	1.0	-	The fraction of rated catalog heating power that will be used for this heat pump.
28	Fraction of Rated Heating Capacity	1.0	-	The fraction of rated catalog heating capacity that will be used for this heat pump.
29	Pressure Rise Through Heat Pump	0.0	atm	The pressure rise (positive) of the air as it flows through the heat pump. The pressurization is due to the internal heat pump fan.

## APPENDIX 4. Manufacture's catalogue data for ASHP and GSHP.

---

### a) ASHP catalogue data



### TECHNICAL GUIDE

#### R-410A ZE/XN SERIES 3 - 6 TON 60 Hertz



#### Description

YORK® ZE/XN Series units are convertible single package rooftops with a common roof curb for the 3, 4, 5, and 6 Ton sizes. Although the units are primarily designed for curb mounting on a roof, they can also be slab-mounted at ground level or set on steel beams above a finished roof.

All ZE/XN Series units are self-contained and assembled on rigid full perimeter base rails allowing for overhead rigging. Every unit is completely charged, wired, piped and tested at the factory to provide a quick and easy field installation.

All models (including those with an economizer) are convertible between bottom and horizontal duct connections. ZE Series units are available in the following configurations: cooling only, cooling with electric heat, and cooling with one or two stage gas heat. Electric heaters are available as factory- installed option or field installed accessory.

XN Series units are available in the following configurations: cooling and heating only and cooling and heating with electric heat.

## Physical Data

### ZE036-072 Physical Data

Component	Models															
	ZE036				ZE048				ZE060				ZE072			
<b>Nominal Tonnage</b>	3				4				5				6			
<b>ARI COOLING PERFORMANCE</b>																
Gross Capacity @ AHRI A point (Btu)	36600				49100				59000				68000			
AHRI net capacity (Btu)	35500				47500				57000				66000			
EER	12.0				12.0				11.8				11.20 <sup>1</sup> /11.00 <sup>2</sup>			
SEER	14.0				14.0				14.0							
IEER																
IEER IntelliSpeed													14.2			
CFM	1200				1450				1680				2057			
System power (KW)	2.96				3.96				4.83				5.9			
Refrigerant type	R-410A				R-410A				R-410A				R-410A			
Refrigerant charge (lb-oz)																
System 1	4-4				5-6				6-4				6-6			
<b>AHRI HEATING PERFORMANCE</b>																
Heating model	H05	H10	N07	N11	H07	H12	N07	N12	H10	H12	N07	N12	H10	H12	N07	N12
Heat input (K Btu)	50	100	75	115	75	125	75	125	100	125	75	125	100	125	75	125
Heat output (K Btu)	40	80	60.8	92	60	100	60.8	100.6	80	100	60.8	100.6	80	100	61	100.6
AFUE% (Single Phase Only)	81	81	-	-	81	81	-	-	81	81	-	-	-	-	-	-
FER Compliant Direct Drive (Single Phase Gas Heat Only) <sup>3</sup>	Yes	Yes	-	-	Yes	Yes	-	-	Yes	Yes	-	-	-	-	-	-
FER Compliant Belt Drive (Single Phase Gas Heat Only) <sup>3</sup>	Yes	Yes	-	-	Yes	Yes	-	-	No	Yes	-	-	-	-	-	-
Steady state efficiency (%) (3 Phase Only)	80	80	81.1	80.2	80	80	81.1	80.5	80	80	81.1	80.5	80.0	80.0	81.1	80.5
No. burners	2	4	3	5	3	5	3	5	4	5	3	5	4	5	3	5
No. stages	1	1	2	2	1	1	2	2	1	1	2	2	1	1	2	2
Temperature Rise Range (°F)	15-45	45-75	35-70	55-90	25-70	45-75	25-70	45-75	25-55	35-75	20-55	35-75	25-55	30-75	15-45	30-75
Gas Limit Setting (°F) - Direct Drive	240	190	210	200	210	165	210	165	170	165	210	165	-	-	-	-
Gas Limit Setting (°F) - Belt Drive	240	210	240	200	240	210	240	210	210	210	210	210	210	210	210	210
Gas piping connection (in.)	1/2	1/2	1/2	1/2	1/2	1/2	1/2	1/2	1/2	1/2	1/2	1/2	1/2	1/2	1/2	1/2
<b>DIMENSIONS (inches)</b>																
Length	82 1/4				82 1/4				82 1/4				82 1/4			
Width	44 7/8				44 7/8				44 7/8				44 7/8			
Height	32 5/8				32 5/8				32 5/8				32 5/8			
<b>OPERATING WT. (lbs.)</b>	470				598				632				665			
<b>COMPRESSORS</b>																
Type	Scroll				Scroll				Scroll				2-stage scroll			
Quantity	1				1				1				1			
Unit Capacity Steps (%)	100				100				100				67/100			
<b>CONDENSER COIL DATA</b>																
Face area (Sq. Ft.)	16.3				16.3				16.3				16.3			
Rows	1				1				1				1			
Fins per inch	23				23				23				23			
Tube diameter (in.)	0.71 / 18				0.71 / 18				1.00 / 25.4				1.00 / 25.4			
Circuitry Type	2-pass Microchannel				2-pass Microchannel				2-pass Microchannel				2-pass Microchannel			

ZE036-072 Physical Data (Continued)

Component	Models							
	ZE036		ZE048		ZE060		ZE072	
Nominal Tonnage	3		4		5		6	
<b>EVAPORATOR COIL DATA</b>								
Face area (Sq. Ft.)	5.06		5.06		5.06		5.01	
Rows	3		4		4		4	
Fins per inch	13		13		13		13	
Tube diameter	0.375		0.375		0.375		0.375	
Circuitry Type	Intertwined		Intertwined		Intertwined		Intertwined	
Refrigerant control	Orifice		Orifice		TXV		TXV	
<b>CONDENSER FAN DATA</b>								
Quantity of fans	1		1		1		1	
Fan diameter (Inch)	24		24		24		24	
Type	Prop		Prop		Prop		Prop	
Drive type	Direct		Direct		Direct		Direct	
Quantity of motors	1		1		1		1	
Motor HP each	1/2		1/2		1/2 <sup>4</sup>		1/2 <sup>4</sup>	
No. speeds	1		1		1		2	
RPM	1090		1090		1100		900 / 1150	
CFM	4000		4000		4200		3300 / 4200	
<b>BELT DRIVE EVAP FAN DATA</b>								
Quantity	1		1		1		1	
Fan Size (Inch)	11 x 10		11 x 10		11 x 10		11 x 10	
Type	Centrifugal		Centrifugal		Centrifugal		Centrifugal	
Motor Sheave	1VL44	1VP56	1VL44	1VP56	1VL44	1VP56	VL44	1VP56
Blower Sheave	AK64	AK66	AK56	AK61	AK56	AK56	AK56	AK56
Belt	A37	A39	A36	A38	A36	A38	A36	A38
Motor HP each	1-1/2	1-1/2	1-1/2	1-1/2	1-1/2	2	1-1/2	3
RPM	1740		1740		1740		1740	
Frame size	56		56		56		56	
<b>DIRECT DRIVE EVAP FAN DATA<sup>5</sup></b>								
Quantity	1		1		1		-	
Fan Size (Inch)	11 x 10		11 x 10		11 x 10		-	
Type	Centrifugal		Centrifugal		Centrifugal		-	
Motor HP each	3/4		1		1		-	
RPM	1050		1050		1050		-	
<b>FILTERS</b>								
15" x 20" x 1" or 2"	2		2		2		2	
14" x 25" x 1" or 2"	1		1		1		1	

ZE060 (5.0 Ton)

Air on Evaporator Coil		Temperature of Air on Condenser Coil																															
CFM	WB (°F)	Total Capacity <sup>1</sup> (MBh)	Total Input (kW) <sup>2</sup>	Sensible Capacity (MBh)						Total Capacity <sup>1</sup> (MBh)	Total Input (kW) <sup>2</sup>	Sensible Capacity (MBh)																					
				Return Dry Bulb (°F)								Return Dry Bulb (°F)																					
				90	85	80	75	70	65			90	85	80	75	70	65																
<b>75°F</b>																	<b>85°F</b>																
1250	77	74.6	3.2	34.0	28.7	23.4	-	-	-	70.6	3.8	31.6	26.4	21.1	-	-	-																
	72	69.2	3.2	42.2	36.9	31.6	26.3	-	-	65.3	3.7	39.7	34.4	29.2	23.9	-	-																
	67	63.8	3.2	50.4	45.1	39.8	34.5	29.2	-	60.1	3.7	47.7	42.5	37.2	32.0	26.7	-																
	62	58.4	3.1	58.4	56.3	48.8	43.5	38.2	32.9	55.1	3.7	55.1	53.7	45.6	40.4	35.1	29.9																
1500	77	76.5	3.3	37.3	31.2	25.1	-	-	-	72.4	3.8	35.0	29.0	23.0	-	-	-																
	72	71.0	3.2	46.1	40.0	33.9	27.9	-	-	67.1	3.7	43.8	37.7	31.7	25.7	-	-																
	67	65.4	3.2	54.9	48.8	42.8	36.7	30.6	-	61.7	3.7	52.5	46.5	40.5	34.5	28.5	-																
	62	59.9	3.2	59.9	58.5	52.4	46.4	40.3	34.2	56.6	3.7	56.6	55.6	49.6	43.6	37.6	31.6																
	57	59.0	3.1	59.0	59.0	54.1	48.0	41.9	35.9	56.2	3.7	56.2	56.2	50.6	44.5	38.5	32.5																
1750	77	78.4	3.3	40.6	33.7	26.9	-	-	-	74.3	3.8	38.4	31.6	24.9	-	-	-																
	72	72.7	3.3	50.0	43.1	36.3	29.5	-	-	68.8	3.8	47.8	41.1	34.3	27.5	-	-																
	67	67.1	3.2	59.4	52.5	45.7	38.9	32.1	-	63.3	3.7	57.3	50.5	43.8	37.0	30.2	-																
	62	61.4	3.2	61.4	60.7	56.1	49.2	42.4	35.6	58.1	3.7	58.1	57.6	53.6	46.9	40.1	33.3																
	57	60.5	3.2	60.5	60.5	57.8	51.0	44.2	37.4	57.7	3.7	57.7	57.7	54.6	47.9	41.1	34.3																
2000	77	80.3	3.3	43.8	36.3	28.7	-	-	-	76.1	3.8	41.8	34.2	26.7	-	-	-																
	72	74.5	3.3	53.9	46.3	38.7	31.1	-	-	70.5	3.8	51.9	44.4	36.9	29.4	-	-																
	67	68.7	3.2	63.9	56.3	48.7	41.1	33.6	-	64.9	3.8	62.1	54.6	47.0	39.5	32.0	-																
	62	62.8	3.2	62.8	62.8	59.7	52.1	44.6	37.0	59.5	3.7	59.5	59.5	57.7	50.1	42.6	35.1																
	57	62.0	3.2	62.0	62.0	61.6	54.0	46.5	38.9	59.1	3.7	59.1	59.1	58.7	51.2	43.7	36.2																
2250	72	81.4	2.6	59.5	51.3	43.0	34.7	-	-	71.7	3.8	55.7	47.5	39.3	31.1	-	-																
	67	75.0	2.6	72.6	63.7	54.1	45.8	37.5	-	66.0	3.8	64.6	58.3	50.1	42.0	33.8	-																
	62	68.6	2.5	68.6	68.6	67.1	58.8	50.5	42.2	60.5	3.7	60.5	60.5	59.6	51.4	43.3	35.1																
	57	67.8	2.5	67.8	67.8	67.6	59.3	51.0	42.7	60.1	3.7	60.1	60.1	59.9	51.8	43.6	35.4																
2500	72	88.2	1.9	65.2	56.2	47.2	38.2	-	-	73.0	3.8	59.4	50.6	41.7	32.9	-	-																
	67	81.3	1.9	81.3	71.2	59.6	50.5	41.5	-	67.1	3.8	67.1	62.1	53.2	44.4	35.6	-																
	62	74.4	1.9	74.4	74.4	74.4	65.4	56.4	47.4	61.6	3.7	61.6	61.6	61.6	52.7	43.9	35.1																
	57	73.6	1.9	73.6	73.6	73.6	64.5	55.5	46.5	61.1	3.7	61.1	61.1	61.1	52.3	43.5	34.7																
<b>95°F</b>																	<b>105°F</b>																
1250	77	66.5	4.3	29.3	24.1	18.9	-	-	-	61.4	4.9	24.0	19.8	14.7	-	-	-																
	72	61.5	4.2	37.1	32.0	26.8	21.6	-	-	56.9	4.9	34.1	29.0	23.9	18.7	-	-																
	67	56.4	4.2	45.0	39.8	34.6	29.4	24.2	-	52.5	4.9	44.2	38.1	33.0	27.9	22.8	-																
	62	51.9	4.2	51.9	51.1	42.4	37.3	32.1	26.9	48.7	4.8	48.7	48.3	39.8	34.7	29.6	24.4																
1500	77	68.3	4.3	32.7	26.8	20.8	-	-	-	62.8	5.0	27.9	22.1	16.2	-	-	-																
	72	63.2	4.3	41.4	35.5	29.5	23.6	-	-	58.3	4.9	38.0	32.2	26.3	20.4	-	-																
	67	58.0	4.2	50.1	44.2	38.2	32.3	26.3	-	53.7	4.9	48.1	42.2	36.4	30.5	24.6	-																
	62	53.3	4.2	53.3	52.8	46.8	40.9	34.9	29.0	49.9	4.8	49.9	49.6	43.8	38.0	32.1	26.2																
	57	53.4	4.2	53.4	53.0	47.1	41.1	35.1	29.2	50.2	4.8	50.2	50.0	44.1	38.3	32.4	26.5																
1750	77	70.2	4.3	36.2	29.5	22.8	-	-	-	64.3	5.0	31.9	24.3	17.7	-	-	-																
	72	64.9	4.3	45.7	39.0	32.3	25.6	-	-	59.7	5.0	42.0	35.3	28.7	22.1	-	-																
	67	59.5	4.3	55.2	48.5	41.8	35.1	28.4	-	55.0	4.9	52.0	46.3	39.7	33.1	26.4	-																
	62	54.8	4.2	54.8	54.5	51.2	44.5	37.8	31.1	51.0	4.9	51.0	50.9	47.9	41.2	34.6	28.0																
	57	54.8	4.2	54.8	54.6	51.5	44.7	38.0	31.3	51.4	4.9	51.4	51.3	48.2	41.6	34.9	28.3																
2000	77	72.0	4.3	39.7	32.2	24.7	-	-	-	65.8	5.0	35.9	26.6	19.2	-	-	-																
	72	66.5	4.3	50.0	42.5	35.1	27.6	-	-	61.0	5.0	45.9	38.5	31.1	23.7	-	-																
	67	61.1	4.3	60.3	52.9	45.4	37.9	30.4	-	56.3	5.0	55.9	50.4	43.0	35.6	28.3	-																
	62	56.2	4.2	56.2	56.2	55.6	48.2	40.7	33.2	52.2	4.9	52.2	52.2	51.9	44.5	37.1	29.7																
	57	56.2	4.2	56.2	56.2	55.9	48.4	40.9	33.4	52.6	4.9	52.6	52.6	52.3	44.9	37.5	30.1																
2250	72	62.1	5.0	51.8	43.7	35.7	27.6	-	-	59.2	5.3	48.5	40.5	32.4	24.4	-	-																
	67	57.0	4.9	56.6	52.9	46.2	38.1	30.0	-	54.6	5.3	54.4	51.7	45.0	37.0	29.0	-																
	62	52.5	4.9	52.5	52.5	52.2	44.1	36.1	28.0	50.7	5.2	50.7	50.7	50.5	42.5	34.5	26.5																
	57	52.5	4.9	52.5	52.5	52.3	44.2	36.2	28.1	51.1	5.2	51.1	51.1	50.9	42.9	34.9	26.9																
2500	72	57.7	5.6	53.5	44.9	36.3	27.6	-	-	57.4	5.6	51.1	42.4	33.8	25.1	-	-																
	67	53.0	5.6	53.0	53.0	46.9	38.3	29.6	-	53.0	5.6	53.0	53.0	46.9	38.3	29.6	-																
	62	48.7	5.5	48.7	48.7	48.7	40.1	31.4	22.8	49.2	5.5	49.2	49.2	49.2	40.5	31.9	23.2																
	57	48.7	5.5	48.7	48.7	48.7	40.1	31.5	22.8	49.6	5.5	49.6	49.6	49.6	40.9	32.3	23.7																

ZE060 (5.0 Ton) (Continued)

Air on Evaporator Coil		Temperature of Air on Condenser Coil																	
CFM	WB (°F)	Total Capacity <sup>1</sup> (MBh)	Total Input (kW) <sup>2</sup>	Sensible Capacity (MBh)						Total Capacity <sup>1</sup> (MBh)	Total Input (kW) <sup>2</sup>	Sensible Capacity (MBh)							
				Return Dry Bulb (°F)								Return Dry Bulb (°F)							
				90	85	80	75	70	65			90	85	80	75	70	65		
		<b>115°F</b>												<b>125°F</b>					
1250	77	56.2	5.6	18.7	15.6	10.5	-	-	-	51.0	6.2	13.2	11.3	6.3	-	-	-		
	72	52.4	5.6	31.1	26.0	20.9	15.9	-	-	47.8	6.3	28.0	23.0	18.0	13.0	-	-		
	67	48.5	5.6	43.4	36.5	31.4	26.3	21.3	-	44.6	6.3	42.7	34.8	29.8	24.8	19.8	-		
	62	45.5	5.5	45.5	45.5	37.2	32.1	27.1	22.0	42.2	6.1	42.2	42.2	34.6	29.6	24.6	19.6		
1500	77	57.3	5.6	23.1	17.3	11.5	-	-	-	51.8	6.3	18.3	12.6	6.9	-	-	-		
	72	53.4	5.6	34.6	28.8	23.0	17.2	-	-	48.5	6.3	31.2	25.5	19.8	14.0	-	-		
	67	49.5	5.6	46.1	40.3	34.5	28.7	22.9	-	45.2	6.3	44.1	38.4	32.6	26.9	21.2	-		
	62	46.4	5.5	46.4	46.4	40.9	35.0	29.2	23.4	42.9	6.2	42.9	42.9	37.9	32.1	26.4	20.7		
	57	47.1	5.5	47.1	47.0	41.2	35.4	29.6	23.8	44.0	6.2	44.0	44.0	38.3	32.6	26.9	21.1		
1750	77	58.4	5.6	27.6	19.1	12.6	-	-	-	52.6	6.3	23.5	13.9	7.4	-	-	-		
	72	54.4	5.6	38.2	31.6	25.1	18.5	-	-	49.2	6.3	34.4	27.9	21.5	15.0	-	-		
	67	50.5	5.6	48.8	44.1	37.6	31.0	24.5	-	45.9	6.3	45.5	41.9	35.5	29.0	22.5	-		
	62	47.3	5.5	47.3	47.3	44.5	38.0	31.4	24.9	43.5	6.2	43.5	43.5	41.2	34.7	28.2	21.8		
	57	48.1	5.5	48.1	48.0	44.9	38.4	31.8	25.3	44.7	6.2	44.7	44.7	41.7	35.2	28.7	22.3		
2000	77	59.6	5.7	32.0	20.9	13.6	-	-	-	53.3	6.3	28.6	15.2	8.0	-	-	-		
	72	55.5	5.7	41.7	34.4	27.1	19.8	-	-	50.0	6.3	37.6	30.4	23.2	16.0	-	-		
	67	51.4	5.7	51.4	48.0	40.7	33.4	26.1	-	46.6	6.3	46.6	45.5	38.3	31.1	23.9	-		
	62	48.2	5.5	48.2	48.2	48.2	40.9	33.6	26.3	44.2	6.2	44.2	44.2	44.2	37.3	30.1	22.8		
	57	49.0	5.6	49.0	49.0	48.6	41.3	34.0	26.7	45.4	6.3	45.4	45.4	45.0	37.8	30.6	23.4		
2250	72	56.3	5.6	45.2	37.2	29.2	21.3	-	-	53.4	6.0	41.8	33.9	26.0	18.1	-	-		
	67	52.2	5.6	52.2	50.5	43.8	35.8	27.9	-	49.8	6.0	49.8	49.2	42.6	34.7	26.8	-		
	62	48.9	5.5	48.9	48.9	48.9	40.9	33.0	25.0	47.1	5.9	47.1	47.1	47.1	39.3	31.4	23.5		
	57	49.7	5.6	49.7	49.7	49.5	41.6	33.6	25.6	48.3	5.9	48.3	48.3	48.1	40.2	32.3	24.4		
2500	72	57.1	5.6	48.6	39.9	31.3	22.7	-	-	56.9	5.6	46.1	37.5	28.8	20.2	-	-		
	67	53.0	5.6	53.0	53.0	46.9	38.3	29.6	-	53.0	5.6	53.0	53.0	46.9	38.3	29.6	-		
	62	49.6	5.5	49.6	49.6	49.6	41.0	32.3	23.7	50.1	5.5	50.1	50.1	50.1	41.4	32.8	24.1		
	57	50.4	5.5	50.4	50.4	50.4	41.8	33.2	24.5	51.3	5.5	51.3	51.3	51.3	42.6	34.0	25.4		



**XN036-060 Heating Capacities**

Size (Tons)	Model	Air Over Evaporator Coil		Capacity <sup>1</sup> & kW	Outdoor Temperature (°F @ 72% RH)							
		CFM	DB (°F)		-10	0	10	20	30	40	50	60
036 (3.0)	XN	900	55	MBH	6.6	11.5	16.4	21.3	26.2	31.1	36.1	41.0
			70	MBH	2.02	2.14	2.26	2.38	2.49	2.61	2.73	2.85
			80	MBH	4.6	9.5	14.4	19.3	24.2	29.1	34.0	39.0
				KW	2.55	2.67	2.78	2.90	3.02	3.14	3.26	3.37
		1200	55	MBH	3.3	8.2	13.1	18.1	23.0	27.9	32.8	37.7
			70	MBH	3.02	3.13	3.25	3.37	3.49	3.60	3.72	3.84
			80	MBH	8.0	12.9	17.8	22.8	27.7	32.6	37.5	42.4
				KW	1.69	1.81	1.92	2.04	2.16	2.28	2.39	2.51
		1500	55	MBH	6.0	10.9	15.8	20.7	25.7	30.6	35.5	40.4
			70	MBH	2.21	2.33	2.45	2.56	2.68	2.80	2.92	3.04
			80	MBH	4.7	9.7	14.6	19.5	24.4	29.3	34.2	39.2
				KW	2.68	2.79	2.91	3.03	3.15	3.27	3.38	3.50
048 (4.0)	XN	1200	55	MBH	8.3	13.2	18.2	23.1	28.0	32.9	37.8	42.7
			70	MBH	1.51	1.63	1.74	1.86	1.98	2.10	2.21	2.33
			80	MBH	6.3	11.2	16.1	21.1	26.0	30.9	35.8	40.7
				KW	2.03	2.15	2.27	2.39	2.50	2.62	2.74	2.86
		1600	55	MBH	5.1	10.0	14.9	19.8	24.7	29.6	34.6	39.5
			70	MBH	2.50	2.62	2.74	2.85	2.97	3.09	3.21	3.33
			80	MBH	7.6	14.0	20.3	26.7	33.1	39.4	45.8	52.2
				KW	2.43	2.52	2.62	2.72	2.82	2.91	3.01	3.11
		2000	55	MBH	4.8	11.2	17.6	24.0	30.3	36.7	43.1	49.4
			70	MBH	2.98	3.08	3.18	3.27	3.37	3.47	3.57	3.66
			80	MBH	2.8	9.2	15.5	21.9	28.3	34.6	41.0	47.4
				KW	3.44	3.54	3.64	3.73	3.83	3.93	4.03	4.12
060 (5.0)	XN	1500	55	MBH	9.2	15.5	21.9	28.3	34.6	41.0	47.4	53.8
			70	MBH	2.08	2.18	2.28	2.37	2.47	2.57	2.67	2.77
			80	MBH	6.4	12.8	19.2	25.5	31.9	38.3	44.6	51.0
				KW	2.63	2.73	2.83	2.93	3.02	3.12	3.22	3.32
		2000	55	MBH	4.8	11.2	17.5	23.9	30.3	36.7	43.0	49.4
			70	MBH	3.22	3.32	3.42	3.52	3.61	3.71	3.81	3.91
			80	MBH	10.1	16.4	22.8	29.2	35.5	41.9	48.3	54.7
				KW	1.58	1.68	1.78	1.87	1.97	2.07	2.17	2.27
		2500	55	MBH	7.3	13.7	20.1	26.4	32.8	39.2	45.5	51.9
			70	MBH	2.14	2.23	2.33	2.43	2.53	2.62	2.72	2.82
			80	MBH	5.3	11.6	18.0	24.4	30.8	37.1	43.5	49.9
				KW	2.60	2.69	2.79	2.89	2.99	3.08	3.18	3.28
1500	55	MBH	5.9	13.9	21.9	29.9	38.0	46.0	54.0	62.0		
	70	MBH	2.90	3.02	3.13	3.25	3.37	3.49	3.60	3.72		
	80	MBH	2.9	10.9	18.9	26.9	35.0	43.0	51.0	59.0		
		KW	3.43	3.55	3.67	3.79	3.90	4.02	4.14	4.26		
2000	55	MBH	0.6	8.6	16.6	24.6	32.7	40.7	48.7	56.7		
	70	MBH	3.91	4.03	4.14	4.26	4.38	4.50	4.62	4.73		
	80	MBH	8.1	16.1	24.1	32.1	40.1	48.2	56.2	64.2		
		KW	2.60	2.72	2.83	2.95	3.07	3.19	3.30	3.42		
2500	55	MBH	5.0	13.0	21.1	29.1	37.1	45.1	53.1	61.2		
	70	MBH	3.12	3.24	3.36	3.47	3.59	3.71	3.83	3.94		
	80	MBH	2.7	10.7	18.8	26.8	34.8	42.8	50.9	58.9		
		KW	3.59	3.71	3.83	3.95	4.07	4.18	4.30	4.42		
1500	55	MBH	12.2	20.2	28.2	36.3	44.3	52.3	60.3	68.4		
	70	MBH	2.63	2.74	2.86	2.98	3.10	3.21	3.33	3.45		
	80	MBH	9.2	17.2	25.2	33.3	41.3	49.3	57.3	65.4		
		KW	3.16	3.28	3.40	3.51	3.63	3.75	3.87	3.98		
1500	55	MBH	6.9	14.9	23.0	31.0	39.0	47.0	55.1	63.1		
	80	MBH	3.64	3.76	3.87	3.99	4.11	4.23	4.34	4.46		

1. These capacities do not include the supply air blower motor heat. For net capacity, add motor heat, MBh = 3.415 x kW.

## b) GSHP catalogue data

Climate Master: Tranquility® 30 Digital TE Series 2 Tons Two-Stage Heat Pump

### Reference Calculations & Legend

Heating	Cooling	
$LWT = EWT - \frac{HE}{GPM \times 500}$	$LWT = EWT + \frac{HR}{GPM \times 500}$	$LC = TC - SC$
$LAT = EAT + \frac{HC}{CFM \times 1.08}$	$LAT (DB) = EAT (DB) - \frac{SC}{CFM \times 1.08}$	$S/T = \frac{SC}{TC}$

CFM = airflow, cubic feet/minute	HE = total heat of extraction,
EWT = entering water temperature,	HWC = Hot Water Generator (desuperheater) capacity,
EA = entering air temperature, Fahrenheit (dry bulb/wet bulb)	Mbtuh WPD = Water coil pressure drop (psi & ft hd)
T = air heating capacity, Mbtuh	EER = Energy Efficiency Ratio = BTU output/Watt
HC = total cooling capacity, Mbtuh	LW = leaving water temperature, °F
TC = sensible cooling capacity, Mbtuh	T = leaving air temperature, °F
TC = total power unit input, KiloWatts	LA = latent cooling capacity,

### Full Load Correction Factors

#### Air Flow Correction Table

Airflow % of Rated	Cooling				Heating		
	Total Capacity	Sensible Capacity	Power	Heat of Rejection	Heating Capacity	Power	Heat of Extraction
60%	0.925	0.788	0.913	0.922	0.946	1.153	0.896
69%	0.946	0.829	0.926	0.942	0.959	1.107	0.924
75%	0.960	0.861	0.937	0.955	0.969	1.078	0.942
81%	0.972	0.895	0.950	0.968	0.977	1.053	0.959
88%	0.983	0.930	0.965	0.979	0.985	1.032	0.974
94%	0.992	0.965	0.982	0.990	0.993	1.014	0.988
100%	1.000	1.000	1.000	1.000	1.000	1.000	1.000
106%	1.007	1.033	1.020	1.009	1.006	0.989	1.011
113%	1.012	1.064	1.042	1.018	1.012	0.982	1.019
119%	1.016	1.092	1.066	1.025	1.018	0.979	1.027
125%	1.018	1.116	1.091	1.032	1.022	0.977	1.033
130%	1.019	1.132	1.112	1.037	1.026	0.975	1.038

### Entering Air Correction Table

Heating			
Entering Air DB°F	Heating Capacity	Power	Heat of Extraction
40	1.052	0.779	1.120
45	1.043	0.808	1.102
50	1.035	0.841	1.084
55	1.027	0.877	1.065
60	1.019	0.915	1.045
65	1.010	0.957	1.023
68	1.004	0.982	1.010
70	1.000	1.000	1.000
75	0.989	1.045	0.974
80	0.976	1.093	0.946

\* = Sensible capacity equals total capacity

Cooling														
Entering Air WB°F	Total Capacity	Sensible Cooling Capacity Multiplier - Entering DB °F										Power	Heat of Rejection	
		60	65	70	75	80	80.6	85	90	95	100			
45	0.832	*	*	*	*	*	*	*	*	*	*	*	0.946	0.853
50	0.850	1.004	1.174	*	*	*	*	*	*	*	*	*	0.953	0.870
55	0.880	0.694	0.902	1.115	*	*	*	*	*	*	*	*	0.964	0.896
60	0.922		0.646	0.875	1.103	1.329	*	*	*	*	*	*	0.977	0.932
65	0.975			0.639	0.869	1.096	1.123	1.320	*	*	*	*	0.993	0.979
66.2	0.990			0.582	0.812	1.039	1.066	1.262	*	*	*	*	0.997	0.991
67	1.000			0.545	0.774	1.000	1.027	1.223	1.444	*	*	*	1.000	1.000
70	1.040				0.630	0.853	0.880	1.075	1.297	*	*	*	1.011	1.035
75	1.117					0.601	0.627	0.821	1.046	1.275	1.510	*	1.033	1.101

# Heating Performance Data - Full Load - capacity 026

Performance capacities shown in thousands of Btuh

Antifreeze use recommended in this range. Also Clip JW3 on DXM2 board.

EWT °F	Cooling - EAT 80/67 °F											Heating - EAT 70°F										
	GPM	WPD		CFM	TC	SC	kW	EER	HR	LWT	HWC	GPM	WPD	CFM	HC	kW	COP	HE	LAT	LWT	HWC	
		PSI	FT																			PSI
20	1.3	0.3	0.6	750	29.3	18.1	1.16	25.3	33.2	70.0	1.4	6.0	1.9	4.4	840	16.5	1.73	2.8	10.7	88.2	16.4	1.5
	1.4	0.3	0.6	850	29.8	19.5	1.20	24.9	33.9	70.0	1.4	6.0	1.9	4.4	950	16.8	1.68	2.9	11.0	86.3	16.3	1.5
30	1.7	0.3	0.7	750	29.3	18.1	1.16	25.3	33.2	70.0	1.4	3.0	0.7	1.6	840	18.2	1.69	3.2	12.6	90.1	21.6	1.7
	1.7	0.3	0.7	850	29.8	19.5	1.20	24.9	33.9	70.0	1.4	3.0	0.7	1.6	950	18.5	1.64	3.3	12.9	88.0	21.4	1.8
	1.7	0.3	0.7	750	29.3	18.1	1.16	25.3	33.2	70.0	1.4	4.5	1.1	2.6	840	19.1	1.68	3.3	13.4	91.0	24.0	1.8
	1.7	0.3	0.7	850	29.8	19.5	1.20	24.9	33.9	70.0	1.4	4.5	1.1	2.6	950	19.4	1.63	3.5	13.8	88.9	23.9	1.9
	1.7	0.3	0.7	750	29.3	18.1	1.16	25.3	33.2	70.0	1.4	6.0	1.8	4.0	840	19.5	1.67	3.4	13.9	91.5	25.4	1.9
	1.7	0.3	0.7	850	29.8	19.5	1.20	24.9	33.9	70.0	1.4	6.0	1.8	4.0	950	19.8	1.62	3.6	14.3	89.3	25.2	1.9
40	2.2	0.4	1.0	750	29.3	18.1	1.16	25.3	33.2	70.0	1.4	3.0	0.6	1.5	840	21.0	1.66	3.7	15.4	93.1	29.7	2.1
	2.3	0.4	1.0	850	29.8	19.5	1.20	24.9	33.9	70.0	1.4	3.0	0.6	1.5	950	21.3	1.61	3.9	15.8	90.8	29.5	2.1
	2.2	0.4	1.0	750	29.3	18.1	1.16	25.3	33.2	70.0	1.4	4.5	1.1	2.5	840	22.0	1.65	3.9	16.5	94.3	32.7	2.2
	2.3	0.4	1.0	850	29.8	19.5	1.20	24.9	33.9	70.0	1.4	4.5	1.1	2.5	950	22.4	1.60	4.1	16.9	91.8	32.5	2.3
	2.2	0.4	1.0	750	29.3	18.1	1.16	25.3	33.2	70.0	1.4	6.0	1.6	3.8	840	22.6	1.64	4.0	17.1	94.9	34.3	2.3
	2.3	0.4	1.0	850	29.8	19.5	1.20	24.9	33.9	70.0	1.4	6.0	1.6	3.8	950	23.0	1.59	4.2	17.5	92.4	34.2	2.3
50	3.0	0.6	1.4	750	29.1	18.0	1.19	24.5	33.1	72.0	1.4	3.0	0.6	1.4	840	23.8	1.64	4.2	18.2	96.2	37.8	2.4
	3.0	0.6	1.4	850	29.6	19.4	1.23	24.0	33.8	72.5	1.5	3.0	0.6	1.4	950	24.1	1.59	4.5	18.7	93.5	37.5	2.5
	3.3	0.7	1.6	750	29.3	18.1	1.16	25.3	33.2	70.0	1.4	4.5	1.0	2.3	840	25.1	1.64	4.5	19.5	97.6	41.3	2.6
	3.4	0.7	1.6	850	29.8	19.5	1.20	24.9	33.9	70.0	1.4	4.5	1.0	2.3	950	25.4	1.59	4.7	20.0	94.8	41.1	2.6
	3.3	0.7	1.6	750	29.3	18.1	1.16	25.3	33.2	70.0	1.4	6.0	1.6	3.6	840	25.8	1.64	4.6	20.2	98.4	43.3	2.7
	3.4	0.7	1.6	850	29.8	19.5	1.20	24.9	33.9	70.0	1.4	6.0	1.6	3.6	950	26.2	1.59	4.8	20.7	95.5	43.1	2.7
60	3.0	0.6	1.3	750	27.9	17.6	1.30	21.4	32.3	81.5	1.9	3.0	0.6	1.3	840	26.7	1.64	4.8	21.1	99.4	45.9	2.8
	3.0	0.6	1.3	850	28.4	18.9	1.35	21.0	33.0	82.0	1.9	3.0	0.6	1.3	950	27.1	1.59	5.0	21.6	96.4	45.6	2.8
	4.5	1.0	2.3	750	28.8	17.9	1.22	23.7	32.9	74.6	1.5	4.5	1.0	2.3	840	28.2	1.65	5.0	22.5	101.0	50.0	2.9
	4.5	1.0	2.3	850	29.3	19.3	1.26	23.3	33.6	74.9	1.6	4.5	1.0	2.3	950	28.6	1.60	5.2	23.1	97.9	49.7	3.0
	6.0	1.5	3.5	750	29.2	18.1	1.18	24.8	33.1	71.0	1.4	6.0	1.5	3.5	840	29.0	1.66	5.1	23.3	102.0	52.2	3.0
	6.0	1.5	3.5	850	29.7	19.4	1.22	24.3	33.8	71.3	1.4	6.0	1.5	3.5	950	29.4	1.61	5.4	24.0	98.7	52.0	3.1
70	3.0	0.6	1.3	750	26.4	17.0	1.43	18.5	31.3	90.9	2.4	3.0	0.6	1.3	840	29.6	1.66	5.2	23.9	102.6	54.1	3.1
	3.0	0.6	1.3	850	26.9	18.3	1.48	18.2	32.0	91.3	2.4	3.0	0.6	1.3	950	30.1	1.61	5.5	24.6	99.3	53.6	3.2
	4.5	1.0	2.2	750	27.5	17.5	1.33	20.7	32.0	84.2	2.0	4.5	1.0	2.2	840	31.4	1.69	5.4	25.6	104.6	58.6	3.3
	4.5	1.0	2.2	850	28.0	18.8	1.38	20.3	32.7	84.5	2.1	4.5	1.0	2.2	950	31.8	1.64	5.7	26.2	101.0	58.3	3.3
	6.0	1.5	3.4	750	28.0	17.7	1.28	21.8	32.4	80.8	1.8	6.0	1.5	3.4	840	32.3	1.71	5.5	26.5	105.7	61.2	3.4
	6.0	1.5	3.4	850	28.5	19.0	1.33	21.4	33.1	81.0	1.9	6.0	1.5	3.4	950	32.8	1.66	5.8	27.2	102.0	60.9	3.4
80	3.0	0.6	1.3	750	24.8	16.3	1.58	15.7	30.2	100.1	3.0	3.0	0.6	1.3	840	32.6	1.71	5.6	26.7	106.0	62.2	3.4
	3.0	0.6	1.3	850	25.2	17.5	1.64	15.4	30.8	100.5	3.0	3.0	0.6	1.3	950	33.1	1.66	5.8	27.5	102.3	61.7	3.5
	4.5	0.9	2.2	750	26.0	16.8	1.48	17.6	31.0	93.8	2.6	3.7	0.7	1.7	840	33.9	1.74	5.7	27.9	107.4	65.0	3.5
	4.5	0.9	2.2	850	26.4	18.1	1.53	17.3	31.6	94.1	2.6	3.8	0.8	1.8	950	34.4	1.69	6.0	28.7	103.6	65.0	3.6
	6.0	1.4	3.3	750	26.2	16.9	1.45	18.1	31.1	90.4	2.4	3.7	0.7	1.7	840	33.9	1.74	5.7	27.9	107.4	65.0	3.5
	6.0	1.4	3.3	850	26.7	18.2	1.50	17.8	31.8	92.7	2.4	3.8	0.8	1.8	950	34.4	1.69	6.0	28.7	103.6	65.0	3.6
90	3.0	0.6	1.3	750	23.1	15.5	1.75	13.2	29.0	109.4	3.7	2.2	0.4	0.9	840	33.9	1.74	5.7	27.9	107.4	65.0	3.5
	3.0	0.6	1.3	850	23.5	16.7	1.81	13.0	29.7	109.8	3.7	2.3	0.4	1.0	950	34.4	1.69	6.0	28.7	103.6	65.0	3.6
	4.5	0.9	2.2	750	24.3	16.1	1.63	14.9	29.8	103.2	3.2	2.2	0.4	0.9	840	33.9	1.74	5.7	27.9	107.4	65.0	3.5
	4.5	0.9	2.2	850	24.7	17.3	1.69	14.6	30.4	103.5	3.3	2.3	0.4	1.0	950	34.4	1.69	6.0	28.7	103.6	65.0	3.6
	6.0	1.4	3.2	750	24.9	16.3	1.57	15.8	30.2	100.1	3.0	2.2	0.4	0.9	840	33.9	1.74	5.7	27.9	107.4	65.0	3.5
	6.0	1.4	3.2	850	25.3	17.5	1.63	15.5	30.9	100.3	3.0	2.3	0.4	1.0	950	34.4	1.69	6.0	28.7	103.6	65.0	3.6
100	3.0	0.6	1.3	750	21.3	14.8	1.95	10.9	28.0	118.7	4.4	1.6	0.2	0.6	840	33.9	1.74	5.7	27.9	107.4	65.0	3.5
	3.0	0.6	1.3	850	21.7	15.9	2.02	10.7	28.6	119.1	4.5	1.6	0.3	0.6	950	34.4	1.69	6.0	28.7	103.6	65.0	3.6
	4.5	0.9	2.1	750	22.5	15.3	1.81	12.4	28.7	112.7	3.9	1.6	0.2	0.6	840	33.9	1.74	5.7	27.9	107.4	65.0	3.5
	4.5	0.9	2.1	850	22.9	16.4	1.88	12.2	29.3	113.0	4.0	1.6	0.3	0.6	950	34.4	1.69	6.0	28.7	103.6	65.0	3.6
	6.0	1.4	3.2	750	23.1	15.5	1.76	13.1	29.0	109.7	3.7	1.6	0.2	0.6	840	33.9	1.74	5.7	27.9	107.4	65.0	3.5
	6.0	1.4	3.2	850	23.5	16.7	1.82	12.9	29.7	109.9	3.7	1.6	0.3	0.6	950	34.4	1.69	6.0	28.7	103.6	65.0	3.6
110	3.0	0.6	1.3	750	19.7	14.2	2.18	9.0	27.1	128.1	5.3	1.2	0.1	0.3	840	33.9	1.74	5.7	27.9	107.4	65.0	3.5
	3.0	0.6	1.3	850	20.0	15.2	2.26	8.9	27.7	128.5	5.4	1.3	0.1	0.3	950	34.4	1.69	6.0	28.7	103.6	65.0	3.6
	4.5	0.9	2.1	750	20.7	14.6	2.04	10.2	27.7	122.3	4.7	1.2	0.1	0.3	840	33.9	1.74	5.7	27.9	107.4	65.0	3.5
	4.5	0.9	2.1	850	21.1	15.7	2.11	10.0	28.2	122.6	4.8	1.3	0.1	0.3	950	34.4	1.69	6.0	28.7	103.6	65.0	3.6
	6.0	1.4	3.1	750	21.3	14.8	1.96	10.8	28.0	119.3	4.4	1.2	0.1	0.3	840	33.9	1.74	5.7	27.9	107.4	65.0	3.5
	6.0	1.4	3.1	850	21.6	15.9	2.03	10.6	28.6	119.5	4.5	1.3	0.1	0.3	950	34.4	1.69	6.0	28.7	103.6	65.0	3.6
120	3.0	0.5	1.2	750	18.2	13.7	2.46	7.4	26.6	137.7	6.2	1.0	0.1	0.2	840	33.9	1.74	5.7	27.9	107.4	65.0	3.5
	3.0	0.5	1.2	850	18.5	14.7	2.55	7.3	27.2	138.1	6.4	1.0	0.1	0.2	950	34.4	1.69	6.0	28.7	103.6	65.0	3.6
	4.5	0.9	2.0	750	19.1	14.0	2.29	8.3	26.9	132.0	5.6	1.0	0.1	0.2	840	33.9	1.74	5.7	27.9	107.4	65.0	3.5
	4.5	0.9	2.0	850	19.4	15.0	2.37	8.2	27.5	132.2	5.8	1.0	0.1	0.2	950	34.4	1.69	6.0	28.7	103.6	65.0	

### Cooling Performance Data – (Full Load) – capacity 064

EWT °F	GPM	WPD		COOLING - EAT 80/67 °F							HEATING - 70°F						
		PSI	FT	CFM	TC	SC	kW	HR	EER	HWC	CFM	HC	kW	HE	LAT	COP	HWC
20	15.0	7.3	16.8								1800	42.8	3.89	29.8	92.0	3.2	3.8
	15.0	7.3	16.8								2050	43.5	3.77	30.6	89.6	3.4	3.8
30	7.5	1.7	3.9	1630	75.3	49.7	2.68	84.3	28.1	1.9	1800	46.9	3.94	33.6	94.1	3.5	3.9
	7.5	1.7	3.9	1850	76.6	53.4	2.78	86.1	27.5	2.0	2050	47.6	3.82	34.5	91.5	3.7	4.0
	11.3	3.7	8.6	1630	74.9	50.3	2.58	83.5	29.1	1.8	1800	49.1	3.98	35.8	95.3	3.6	4.0
	11.3	3.7	8.6	1850	76.2	54.0	2.67	85.3	28.5	1.8	2050	49.9	3.86	36.7	92.5	3.8	4.1
	15.0	6.1	14.1	1630	74.2	50.5	2.53	82.7	29.4	1.8	1800	50.4	4.00	36.9	95.9	3.7	4.0
	15.0	6.1	14.1	1850	75.5	54.3	2.62	84.5	28.8	1.8	2050	51.2	3.88	37.9	93.1	3.9	4.1
40	7.5	1.2	2.7	1630	74.4	48.8	2.87	84.0	26.0	2.3	1800	53.9	4.07	40.2	97.7	3.9	4.2
	7.5	1.2	2.7	1850	75.7	52.5	2.97	85.8	25.5	2.3	2050	54.7	3.94	41.3	94.7	4.1	4.2
	11.3	3.0	7.0	1630	75.2	49.5	2.72	84.3	27.6	2.0	1800	56.7	4.12	42.8	99.2	4.0	4.3
	11.3	3.0	7.0	1850	76.5	53.2	2.82	86.1	27.1	2.1	2050	57.6	3.99	44.0	96.0	4.2	4.4
	15.0	5.3	12.2	1630	75.3	49.8	2.66	84.2	28.3	1.9	1800	58.3	4.15	44.3	100.0	4.1	4.3
	15.0	5.3	12.2	1850	76.6	53.6	2.76	86.0	27.7	1.9	2050	59.2	4.02	45.5	96.7	4.3	4.4
50	7.5	0.9	2.0	1630	72.4	47.8	3.09	82.8	23.4	2.8	1800	61.1	4.21	46.9	101.5	4.3	4.5
	7.5	0.9	2.0	1850	73.6	51.4	3.20	84.5	23.0	2.9	2050	62.1	4.08	48.2	98.0	4.5	4.6
	11.3	2.6	6.0	1630	74.0	48.6	2.91	83.8	25.4	2.4	1800	64.5	4.28	50.0	103.2	4.4	4.6
	11.3	2.6	6.0	1850	75.3	52.2	3.02	85.6	24.9	2.5	2050	65.5	4.15	51.3	99.6	4.6	4.7
	15.0	4.7	10.8	1630	74.6	48.9	2.84	84.1	26.3	2.2	1800	66.3	4.32	51.7	104.1	4.5	4.7
	15.0	4.7	10.8	1850	75.9	52.6	2.94	85.9	25.8	2.3	2050	67.3	4.19	53.0	100.4	4.7	4.8
60	7.5	0.8	1.7	1630	69.5	46.7	3.35	80.9	20.8	3.5	1800	68.5	4.38	53.6	105.2	4.6	4.9
	7.5	0.8	1.7	1850	70.7	50.3	3.47	82.6	20.4	3.6	2050	69.5	4.24	55.1	101.4	4.8	5.0
	11.3	2.4	5.4	1630	71.7	47.6	3.15	82.3	22.8	3.0	1800	72.3	4.47	57.1	107.2	4.7	5.1
	11.3	2.4	5.4	1850	73.0	51.1	3.26	84.1	22.4	3.1	2050	73.4	4.33	58.6	103.2	5.0	5.2
	15.0	4.3	10.0	1630	72.7	48.0	3.05	83.0	23.8	2.8	1800	74.4	4.52	59.0	108.3	4.8	5.2
	15.0	4.3	10.0	1850	74.0	51.6	3.16	84.8	23.4	2.8	2050	75.5	4.38	60.6	104.1	5.1	5.3
70	7.5	0.7	1.7	1630	66.1	45.5	3.68	78.6	18.0	4.4	1800	75.8	4.55	60.3	109.0	4.9	5.3
	7.5	0.7	1.7	1850	67.3	48.9	3.81	80.3	17.7	4.5	2050	77.0	4.41	61.9	104.8	5.1	5.4
	11.3	2.3	5.2	1630	68.6	46.4	3.44	80.3	20.0	3.8	1800	80.1	4.66	64.2	111.2	5.0	5.6
	11.3	2.3	5.2	1850	69.8	49.9	3.56	82.0	19.6	3.8	2050	81.3	4.52	65.9	106.7	5.3	5.7
	15.0	4.1	9.6	1630	69.9	46.9	3.32	81.1	21.0	3.5	1800	82.4	4.74	66.3	112.4	5.1	5.7
	15.0	4.1	9.6	1850	71.1	50.4	3.44	82.8	20.7	3.5	2050	83.7	4.59	68.0	107.8	5.3	5.8
80	7.5	0.8	1.8	1630	62.5	44.1	4.04	76.2	15.4	5.5	1800	83.1	4.76	66.9	112.8	5.1	5.8
	7.5	0.8	1.8	1850	63.5	47.5	4.19	77.8	15.2	5.6	2050	84.4	4.61	68.7	108.1	5.4	5.9
	11.3	2.2	5.2	1630	65.1	45.1	3.77	77.9	17.2	4.7	1800	87.8	4.89	71.1	115.2	5.3	6.1
	11.3	2.2	5.2	1850	66.2	48.5	3.91	79.6	16.9	4.8	2050	89.1	4.74	73.0	110.3	5.5	6.2
	15.0	4.1	9.4	1630	66.4	45.6	3.65	78.7	18.2	4.3	1800	90.3	4.96	73.3	116.5	5.3	6.7
	15.0	4.1	9.4	1850	67.5	49.0	3.78	80.4	17.9	4.4	2050	91.7	4.81	75.3	111.4	5.6	6.9
85	7.5	0.6	1.3	1630	60.6	43.4	4.3	75.1	14.3	6.1	1800	86.7	4.86	70.1	114.6	5.2	6.0
	7.5	0.6	1.3	1850	61.6	46.7	4.42	76.7	14.0	6.2	2050	88.0	4.7	72.0	109.8	5.5	6.2
	11.3	1.8	4.2	1630	63.2	44.4	3.98	76.7	16.0	5.3	1800	91.5	5.0	74.4	117.1	5.4	6.4
	11.3	1.8	4.2	1850	64.3	47.7	4.12	78.3	15.7	5.4	2050	92.9	4.9	76.3	112.0	5.6	6.5
	15.0	3.3	7.7	1630	64.5	44.9	3.84	77.5	16.9	4.9	1800	94.1	5.1	76.7	118.4	5.4	6.8
	15.0	3.3	7.7	1850	65.6	48.3	3.98	79.2	16.6	5.0	2050	95.5	4.9	78.7	113.1	5.7	7.0
90	7.5	0.3	0.7	1630	58.7	42.6	4.49	74.0	13.1	6.7	1800	90.3	4.96	73.3	116.4	5.3	6.3
	7.5	0.3	0.7	1850	59.8	45.8	4.65	75.6	12.8	6.8	2050	91.7	4.81	75.2	111.4	5.6	6.4
	11.3	1.4	3.2	1630	61.3	43.7	4.18	75.5	14.7	5.8	1800	95.2	5.12	77.7	119.0	5.5	6.7
	11.3	1.4	3.2	1850	62.3	47.0	4.33	77.1	14.4	6.0	2050	96.7	4.96	79.7	113.7	5.7	6.9
	15.0	2.6	6.0	1630	62.6	44.2	4.03	76.3	15.5	5.4	1800	97.9	5.21	80.0	120.3	5.5	7.0
	15.0	2.6	6.0	1850	63.7	47.5	4.18	77.9	15.2	5.5	2050	99.4	5.05	82.1	114.9	5.8	7.1
100	7.5	0.3	0.8	1630	55.2	41.1	5.00	72.3	11.0	8.1							
	7.5	0.3	0.8	1850	56.2	44.2	5.18	73.9	10.8	8.3							
	11.3	1.4	3.2	1630	57.5	42.1	4.65	73.4	12.4	7.2							
	11.3	1.4	3.2	1850	58.5	45.3	4.82	75.0	12.1	7.3							
	15.0	2.6	6.0	1630	58.8	42.6	4.49	74.0	13.1	6.7							
	15.0	2.6	6.0	1850	59.8	45.9	4.65	75.6	12.9	6.8							
110	7.5	0.3	0.6	1630	52.2	39.6	5.60	71.4	9.3	9.8							
	7.5	0.3	0.6	1850	53.1	42.6	5.80	72.9	9.2	10.0							
	11.3	1.3	3.1	1630	54.1	40.6	5.20	71.9	10.4	8.7							
	11.3	1.3	3.1	1850	55.0	43.6	5.39	73.4	10.2	8.9							
	15.0	2.5	5.8	1630	55.2	41.1	5.01	72.3	11.0	8.2							
	15.0	2.5	5.8	1850	56.1	44.2	5.19	73.8	10.8	8.3							
120	7.5	0.0	0.0	1630	50.0	38.5	6.30	71.6	7.9	11.7							
	7.5	0.0	0.0	1850	50.8	41.4	6.53	73.1	7.8	11.9							
	11.3	1.1	2.6	1630	51.3	39.2	5.83	71.3	8.8	10.4							
	11.3	1.1	2.6	1850	52.2	42.1	6.04	72.8	8.6	10.6							
	15.0	2.4	5.4	1630	52.1	39.6	5.62	71.3	9.3	9.8							
	15.0	2.4	5.4	1850	53.0	42.6	5.82	72.9	9.1	10.0							